South Dakota State University

Open PRAIRIE: Open Public Research Access Institutional Repository and Information Exchange

Electronic Theses and Dissertations

2023

Simulating The Impact of Emissions Control on Economic Productivity Using Particle Systems and Puff Dispersion Model

Najam Khan

Follow this and additional works at: https://openprairie.sdstate.edu/etd2

Part of the Industrial Organization Commons, Mechanical Engineering Commons, and the Operational Research Commons

SIMULATING THE IMPACT OF EMISSIONS CONTROL ON ECONOMIC PRODUCTIVITY USING PARTICLE SYSTEMS AND PUFF DISPERSION MODEL

BY

NAJAM KHAN

A dissertation submitted in partial fulfillment of the requirements for the

Doctor of Philosophy

Major in Agriculture, Biosystems, and Mechanical Engineering

South Dakota State University

2023

DISSERTATION ACCEPTANCE PAGE
Najam Khan

This dissertation is approved as a creditable and independent investigation by a candidate for the Doctor of Philosophy degree and is acceptable for meeting the dissertation requirements for this degree. Acceptance of this does not imply that the conclusions reached by the candidate are necessarily the conclusions of the major department.

Huitian Lu
Advisor Date

Kasiviswanathan Muthukumarappan
Department Head Date

Nicole Lounsbery, PhD
Director, Graduate School Date

ACKNOWLEDGEMENTS

I am extremely grateful to my advisor, Dr. Huitian Lu. for all his support and guidance throughout my research work. I would like to extend my sincere thanks to Joe Wadsworth (CEO) at CSW, Paul Hitchcock (CEO) at Crowsnest and my dad Saeed Khan for their support and motivation. Additionally, I want to express my gratitude for the time and help of my committee members, Stephen Gent (Mechanical Engineering), Bryan Logue (Chemistry & Biochemistry), Gary Anderson (Agriculture & Biosystems Engineering), Gary Hatfield (Mathematics & Statistics), and Robin Arends. Finally, I want to express my gratitude to the departments of Construction & Operations Mgmt. and Agriculture, Biosystems, and Mechanical Engineering for allowing me the opportunity to undertake this challenge.

CONTENTS

LIST OF FIGURES vii

LIST OF TABLES ix

ABSTRACT x

1. INTRODUCTION 1

1.1 Statement of need 7

1.2 Problem of study 9

1.3 Purpose of study 9

1.4 Research question 11

2. LITERATURE REVIEW 13

2.1 Commodities demand 13

2.2 Effects of emissions on health 22

2.3 Emissions control 24

2.4 Mobile emissions 26

2.5 Atmospheric emissions modeling 28

2.6 Production 30

2.7 Consumption 40

2.8 Transport / Graph Theory 49

2.9 Emissions impact modeling 68

2.10 Summary 71

3. MATERIALS AND METHODS 72

3.1 Object / class / particle system 75

3.2 Vectors 76

3.3 Prim's algorithm 77

3.4 Floyd Warshall algorithm 78

3.5 Equilibrium order quantity (EOQ) / Reorder point (ROP) 80

3.6 Vehicle routing problem 82

3.7 Genetic algorithm (GA) 85

3.8 Production function (Profit maximization, cost minimization) 87

3.9 Demand function 90

3.10 Warehouse location problem 91
3.12 Navier-Stokes Equation 94
3.13 Puff dispersion model 95
3.14 Population growth 100
3.15 Commodities pricing 101
3.16 Liquidity preference-money supply (LM) model 102
3.17 Labor-Leisure model 103
3.18 Intertemporal choices 104
3.19 Land price gradient 106
3.20 Fisher index 107
3.21 Emission` exposure 107
FLOW CHART OF THE SIMULATION 109

4. ASSUMPTIONS OF STUDY 110

5. LIMITATIONS 112

6. DELIMITATION 113

7. NUMERICAL SIMULATION 114

7.1 Experiments 114
7.2 Software 115
7.3 Global Parameters 115
7.4 Termination conditions 117
7.5 Validation of key concepts 117
7.5a Prim's Minimum Spanning Tree (MST) 117
7.5b Floyd Warshall algorithm 118
7.5c Production function 119
7.5d Demand function 122
Hicksian Demand 123
Marshallian Demand 124
7.5e Puff Dispersion model 126
7.5f VRPSPD 133
7.5g Commodities Pricing 136
7.5h Labor-Leisure model 137
7.5i Liquidity Preference-Money Supply model 138

7.5j Intertemporal Choice model 139
7.5k Land Price gradient 141
7.5l Hub Location problem 142
8. RESULTS 145
8.1 Passive emissions controls 153
8.1a Earnings ($) / spending ($) / foregone sales ($) 153
8.1b Units produced versus units consumed 156
8.1c Maximum product moved ($) vs transportation costs ($) 158
8.1d Average and maximum emission's exposure 159
8.1e Active transport hubs, delivery delays 162
8.2 Active emissions controls 165
8.2a Earnings ($) / spending ($) / foregone sales ($) 165
8.2b Units produced versus units consumed 167
8.2c Maximum product moved ($) vs transportation costs ($) 170
8.2d Average and maximum emission's exposure 173
8.2e Active transport hubs, delivery delays 176
9. DISCUSSION 179
10. CONCLUSION 188
11. RECOMMENDATIONS 190
12. REFRENCES 191

LIST OF FIGURES

Figure 2-1: Delaunay Triangulation (Left), Voronoi Diagram (Center) (Kopsch, 2012), Steiner Tree (Right) (Smith, 1998) 55
Figure 2-2: (L) Spatial map of ozone monitoring sites in US (max 8hr ozone concentration). (R) Spatial map of max-8hr ozone concentration predicted by CMAQ (EPA, 2022)..... 69
Figure 3-1: Application of vectors to simulate attraction between a central body and 2,000 particles (Henderson, n.d.). 77
Figure 3-2: Application of Prim's Algorithm on 29 vertices to generate an MST. 78
Figure 7-1: Prim's Minimum Spanning Tree output on 32 vertices in simulation (Left) vs Graph Online output (Right)..... 117
Figure 7-2: Shortest path reconstruction between vertices (1 → 32) using Floyd Warshall Algorithm. Simulation's shortest path output (Left) edges with red highlight is identical to the Graph-Online shortest path output (Right) red vertices with yellow highlighted edges. 118
Figure 7-3: Ground level emission's concentration estimated using Puff dispersion model under the atmospheric stability class (A). The central point of gaseous plumes is indicated by white points..... 128
Figure 7-4: Comparison of the steady state concentrations produced by the Puff dispersion model and the EPA Screen 3 model under the stability class (A). 128
Figure 7-5: Ground level emission's concentration estimated using Puff dispersion model under the atmospheric stability class (B). The central point of gaseous plumes is indicated by white points..... 129
Figure 7-6: Comparison of the steady state concentrations produced by the Puff dispersion model and the EPA Screen 3 model under the stability class (B)..... 129
Figure 7-7: Ground level emission's concentration estimated using Puff dispersion model under the atmospheric stability class (C). The central point of gaseous plumes is indicated by white points..... 130
Figure 7-8: Comparison of the steady state concentrations produced by the Puff dispersion model and the EPA Screen 3 model under the stability class (C)..... 130
Figure 7-9: Ground level emission's concentration estimated using Puff dispersion model under the atmospheric stability class (D). The central point of gaseous plumes is indicated by white points..... 131
Figure 7-10: Comparison of the steady state concentrations produced by the Puff dispersion model and the EPA Screen 3 model under the stability class (D). 131
Figure 7-11: Ground level emission's concentration estimated using Puff dispersion model under the atmospheric stability class (E). The central point of gaseous plumes is indicated by white points..... 132
Figure 7-12: Comparison of the steady state concentrations produced by the Puff dispersion model and the EPA Screen 3 model under the stability class (E). 132
Figure 7-13: The Genetic Algorithm (GA) Heuristic approach is used to solve the VRPSPD problem. To transfer 12 orders between firms, 657 KM must be covered. 133
Figure 7-14: Simulation results showing supply, demand, and price changes. 136
Figure 7-15: Simulation output depicting transient behavior of money supply and interest rate. The approximate money supply equilibrium is established at $ 1,695.70. 139
Figure 7-16: (Top) Simulation output of land price gradient achieved using finite differencing scheme. The Po is the price of land at each city center. (Left) A comparison of land price gradient

around a city in the simulation versus the land price gradient for the city of Paris. (The two diagrams shown above are not connected) 141
Figure 7-17: The Genetic Algorithm (GA) Heuristic approach is used to solve the HLP problem. To accomplish the shortest possible total transit distance, the 12 demand sites (blue triangles) are each individually connected to 4 hubs. 143
Figure 8-1: A 2D spatial output of the economic assessment platform. The display shows random distribution of various resources, industries, transport hubs and markets over a 500KM x 500 KM area. The road network is conceived by the application of Prim's Minimum Spanning Tree (MST) algorithm, with extra edges added to create close loops. Trucks use the road network to channel goods between pickup and drop-off points. 148
Figure 8-2: Ground level emissions concentrations from mobile and point sources. Emissions concentrations are estimated using the PUFF dispersion model. 149
Figure 8-3: Spatial distribution of various entities used in calculating the impact of passive and active emissions control on productivity. 150
Figure 8-4: The interdependence of firms on each other's productivity 151
Figure 8-5: Vehicle routing problem with multiple pickups-drop offs. 152
Figure 8-6: Plots of earnings, spending, and foregone sales as a function of production firm's shutoff time between consecutive operations (Low Inventory) 153
Figure 8-7:Commodities production and consumption as a function of production firm's shutoff time between consecutive operations (Low Inventory) 156
Figure 8-8: Total nominal value of product moved, and the associated transport cost observed at various levels of shutoff time. 158
Figure 8-9: Plots of (average) and (maximum) emissions exposure as a function of firm's shutoff time between each production 160
Figure 8-10: Active transport hubs and delivery lead times as a function of shutoff time periods between consecutive production 162
Figure 8-11: Plots of earnings, spending, and foregone sales as a function of production firm's shutoff time between consecutive operations (Active Control) 165
Figure 8-12: Commodities production and consumption as a function of production firm's shutoff time between consecutive operations (Active Control) 167
Figure 8-13: Total nominal value of product moved, and the associated transport cost observed at various levels of shutoff time (Active Control) 170
Figure 8-14:Plots of (average) and (maximum) emissions exposure as a function of firm's shutoff time between each production (Active Control) 173
Figure 8-15: Active transport hubs and delivery lead times as a function of shutoff time periods between consecutive production (Active Control) 176
Figure 10-1: Average and maximum ground level concentrations experienced by a set of 1000 boids from industrial clusters (alpha) and (delta) as a function of varying distances. 189

LIST OF TABLES

Table 2.1: Fertilizer input per capita (1960 versus 2019) 15

Table 2.2: Chemicals released per 1 kg production of cement 18

Table 2.3: Metal sector – Greenhouse Gas Emissions (Mt CO2e) 19

Table 2.4: 2020 emissions (CO2e) per metals industry subsector 19

Table 2.5: Emission factors of various compounds for Boilers and Process Heaters firing 21

Table 2.6: Nitrogen oxides emission control techniques 25

Table 2.7: Average Heavy-Duty Truck Emission Rates by GVW^{ref} Class (g/Mile) 27

Table 2.8: Cobb Douglas production function estimates for various industries 38

Table 2.9: US technical coefficients for various industries (Year - 2006) 39

Table 2.10: Summary of air pollution exposure & epidemiology studies on pollutants .. 70

Table 7.1: Simulation global parameters 115

Table 8.1: Summary of earnings, spending, and foregone sales 154

Table 8.2: Units produced versus units consumed 156

Table 8.3: Product moved and corresponding transport cost 158

Table 8.4: Average and Max Emissions Exposure 160

Table 8.5: Active Transportation Hubs, Delivery Lead Time 163

Table 8.6: Summary of earnings, spending, and foregone sales (Active control) 166

Table 8.7: Units produced versus units consumed (Active control) 168

Table 8.8: Product moved and corresponding transport cost (Active control) 170

Table 8.9: Average and Max Emissions Exposure (Active control) 174

Table 8.10: Active Transportation Hubs, Delivery Lead Time (Active control) 177

ABSTRACT

SIMULATING THE IMPACT OF EMISSIONS CONTROL ON ECONOMIC PRODUCTIVITY USING PARTICLE SYSTEMS AND PUFF DISPERSION MODEL

NAJAM KHAN

2023

A simulation platform is developed for quantifying the change in productivity of an economy under passive and active emission control mechanisms. The program uses object-oriented programming to code a collection of objects resembling typical stakeholders in an economy. These objects include firms, markets, transportation hubs, and boids which are distributed over a 2D surface. Firms are connected using a modified Prim's Minimum spanning tree algorithm, followed by implementation of an all-pair shortest path Floyd Warshall algorithm for navigation purposes. Firms use a non-linear production function for transformation of land, labor, and capital inputs to finished product. A GA-Vehicle Routing Problem with multiple pickups and drop-offs is implemented for efficient delivery of commodities across multiple nodes in the economy. Boids are autonomous agents which perform several functions in the economy including labor, consumption, renting, saving, and investing. Each boid is programmed with several microeconomic functions including intertemporal choice models, Hicksian and Marshallian demand function, and labor-leisure model.

The simulation uses a Puff Dispersion model to simulate the advection and diffusion of emissions from point and mobile sources in the economy. A dose-response function is

implemented to quantify depreciation of a Boid's health upon contact with these emissions.

The impact of emissions control on productivity and air quality is examined through a series of passive and active emission control scenarios. Passive control examines the impact of various shutdown times on economic productivity and rate of emissions exposure experienced by boids. The active control strategy examines the effects of acceptable levels of emissions exposure on economic productivity. The key findings on 7 different scenarios of passive and active emissions controls indicate that rate of productivity and consumption in an economy declines with increased scrutiny of emissions from point sources. In terms of exposure rates, the point sources may not be the primary source of average exposure rates, however they significantly impact the maximum exposure rate experienced by a boid. Tightening of emissions control also negatively impacts the transportation sector by reducing the asset utilization rate as well as reducing the total volume of goods transported across the economy.

[1] Najam Khan
Operations Research (M.S.OM) J.J College of Engineering
Ag, Biosystems, and Mechanical Engineering Program (Ph.D.)
South Dakota State University, Brookings, SD, USA. e-mail: najam.khan@jacks.sdstate.edu

Simulating the impact of emissions control on economic productivity (PUFF, IS-LM, GA, O.R, MST, O.M) - YouTube

1. INTRODUCTION

Industrial activities play a vital role in satisfying a country's socio-economic needs. The rapid rise in population and purchasing power in various regions has led to a considerable strain on the supply streams of various commodities. To quench the gap between supply and demand, industries have continuously responded by expanding operations either through innovation or investment in new plants. Typically, have expansion of industrial activities has contributed positively to the gross domestic product (GDP) of a region but has also heightened the risks to the environment. Consequently, governing bodies in many regions around the globe are faced with the dilemma of how to achieve a balance between economic productivity and environmental security.

The world population in 1985 stood at 5 billion and by mid-2020 had risen to 7.8 billion with a projected increase to > 9.0 billion by 2050 (Danan Gu, 2021). Between 1985-2020, the per capita GDP increased from $2,311 to $ 10,926 which combined with population growth led to a substantial increase in demand for various commodities. In 1985, the domestic material consumption of metals, non-metallic minerals, and fossil energy stood at 1,159 tons per capita which by 2019 had risen to 2,087 tons per capita (OECD, Material consumption, 2023). A detailed breakdown of metals consumption between 1970 and 2005 indicates that the global consumption of aluminum grew by 300%, steel, copper, zinc, and chromium by 200%, lead by 150%, and nickel by 75% respectively. During the same period, the extraction of nitrogen-based fertilizers increased 4 folds, from approximately 30 million metric tons to around 120 million metric tons. Meanwhile, global consumption of cement increased from 550 million metric tons (1970) to 2,100 million metric tons (2005) (Donald G. Rogich, 2008). The continuous rise in demand for

commodities has been satisfied with the expansion of the industrial base in many regions around the globe.

The industrial production index monitors output from mining, manufacturing, electricity, gas, steam, and air conditioning sectors. Between 1970-2005 the U.S industrial production index[2] increased 291% from 35 to 102 points, whereas Turkey increased 600% from 10 to 60 points, the UK by 150% from 60 to 90, and France by 167% from 67 to 112. Data on India from 1994-to 2018 indicates that the industrial production index soared 500% from 23 to 115 points (OECD, Industrial production, 2023). The contribution of industrial production to a country's gross domestic product (GDP) varies greatly across the globe. For example, in 2017 the U.S industrial activity contributed 19.1% to the country's total GDP, whereas in Turkey industrial activity contribution was 32.2%, the UK 20.2%, France 19.5%, India 23%, China 40.5%, Pakistan 19.1%, Nigeria 22.5%, Germany 30.7%, and the Republic of Congo at 51% (CIA, 2023). Generally, the expansion of industrial activity has contributed positively to economic growth through the production of goods, employment opportunities, trade, and taxes as well as serving as a support for sectors including logistics and services. A major drawback of industrial expansion has been its detrimental effect on the environment since many industrial installations are major emitters of atmospheric pollutants, emissions to water and soil, waste generation, and consumption of energy (AMEC Environment & Infrastructure UK Limited, 2014).

[2] 2005 – Baseline Year

A 2010 European Union (EU) study on emissions of 17 air pollutants concluded that 23% of air pollutants emitted across the EU originated from (agro-) industrial sources. A breakdown of the contribution of individual pollutants indicates that industrial activity was responsible for 15% of the carbon monoxide emissions (CO), 30% of nitrogen oxides (NO_x) emissions, 12% of particulate matter (PM_{10}), 73% of sulfur oxides (SO_x), 57% of arsenic, 44% of chrome, 44% of lead, 62% of mercury, 47% of nickel, 5% of ammonia, 68% of dioxins and furans, 60% of polychlorinated biphenyls (PCBs), and 86% of polycyclic aromatic hydrocarbon (PAH) emissions (AMEC Environment & Infrastructure UK Limited, 2014). A study of the emissions trend from the Pearl River Delta Region in China indicated that power plants and industrial sources were responsible for 82% of SO_x emissions, 48% of NO_x emissions, 32% of PM_{10}, and 33% of volatile organic compounds (VOC) emissions (Qing Lu, 2013). A 1997 study on India's atmospheric emissions indicated that industrial activity, including power generation, was responsible for 85% of SO_x emissions, 87% of $PM_{2.5,}$ and 18% of carbonaceous aerosol emissions (M.Shekar Reddy, 2002). In 2014, total SO_x emissions in the US stood at 4.68 million tons with industrial activity accounting for 94.70%, total NO_x emissions stood at 13.60 million tons with industrial activity accounting for 34.8%, total $PM_{2.5}$ emissions stood at 5.4 million tons with industrial activity accounting for 61.5%, total PM_{10} emissions stood at 18.2 million tons with industrial activity accounting for 86.0% of emissions, and total VOC emissions stood at 55.4 million tons with industrial activity accounting for 15.1% of emissions (EPA, n.d.). Exposure to these emissions carries the risk of adverse effects on human health and the environment.

The environmental impact of SO_2, NO_x, CO_2, and chlorofluorocarbons emissions include stratospheric ozone depletion, acid precipitation, and global climate change (An empirical investigation of air pollution from fossil fuel combustion and its impact on health in India during 1973–1974 to 1996–1997, 2005). Exposure to a mix of pollutants, i.e., gases, dioxins, heavy metals, and particulate matter, can lead to adverse health effects in humans. These health effects can range from nausea, difficulty breathing, skin inflammation, birth defects, compromised immune systems, and cancer (Marilena Kampa, 2008). Long-term exposure to even lower concentrations of pollutants can affect the respiratory system. For example, exposure to increased levels of SO_x, NO_x, arsenic, and nickel can cause throat irritation, followed by bronchoconstriction and dyspnea (John R. Balmes, 1987). Exposure to heavy metal pollutants can lead to tachycardia, increased blood pressure, and anemia (Andrew J Ghio, 2004). Exposure to dioxins and heavy metals such as lead, mercury, and arsenic can lead to neuropathies with symptoms including fatigue, hand tremors, blurred vision, injuries to dopamine systems, N-methyl-D-Aspartate (NMDA) receptor complex, certain cases of neurological cancers, and impaired mental development in children (Ewan KB, 1996) (Ratnaike, 2003) (Lasley SM, 2000). In addition, heavy metals exposure can lead to tubular dysfunction and can increase the risk of stone formation in the kidneys. Dioxins can result in damage to liver cells which can result in gastrointestinal and liver cancers. Exposure to heavy metals during pregnancy has been observed to prompt spontaneous abortion, congenital malformations, and lesions to the developing nervous system (Marilena Kampa, 2008).

A 1992 study by the World Bank estimated that in India, SO_2 and particulate emissions were responsible for 50,000 premature deaths and 4-5 million new cases of chronic

bronchitis (An empirical investigation of air pollution from fossil fuel combustion and its impact on health in India during 1973–1974 to 1996–1997, 2005). Epidemiological studies in China found that long-term exposure to emissions resulted in various respiratory and cardiovascular complications. In 2010, China's death toll from particulate and ozone exposure accounted for 1.36 million premature deaths (Zhenyu Luo, 2022), and a loss of 41% of crop production. The sectoral emissions in China were estimated to have cost 0.66% of the annual GDP (Gu Y, 2018). In 2005, US industrial and transport emissions of $PM_{2.5}$ accounted for 200,000 premature deaths, and about 10,000 deaths from ozone concentrations, with road transport being the largest contributor (Fabio Caiazzo, 2013). A 2021 publication estimated that the health effects associated with mercury exposure during 2010-to 2050 are estimated to be $19 trillion. Methylmercury (MeHg) exposure is attributable to 10,000 fatal heart attacks in China, and an economic loss of $16 billion in the U.S. and European Union due to a decrease in intelligence quotient (IQ) (Zhang, 2021). Overall, the annual global premature deaths from $PM_{2.5}$ emissions are estimated to be 2.2 million, and 493,000 from ozone emissions. Land transport had the highest impact on ozone respiratory mortality globally, accounting for 16% of the global burden, whereas the residential and commercial sectors contributed the most to $PM_{2.5}$ emissions, accounting for 30% of the global burden (Raquel A. Silva, 2016).

The perpetual worsening of air quality and the rise in average global temperatures have prompted many governments to start taking stringent actions against emissions. However, ill-defined execution of emissions control policies has contributed to short-term job losses, increased dependence on imports, supply disruptions, inflation, and, in certain

instances, led to the contraction of certain sectors of the economy. Governments, in many cases, have doubled down on emissions control pledges due to political pressures, lack of access to alternatives, and skepticism among a major minority regarding environmentalism (Alexander H. DeGolia, 2019).

In 2021, the COP26 climate conference noted pledges from 200 nations regarding the fight against climate change, methane gas emissions, deforestation, coal financing, and rules on carbon trading. However, differences between nations were apparent when India, China, and Russia, which make up 35% of total methane emissions, decided not to join the coalition on methane emissions. Words regarding coal usage were switched from "phase out" to "phase down" upon insistence from China and India (Newburger, 2021). In May 2022, India, to combat the worst energy crisis in six years, granted environmental clearances to coal producers to increase production capacity by 50% (Varadhan, 2022). Atmospheric emissions, by nature, do not stay restricted to a given region due to the dynamic nature of the atmosphere. Cutting down on gaseous emissions like CO_2, CH_4, and CFC in Europe and the U.S. will have no impact on global warming if China, India, and Russia are going to stay passive or, in the worst case, increase such emissions. Exposure to pollutants like SO_2, heavy metals, and particulate matter is subject to local weather conditions like inversion, wind direction, solar radiation, wind velocity, decay rate, regional precipitation levels, terrain, emissions rate, and temperature (Air quality monitoring, 2017). Limiting economic growth to safeguard the environment involves a reevaluation at the regional level due to the dynamic nature of pollutant dispersion, the limited success of emissions management across many regions, unclear commitments by

important emitters, emissions from natural resources, a growing population, rising commodities demand, and geopolitical dangers to the global supply chain.

1.1 Statement of need

The projected increase in demand for various commodities incentivizes many industries to increase production, either through innovation or investment in new plants. The location choice of many industries includes factors like agglomeration, proximity to skilled labor, resources, suppliers, and customers, which tend to put industrial expansion in proximity to population centers (Timms H. L., 1962). Emissions from the ever-increasing cycle of industrial production of even core commodities put additional strain on the environment. In response, governing bodies in many regions have attempted to enact emissions control measures, but the results have not been conclusive.

The key predicament faced by many governing bodies is that excessive restrictions on emissions can be economically counterproductive. The rising population and purchasing power in many regions have given rise to increased demand for products. Excessive restrictions on emissions in the absence of alternatives can lead to job losses, increased dependence on imports, supply chain disruptions, inflation, and the contraction of certain sectors of the economy. Contradictory national and international policies regarding emissions control and large-scale emission events from natural sources also make the justification for emissions control at a regional level questionable by a major minority of the public.

The U.S. during the Trump administration's tenure (2017–2021) rolled back more than 100 environmental rules enacted by previous administrations. These included the withdrawal of the U.S. from the Paris climate agreement; the cancellation of requirements

on oil and gas companies to report methane emissions; the withdrawal of Clinton-era rules on limits of toxic emissions from major industrial polluters; the overturning of Obama-era guidance meant to reduce emissions during power plant start-ups, shutdowns, and malfunctions; relaxing air pollution regulations for a handful of plants that burn waste coal for electricity; and lifting an Obama-era freeze on new coal leases on public lands, etc. (Nadja Popovich, 2021). On November 2nd, 2021, the Biden administration released initiatives to tackle methane emissions, deep decarbonatization, clean energy demand initiative (CEDI), and supporting agriculture and critical ecosystems, which overrides practically all of Trump's earlier rollbacks (House, 2021). In March 2022, the U.S. inflation rose to 7.9%, with the price of gasoline jumping 43.6%, the cost of electricity by 9%, and the cost of used cars and trucks by 41.2%, while wages rose only by 5.1% compared to March 2021. Biden's energy policies restrained oil producers to the extent that gas prices, which is a key component of CPI, were rising before the start of the Russia-Ukraine conflict (Gasparino, 2022). To control the increase in energy prices, the Biden administration announced a record release of 180 million barrels from the strategic petroleum reserves, which led other member countries of the International Energy Agency to release reserves from their inventories (Zhdannikov, 2022). The directive and counter directive between successive administrations on environmental policies is unproductive for both the environment and economic stability.

1.2 Problem of study

Excessive restrictions on atmospheric emissions can negatively impact the productivity of certain industrial and transportation sectors. In the absence of technological improvements, these restrictions can have a prohibitive effect towards value added operations, sector's expansion, and in certain cases yield to sector's collapse. Given that firms are highly dependent on each other's output, these restrictions can have a negative cascading effect on productivity of certain sectors, which ultimately yields to disruption of the supply – demand equilibrium of various commodities. Restriction on emissions can assist in environmental protection and mitigation, however in the absence of reliable alternatives can make an economy vulnerable to supply chain shocks, employment growth, inflation, increased dependence on imports, and inadvertent retraction in other sectors of the economy. The globe is currently confronted with a conundrum in which the simultaneous increase in population growth and purchasing power will need the development of supply chains to fulfill expected demand. Additionally, governments must promote economic growth in order to provide jobs for the growing population. How should governments respond to the dichotomy of preserving economic stability without sacrificing the wellbeing of the regional atmospheric conditions?

1.3 Purpose of study

The purpose of the research is to determine how emissions control effect a region's productivity. The goal of the research is to determine the optimal policy that can maximize economic productivity while minimizing the detrimental effects of emissions on the regional environment and its inhabitants. This research will have an economic, social, and environmental impact in many regions that are struggling to strike a balance

between economic prosperity and environmental protection. The primary objectives of the research are as follows:

1. Create a simulation platform that can support rapid scalability and customization to evaluate a wide range of scenarios that influence economic productivity and environment.
2. A platform capable of supporting the spatial distribution of multiple production and consumption nodes on a 2D plane, as well as the ability to execute autonomous trade decisions between entities that adhere to general microeconomic principles such as production (Leontief, Cobb Douglas, CES, etc.), consumption (Marshallian, Hicksian, Slutsky, etc.), Walrasian price stability, intertemporal choice, and labor-leisure model.
3. Create a transport system in the platform that permits the movement of unfinished and finished goods between different simulation nodes. The implementation of transport systems includes establishing a transportation network using concepts from graph theory and a navigation system employing ideas from field of operations research.
4. Integration of an EPA recommended pollutant dispersion model that can facilitate transient modeling of emission's dispersion from point and mobile sources. Quantify the resultant exposure of emissions on the boids[3] as a function of emissions control at the regional level.

[3] An artificial intelligence with limited capabilities programmed to follow basic rules and behaviors. They are perfect for modeling schools, herds, swarms, and flocks of diverse animals, insects, and fish, as well as simulations of predators and prey. They may respond to the presence of other items as well as to the individuals inside their own system (Blender, 2023).

1.4 Research question

Given an economy that generates *Y* units of output: $Y = \int_{t=0}^{n} y_{(t)}$ where t is time span 0, 1,..., *n*. Let T be a set of unique commodities in the economy such that $T = \{t_1, t_2, \dots, t_n\}$, where each commodity type t_i is produced by p set of production units. The production units are represented by an array $I = \{ p_0^{t_1}, p_1^{t_1}, \dots, p_z^{t_n}\}$, where z is the total number of firms in the economy. The economy consists of M market centers: $M = \{m_1, m_2, \dots, m_n\}$, L transport hubs: $L = \{l_1, l_2, \dots, l_n\}$ where each hub l_i holds K set of delivery units. Each delivery unit $k \in K$, covers a distance d during delivery of a given commodity between two locations. The economy also contains a set of boid objects $B|B = \{b_0, b_1, \dots, b_n\}$ where each boid b_i consumes a portion of finished output Δy in per unit time t. A subset of B provides l units of labor in the economy, in exchange for wages. Each boid trades a portion of savings Δs with a market m_i in exchange for Δy.

Given that the p set of production units and k set of delivery units each introduce Q units of pollutants in the atmosphere, where $Q \propto Y,\ Q \propto d$ respectively. The emitted pollutants are dispersed in the atmosphere using advection and diffusion mechanism, resulting in a final ground level concentration $C_{x,y,t}$. The $C_{x,y,t}$ negatively impacts the health index *H* of a given boid b_i such that $H_{bi} = -f(C_{x,y,t})$.

If the economy needs to produce *Y* units of output to meet total demand $D|D = \sum_{i=1}^{B} \Delta y$ and maximize labor opportunity $l \subseteq B$. Calculate the economic productivity *Y* of a closed loop economy and the corresponding health indices $H \in B$ as a function of constrain on point emissions. To assist the resolution of the problem, the following set of assignments have been proposed:

1. Calculate the change in industrial production in a geographically confined, closed-loop economy as a function of emission restrictions, assuming no breakthroughs in emissions control technologies.
2. Calculate the change in consumption in a geographically confined, closed-loop economy as a function of emission restrictions, assuming no breakthroughs in emissions control technologies.
3. Calculate the change in emissions exposure levels experienced by boids as a function of change in emissions restrictions.
4. Quantify the impact on transportation sector as a function of emissions restrictions on point sources.

2. LITERATURE REVIEW

The purpose of the study requires a broad literature review across multiple disciplines including economics, pollution, graph theory, logistics, operations research, operations management, mechanics, and environmental sciences. The literature review establishes correlation between population growth, increased demand of commodities, and resultant atmospheric pollution. Additionally, it covers the dynamics of emissions regulation and its potential effects on the economy, as well as the effects of emissions on the environment and public health. The review then covers a variety of subjects from the fields of mathematics, microeconomics, and computer sciences that play an important role towards constructing the simulation platform.

2.1 Commodities demand

Industrial and transportation operations play an important part in meeting a country's different socioeconomic demands and achieving long-term growth. The world population in 1950 stood at 2.5 billion which by the end of the century rose to 6.1 billion with a projected increase to 8.8 to 10 billion by 2050 (Cleland, 2013). In 1960, the global GDP per capita[4] was $ 3,585.8, but by 2019 it had risen to $11,012.90 (The World Bank, n.d.). The significant surge in population and purchasing power in various regions across the world has put additional strain on supplies of various commodities. For example, since late 1990, China's rapid industrialization has resulted in a dramatic increase in global steel and concrete consumption (6% per year), aluminum consumption (5% per year), copper consumption (3% per year), chromium consumption (5% per year), manganese consumption (6% per year), nickel consumption (5% per year), and zinc consumption

[4] Constant (2015 US$)

(4% per year). In 2015, the global consumption of mineral resources reached an unprecedented level of 70 Gt/year. The expected shift to 100% renewable energy by 2050 may require up to 330 Mt of copper (20 x the present world annual supply), 8 Mt of lithium (190 x), 66 Mt of nickel (30 x), and 31 kilotons of platinum (15 x). The rising demand for rare metals such as Germanium, Indium, Selenium, Tellurium, Dysprosium, Neodymium, and Praseodymium is predicted to necessitate a 10% to 230 percent rise in production levels[5] by 2030. Overall, the demand for all metals during the next 35 years (2015-2050) for all goods would exceed the total quantity produced to date (Olivier Vidal, 2017).

Fertilizer sales were $ 172 billion in 2014, supporting 2.3 million jobs both directly and indirectly (Patrick Heffer, 2014). In 1961, the global production of nitrogen-based fertilizer was 12.94 Mt, 11.21 Mt of phosphate, and 9.37 Mt of potash. By 2019, global demand for nitrogen-based fertilizer had increased to 113.3 Mt, 53.3 Mt of phosphate, and 41.37 Mt of potash (Hannah Ritchie, Fertilizers, 2013). Between 1961 – to 2019 the fertilizer input per capita across multiple regions is summarized in Table 1. To feed 9 billion people by 2050, food production will need to increase by roughly 60% between 2007 and 2050, necessitating further increases in fertilizer production (Patrick Heffer, 2014).

[5] Base Year - 2010

Table 2.1: Fertilizer input per capita (1960 versus 2019)

Country	Kg/Yr. (1960)	Kg/Yr. (2019)	%
China	3.5	35.67	919.1
India	3.7	22.88	518.4
US	52.57	68.08	29.5
Russia	37.94	26.73	-29.5
Germany	58.58	33.04	-43.6
Sudan	5.33	6.81	27.8
South Africa	14.84	13.9	6.3
Pakistan	4.72	25.9	448.7

In 1950, global plastic production was 2 million tons, but by 2015, it had increased 200 x to 381 million tons per year, equating to one ton of plastic per live person. The packaging sector accounted for 42 percent of total plastic use, followed by construction at 19 percent and textile at 17 percent (Hannah Ritchie, Plastic Pollution, 2018). Based on current growth rates, plastic production is expected to double in the next 20 years. Plastics manufacture and processing are expected to account for 20% of yearly petroleum consumption and 15% of annual carbon emissions by the year 2050 (Laurent Lebreton, 2019).

Worldwide energy consumption and carbon dioxide emissions will rise by over half by 2050 due to population and economic expansion. In 2020, the fossil fuels accounted for nearly 80% of global primary energy consumption, and by 2050, they will still account for around 70%, with a bigger market. In 2050, renewable energy sources such as hydroelectricity, solar, and wind will have roughly equal prevalence in the electric

producing sector as petroleum and other liquid fuels. OPEC and non-OPEC crude oil production is expected to increase from 92.57 million barrels per day in 2020 to 125.9 million barrels per day in 2050. Natural gas production is predicted to rise by 31% from 3.85 trillion cubic meters in 2020 to 5.04 trillion cubic meters in 2050. The global coal consumption is expected to grow from 8 billion tons in 2020 to 9.2 billion tons by 2050 with India and China being the primary consumers. Electricity generation is expected to increase by 68% by 2050, from 25 trillion kWh in 2020 to 42 trillion kWh in 2050, with renewable energy accounting for 56% of worldwide generation in 2050, followed by coal (20%), natural gas (17%), and nuclear (7%) (Institue for energy reseach (IER), 2021).

The chemical industry is critical to the global production of many goods. Hydrochloric acid is used in 110 different chemical manufacturing processes, with ethylene dichloride (EDC) accounting for 37% of usage and organic compounds accounting for 61%. The sulfuric acid is used in production of phosphate fertilizer, metal leaching, steel pickling, ammonium sulfate and titanium dioxide. Nitric acid is one of the most widely used chemicals in the world, with applications including calcium ammonium nitrate, nitrobenzene, adipic acid, toluene diisocyanate (TDI), nitro-chlorobenzenes, and explosives (CEH, 2020). In the next few decades, the chemical industry is expected to grow from $3.1 trillion to $14.9 trillion. Chemical consumption per capita in the world was $456 in 2010, and it is anticipated to increase to $1,631 by 2050 (Cayuela, 2013). In the next 10 years[6], the production of High-value chemicals is expected to rise 28%,

[6] Base Year - 2020

ammonia 11% and methanol 20.69% (Tiffany Vass, 2021). A 300 % increase in global ethylene demand is predicted from 140 Mt in 2010 to 500 Mt in 2050 (Cayuela, 2013).

The United States Environmental Protection Agency (EPA) classifies ground level ozone, lead, SO_2, CO, NO_x, and particulate matter as 6 criteria pollutants. In addition, another 187 toxic pollutants are monitored throughout U.S whose exposure to public has been linked to cancer, birth defects, serious health complications as well as environmental damage. Examples of such pollutants include asbestos, chlorine, formaldehyde, hydrazine, hydrogen sulfide, hydrochloric acid, methanol, phosgene, phosphine, toluene, coke, arsenic, chromium, mercury, and cyanide compounds (EPA, 2022). The global economy is predicted to quadruple by 2050, putting further strain on natural resources and the environment. Because of operational waste, energy, and critical pollutant emissions, many industrial facilities have a substantial impact on human health and the environment. For example, Cement plants are key contributors of NO_x, SO_x, $PM_{2.5}$, PM_{10} and mercury emissions in the atmosphere. A cement plant with 1 Mt/Yr. production capacity would emit roughly 2.25 tons of SO_x, 3.29 tons of NO_x, 1.34 tons of PM, 9 kg benzene, and 0.6 kg of lead per day. Summary of the chemicals emitted in air (in kg) by the cement factory during the production of one kilogram of cement CEM I (C.Chen, 2010) are summarized in Table 2.

Table 2.2: Chemicals released per 1 kg production of cement

Chemical		Mean (kg)
Arsenic	(As)	3.2×10^{-8}
Antimony	(Sb)	1.8×10^{-9}
Cadmium	(Cd)	2.6×10^{-8}
Chromium	(Cr)	6.4×10^{-8}
Lead	(Pb)	2.2×10^{-7}
Ammonia	(NH_3)	7.2×10^{-4}
Carbon dioxide	(CO_2)	6.9×10^{-1}
NMVOC		4.5×10^{-5}

Metal production releases a wide range of hazardous atmospheric emissions. Emissions from iron and steel production include iron oxides, SO_x, aliphatic hydrocarbons, chlorides, calcium oxides, silicon oxide and magnesium oxide. Emissions from copper production include SO_x, metallic sulfates, arsenic, antimony, cadmium, lead, mercury, and zinc oxides. The aluminum metal is produced by reduction of Alumina (Al_2O_3) using the Hall-Heroult electrolytic process. Emissions from the electrolytic process include particulate fluorides, SO_x, aluminum fluoride, tetrafluoromethane, carbon dioxide, VOC, and CO, etc. Zinc extraction starts with conversion of zinc sulfide to zinc oxide using a roasting process. Purified zinc metal is recovered by an electrolysis process with zinc metal deposition on an aluminum cathode. Emission from zinc production include SO_x and metal particulates including cadmium, chromium, lead, mercury, and nickel (EPA, 2021). Table 3 and Table 4 show a summary of greenhouse gaseous emissions (GHG) from the US metal industry for FY 2020 (EPA, 2021).

Table 2.3: Metal sector – Greenhouse Gas Emissions (Mt CO2e)

	2015	2016	2017	2018	2019	2020
Number of facilities	303	304	298	306	300	294
Total emissions (CO_2e)	91.4	88.3	88.8	92.2	90.0	77.9
Emissions by greenhouse gas (CO_2e)						
Carbon Dioxide (CO_2)	88.6	86.0	87.0	89.8	87.7	75.7
Methane (CH_4)	**	**	**	**	**	**
Nitrous oxide (N_2O)	**	**	**	**	**	**
Hydrofluorocarbons (HFCs)	**	**	0.1	0.1	0.1	0.1
Perfluorocarbons (PFCs)	2.0	1.4	1.0	1.6	1.7	1.6
Sulfur hexafluoride (SF_6)	0.7	0.8	0.7	0.7	0.6	0.5

Table 2.4: 2020 emissions (CO2e) per metals industry subsector

Production Industry	Reporters	Emissions (Mt CO_2e)
Aluminum	7	3.8
Ferroalloy	9	1.6
Iron and Steel	122	62.1
Lead	11	1
Magnesium	9	0.9
Zinc	5	0.7
Other metals	131	8

Phosphorus fertilizers production starts with the chemical treatment of phosphate rock with sulfuric acid (H_2SO_4) to form phosphoric acid (H_3PO_4) which is then used in synthesis of monocalcium phosphate, monoammonium phosphate, and diammonium phosphate (Eric Walling, 2020). Emissions from phosphate fertilizer production include hydrogen fluoride (HF), SO_2, sulfur trioxide SO_3, ammonia (NH_3) and particulates (PM). A 1 Mt/year phosphate fertilizer facility is expected to emit roughly 26 tons of HF, 587 t of SO_2, 120 t of SO_3, 22 t of NH_3 and 437 t of PM (Salam, 2013). The N-fertilizers is produced using the Haber-Bosch process which uses methane from natural gas and combines it with nitrogen extracted from air to generate ammonia. The ammonia is then used in synthesis of N-fertilizers specially the urea ($CO(NH_2)_2$) and ammonium nitrate (NH_4NO_3). Each kg of NH_4NO_3 generates roughly 3.6-10.3 kg CO_2e with higher emissions due to increased N_2O emissions from the nitric acid production (Eric Walling, 2020). Urea is produced by reaction of ammonia (NH_3) and carbon dioxide (CO_2) with 1.01 t of CO_2, 0.02 t of non – CO_2, 0.26 t of GHGs and 3.54 t of CO_2, CH_4, CO and NO_x emissions released per one thousand metric tons of urea produced (Edi Munawar, 2003).

Electricity power generation from fuel sources (Coal, Petroleum, LNG, Gas, etc.) is responsible for CO_2, SO_2, NO_x, and CO emissions (Mahlia, 2002). Emissions from coal power plants are linked to asthma, cancer, heart and lung illnesses, neurological problems, acid rain, and global warming. In 2014, US coal power plants emitted 22.8 t of mercury (Hg), 3.1 Mt of SO_2, 1.5 Mt of NO_x, 197,286 t of $PM_{\leq 10}$, 41.2 t of lead, 4.7 t of cadmium, 576,185 t of CO, 22,1123 t of VOC and 38.6 t of arsenic to generate ~1,500 billion kWh of electricity (Coal and Air Pollution, 2017). Coal is predominant primary energy source in China with ½ of coal used for power industry with SO_2, NO_x, $PM_{2.5}$

accounting for 28.4%, 32.4%, and 7.3% of the total emissions in China (Gang Wang, 2020). Emissions from oil refineries include VOC (Hexane, Benzene, Toluene, etc.) leaks from equipment, storage tanks, catalytic converters, fluid cooking units, catalytic reforming units and flares, etc. The catalytic cracking units vent a range of pollutants including PM, SO_2, NO_x, CO, and NH_3. A summary of few emissions from a refinery facility is summarized in Table 5 (RTI International, 2015).

Table 2.5: Emission factors of various compounds for Boilers and Process Heaters firing

Compound	Natural Gas (lb/MMBtu[7])	Crude Oil (lb/MMBtu)	Residential Fuel (lb/MMBtu)	Distillate Fuel (lb/MMBtu)
Arsenic	2.0×10^{-7}	6.7×10^{-6}	8.8×10^{-6}	4.0×10^{-6}
Benzene	2.1×10^{-6}	4.1×10^{-6}	1.4×10^{-6}	**
Cadmium	1.1×10^{-6}	2.2×10^{-6}	2.7×10^{-6}	3.0×10^{-6}
Chromium	1.4×10^{-6}	8.7×10^{-6}	5.6×10^{-6}	3.0×10^{-6}
Lead	4.9×10^{-7}	1.9×10^{-6}	1.0×10^{-5}	9.0×10^{-6}
Mercury	2.5×10^{-7}	1.0×10^{-5}	7.5×10^{-7}	3.0×10^{-6}
Toluene	3.3×10^{-6}	3.5×10^{-5}	4.1×10^{-5}	**
Hydrogen Sulfide	8.5×10^{-5}	**	**	**
Cobalt	8.2×10^{-8}	**	4.0×10^{-5}	**

[7] lb/MMBtu – pounds per million British thermal unit

2.2 Effects of emissions on health

Toxicological and epidemiological studies correlate air pollution to a wide range of adverse health effects, ranging from mortality to sub clinical respiratory symptoms. For example, SO_2 exposure can result in respiratory tract inflammation, mucus secretion, chromonic bronchitis and aggravation of asthma. A healthy individual can experience bronchoconstriction at 1.6 ppm of SO_2, development of throat irritation at 8-12 ppm level, and immediate cough and eye irritation at 20 ppm exposure (Rahila Rahman Khan, 2014). Fuel combustion and motor vehicle emissions are one of the primary sources of NO_2. Long term exposure to NO_2 is associated with cardiovascular and respiratory mortality. NO_2 increases levels of oxidative free radicals, inflammation, and vascular oxidative stress reaction. Radical oxygen species can contribute to endothelial dysfunction, monocyte activation and certain pro-atherosclerotic changes in lipoproteins resulting in plaque formation aggravating diseases, and increased mortality (Shiwen Huang, 2021). $PM_{2.5}$ emissions have been associated of various respiratory and cardiovascular ailments including breathing disorders, asthma, chronic bronchitis, arrhythmia, heart disease and cardiopulmonary (Li Li, 2018).

Arsenic emissions are generated during fly ash disposal, smelting of sulfide ores, coal combustion, pigment production, pesticide manufacturing, copper refining and hardening of metal alloys. Upon inhalation arsenic targets multiple organs including liver, kidneys, lungs, lymphatic system, and skin. Long term exposure of arsenic can damage the nervous system, blood circulation, and increase the risk of skin and liver cancer (Vimal Chandra Pandeya, 2011). Asbestos exposure symptoms include dyspnea, interstitial fibrosis, restricted pulmonary function, finger clubbing and eye irritation with long term

exposure linked to lung cancer (NIOSH, 2007). The exposure symptoms of CO include headache, tachypnea, nausea, lassitude, dizziness, confusion, angina, and syncope (NIOSH, 2007). Chromium emissions are generated during chromate ore refining, coal and oil combustion, and production of ferrochromium, steel, and cement, etc. The chromium reactivity to environment and biology depends strongly on its oxidation state which ranges between -2, +6. Exposure to chrome oxide (+3) can result in kidney and liver damage, leukocytosis, skin ulcer, conjunctivitis, and lung cancer. Chromium chloride (+2) exposure can result in eye and skin burn and in extreme cases lung cancer (EPA, Locating and estimating emissions from sources of chromium , 1984). Coke is produced by carbonation of bituminous coal which generates a wide range of emissions including polycyclic aromatic hydrocarbons, benzene, b-naphthylamine, NO_x, SO_2, arsenic, cadmium, chromium, lead, and nickel. Long term exposure to coke emissions can result in skin, lung, kidney, and bladder cancer (NIOSH, 2007), (NTP, 2018). Cyanide compounds are used in the production of adiponitrile, acetone cyanohydrin, cyanic chloride, carbon black, carbon fiber and refining of petroleum and gold. Exposure to cyanide can yield in eye irritation, miosis, delayed pulmonary edema, dizziness, vomiting, irregular heartbeat, and skin irritation. Target organs of cyanide derivatives include respiratory, cardiovascular, and central nervous system (NIOSH, 2007), (Midwest Research Institute, 1993). Sources of hydrogen sulfide emissions include petroleum refineries, coke ovens, tanneries, natural gas, and petrochemical processing plants. Exposure to hydrogen sulfide emissions results in irritated eyes, apnea, lacrimation, corneal vesiculation, lassitude, gastrointestinal disturbances, and convulsions (NIOSH, 2007), (ATSDR, 2016).

2.3 Emissions control

To protect the environment, several regions have established pollution control standards to reduce industrial and mobility emissions. For example, in 1998 India's Central Pollution Control Board issued a 2nd print on emissions threshold for various industrial pollutants. This established a limit on calcium carbide PM emissions from arc furnace operations at 150 mg/Nm^2, ban on SO_2/SO_3 release from copper, zinc and lead smelting operations and channeling of off-gases for H_2SO_4 manufacturing, restricted carbon based PM emissions from newly constructed plants to 150 mg/Nm^2, introduced limit on fluoride emissions from phosphate fertilizer production at 25 mg/Nm^2, limit on fluoride emissions from aluminum smelting operations at 1 kg/ ton of aluminum processed, and limit on SO_x emissions from oil refinery catalytic cracker at 2.5 kg/ton of feed (Parivesh Bhawan, 1998). In US, the standard for NO_x emissions from cement and concrete product manufacturing using preheater kiln has been set at 2.3lb/ton, the NO_x emissions from Iron and Steel oxygen blast furnace set at 0.07 lb./ton, and NO_x emissions from flat glass manufacturing furnace set at 9.2 lb./ton (EPA, 2022). In terms of air quality, the national standard for NO_2 has been set at 100 ppb[8], SO_2 at 75 ppb, CO at 9 ppm, ozone at 0.075 ppm, lead at 0.15 ug/m^3, PM_{10} at 150 ug/m^3, and $PM_{2.5}$ at 12 ug/m^3 (EPA, 2021). In EU, the hourly air quality standard for NO_2 is set at 200 ug/m^3, SO_2 at 350 ug/m^3, CO at 4 mg/m^3, ozone at 120 ug/m^3, lead at 0.5 ug/m^3, PM_{10} at 50 ug/m^3, and $PM_{2.5}$ at 15 ug/m^3 (Agency, 2021).

Currently in various parts of the globe, the coal power plants with generational capacity of $\leq$ 100 MWe are also being phased out, while units with 100-300 MWe capacity are

[8] ppb – Part Per Billion

being modernized. High-capacity power plants operating at super critical temperatures and pressures, ensure efficient burning of coal derivatives. Several technologies are being developed to reduce the negative environmental impacts of the coal fuel cycle, including (1) removing sulfur and nitrogen from coal before it is burned, (2) in-furnace measures to prevent pollution during combustion, and (3) removing pollutants from flue gases using "end of pipe" methods prior to emissions. The quantity of NO_x generated during a combustion process depends on fuel type, combustion conditions, air ratio and flame type. Post treatment of NO_x using selective catalytic reduction (SCR) operating between 300-400 °C reduces 90% of NO_x emissions. Other technologies available for NO_x controls are summarized in Table.6.

Table 2.6: Nitrogen oxides emission control techniques

Control technique	NO reduction potential (%)
Overfire air (OFA)	20–30
Low-NO*x* burners (LNB)	35–55
LNB+OFA	40–60
Reburn	50–60
Selective non-catalytic reduction (SNCR)	30–60
Selective catalytic reduction (SCR)	75–85
LNB with SCR	50–80
LNB with OFA and SCR	85–95

A variety of technologies are available to reduce SO_x emissions. The precombustion sulfur removal from coal can reduce SO_x emissions by 30-50%, application of dry

sorbent injection (DSI) can reduce SO_x emissions by 50%, wet flue gas desulfurization (FGD) by 80-90%, and chemical and biological cleaning by 90%. Particulate matter (PM) emissions can be reduced by the application of wet scrubber by 95-99%, cyclone by 90-95%, electrostatic precipitator (ESP) by 99%, and filters by ~ 99.9%. Mercury emissions can be reduced by using oxidizing agents in flue gas scrubbers, which convert gaseous mercury into sulfate byproducts (Franco, 2009).

2.4 Mobile emissions

The emission from vehicular traffic includes NO_x, SO_x, hydrocarbons (HC), particulate matter ($PM_{2.5}$, PM_{10}), volatile organic compounds (VOC), and metallic compounds such as Cobalt, Carbon, Arsenic, Chromium, Cadmium, Lead and Nickel. Heavy-duty diesel trucks, which transport a major portion of goods, also generate significant quantities of NO_x and smog. Communities near freight hubs, such as ports, railyards, and distribution centers, experience elevated levels of diesel-related air pollution resulting in various health complications (Ji Luo, 2022). In China, 80% of CO and over 70% of hydrocarbon emissions are from passenger cars while over 80% of NO_x and over 90% of PM emissions are from trucks. GHG emissions are a major contributor to global warming while NO_x and PM emissions result in severe haze weather and acid rain. VOC emissions contribute to the formation of ground-level ozone, photochemical smog, and secondary organic aerosol (SOA), that are carcinogenic, mutagenic, and teratogenic. Emissions testing on different vehicles detected 57 different VOC including Ethylene, Alkyne ethyne, Ethane, Propylene, Isobutane, 1-Butene, Butane, 1,3-Butadiene, trans-2-Butene, Benzene, Heptane, Toluene, Styrene, Undecane, and Cumene (Wang, 2013). Emissions control techniques for mobile sources include substituting fuel oil with green hydrogen

(Junming Lao, 2022), selective catalytic reduction (SCR) (Kröcher, 2018), diesel particulate filters (DPFs) and use of lower sulfur – diesel fuel (D Durbin, 2003). A summary of average emissions rate from heavy duty trucks are summarized in Table 7 (Quality, 2008).

Table 2.7: Average Heavy-Duty Truck Emission Rates by GVW[ref] Class (g/Mile)

Pollutant	Fuel	Hb	III	IV	V	VI	VII	VIIIa	VIIIb
VOC	Petroleum	1.353	1.667	4.234	2.632	2.477	2.857	3.628	~
	Diesel	0.189	0.201	0.262	0.274	0.365	0.453	0.455	0.545
CO	Petroleum	11.22	15.81	33.86	19.58	18.130	23.13	28.560	~
	Diesel	0.839	0.908	1.163	1.189	1.367	1.719	2.395	3.109
NO_x	Petroleum	2.734	2.920	4.133	3.735	3.650	4.199	4.892	~
	Diesel	3.088	3.298	4.352	4.548	5.990	7.471	9.191	10.99
$PM_{2.5}$	Petroleum	0.043	0.045	0.058	0.046	0.045	0.046	0.049	~
	Diesel	0.091	0.073	0.089	0.079	0.172	0.177	0.215	0.238
PM_{10}	Petroleum	0.049	0.051	0.074	0.055	0.054	0.056	0.061	~
	Diesel	0.099	0.079	0.096	0.088	0.186	0.192	0.233	0.259

[ref] Heavy-Duty Vehicle Classifications GRW (Gross Vehicle Weight Rating)

IIb:	8,501-10,000 lb	… full-size pick-up, large passenger vans
III:	10,001-14,000 lb	… panel trucks, enclosed delivery trucks
IV:	14,001-16,000 lb	… city delivery and rental trucks
V:	16,001-19,500 lb	… bucket utility and large walk-in trucks
VI:	19,501-26,000 lb	… rack trucks, single axle vans
VII:	26,001-33,000 lb	… tow, garbage collections trucks
VIIIa:	33,001-60,000 lb	… long haul semi-tractor trailer rigs
VIIIb:	> 60,000 lb	. double long-haul semi-tractor trailer rigs

2.5 Atmospheric emissions modeling

Aside from regulatory and technical controls, attempts are being undertaken to incorporate pollutant dispersion models to analyze the impact of various sources of emissions on the local environment and devise mitigation measures. Pollutant dispersion models use mathematical and numerical techniques to simulate the physical and chemical processes that affect air pollutants. A dispersion model can forecast concentrations at specific receptor locations based on emissions and atmospheric inputs. The US Environmental Protection Agency offers a list of dispersion models that is divided into Preferred, Alternative, and Screening Tools categories. The preferred category includes AERMOD modeling system, CTDMPLUS, and OCD. The alternative category includes ADAM, ADMS, AFTOX, ASPEN, BLP, CALPUFF, HGSYSTEM, ISC3, OZIPR, SDM, and SLAB, etc. The AERMOD system is a steady-state plume model with air dispersion based on planetary boundary layer turbulence structure and scaling concepts, with consideration of both surface and elevated sources, as well as simple and complex topography. The CALPUFF system, which was part of the EPA's recommended model until 2017, simulates the impacts of time and space variable meteorological circumstances on pollution transport, transformation, and removal using a multi-layer, multi-species non-steady-state puff dispersion model (EPA, 2022).

The Gaussian plume dispersion Equation (2.1) is fundamental in modeling of emissions from point, line, and area sources.

$$C(x,y,z) = \frac{Q}{2\pi u \sigma_y \sigma_z} exp\left[\frac{-(y-y')^2}{2\sigma_y^2}\right]\left\{exp\left[\frac{-(z-H)^2}{2\sigma_z^2}\right] + exp\left[\frac{-(z+H)^2}{2\sigma_z^2}\right]\right\} \quad (2.1)$$

(Wm. J. Veigele, 1978)

Gaussian plume dispersion model has been used by Enkeleide Lushi, John M. Stockie in modelling emission from lead-zinc smelters located in Trail, British Columbia (Enkeleida Lushi, 2010), Khandakar Md Habib Al Razi and Moritomi Hiroshi used the Gaussian based model (METI-LIS) for simulating atmospheric dispersion of mercury from coal fired power plant (Al Razi, 2012), A.D. Bhanarkar and others used the Gaussian based ISCST3 model for assessment of SO_2 and NO_2 contribution from different steel mills in Jamshedpur (A.D. Bhanarkar, 2005), José I.Huertas and others used the Gaussian based ISC3/AERMOD programs to model dispersion of total suspended particulate (TSP) from multiple open pit coal mines in northern Colombia (José I. Huertas, 2012), Yaroslav Bezyk and others used the CALPUFF dispersion model to estimate urban ecosystem CO_2 flux (Yaroslav Bezyk, 2021), and Hui Xu and others used the CALPUFF-Hg dispersion model to analyze mercury deposition in the central Pearl River Delta, China (Hui Xu, 2019).

Despite the development of legislation, technologies, and models relating to the management of various pollutants' emissions, global achievements have been inconsistent. Between 1980 and 2020, ambient NO_2 levels in the US reduced by 64%, SO_2 by 94%, ozone by 33%, CO by 81%, and lead by 86%. The PM concentration also reduced 26% between 1990-2020 (EPA, National Air Quality: Status and Trends of Key Air Pollutants, 2021). However even with these reductions, the premature deaths in US from air pollution are estimated to be at 53,000 (Mailloux, 2022). In 2018, the European Environment Agency (EEA) estimated that even with the progress on emissions control, the air pollution caused almost 0.5 M premature deaths in Europe per year (European Environment Agency, 2018). A 2017 study by Health Effects Institute (HEI) estimated

that in India premature deaths from air pollution were at 1.07 M, while in China this number stood at 1.10 M (Venkatachalam, 2017). With identical GDPs, how come China's premature mortality significantly outweigh those in the US, despite general agreement that industrial and mobile emissions are harmful to the environment?

2.6 Production

The systematic design, guidance, and control of processes that transform inputs into services and products for both internal and external clients is defined as "operations management." A firm needs to focus on 10 decision areas to maximize operational efficiency and built strategic capabilities (Krajewski, 2022):

1	Design of goods and services	2	Quality management
3	Process and capacity design	4	Location strategy for stores
5	Layout design and strategy	6	Job design and human resources
7	Supply chain management	8	Inventory management
9	Scheduling	10	Maintenance

A production process converts low-value raw materials into high-value final goods. A production function is a mathematical statement that describes how inputs (land, labor, capital, and raw materials including crude oil, hematite, chalcocite, and natural gas etc.) and outputs (commodities including gasoline, steel, copper, fertilizers, and polymers, etc.) are related in a systematic way. Types of production function include Leontief, Cobb-Douglas, Constant Elasticity of Substitution (CES), Trans-log, and Normalized Indirect (Silberberg, 1990). The key properties of a production function include (Reynès, 2019):

1. a continuous and twice differentiable function: $Q = Q(X_1, X_2, \dots, X_i, \dots, X_n)$ where X_i is a quantity input $i \in [1,2, \dots, n]$ used to produce output Q.
2. homogenous of degree 1 (constant return to scales)
3. increasing in inputs: $Q'X_i = \frac{\partial Q}{\partial X_i} > 0$ (increase in inputs, increases output)
4. strictly concavity (law of diminishing returns)

$$Q^n(X_i) = \frac{\partial^2 Q}{(\partial X_i)^2} < 0 \; and \; \frac{\partial (Q'(X_i))}{\partial X_j} = \frac{\partial^2 Q}{\partial X_i \partial X_j} > 0 \; for \; i \neq j \text{ where } i, j \in [1,2, \dots, n] \qquad (2.2)$$

Leontief production function → $Y = \; Y_o \min \left(\frac{x_1}{x_{10}}, \frac{x_2}{x_{20}}, \dots, \frac{x_n}{x_{n0}}\right)$ (2.3) where x_i are inputs, x_{i0} are the constant per unit input requirements, Y is output, and Y_o is the scale factor having the dimension of *Y*. The Leontief production function applications can be traced in Liebig function, queuing models, job shop scheduling, and liner supply chain, etc. (A. Mustafin, 2018).

Cobb-Douglas production function: $Y = \; A \prod_{i=1}^{n} x_i^{\varepsilon_i}$ (2.4) where $x = (x_1, x_2, \dots, x_n), x_i > 0, \; i = 1,2,3 \dots n$, is inputs, A is the technology factor and ε_i are exponents with range $0 < \varepsilon_i < 1$.

CES production function : $Y = \gamma(\sum_{i=1}^{n} \delta_i z_i^{\frac{\rho}{\rho_i}})^{\frac{-\upsilon}{\rho}}, z_i = \sum_{i=1}^{n} \delta_{j,i} \, x_{j,i}^{-\rho_i} \forall i = 1, \dots, n$ (2.5). Y is the output quantity, and $\gamma, \delta, \rho, \upsilon$ are parameters, where $\gamma \in (0, \infty)$ determines the productivity, $\delta \in [0,1]$ determines optimal distribution of the inputs, $\rho \in [-1,0) \cup (0, \infty)$ determines the constant elasticity of substitution, which is $\sigma = \frac{1}{1+\rho}, and \; \upsilon \in (0, \infty)$ refers to elasticity of scale. The inputs are subdivided into n groups, where n_i donates the number of inputs in the ith group and $x_{j,i}$ donates the jth input in the ith

group. Specification requires the normalizations $\sum_{i=1}^{n} \delta_i = 1$ and $\sum_{j=1}^{n_i} \delta_{j,i} = 1 \; \forall \; i = 1, \ldots, n$. Application of CES production can be found in areas of economic growth, international trade, and energy economics (Henningsen, 2012).

Trans log production function:

$$\ln \; Y = \ln A_{\alpha_i, \beta_{ij}} + \sum_{i=1}^{n} \alpha_i \ln X_i + \left(\frac{1}{2}\right) \sum_{i=1}^{n} \sum_{j=1}^{n} \beta_{ij} \ln X_i \ln \; X_j \qquad (2.6)$$

where ln is natural algorithm, Y is output, X_i is factors of input, A, α, β are parameters (Pavelescu, 2014).

A firm's *profit* π corresponding to a production function f can be written as:

$$\pi = pf(x_1, \ldots \; x_n) - \sum_{i=1}^{n} w_i x_i \qquad (2.7)$$

where x_i is quantity of each input factor, w_i cost of each input, p is sales price of product. The π^* can be obtained by solving for $x_1, \ldots \; x_n$ by solving for derivatives $\frac{d\pi}{dx_1}, \ldots, \frac{d\pi}{dx_n}$ simultaneously.

A firm's *cost* C to achieve an arbitrary level of output y^o can be written as:

$$C = \sum_{i=1}^{n} w_i x_i \text{, subject to } f(x_1, \ldots, x_n) = y^0 \qquad (2.8)$$

The minimum cost C^* corresponding to y^o for inputs $x_1, \ldots \; x_n$ can be obtained by applying Lagrangian function on Eq. (2.8):

$$\mathcal{L} = \sum_{i=1}^{n} w_i x_i + \; \lambda[\, y^0 - f(x_1, \ldots, x_n)] \qquad (2.9)$$

The equilibrium price p of a product or intermediates moves directly as response to change in demand and supply quantities: $\frac{dp}{dt} = g\big(D(p, M) - S(p)\big)$ (2.10) where $g' > 0$, M is money income, p is product pricing, D is quantity demanded, and S is quantity supplied

(Silberberg, 1990). The production capacity of a firm is subject to supply and price of land, labor, capital, and intermediates. The following are details of each of these inputs:

Land has a limited supply compared to other commercial commodities, and each piece of land has a fixed location, influencing its price and the value of surrounding parcels. Various theories and models exist to explain the land price in relation to its usage. For example, in a completely free market system of competition beyond monopoly, Ricardian popular theory on "economic rent" describes land price as a function of its productivity. It invariably means that every component of productivity, such as capital, labor, technical advancement, or a favorable environment, that affects land output can be reflected in the selling land value or land rent (Uzair Ali, 2021). Von Thünen model described land cost as a function of its location, utilization, and transportation costs. Randall and Castle described land price in relation to other inputs as well as institutional factors other than land itself (Hubacek, 2002). The bid rent theory based on work of Alonso, Muth describes relationship between urban land use and urban land value. Households and businesses make a trade-off between land price, transportation costs, and the amount of land they use. As a result, the land price curve is convex, with the highest prices near the city center (Eric Koomen, 2002). The Transit Oriented Development (TOD) concept uses regional transit plans to achieve economic growth through the distribution of firms and employment locations, land development, and land prices by altering the level of accessibility between locations. Transportation has the potential to increase employment or firm density by improving access to labor and connecting businesses. Transportation access affects firm costs of doing business because firms require access to materials, workers, customers, and information.

A firm` location decision is influenced by a variety of factors, including transportation costs for inputs and outputs, agglomeration economics, and differences in factor costs, which include taxes, labor costs, political factors, and amenities that influence quality of life. Agglomeration may benefit firms through the following mechanisms (Hiroyuki Iseki, 2018):

1. sharing consumer-side service, retail, and entertainment amenities "increasing the city size or the CBD size enabling the provision of urban amenities that are attractive to households." (by enabling city growth and densification)
2. sharing/matching pools of labor (enabling better matching of workers to jobs; less turnover)
3. matching firms in disaggregated production processes (enabling vertical disaggregation and supplier specialization)
4. learning innovative practices (i.e., knowledge spillovers) (skilled labor learning from each other; quick dissemination of innovative practices)
5. sharing production inputs
6. sharing transport infrastructure

Labor input is critical in production. Firms adjust the quantities of capital and labor they use when they expand or contract in response to changes in prices and technology (Tang, 2022). The labor input is measured as number of people, or number of hours worked. The average product of labor, $(\frac{Y}{L})$ is defined as the ratio of output to labor input. The marginal product of labor is defined as $\frac{\partial Y}{\partial L}$. Firms hire workers until the marginal product of additional unit of labor equals the wage. Worker's productivity is greatly impacted by

technology factor, countries with a high technology factor also have more capital per worker (Cedergren, 2012).

A worker's preference over consumption (c_t) and work hours (h_t) can be defined by a utility function $U(c_t, h_t)$. The utility maximization problem for a given worker can be defined as:

$$\mathbb{E}\sum_{t=0}^{\infty} \beta^t \, U(c_t, h_t),$$

$$s.t: c_t + k_{t+1} = (1-\tau)w_t h_t + (1 - r_t - \delta)k_t + T_t \tag{2.11}$$

where k_t is capital, τ is the marginal labor income tax rate, w_t is the wage rate, r_t is the rental price of capital, δ is the depreciation rate of capital, and T_t is the lump sum transfers. The 1st-order optimality conditions for Eq 2.11 are:

$$U_c(c_t, h_t) = \beta(1 + r_{t+1} - \delta)U_c(c_{t+1}, h_{t+1}) \text{ and } -\frac{U_{h(c,h)}}{U_c(c,h)} = w_t(1-\tau) \tag{2.12}$$

A worker chooses a consumption level that equalizes the current period's marginal utility of consumption to the discounted marginal utility of consumption of tomorrow. Units of labor hours supplied by a given worker is such that the marginal utility rate between consumption and labor approximates the wage rate. The wage rate supplied by a given firm employing Cobb-Douglas production function equates to:

$$w_t = (1-\alpha)\left(\frac{k_t}{h_t}\right)^{\alpha} \tag{2.13}$$

where α represents the share of capital (Charles Gottlieb, 2021). A reservation wage is defined implicitly as an optimal stopping rule in the job search behavior of the

unemployed. Simply put the 'reservation wage' in the minimum wage an unemployed worker is willing to accept for a unit of labor. Reservation wages may adjust positively in response to increases in observed worker wages or negatively in response to a decrease in the job offer arrival rate. Mathematically reservation wage can be approximated using following Equation:

$$w^{res} = b + \frac{\alpha}{\rho}\int_{w^{res}}^{\bar{w}}[1 - F(w)]dF(w) \quad (2.14)$$

where b is donates money received while not working, ρ is time discounting factor, α is the job arrival rate, and $F(w)$ is the observed wage distribution (Alexandra Fedorets, 2021). The work force (occupied work force vs unemployed) evolution in a region can be modelled using the following Equation:

$$\frac{dL}{dt} = \gamma U - (\sigma + \mu)L, \frac{dU}{dt} = \rho\left(1 - \frac{L_\tau + U_\tau}{N_c}\right)L_\tau + \sigma L - (\mu + \gamma)U \quad (2.15)$$

The initial conditions for Eq.2.15 are:

$$L(0) > 0, U(0) > 0, \big(L(\theta), U(\theta)\big) = \big(\varphi_1(\theta), \varphi_2(\theta)\big), \forall\theta \in [-\tau, 0] \quad (2.16)$$

where $\varphi_i \in C([-\tau, 0], \mathbb{R}^+), i = 1,2$

where L is occupied labor force, U is number of unemployed, γ is unemployment rate, σ is rate of job loss, μ is mortality rate, ρ is maximum population growth rate, N_c is the carrying capacity, and τ is time lag needed to contribute to the reproduction process of a new individual looking for work (Sanaa ElFadily, 2019).

Capital inputs are stock of physical assets utilized in production of goods for current and future production. Examples of capital inputs include machinery, infrastructure,

equipment, tools, and transportation assets, etc. Capital assets depreciate in geometric or in exponential terms. A firm's wealth maximization objective concerning capital can be written as:

$$\max \int_0^{\infty} [R\big(x(t)\big) - c\big(u(t)\big)]e^{-rt}dt,$$

$$\text{subject to: } x'(t) = u(t) - bx(t), x(0) = x_0 > 0 \qquad (2.17)$$

where $x(t)$ is stock of capital at time t, $R(x)$ is stream of rents, $b(x)$ is the capital depreciation rate (linear), $c(u)$ is the cost of investing new capital, and r is the interest rate of capital. The state Equation $u(t) - bx(t)$ states that the rate of change in capital stock is equal the rate of acquisition of new capital minus the depreciation at time t. The control variable in the wealth maximization Equation is the rate of investment (Silberberg, The structure of economics: A mathemetical analysis, 1990). The System of National Accounts (SNA) distinguishes capital between "productive capital" and "wealth capital stock". The SNA defines wealth depreciation as "the reduction in the value of the fixed assets used in production during the accounting period resulting from physical deterioration, normal obsolescence or normal accidental damage". Productive depreciation refers to the *decay* of the productive capacity of fixed assets in the production process. In terms of capital, the assets can be distinguished between productive and non-productive investments. Within the industrial and manufacturing sector, the non-productive part of fixed assets are investments that are not transformed into fixed assets. Examples include residential building, schools, hospital, and other welfare structures (Lili Wang, 2012).

The *q*-ratio is the market value of a company divided by the cost of replacing its assets. The *market value* of the company is the discounted expected cash flows generated by the firm's assets. Given that the replacement cost of assets is expressed in present value terms, there is an implied positive relationship between a firm's Tobin's q ratio and its future cash flows. The future performance of a firm is dependent on the investment made in the current period (Liang Fu, 2016). The present value of discounted future cash flows up to time T is given by:

$$P = \int_0^T [FV(t)]e^{-rt}dt$$

where $FV(t)$ is expected cash inflow at time t and r is the interest rate. The contribution of production inputs like land, labor and capital varies greatly depending on the industry type. For example, application of Cobb-Douglas production function to industries based in West Sumatra, provided following coefficient estimates of labor and capital (See Table.8) (Ahfazh Fauzy Nurunnajib, 2018).

Table 2.8: Cobb Douglas production function estimates for various industries

Plastic, rubber	$Y = 4.0357\ L^{0.0609}K^{0.7815}$
Publishing, printing	$Y = 1.3185\ L^{0.0863}K^{0.9597}$
Textile	$Y = 1.5132\ L^{0.0715}K^{0.9303}$
Nonmetal mining	$Y = 0.1537\ L^{0.7430}K^{0.5954}$
Beverage	$Y = 2.8305\ L^{0.2752}K^{0.5744}$

In addition to land, labor, and capital, firms typically require low-value finished outputs (Tier 1) from other industries as inputs, that are then transformed into high-value outputs (Tier 2) for either direct consumption or to serve as input feeds for the next hierarchy (Tier 3)

of production. For example, the production of Lithium Carbonate from Spodumene ore requires a variety of inputs including natural gas, sulfuric acid, lime, hydrogen peroxide and sodium carbonate. The finished product is then used in lithium-ion batteries, chemicals, pharmaceuticals, and metallurgical industries (Pratima Meshram, 2014). An *input-output* (IO) analysis determines the flow of production from one sector of the economy to the next, all the way to final consumption (Hewings, 1985). Table.9 summarizes a matrix of technical coefficients derived from a highly aggregated IO table for seven U.S. sectors. The column of the matrix describes the inputs required by a specific sector to produce a unit of output. For example, the technical coefficient (a_{24} – 0.00756) identifies that the manufacturing sector purchased mining products worth 0.0756 to produce 1$ worth of output (A. Mustafin, 2018).

Table 2.9: US technical coefficients for various industries (Year - 2006)

			Producers as Consumers						
			1	2	3	4	5	6	7
Producers	1	Agriculture	0.2403	0.0000	0.0014	0.0345	0.0001	0.0018	0.0007
	2	Mining	0.0028	0.1307	0.0079	0.0756	0.031	0.0004	0.0066
	3	Construction	0.0035	0.0002	0.001	0.0019	0.0039	0.0072	0.0242
	4	Manufacturing	0.1858	0.0959	0.2673	0.3311	0.0581	0.0558	0.1027
	5	Transport, util	0.0774	0.0379	0.1063	0.1003	0.0698	0.0329	0.0439
	6	Services	0.0875	0.1298	0.1262	0.1239	0.0698	0.2889	0.2029
	7	Others	0.0102	0.0096	0.0095	0.0233	0.0223	0.0192	0.0225

The basic Equation for input-output analysis is: $y = (1 - A)x$ (2.18), where y is an $n \times 1$ vector of final deliveries, x is an $n \times 1$ vector of sectoral outputs, and A is the $n \times n$ matrix of coefficients of inputs per unit of output (Helga Weisz, 2006).

Given the high level of interdependence among firms, a *seamless* supply chain is paramount to a working economy since any form of disruption can have a cascading impact on the productivity of dependent firms. For example, the 2021-2022 global chip shortage due to plant closures in South-East Asia directly impacted several manufacturing sectors in the U.S including equipment, automobile, and telecommunications (Ellyatt, 2021). The 2022 conflict between Russia and Ukraine impacted global supply of various commodities including crude oil, natural gas, wheat, titanium, nickel, platinum, palladium, aluminum, uranium, ammonia, urea, potash, and diamonds. In consequence, global energy and metal skyrocketed, food prices in Africa increased by 34% whereas price of wheat prices soared by 64%. The disruption in titanium supply impacted the global aerospace industry, resulting in formation of arbitrary delivery timelines of aircrafts (Lazenby, 2022). Supply chain disruptions due to COVID-19 pandemic and Russia-Ukraine conflict is estimated to cause European economies up to €920 billion in GDP in FY 2023 (SCMR Staff, 2022).

2.7 Consumption

A supply chain is defined as the flow of material, information, and services, typically crossing several different organizations that are involved in producing and delivering a product or service to an end user. Consumer choice theory investigates the equilibrium relationship between an individual's preferences and expenditures such *to maximize one's utility under a budget constraint*. Mathematically this relationship can be written as:

$$\max U(x_1, x_2, \dots, x_n)$$

$$\text{s.t } \sum p_i x_i = M \tag{2.19}$$

where $x_1, \dots, x_n$ represents a basket of goods a customer consumes, $U(x_1, \dots, x_n)$ is the utility derived from consuming the commodities, p_i is the unit price of commodity x_i, and M is the total budget. A utility function is a cumulation of an individual's preferences regarding consumption of various bungles of goods. The important properties of a differentiable utility function U are:

1. More is preferred to less – if $x_1, \dots, x_n$ are goods consumed, the marginal utility of any good x_i is positive, or $U_i = \frac{\partial U}{\partial x_i} > 0$.
2. Substitution $\frac{\partial x_i}{\partial x_j} = \frac{-U_j}{U_i} < 0$
3. The marginal value of a good decreases as more of that good is consumed - $\left(\frac{\partial^2 x_j}{\partial x_i^2}\right) U^0 > 0 \qquad i, j = 1, \dots, n, i \neq j$

Application of Lagrange function on Equation.2.19 yields following Marshallian demand Equation (Silberberg, The structure of economics: A mathemetical analysis, 1990):

$$\mathcal{L} = U(x_1, x_2, \dots, x_n) + \lambda(M - \sum p_i x_i) \qquad (2.20)$$

The Marshallian demand theory assumes that the individual assigns a different utility function to each good it consumes, and that the marginal utility of money is constant. The equilibrium condition for consumption of good x_i is:

$$\frac{\partial U}{\partial x_i} = \frac{\partial U}{\partial M}\frac{\partial p_i}{\partial x_i} \qquad (2.21)$$

The maximum amount a consumer would be willing to pay for an additional unit of x_i will be a quantity such that the utility that is lost in the giving of this amount of money $\frac{\partial U}{\partial M}\frac{\partial p_i}{\partial x_i}$ will be equal to the utility that will be received instead $\frac{\partial U}{\partial x_i}$ (Zaratiegui, 2002).

An alternative to Marshallian demand is the 'Hicksian' demand theory proposed by Sir John R. Hicks. A Hicksian demand of a good is determined by its price, price of other goods and a fixed level of utility. Mathematically:

$$\min C = \sum_{i=1}^{n} p_i x_i$$

$$\text{s.t } U(x_1, \dots, x_n) = U^0 \tag{2.22}$$

Equation 2.22 provides us the minimum cost an individual needs to maintain a fixed level of utility U^0. The Hicksian demand is also known as "compensated demand" because it indicates how much an individual must be compensated in order to maintain the same level of utility. The amount of each good x_i to satisfy U^0 can be obtained by the application of Lagrangian mechanism on Eq 2.22.

$$\mathcal{L} = \sum p_i x_i + \lambda[U^0 - U(x_1, x_2, \dots, x_n)] \tag{2.23}$$

The Slutsky Equation is another important contribution to consumption theory; it relates the rate of change in consumption with respect to price changes when income is held constant to the corresponding change when real income, or utility, is held constant. Mathematically for n different goods, the relationship is as follows:

$$\frac{\partial x_i^M}{\partial p_j} = \frac{\partial x_i^U}{\partial p_j} - x_j^M \frac{\partial x_i^M}{\partial M} \quad i, j = 1, \dots, n \tag{2.24}$$

The Slutsky Equation demonstrates that a utility-maximizing consumer's response to a change in good price can be divided into a pure substitution effect and a pure income effect. When the price of a good p_j rises, the consumer substitutes away from it, whereas when the price falls, the consumer can achieve a certain level of consumption that was previously outside their former budget constraint – a decrease in price produces a similar effect to an increase in income. The negative sign in $-x_j^M \frac{\partial x_i^M}{\partial M}$ indicates that the applied change in income is in the opposite direction to the price change. The x_j^M multiplier implies the relative intensity of a good getting consumed and effect of its price change on an individual's utility.

A utility function can have an additive or multiplicate behavior. An additive utility function for n goods can be written as:

$$U(x_1, \dots, x_n) = U_1(x_1) + U_2(x_2) \dots + U_n(x_n) \quad (2.25)$$

The additive utility function is appropriate when analyzing utility of *independent* goods. The marginal utility derived from consuming good x_i is a function of x_i only and is unaffected by changes in consuming some other good x_j, $\frac{\partial Ui'(x_i)}{\partial x_j} = 0$. The strong separability imposes various restrictions on the observable behavior. For example, either all goods are noninferior and net substitutes for each other or all goods, but one is inferior, and the inferior good is a net substitute for the other goods, while the others are all net complements to each other. The multiplicate utility function concerning consumption of n goods can be written as: $V = U_1(x_1) \times U_2(x_2) \dots \times U_n(x_n)$. (2.26)
The multiplicative utility function is appropriate when analyzing consumption of substitute goods.

In consumer theory, several functions have been established for describing the empirical demand of customers. For example, the Linear Expenditure System (LES) describes consumers first buying subsistence quantities of goods, and then dividing the remaining expenditure among the goods in fixed proportions. A LES function on two goods can be written as:

$$U(x_1, x_2) = \alpha_1 \log(x_1 - \beta_1) + \alpha_2 \log(x_2 - \beta_2) \quad (2.27)$$

s.t $x_i - \beta_i > 0, \alpha_i (i = 1,2) > 0, \alpha_1 + \alpha_2 = 1$

where (β_1, β_2) are subsistence quantities of each good, $(\alpha_{1,}\alpha_2)$ are proportions for each good, and $(x_{1,}x_2)$ are quantities of each good. Maximizing the (LES) function per budget constrain M yields following solution for quantity demanded per good:

$p_i x_i^M = p_i \beta_i + \alpha_i (M - p_1\beta_1 - p_2\beta_2),\ i = 1,2$ (2.28).The indirect utility of LES → $U^* = \frac{M - p_1\beta_1 - p_2\beta_2}{p_1^{\alpha_1} p_2^{\alpha_2}}$; the inversion of the indirect utility yields *an* expenditure function:

$$M^* = U p_1^{\alpha_1} p_2^{\alpha_2} + p_1\beta_1 + p_2\beta_2 \quad (2.29)$$

An indirect utility function was introduced by Houthakker as a dual to a utility function with no available closed-form solution. If a function is nondecreasing in income, has nonincreasing and quasi-convex pricing, and is continuous and homogeneous of degree zero in prices and income, it is a legitimate indirect utility function to express consumer preferences. Mathematically: $U^*(p_1, p_2, M) = \alpha_1 \left(\frac{M}{p^1}\right)^{\beta_1} + \alpha_2 \left(\frac{M}{p^2}\right)^{\beta_2}$ (2.30)

The translog indirect utility function is widely used in empirical demand analysis. The translog flexible function form can be a 2nd order local approximation to an arbitrary indirect utility function. A basic translog specification can be written as:

$$\log U^*(p_1, \dots, p_n;\ M) = -\sum_j\ \alpha_j \log\frac{p_j}{M} - \frac{1}{2}\sum_k\ \sum_j\ \beta_{kj}\log\frac{p_k}{M}\log\frac{p_j}{M} \quad (2.31)$$

where $\sum_j\ \alpha_j = 1, \beta_{kj} = \beta_{jk}$ for all k and j. Other functions include Almost ideal demand system, Cobb-Douglas, etc. (Silberberg, 1990).

Random Utility Model (RUM) attempts to model individuals' choices among discrete sets of alternatives. The RUM model's key assumptions are that choice is a discrete event, utility of choices is a random variable, and customer behavior is rational (*it chooses item with the highest utility*). The observed attributes are represented using a utility function using explanatory variables whereas the unobserved ones are represented by random variables. Given that utility is a random variable in RAM, such a model cannot accurately predict a customer's choice; instead, RAM assigns a probability to each alternative. For example, consider an individual who chooses among J alternatives. Let the utility of alternative j be: $U_j = \beta' X_j + \varepsilon_j$ where X_j is a column vector of observed attributes of alternative j, β' is a conformable vector of constant parameters, and ε_j is a random variable that accounts for effects on preferences of unobserved attributes of the alternative and individual. The probability that an individual chooses alternative i is given by:

$$P(i|X) = P(B'X_i + \varepsilon_i > B'X_j + \varepsilon_j \text{ for all } j = 1, \dots, J;\ j \neq i),\ X = (X_1', \dots, X_J')' \quad (2.32)$$

$P(i|X)$ can be resolved to a multinomial logit model if $\varepsilon = (\varepsilon_1, \dots, \varepsilon_j)'$ are independent and identically distributed across alternatives with the Type 1 extreme value distribution. The multinomial logit model is given by (Horowitz, 1994):

$$P(i|X) = [\exp(\beta' X_i)] / \sum_{j=1}^{J}[\exp\ (\beta' X_j)] \quad (2.33)$$

The consumption models discussed above were limited to choices between contemporaneous commodities, with no consideration for consumption over time. Intertemporal choice models, on the other hand, look at everyday decisions that involve choosing between outcomes at different points in time. Intertemporal decisions may include, for example, determining whether additional money offered later is worth the waiting period to receive a larger sum (Samanez-Larkin, 2015). Economists observed that individuals prefer immediate payoff when provided with a choice between current and future utilization – the key reason being the devaluation of payoffs with passage of time. Devaluations of payoffs can occur due to inflation, investment, and uncertainty (Stevens, 2010).

A simple example of intertemporal choice model is the problem of maximizing utility $U(c_1, c_2)$ through consumption of goods in two time periods (c_1, c_2), earning (I_1, I_2) and interest rate r. Earnings not spent in period 1 can be loaned out to other individuals at an interest rate r. Alternatively, an individual can borrow money at an interest rate r to increase consumption c_1 and repay (principal + interest) in $t + 1$. Mathematically this relationship can be written as:

$$\max U(c_1, c_2) \text{ s.t } c_1 + \frac{c_2}{(1+r)} = I_1 + \frac{I_2}{(1+r)} = W \tag{2.34}$$

where W is defines as the present value of current and future income. The Lagrangian of the above problem is written as:

$$\mathcal{L} = U(c_1, c_2) + \lambda \left[(I_1 - c_1) + \frac{(I_2 - c_2)}{(1+r)} \right] \tag{2.35}$$

Solving for 1st order condition provides yields $\frac{U_1}{U_2} = 1 + r$, the customer's marginal value of present consumption $\frac{U_1}{U_2}$, equals the opportunity cost of present consumption. An n period utility function with impatience ρ can be written as $\sum_{i=1}^{n} \frac{U(x_i)}{(1+\rho)^{(i-1)}}$ (2.36). The consumption in the future is valued less than present consumption. The $V(x)$ is strictly increasing and quasi-concave, by which the "goods" x_i are given less weight as i increases. The dynamic consistency property states that the marginal value of consumption in period i in terms of foregone consumption in period j be independent of the date and dependent only on the consumption level in two time periods. The marginal rate of substitution for n period utility function is given by:

$$\frac{dx_j}{dx_i} = \frac{-V_i}{+V_j} = \frac{-(1+\rho)^{(j-1)} U_{i'}(x_i)}{U_{j'}(x_j)} \tag{2.37}$$

Maximizing the n period utility function per wealth constraint produces the following tangency condition for periods $i, j \rightarrow \frac{U'(x_i)}{U'(j)} = \frac{(1+r)}{(1+p)}$. The consumption of income is affected by relation between the consumer's preference for earlier availability measured by $(1 + \rho)$ and market price of earlier availability $(1 + r)$ (Silberberg, 1990).

The consumption of commodities is sensitive to interest rates in the economy. Low interest rates help customers to spend more due to the reduced cost of borrowing. However, excessive consumer spending can cause an imbalance in supply and demand, which can lead to price escalation of commodities and inflation. The central bank in an economy constantly monitors the inflation and employment rate and adjusts the interest rates in response. In 2022, the U.S. Federal Reserve in response to a 40-year high inflation (> 8%) started increasing interest rates to discourage customer spending. The

key reasons for high inflation were excessive liquidity in the market as well as contraction of manufacturing activity due to COVID 19 pandemic (Sommer, 2022). The IS-LM model is used by governments and commercial firms to analyze the effects of exogenous macroeconomic variables on alternative monetary and fiscal policy (Gali, 1992). The model is used to investigate how output effects of given changes in money supply and government spending depend on model's parameters and on the slopes of IS (investment-saving) and LM (liquidity preference - money supply) curves. The equilibrium in the market for good Y is given by:

$$Y = k(A_0 - br) \tag{2.38}$$

where k is a function of marginal propensity to consume, the tax rate, and the marginal propensity to import, A_0 is the aggregate expenditures independent of both interest rate r and output, and b represents the interest rate responsiveness of aggregate expenditures. Solving for r yields following IS Equation:

$$r = \frac{A_0}{b} - \left(\frac{1}{kb}\right) Y \tag{2.39}$$

The equilibrium in the money market is given by $\frac{M}{P} = hY - fr$ (2.40) where $\frac{M}{P}$ is the real money supply, h is the income responsiveness of the demand for money, and f is the interest rate responsiveness of money demand. Solving for r yields following $LM\ equation$ (Findlay, 1999):

$$r = \left(\frac{h}{f}\right) Y - \left(\frac{1}{f}\right) M/P \tag{2.41}$$

The future value of a loan in absence of inflation is calculated as $P' = Pe^{rt}$ where P is the initial principle, r is the real-interest rate, and t is the number of years. In case of inflation g, the future value of the loan is given by $P' = Pe^{(r-g)t}$. To offset the effect of inflation, an anticipated rate of inflation is incorporated into the real rate of interest – yielding to nominal rate of interest i, where $i = r + g$.

2.8 Transport / Graph Theory

Transport systems allow economic activities to be linked by identification of locations that produce favorable conditions of production. A poorly established transport infrastructure can stifle industrial output by acting as a bottleneck, but a well-built transportation system can stifle industrial development by providing a cost-effective means of importing goods from industrialized areas. The direct impact of improvements in transport system includes establishment of connection between large markets and savings in time and money. Increased specialization, distinct separation phases in value addition, and increased business activities result in higher transport volumes and average haul lengths. The indirect impact of transportation infrastructure includes the economic multiplier effect caused by price rises in goods or services when diversification occurs. Between 1970-1998, the European Union freight transport increased 54% while the GDP growth was estimated at 35% in the same period. Although integrated transportation increases productivity and facilitates the flow of goods, it also makes different regions more vulnerable to economic shocks. For example, the financial crises of 2008 and 2019 COVID pandemic led to substantial decrease in exports and imports across various regions (Filip, 2014). One of the most common transport infrastructures is the road

network system composed of spatial points (industries, mining facilities, hubs, and markets), pathways and transport assets.

Graph theory is an area of mathematics concerned with formal mathematical structures of graphs. A minimal spanning tree (MST) is a graph of connected edges that connect all vertices without generating a cycle, with the sum of total edges' weights being minimal. The MST algorithms have been utilized in route optimization, formulation of transport plans, dual carriageways in Sokoto city, gas pipeline layout in West Africa, taxonomy, cluster analysis, image processing, circuit design, regionalization of socio-geographic areas, comparison of ecotoxicology data, power systems topology, and minimax process control, etc. (Akpan, 2017), (Bereg, n.d.). Examples of MST algorithms include Prim's, Kruskal and Steiner Tree. Details on algorithms are as follows:

Prim's Minimum Spanning Tree

Input: A digraph G with vertices $V(G) = [1, \dots, n]$

Output: (1) A subset of the edges that connects all vertices such total weight (distance) of all the edges in the tree is minimized – MST (Minimum Spanning Tree)

(2) Modification - A subset of new edges* that connects all vertices of degree 1 ∈ MST (1): total weight of new edges* is minimum

Prim-Heap Algorithm

Select an arbitrary vertex s

for each neighbor u of s; set near (u) to $w(u, s)$, the weight of the edge (u, s)

All other vertices have their near value set to '∞'

Add the other $n - 1$ vertices as follow:

1. Find the vertex v not in G with minimum distance value.
2. $for\ each\ neighbour\ u\ of\ v$

   $if(w(u,v) < near(u)\ and\ u\ not\ in\ T)$

   $then\ near(u) \leftarrow w(u,v);$
3. $Add\ v\ to\ G$

The worst-case time for step (1) is $O(n \log n)$ and $O(m \log n)$ for step (2) (Martel, 2002).

Kruskal's Minimum Spanning Tree

The Kruskal algorithm identifies an MST in a linked graph by adding consecutive edges from lowest to highest weight without producing a cycle. The pseudo code for Kruskal is as follow:

Kruskal Algorithm

function Kruskal (*Graph):*

create a new empty tree *F*

for each vertex v in the *Graph*:

$make_set(v)$

for each edge (u, v) in the *Graph* ordered by weight (ascend):

$u_set = find_set(u)$

$v_set = find_set(v)$

$if\ u_set \neq v_set$:

add the edge (u, v) in the tree *F*

$u_{set} \cup v_set$

return *F*

The time complexity of Kruskal algorithm is $O(n \log n)$ (Soularidis, n.d.).

Steiner Tree

The Steiner trees appear frequently in network design problems because they show how to connect a given set of locations with the least amount of wire. Other applications include water pipe networks, heating ducts, and VLSI circuit design. In contrast to the above MST algorithms, a Steiner tree introduces additional pseudo points in the graph, to reduce the total weight of the network. An equilateral triangle is the worst-case scenario for an MST approximation; application of an MST algorithm on an equilateral triangle produces a network with a combined edge weight of 2, in comparison the Steiner tree connects the vertices of an equilateral triangle by introducing an intermediate point in the center of triangle resulting in combined edge weight of $\sqrt{3}$ (Skiena, 2008). The $\sqrt{3}/2$ represents the Steiner ratio: the ratio of Steiner tree weight to that of Euclidean Minimal Spanning Tree (EMST) weight. The Steiner tree inherently is an NP-Hard problem: a non-deterministic polynomial-time hardness (NP-Hard) are complex problems that cannot be solved and verified in polynomial time. In response to the NP nature of Steiner tree, various approximation and heuristic algorithms have been developed to deal with the problem of Steiner tree.

Steiner – Heuristic Algorithm

> The heuristic approach is a greedy one based on using the MST as a decomposition guide and Delaunay Triangulation to construct the edges R of tetrahedra. The heuristic seeks to decompose the chain data structure in a such a way as to minimize the Steiner ratio for each piece. The Steiner ratio depends on

the *length of each edge and the degree of each junction.* The algorithm tries to maximize the *minimum length edge* while simultaneously reducing the degree of each junction in the chain data structure. General algorithm description is as follow (Smith, 1998):

(1) Establish the computational geometry data structure: Construct the Convex Hull and Delaunay Triangulation (DT) data structure. *Time complexity:* $\Omega(n^2)$

(2) Establish an upper bound on the Steiner Minimal Tree (SMT): Solve the minimum spanning tree (MST) with the Delaunay Triangulation (V) edge set. *Time complexity:* $O(N^2)$

(3) Construct the *R Data Structure*: Identify the tetrahedra $t_i, t_j, \dots, t_q$ sharing edges in the minimum spanning tree. *Time complexity:* $O(N^2)$

   a. Utilize the Voronoi locus information to determine adjacent tetrahedra in the minimum spanning tree.

   b. Utilize the centroid spanning tree (CST) to construct the largest chains R_i of the tetrahedra in the minimum spanning tree.

   c. Identify p^i within each R_i.

   d. Identify the junctions of the R_i.

(4) *Local Optimal Solutions:* Create a Priority Queue Q of R_i sorted on their Steiner ratio. *Time complexity:* $O(2^N N!)$

   a. Select a R_i and determine adjacent R_j incident to R_i at both ends of possible of R_i.

b. Choose the largest junction and determine the adjacent R_j which *Maximize* the minimum length R_j. If the sets of edges can be unionized together, go to step 4.c, otherwise:
    i. Using the longest R_i at the junction, determine the face F_i of the tetrahedron which chain R_i is adjacent.
    ii. Using this face F_i determine the vertex of the tetrahedral junction nearest to the 1st three vertices of R_i. Call this vertex v_k as the critical root vertex of the R_i.
    iii. Using v_k find a local optimal solution for the R_i.
    iv. Find the local optimal solutions for the remaining $R_j, j = 2,3,4$ using the appropriate root vertex of the junction tetrahedra.
c. Union the R_i and R_j, $j = 2,3,4$ and find the Steiner Minimal Tree (SMT) of the union.
d. Store the SMT solution and $k \leftarrow k + 1$ and return to 4.a.
e. The process is complete once the priority queue Q is empty.

Delaunay triangulation: Given a set of points or a polyhedron, the *triangulation* process partitions the interior of the point set into triangles. Delaunay triangulation of a point set minimizes the maximum angle over all possible triangulations.

Voronoi Diagrams: Given a set S of points $p_1, p_2, \dots, p_n$; decompose space into regions around each point such that all points in the region around p_i are closer to p_i than any other point in S. Applications of Voronoi diagrams include nearest neighbor search, facility location, path planning and quality triangulation (Skiena, 2008).

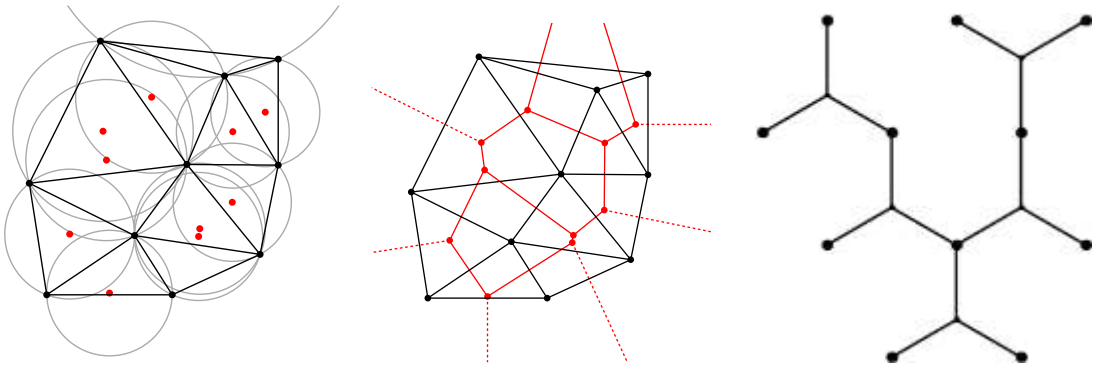

Figure 2-1: Delaunay Triangulation (Left), Voronoi Diagram (Center) *(Kopsch, 2012)*, Steiner Tree (Right) *(Smith, 1998)*

A variety of transportation applications require the use of *shortest path algorithms* to solve the problem of finding the shortest path between two points on a map with the smallest sum of distances. The shortest path problem can be categorized into five types: (a) shortest between two points, (b) shortest path among all nodes, (c) K shortest path, (d) real-time shortest path, and (e) shortest path of the specified path. Classical shortest path algorithms include Dijkstra, Bellman Ford, and Floyd-Warshall (Wang, 2011).

Dijkstra Algorithm

The Dijkstra algorithm is used to find a calculate the shortest path from a source node to all other nodes in a graph. In each iteration, algorithm adds exactly one vertex to the tree of vertices for known shortest path (Skiena, 2008). The time complexity of Dijkstra is $O(E \log V)$.

$ShortestPath - Dijkstra(G, s, t)$

$known = \{s\}$

$for\ i = 1\ to\ n, dist[i] = \infty$

$for\ each\ edge\ (s, v), dist[v] = w(s, v)$

$last = s$

$while\ (last\ \neq t)$

$select\ v_{next}, the\ unkown\ vertex\ minimizing\ dist[v]$

$for\ each\ edge\ (v_{next}, x), dist[x] = \min[dist[x], dist[v_{next}] + w(v_{next}, x)]$

$last = v_{next}$

$known = known \cup \{v_{next}\}$

Bellman Ford Algorithm

The Bellman Ford Algorithm computes the shortest path from a single vertex to all other vertex with the capability to solve graphs in which some of the edge weights being negative. The time complexity of Bellman Ford is $O(VE)$.

$ShortestPath - BellmanFord(G, S)$ (Bellman Ford's Algorithm, n.d.)

$for\ each\ vertex\ V\ in\ G$

$distance\ [V] \leftarrow \infty$

$previous\ [V] \leftarrow NULL$

$distance\ \ [S] \leftarrow 0$

$for\ each\ vertex\ V\ in\ G$

$for\ each\ edge\ (U, V)\ in\ G$

$dist_{temp} \leftarrow distance[U] + edge_weight(U, V)$

$if\ dist_{temp} < distance[V]$

$distance[V] \leftarrow\ dist_{temp}$

$previous[V] \leftarrow U$

$for\ each\ edge\ (U, V)\ in\ G$

$$if\ distance[U] + edge_{weight(U,V)} < distance[V]$$

Error: Negative Cycle Exists

$$return\ distance[\ ], previous\ [\ ]$$

Floyd Warshall Shortest Path

The Floyd Warshall algorithm utilizes dynamic programming to find all-pairs shortest path. The time complexity of Floyd-Warshall algorithm is $O(n^3)$ (Hougardy, 2010).

Input: A digraph G with vectors and distances $c : E(G) \to \mathbb{R}$

Output: A $n \times n$ matrix M such that $M[i, j]$ contains the length of a shortest path from vertex i to vertex j

a. $\mathrm{M[i,j]} \coloneqq \infty\ \forall \mathrm{i} \neq \mathrm{j}$ (Minimum distances initialized as infinite)

b. $\mathrm{M[i,j]} \coloneqq 0\ \forall \mathrm{i}$

c. $\mathrm{M[i,j]} \coloneqq \mathrm{c}\big((\mathrm{i,j})\big), \forall (\mathrm{i,j}) \in \mathrm{E(G)}$

d. $\mathrm{for(int\ i = 0\ ; i < n; i + +)\ do}$

e. $\mathrm{for(int\ i = 0\ ; i < n; i + +)\ do}$

f. $\mathrm{for(int\ i = 0\ ; i < n; i + +)\ do}$

g. $\mathrm{if\ M[j,k] > M[j,i] + M[i,k]\ then\ M[j,k] \coloneqq M[j,i] + M[i.k]}$

h. $\mathrm{for(int\ i = 0\ ; i < n; i + +)\ do}$

$\mathrm{if\ M[i,i] < 0\ then\ return\ ('negative\ cycle\ found')}$

Several heuristic shortest path algorithms have been developed for in-vehicle Route Guidance Systems (RGS), real-time Automated Vehicle Dispatching System (AVDS), and scheduling. The main benefit of utilizing heuristics instead of regular, optimum algorithms (Dijkstra, Bellman, Floyd, etc.) is the reduction in processing time. Different

heuristic approaches include, a) limit the area searched (branch pruning and A*), (b) decompose the search problem (sub-goal and bi-directional search), (c) limit the links searched (hierarchical search), and (d) some combination of above (L. Fu, 2006).

The Vehicle Routing Problem (VRP) is concerned with determining a set of least-cost vehicle routes in which each customer is visited precisely once by one vehicle, each vehicle begins and ends its route at the depot, and the vehicle capacity is not exceeded. Variants of VRP include Mixed Fleet VRP (HFVRP) – fleet w/ varied capacities, VRP with Time Windows (VRPTW) – when deliveries need to occur in a certain time interval, VRP with Pickup and Delivery (VRPPD), VRP with backhauls (VRPB) – vehicle does deliveries as well as pickup in one route, Multi-Depot VRP (MDVRP) – assumes that multiple depots are geographically spread among customers, Periodic VRP (PVRP) – used when planning is made over a certain period and deliveries to client can be made in different days, and VRP with simultaneous pickup and delivery (VRPSPD) - goods must be carried from several origins to various destinations, and each client has a delivery and pickup requirement that must be met at the same time. VRT problems are NP-hard (Kris Braekers, 2016), (Çağrı Koç, 2020).

The Vehicle Routing Problem with simultaneous pickup and delivery (VRPSPD) can be defined on a complete directed graph $G = (V, A)$, where V is the node set and A is the arc set. The depot is represented by node O, *other* nodes of V are the customers: $V' = V \backslash \{0\}$. The depot contains a fleet of homogenous vehicles K each with a carrying capacity Q. The cost of travelling on arc {i, j} is $c_{i,j}$. Each customer i has a non-negative demand d_i for delivery and p_i for pickup. The y_{ij} is the amount of commodity picked and z_{ij}

represents the amount of commodity delivered on arc $(i,j) \in A$. The objective of the model is then:

$$Min \sum_{(i,j)\in A} c_{ij}x_{ij}$$ Minimize the total routing cost.

subject to

$\sum_{j\in V} x_{ij} = 1$	$i \in V'$	..	each customer is visited by exactly one vehicle
$\sum_{j\in V'} x_{0j} \leq K$		..	ensure maximum K vehicles are used
$\sum_{j\in V} x_{ij} = \sum_{j\in V} x_{ji}$	$i \in V$		
$\sum_{j\in V} y_{ij} = \sum_{j\in V} y_{ji} = p_i$	$i \in V'$		quantity delivered at point j = quantity picked up at point i
$\sum_{j\in V} z_{ij} = \sum_{j\in V} z_{ji} = d_i$	$i \in V'$	..	
$y_{ij} + z_{ij} \leq Qx_{ij}$	$(i,j) \in A$		vehicle capacity ≯ total demand of vehicle route
$y_{ij}, z_{ij} \geq 0$	$(i,j) \in A$	..	amount picked up and amount delivered ≥ 0
$x_{ij} \in \{0,1\}$	$(i,j) \in A$		

(Çağrı Koç, 2020)

The Vehicle routing problem being NP-Hard requires the use of heuristics to generate approximate solutions in a polynomial time. Heuristics methods are an alternative way for solving difficult combinatorial problems. For example, the traveling salesman problem[9], with the goal of finding the shortest route through 45 cities while visiting each city only once and returning to the point of origin, necessitates $2.7x10^{54}$ calculations to find the optimal solution. The simplest way to deal with such a complex problem is to use random sampling and stop the search after several iterations or when there is no improvement in the solution, i.e., Monte Carlo. However, random search on the TSP problem has produced results that are far from satisfactory (Skiena, 2008). Heuristic algorithms such as Tabu search, simulated annealing, Particle swarm optimization, Genetic algorithm, Neural Networks, Support vector machines, and Ant colony

[9] Simplest vehicle routing problem

optimization use intelligent simplifications and methodologies to solve computationally complex problems. A brief overview of few heuristic algorithms is as following:

$Simulated - Annealing( )$

Create $initial$ solution S
initialize temperature t
$repeat$
$for\ i = 1 : n\ \boldsymbol{do}$
generate a random transition from S to S_i
$if\ C_{(s)} \geq C_{(s_i)} \rightarrow S = S_i$
$else\ if \left(e^{\frac{C_{(s)} - C_{(s_i)}}{k.t}} > random[0,1) \right) \rightarrow\ S = S_i$
reduce temperature t
$until(no\ change\ in\ C_{(s)})$
$return\ S$

Simulated annealing (SA) is a random approach that simulates the statistical process of growing crystals using the annealing process to reach its global minimum internal energy configuration. The annealing process results in a local minimum state of internal energy if the temperature profile is not gradually reduced over time (Arora, 2004). Upon initialization the program uses randomness to search a wide solution space with a high probability of accepting negative results. The cooling schedule controls the acceptance of negative results with passage of time. Parameters for colling schedule are as following: a) Initial system temperature t_1 = 1, Cooling rate $t_k = \alpha(t_{k-1})$ where $0.8 \leq \alpha \leq 0.99$, number of iterations at each temperature gradient (100 – 1,000), acceptance criteria $s_i \rightarrow s_{i+1}$ given $C_{(s_{i+1})} < C_{s_i}$ or accept $C_{(s_{i+1})} > C_{s_i}$ when $e^{\frac{-(C(s_i) - C(s_i+1))}{k.t_i}} \geq r$ where r is a random number $0 \leq r \leq 1$, stopping criteria: no improvement in current solution (Skiena, 2008).

Genetic Alogrithm( )

select an initial population of chromosomes
while termination conditions not satisfied ***do***
repeat
if crossover condition is satisfied ***then***
select parent chromosomes
choose cross-over parameters
perform crossover

if mutation condition is satisfied ***then***
choose mutation points
perform mutation
evaluate fitness of offspring

until sufficient offspring created
select new population
endwhile (Reeves C. , 2010)

The *Genetic Algorithm Optimization (GA)* technique is based on the Darwinian principle of evolution through genetic selection. Starting with a randomly generated population of chromosomes (combinations of finite real numbers), the GA calculates the fitness function of each chromosome and performs a recombination step in which the genetic material of the parents' chromosomes is recombined and in certain instances mutated to produce a child chromosome. This process is repeated several times, with the average fitness of chromosomes increasing with each generation until a termination criterion is met (McCall, 2005).

The *Particle Swarm Optimization (PSO)* algorithm is metaheuristic based on populations of individuals in which solution candidates evolve through simulation of a simplified

model of social adaptation. The PSO algorithms have been used to solve optimization problems with domain, linear and nonlinear constraints (Manoela Kohler, 2019). The PSO algorithm pseudo code is as follows (Tsitsas, 2021):

Particle Swarm Optimization

Input: $N, x_l, x_u, c_1, c_2, i_{max}, f$

Output: A swarm S of size N

a. Initialize S, randomly generate the position x of each particle per bounds x_l, x_u of the objective function.
b. Initialize all velocities u to 0.
c. Initialize best positions x^* (and respective values) for individual particles & find $g*$
d. Choose randomly two values in $[0,1]$ for r_1 and r_2
e. Iteration $i = 0$
f. Initialize θ_{min}, θ_{max}

   while $i < i_{max}$ do

   Calculate inertia: $\theta = \theta_{max} - \frac{\theta_{max} - \theta_{min}}{i_{max}} i$;

   for each particle in S, the values for iteration i are:

   1. $Update\ velocity$: $u_i = \theta u_{i-1} + c_1 r_1 [x^* - x_{i-1}] + c_2 r_2 [g^* - x_{i-1}]$
   2. $Update\ position$: $x_i = x_{i-1} + u_i$
   3. $Compute\ the\ value\ of\ the\ new\ position\ according\ to\ f$
   4. Check / Update: x^*, g^*

   (Optional) Check for convergence

   Update iteration: $i = i + 1$

   end

   return S;

where f is the objective position, (x_l, x_u) are minimum and maximum range of solution space, i_{max} is maximum number of iterations, g^* is global best position, x^* is individual

best position, x is individual position, u is velocity component, θ inertia weight mechanism ($\theta_{max} = 0.9, \theta_{min} = 0.4$)

The *Support Vector Machines (SVM)* is a supervised classification technique used in building nonlinear classifiers. Let Ω be a set of n records, each associated with a pair (x^i, y^i), with $x^i \in \mathbb{R}^d$ and $y^i \in \{-1,1\}$. The SVM classifier will classify records with predictor vector $x \in \mathbb{R}^d$ by means of a score $s(x)$ of the form

$$s(x) = \sum_{i=1}^{n} \alpha^i \beta^i K(x, x^i) \quad (2.42)$$

where $K: \mathbb{R}^d \times \mathbb{R}^d \rightarrow \mathbb{R}$ is called the SVM kernel. The coefficients α^i are obtained by solving following concave quadratic maximization problem with constraints plus one linear constraint:

$$\max \sum_{i=1}^{n} \alpha^i - \frac{1}{2} \sum_{i=1}^{n} \sum_{j=1}^{n} \alpha^i \alpha^j y^i y^j K\left(x^i x^j\right) s.t. \sum_{i=1}^{n} \alpha^i y^i = 0, \alpha \in [0, C]^n \quad (2.43)$$

Here $C > 0$ is the regularization parameter which limits the influence of each record i in the score function s. The selection of kernel K and regularization parameter C is extremely important for SVM classification accuracy. The SVM parameter tuning problem can be formulated as the optimization problem…The variable neighborhood search (VNS) has been used for parameter tuning problem. The VNS sequentially moves through the feasible region by search solutions in a neighborhood of the current best solution, while systematically changing the size of neighborhood to avoid getting trapped at local optima (Emilio Carrizosa, 2014).

SVM Parameter Tuning using Variable Neighborhood Search (VNS)

INPUT: Kernal set $K = \{K(\theta): \theta \in \Theta\}$.

Max iterations m. Neighborhood structure $\{N_1, N_2, \dots, N_{k_{max}}\}$,

with $N_k(\tilde{\theta}) = \{\theta \in \Theta: \|\theta - \theta\| \leq r_k\}$ and $0 < r_1 < r_2 < \cdots < r_{k_{max}}$.

INTIAL: Select and initial solution $\theta \in \Theta$; set $k \leftarrow 1$; set iter $\leftarrow 0$.

1. Repeat until $iter = m \; or \; k = k_{max}$:
    a. Shaking. Generate a random solution θ' in the k-neighborhood of the incumbent solution $\tilde{\theta}$, $\theta' \in N_k(\tilde{\theta})$
    b. Neighborhood change. If $\hat{a}(\theta') > \hat{a}(\tilde{\theta})$, then move $(\tilde{\theta} \leftarrow \theta')$ and reset the neighborhood $(k \leftarrow 1)$; otherwise, set $k \leftarrow k + 1$
    c. Set iter $\leftarrow$ iter $+ 1$
2. If iter $= m,$ STOP with solution $\tilde{\theta}$; otherwise, reset $k \leftarrow 1$ and go to Step 1.

Ant Colony Optimization (ACO) is a family of nature-inspired metaheuristics that can be used to solve NP-Hard combinatorial optimization problems (COPs). ACO is a problem-solving system in which several information-processing units (agents) interact with one another to improve problem-solving efficiency. Versions of ACO include Ant system, Ant Colony System, MAX MIN Ant System MMAS, Population-based ACO and Beam ACO. The ACO algorithms have been used to solve vehicle routing problems, set cover problems, edge detection on digital images, protein folding and scheduling problems.

MAX MIN Ant System ( )

$global_{best} \leftarrow$ Build initial solution

Calculate pheromone trails limits τ_{min} and τ_{max} using $global_{best}$

Set pheromone trails values to τ_{max}

for $i \leftarrow 0 \; to$ # of iter do

for $j \leftarrow 0 \; to$ # of ants do

$route_{Ant(j)}\ [0] \leftarrow u\{0, n-1\}$ // Select first node randomly

for $k \leftarrow 1\ to$ n $-$ 1 do

$route_{Ant(j)}\ [k] \leftarrow$ select. next. node(route$_{\text{Ant(j)}}$)

$local.search(route_{Ant(j)})$ // Optional

$iter_{best} \leftarrow select_shortest(route_{Ant(0)}, \dots, route_{Ant(\#ants-1)})$

if iter$_{\text{best}} < global_{best}$ then

$global_{best} \leftarrow$ iter$_{\text{best}}$

Update pheromone trails limits τ_{min} and τ_{max} using $global_{best}$

Evaporate pheromone according to p parameter

Deposit pheromone using either $global_{best}$ or $iter_{best}$ solution

In the ACO, a virtual ant traverse through a graph G from current node to neighboring nodes. The route of a given ant becomes its solution. The decision of which node to choose next is based on the costs of edges to unvisited nodes and additional information supplied by pheromone trails. For every edge $(i, j) \in E$ a pheromone trail, $\tau_{ij}(t)$ is defined, where t is discrete time. The use of pheromone trails simulates how certain ant species use chemical substances as a way of indirect communication between individuals. The MAX-MIN Ant System impose limit on pheromone values (τ_{min}, τ_{max}) to control exploration-exploitation behavior induced by the pheromone. Exploitation is triggered by an increase in pheromone levels on a path, whereas exploration is triggered by evaporation. The probability that an Ant k located at node i selects edge (i, j) is:

$$p_{ij}^{k}(t) = \frac{[\tau_{ij}(t)]^{\alpha}[\eta_{ij}]^{\beta}}{\sum l \in N_i^k [\tau_{ij}(t)]^{\alpha}[\eta_{ij}]^{\beta}}\ if\ j \in N_i^k \tag{2.44}$$

where $\tau_{ij}(t)$ is the value of the pheromone trail deposited on edge (i, j), η_{ij} is the value of heuristic information of edge (i, j), α, β are parameters that control influence of

pheromone values and heuristic information, N_i^k is a set of nodes to be visit by ant k. In vehicle routing problem, the value of heuristic information of edge (i, j) is a reciprocal of the edge cost $1/d_{ij}$, *shorter paths are more attractive* (Skinderowicz, 2022).

The Fuzzy Set theory is a research method for dealing with ambiguous, subjective, and imprecise assessments, as well as for quantifying the linguistic aspect of available data and preferences for individual or group decision-making (Bon-Gang, 2018). Fuzzy logic is an alternative to mathematical modeling for many physical processes that are too complex to be described by simple mathematical Equations and formulas. Takagi-Seguno is a popular Fuzzy system that consists of if-then rules with fuzzy antecedents and mathematical functions on the consequent part. The antecedents of fuzzy sets divide the input space into several fuzzy regions, while the consequent functions describe the system's behavior in these regions (Hamad, 2021). A Takagi-Seguno Fuzzy system has the following form for an i^{th} rule:

$$If\ x(k)\ is\ M_i, then\ x(k+1) = A_i x(k) + B_i u(k) \tag{2.45}$$

where $x(k)$ is the state vector, M_i is the vector of the fuzzy set of the i^{th} rule. The similarity ratio of each rule to the actual behavior of the process is described as:

$$w_i\big(x(k)\big) = \prod_{j=1}^{p} M_{ij}(x_j(k)) \tag{2.46}$$

where $M_{ij}(x_j(k))$ is the membership degree of the j^{th} state variable of the i^{th} rule, $w_i\big(x(k)\big)$ is the product of all the membership degrees of the i^{th} rule. Therefore, the weighted average output of all rules:

$$x_i(k+1) = \frac{\sum_{i=1}^{n}\sum_{i=1}^{n}(x(k))(A_i x(k)+B_i u(k))}{\sum_{i=1}^{n} w_i(x(k))} \tag{2.47}$$

In the Takagi-Seguno Fuzzy system, the weighting of the element $x(k)$ is described in the form:

$$\phi_i(x(k)) = \frac{w_i(x(k))}{\sum_{i=1}^{n} w_i(x(k))} \quad (2.48)$$

Thus, the output of Takagi-Seguno Fuzzy system equals:

$$x(k+1) = \sum_{i=1}^{n} x_i(k+1)\phi_i(x(k)) \quad (2.49)$$

A Fuzzy object is a method based on Fuzzy logic that captures and analyzes imprecise requirements by incorporating the concept of fuzziness on object orientation features. The Fuzzy object-oriented modeling technique converts a class to a fuzzy class that classifies objects with similar properties, encapsulates fuzzy rules in a class to describe attribute relationships, evaluates fuzzy class memberships by taking both static and dynamic properties into account, and models uncertain fuzzy associates between classes (Lee, 2013). A *Particle System* is a collection of numerous particles that collectively represent a Fuzzy object. Each particle 'boid' is an individual actor that navigates according to its own perception of the environment, the simulated laws of physics, and a simple set of behavioral patterns.

The sequence of steps performed in a particle system include (Reeves W. T., 1983):

a. Generation of new particles
b. Each particle is assigned individual attributes.
c. Particles are removed from the system after their prescribed lifetime is extinguished.
d. Active particles are moved and transformed according to their dynamic attributes.
e. Image of active particles is rendered in a frame buffer.

The particle systems have been utilized in modeling flow of pedestrians in emergency situations, in testing suitability of building designs, town planning, and entertainment (Leggett, 2004).

2.9 Emissions impact modeling

Several models have been developed to assess the impact of exposure to emissions. The Fuzzy exposure model, for example, has been used to deal with the uncertainties involved in quantifying long-term chronic chemical exposure in humans. In many regions, exposure evaluation is critical in quantitative risk assessment to formulate regulatory decisions. An exposure assessment identifies all individuals or population subgroups who have been exposed to a chemical and quantifies the actual doses received. The Fuzzy model input variables included chemical concentration, duration of exposure and dose absorbed to predict the life average daily exposure (T. Rajkumar, 1996). Fuzzy model has been used to estimate amounts of NO_x emissions from transit vessels passing through Bosphorus strait that connects the Black Sea with Marmara Sea (Kanbay, 2018). EPA's Stochastic Human Expose and Dose Simulation (SHEDS) are probabilistic models that can estimate the amount of chemicals that people are exposed to in their daily lives. The models can forecast aggregate and cumulative exposures over time, which can be used to help with risk evaluations that protect human health. Given a set of demographic variables, SHEDS can estimate the range of total chemical exposures in a population resulting from various exposure pathways throughout time periods (Graham Glen, 2012).

The EPA's Community Multiscale Air Quality (CMAQ) Modeling System is the preeminent modeling system for researching air pollution at local, regional, and global scales. It combines meteorology, emissions, and chemistry modeling to simulate the fate of air pollutants under changing atmospheric conditions. Other models, such as crop management and hydrology models, can be linked with the CMAQ simulations as needed to simulate pollution more comprehensively across environmental media. Various states

use CMAQ model to develop and assess implementation actions needs to attain National Ambient Air Quality Standards (NAAQS). Estimated deposition values from CMAQ model are used to assess the effects of air pollutants on ecosystems, such as eutrophication and acidification (U.S. Environmental Protection Agency, 2019).

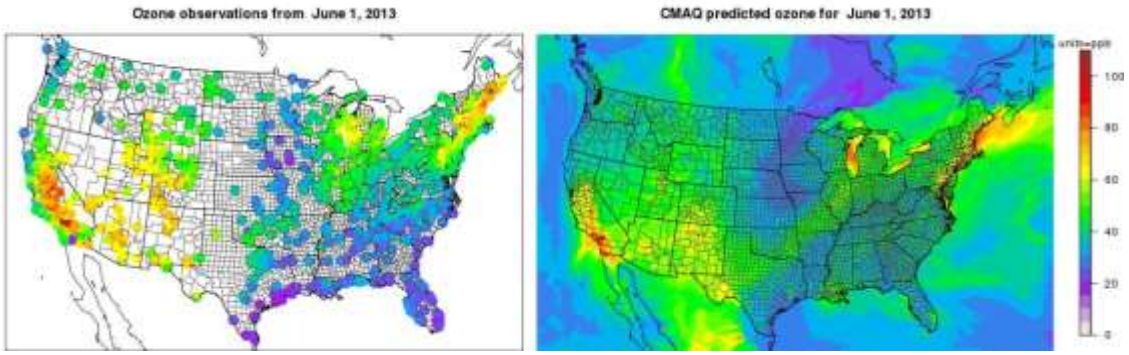

Figure 2-2: (L) Spatial map of ozone monitoring sites in US (max 8hr ozone concentration). (R) Spatial map of max-8hr ozone concentration predicted by CMAQ *(EPA, 2022)*

Furthermore, air quality models that combine emission inventory data with meteorology and atmospheric fate and transport mechanisms have been used to improve the spatial and temporal resolution of exposure estimates while incorporating both regionally transported and local pollution sources. Exposure models that incorporate exposure factors such as time-location-activity budgets and ambient pollutant penetration into the indoor environment have been used in epidemiological studies to provide additional exposure variability (Haluk Ozkaynak, 2013). A summary of epidemiology studies that investigated health effects of various pollutants is summarized in Table.10.

Table 2.10: Summary of air pollution exposure & epidemiology studies on pollutants

Study	Location	Health outcome		Exposure estimation approaches
New Jersey Triggering of Myocardial Infarction	New Jersey, USA	Transmural myocardial infarction	$PM_{2.5}$	1) Ambient monitoring 2) SHEDS 3) LBNL APP and infiltration models 4) Hybrid of (2) and (3)
Study of Particles and Health in Atlanta	Atlanta, GA, USA	Emergency department visits for: 1) respiratory disease 2) asthma/wheeze 3) cardiovascular disease (CVD)	$PM_{2.5}$, EC, SO_4, O_3, NO_x, CO	1) Ambient monitoring 2) Modeled regional background 3) AERMOD modeling 4) Hybrid of (2) and (3) 5) Exposure modeling (APEX and SHEDS)
Air pollution and respiratory health in NYC using case cross-over methods	New York, NY, USA	Hospital admissions for respiratory morbidity from SPARCS	$PM_{2.5}$, O_3	1) Ambient monitoring 2) SHEDS
NCSU SHEDS Study for the Effects of Particulate Matter on Health Outcomes	New York, NY, USA	Hospital admissions for: 1) Respiratory disease 2) Cardiovascular disease (CVD)	$PM_{2.5}$	1) Ambient monitoring 2) CMAQ 3) SHEDS
Satellite-based estimation of PM concentrations: application to COPD in Cleveland	Cleveland, OH, USA	Hospital admissions for acute exacerbation of chronic obstructive pulmonary disease (AECOPD)	$PM_{2.5}$	Hybrid statistical approach combining satellite remote sensing data (Aerosol Optical Depth) with ambient monitoring
Traffic Pollution and Health in London	London, UK		$PM_{2.5}$, NO_2, NO_x, PM_{10}	Hybrid approach combining CMAQ-urban with the KCLurban model

2.10 Summary

The extensive literature review covered various topics related to commodities supply and demand, volume of atmospheric emissions from various industries, emissions modeling, ecological impact of emissions, and mitigation techniques to control various emissions. The review also discussed topics from microeconomics including production and consumption function, labor-leisure model, and intertemporal choice models. The literature review confirms that demand of commodities will stay elevated in the future and companies will need to increase supply to meet these elevated levels of demand. Most production processes generate atmospheric emissions, which disperse in the atmosphere using advective and diffusive processes and exposure to these emissions results in harmful health impacts. In the absence of technological improvements, the scale of emissions around the globe is set to remain elevated causing further environmental damage. The government bodies can enforce emissions regulations to a point, beyond which certain declining sectors of the economy will rather choose to shut down production completely rather than comply with strict emissions control (Mary E Deily, 1991). The shutting down of industries poses negative economic consequences for the economy. Time after time, governments oscillate between tightening and losing emissions control for various reasons to balance environmental well-being as well as economic output. The literature review promotes the need for an integrated tool that can model the phenomena of emissions dispersion from multiple point and mobile sources at various levels of production, quantify impact of emissions on agents within a given geographical boundary and finally establish a quantitative relationship between economic productivity as a function of emissions control.

3. MATERIALS AND METHODS

The overall goal of the study is to create a simulation platform that would allow governments to calculate the economic productivity losses caused by constraints on emissions from both stationary and mobile sources. Population growth, combined with an increase in purchasing power, has increased demand for various commodities, leading to the expansion of industries. Many governments value industrial expansion because it provides appropriate job growth for a growing population. Emissions from the industrial and allied transportation sectors, on the other hand, represent severe environmental and health risks in both regional and global geographies. Efforts have been made to reduce emissions through the implementation of legislative, technical, and alternative green sources. The result of such emissions control has been mixed:

- the developed regions that have enacted stringent emissions controls have caused industries with a high emissions factor to contract and begin to rely on imports of such industries from other regions - pollution haven hypothesis (Arif, 2021).
- underdeveloped and developing regions with lax emissions control policies have expanded industrial expansion due to socioeconomic and geographic pressures, regardless of the scale of morbidity and mortality from industrial and transportation emissions.

In a nutshell, the enactment of stricter emissions limits is beset by the following conundrum: how to strike a balance between socioeconomic necessities and environmental security.

The analysis of emissions control on economic productivity requires integration of multiple concepts including graph theory, production functions, advection-diffusion mechanism, heuristics, consumption theory, vector mechanics, and particle systems. The dynamic nature of the problem necessitates the use of simulation to conduct goal-directed experiments. A simulation platform enables the prediction and evaluation of a system under varying experimental conditions, allows evaluation of alternatives, evaluate model performance, allow sensitivity analysis, virtual prototyping, testing, planning, acquisition, decision making, and proof of concept (Oren, 2018).

Positivism philosophy is used in our research methodology to generate testable hypotheses, identify key variables to manipulate, run empirical simulations, and develop an informed theory to contribute to the literature. The positivism approach is ideal for our problem because we are developing a functional relationship between explanatory factors (maximum discharge of emissions in 24 hrs.) and outcomes (ground level pollution concentration) (Park, 2020). The research uses inductive reasoning as a logical process to bind multiple established concepts, to establish a specific conclusion. In contrast to deductive reasoning, where the conclusion inference is certain, deductive reasoning's conclusion is only probable where the certainty is based on the strength of evidence. Is it advantageous, for example, to ban the formation of specific enterprises at the regional level to reduce emissions at the expense of economic development when emissions from neighboring regions pass through unaffected owing to weather phenomena? Depending on the testing environment, the results to the above question can be supportive or unsupportive. The inductive approach is a suitable approach when dealing with an outcome that is not a scientific certainty (Sauce, 2017).

74

The developed platform encapsulated following concepts to collectively simulate an imprecise economic system:

Programming
- Implementation of object oriented programming concepts including polymorphism and inheritence.

Vectors
- Eucledian vector functions including vector addition, subtraction, multiplication, linear interpolation, cross, and dot products.

Minimum spanning tree
- Implementation of Prim's alogrithm to connect all fixed entities using a minimum weighted graph

All pair shortest path
- Implementation of Floyd Warshall alogrithm to create an all pair shortest path matrix. The matrix is used for routing moveable objects on the minimum spanning tree network.

Metaheuristics
- Implementation of genetic alogrithm to solve NP-Vechile routing problem

Microeconomics
- Production function
- Demand function
- Labor leisure model
- Intertemporal choices
- Walrasian price stability

Exponential functions
- Population growth: population growth rate of boids is modeled using an exponential growth function
- Land rate: land rate distribution away from market centers are modeled using the exponential function.

Supply chain management
- Equilibrium order quantity
- Reorder point

System analysis
- M/M/c queing model: models waiting time, queue length as a function of arrival rate, service rate, and number of servers per station.

Fluid dynamics
- Navier-Stokes equation
- Puff dispersion model: Transient modelling of dispersion of pollutants from multiple point and mobile sources

Operations research
- Vechile routing problem: focuses on how to optimally route multiple trucks from a transport hub to execute multiple pickup and dropoff delivery orders
- Hub location problem

Macroeconomics
- Liquidity preference money supply model: controls the amount of money supply in economy as a function of interest rates, inflation rate, and economic ouput

3.1 Object / class / particle system

The simulation framework is made up of certain classes that are used to build various objects such as resource extraction units, industries, transportation hubs, markets, and population members. Each class is composed of several functions (production, consumption, move, etc.), variables (production inputs, demand utilities, and velocities, etc.) and constants. The simulation is based on a 2D geometry in which firms are randomly distributed and linked via a network for any mass transfers. Firms oversee production of n goods by converting intermediary feeds into finished products using labor, land, and capital inputs, which are subsequently transferred to population members for consumption to achieve a desired level of utility.

Let $\mathbb{C}$ be a special class comprised of constants $c_1, c_2, \dots, c_n$, variables $v_1, v_2, \dots, v_n$ and functions $f_1, f_2, \dots, f_n$. Let S be a basket of raw commodities $S = (s_0, s_1, \dots, s_n)$ and E be a basket of finished commodities $E = (e_0, e_1, \dots, e_n)$ where n is an exogenous variable : $n \geq 2$. The main class $\mathbb{C}$ is extended to 3 distinct subgroups: firms F, population B, and transport hubs H.

The $\mathbb{C}$ is extended to create following classes:

a. Resources R $\in F$
b. Industries I $\in F$
c. Warehouses W $\in F$
d. Markets M $\in F$
e. Hubs H $\in H$
f. Boids B $\in B$
g. Trucks T $\in H$

Each raw commodity s_i is produced by a set of disassociated resource extraction objects $R \rightarrow (r_0^{t_i}, r_1^{t_i} \dots, r_k^{t_i})$, whereas e_i is produced by a set of disassociated firm objects $I \rightarrow (i_0^{e_i}, i_1^{e_i} \dots, i_l^{e_i})$ where k, l are exogenous variable declared at the start of the simulation. The market objects M$\rightarrow (m_0, m_1, \dots, m_p)$ each carry a basket of finished goods E. The boid objects B$\rightarrow (b_0, b_1, \dots, b_q) : q \gg (k + l + q)$ each carry a basket of demand good E and perform functions like $invest()$, $spend$ (), $work$ (), $consume()$, etc. The warehouse objects W$\rightarrow (w_0, w_1, \dots, w_u) : u = p$ with each object w_i holding a basket E. The transport hub objects H$\rightarrow (h_0, h_1, \dots, h_x)$ with each object h_i holding an assortment of transport units $T = (t_0^{h_i}, t_1^{h_i}, \dots, t_{Kh}^{h_i})$. All objects are stored in an Array List < > with each object holding a specific index in the array. Objects are added in the system using various array commands including append () and remove ().

3.2 Vectors

Euclidean vectors are used to move boids and transport units in the 2D plane. Euclidean vector is an entity that has a magnitude and direction. Vector subtraction is used to reduce straight line distances between two objects whereas vector addition is used to expand such distances. The length of a vector is determined by its magnitude. The velocity of a given object per time-step is scaled via vector multiplication. The change in position of a given object $r \rightarrow (r_x, r_y)$ is given by:

$$r_{(t+1)} = r_t + v_t \Delta t + \frac{1}{2} a_t \Delta t^2 \qquad (3.1)$$

where a is acceleration, v is the current velocity, and Δt is time step. The a_t is given by $\hat{r}n$ where $\hat{r} = \frac{\vec{r}}{\sqrt{r_x \times r_x + r_y \times r_y}}$ is normalized vector magnitude and n is a multiplication term (Shiffman, The Nature of Code, Simulating Natural Systems with Processing, 2012).

Figure 3-1: Application of vectors to simulate attraction between a central body and 2,000 particles *(Henderson, n.d.)*.

3.3 Prim's algorithm

Transportation networks (railways, roadways, pipelines, power systems) connect multiple geographical locations to promote the efficient transfer of people, raw materials, commodities and energy. The production and consumption entities in our simulation are seeded at random locations on a 2D plane and require a network to move goods and people between various vertices while minimizing the sum of distances. The Prim's algorithm was selected to generate a minimal spanning - road network to connect geographical vertices (Akpan, 2017) (Bereg, n.d.). Prim's method was chosen above other possibilities (such as Kruskal's, Solin's, and Steiner Tree) due to its widespread use in solving MST problems. Prim's algorithm is a greedy

algorithm that finds a minimum spanning tree network in a weighted undirected graph.

Given a connected graph, $G = [V, E]$, with n vertices and m edges with non-negative weights, $w(e_i)$.Then sorting edges: $w(e_1) \leq \cdots \leq w(e_m)$. The output is a spanning tree, T, with a total weight being minimum. T is initialized with minimum edge weight e_1 and its two endpoints. The number of vertices in T is denoted by $v(T)$.

> Prim's - DO WHILE $v(T) < n$: interrogate edges (in order) until one is found that is incident with a vertex in T and does not form a simple circuit in T. Then, add this edge and its endpoint(s) to T (Greenberg, 1998).

In a nutshell, the algorithm starts with an arbitrary vertex v and expands to form a tree by repeatedly finding the lowest-cost edge that links new vertex. During execution, each vertex is labelled as either in the tree or unseen. In simple data structures, Prim's algorithm is implemented in $O(n^2)$ (Skiena, 2008).

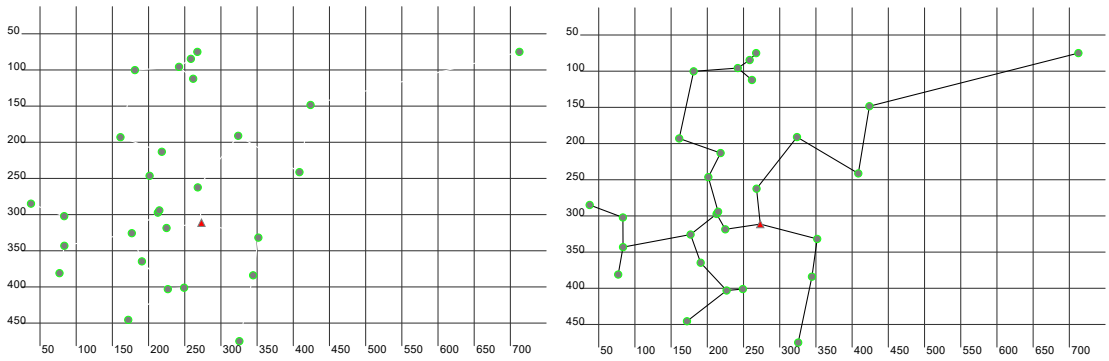

Figure 3-2: Application of Prim's Algorithm on 29 vertices to generate an MST.

3.4 Floyd Warshall algorithm

In everyday life, entities do not move in a straight line between two points, but rather use a shortest path on a network for traversal. In our simulation, Floyd Warshall

algorithm is used to generate all-pair shortest path matrix to facilitate pathfinding between various vertices. The Floyd-Warshall algorithm initiates by numbering each vertex in the graph g from 1 to n. The length of the shortest path from i to j is defined as $W[i,j]^k$, allowing only vertices number $1, \dots, k$ as possible intermediate. Initially, all pair shortest-path matrix consists of the initial minimum spanning tree. A n number of iterations are performed, where kth iteration allow only the first k vertices as possible intermediate steps on the path between each pair of vertices x and y. At each iteration, a new set of possible paths are added by inserting a new vertex as a possible intermediary.

$$W[i,j]^k = \min(W[i,j]^{k-1}, W[i,k]^{k-1} + W[k,j]^{k-1}) \quad (3.2)$$

```
Floyd (adjacency matrix *g)
    int i, j;                    /* dimension counters */
    int k;                       /* intermediate vertex counter */
    int dist_k;                  /* distance through vertex k */
            for(k = 1; k ≤ g; k++) do
                for(i = 1; i ≤ g ; i++) do
                    for(j = 1; j ≤ g; j++) do
                        dist_k = weight[i][k] + weight[k][j];
                        if (dist_k < weight[i][j]) do
                                weight[i][j] = dist_k
```

The Floyd Warshall algorithm is solved in $O(n^3)$ time and was chosen over Dijkstra's algorithm due to its practicality. The shortest path from x to y is the concatenation of the shortest path from x to k with the shortest path from k to y, which is reconstructed recursively given the all-pair shortest path matrix (Skiena, 2008).

3.5 Equilibrium order quantity (EOQ) / Reorder point (ROP)

The industries and mining firms in our simulation use intermediate and raw materials for production of goods. All firms including markets need to maintain sufficient stock levels to ensure uninterrupted production or sales of goods to customers. The two main costs associated with inventory management are the holding (warehousing costs, shrinkage loss, insurance, rent, overhead, etc.) and ordering costs (order communication, cost of ordering and receiving, transport cost, etc.). The Equilibrium Ordering Quantity (EOQ) is an inventory management system that establishes the quantity of a commodity such that the ordering and holding costs are minimized. The Reorder Point (ROP) of an item is a threshold at which the product needs an order placement for the replenishment of the stock to ensure uninterrupted trade operations (Senthilnathan, 2019).

The simulation utilizes the Equilibrium Order Quantity (EOQ) and Reorder Point (ROP) system for inventory management. Details are as follows:

a. All firms are initialized with arbitrary stock levels and reorder points.
b. All firms are initially linked with a supplier based on criteria of minimum distance G.
c. Each firm records unit of each good consumed (industries, mining) or sold (warehouses, markets) per operating cycle in an array → InvConArry
d. At the end of each operating cycle, each firm checks the stock levels of various commodities and if the stock level is below the ROP, a replenishment signal is generated.

e. An optimal supplier routine SUP is then initialized to performs following steps:

Given entity i with input j;

$\min Gidx = -1$

$\min Rcost = \infty$

$for(int\ k = 0; k < \Theta; \mathrm{k}++)\{$

$if(k == j)\{$

i. Calculate distance between entity i and entity k *(supplying input j).*

ii. Given freight rate per unit distance $\frac{T_c}{d}$, calculate total cost of freight between i, k.

iii. Calculate the total cost of procurement $\mathrm{ncstEx} =$ freight cost + commodity cost.

iv. if $(ncstEx < Rcost)$ {

$ncstEx = Rcost$

$Gidx = k$ }

if $\left(\mathrm{supplier(k).Inventory_{Level}} > freight_{carrying\ capacity}\right)\{Gidx = k\ \}$ } }

f. if $(Gidx != -1)$ then

i. Use InvConArry to calculate average daily consumption μ_c and related standard deviation σ_c.

ii. Extrapolate average daily consumption to calculate long-term demand D.

iii. Determine lead time L_t based on time difference between $[order_{time} - receiving_{time}]$ of last shipment. L_t is arbitrary at the start of the simulation.

g. Determine EOQ and ROP using following formula:

$$EOQ = \sqrt{\frac{2 \times c_o \times D}{c_h}} \text{ (3.3); } c_o = B + G\frac{T_c Q \epsilon}{d} \text{ (3.4); } R_p = R_l \times \sigma_c \times \sqrt{L_t} + \bar{c} \times L_t \text{ (3.5)}$$

where c_o is ordering cost, R_p is reorder point, c_h is holding cost, B is base charge, ϵ is transport charge exponent, and R_l is reliability of commodity supply.

h. A delivery order is then introduced with one of the transport hubs for transfer of stock from node k to node i.

3.6 Vehicle routing problem

In our simulation, a transport hub houses several trucks K_h with similar carrying capacities. An idle hub accepts pending delivery orders and signals customers with an acknowledgement. Orders are stored in an integer array $O_L = \{1,2, \dots n\}$ where n is total number of orders. Each order $o \in O_L$ contains following information: pickup vertex $(o \rightarrow i_o)$, drop-off vertex $(o \rightarrow j_o)$, load $(o \rightarrow L_o)$, load price $(o \rightarrow P_o)$. The orders $o \in O_L$ needs to distributed among $k \in K_h$ such that the sum of distances traversed by K_h is minimum.

A VRPSPD model (A. Subramanian, 2010) with one hub can be defined as follow: Let $G = (V, E)$ be a complete graph with set of vertices $V = \{0, \dots, n\}$ with a vertex o representing the depot $(V_o = \{0\})$. Each edge $\{i, j\} \in E$ has a non-negative cost c_{ij}

and each client $i \in V - V_o$ has a demand q_i for delivery and p_i for pickup. Let $C = \{1, \dots, v\}$ be the set of identical vehicles with carrying capacity Q. The VRPSPD consists of constructing a set of routes v such that:

i. all sum of costs is minimized.

j. a customer is visited by only a single vehicle.

k. all the pickup and delivery demands are achieved.

Mathematical formulation (VRPSPD) (Fermin Alfredo Tang Montane, 2002)

V : set of customers

V_o : set of customers including depot: $V_o = V \cup \{0\}$;

$V_P(V_D)$: set of pick up (delivery) clients: $V = V_P = V_D$

N : total number of clients: $N = |V|$;

$N_P(N_D)$: number of pick-up (delivery) clients: $N_P = |V_P|, N_D = |V_D|$ and $N = N_P = N_D$;

c_{ij} : distance between clients i and j

p_i : pick up demand of client $i, i = 1, \dots, N$

d_i : delivery demand of client $i, i = 1, \dots, N$

Q : vehicle capacity

NV : max number of vehicles

Decision variables are as follows:

$$x_{ij} = \begin{cases} 1, \text{if arc(i, j) belongs to the optimal set of routes;} \\ 0, otherwise; \end{cases}$$

y_{ij} : demand picked up in clients routs up to node i and transported in arc (i, j);

z_{ij} : demand to be delivered to clients routed after node i and transported in arc (i, j);

The formulation of VRPSPD is then given by:

$\min \sum_{i=0}^{N} \sum_{j=0}^{N} c_{ij} x_{ij}$ ← objective function seeking to minimize total distance …

subject to

$\sum_{i=0}^{N} x_{ij} = 1, \quad j = 1, \dots, N$

$\sum_{j=0}^{N} x_{ij} = 1, \quad i = 1, \dots, N$ (each client is visited by exactly one vehicle)

$\sum_{j=0}^{N} x_{ij} \leq NV$ … limit on number of vehicles used.

$\sum_{i=0}^{N} y_{ji} - \sum_{i=0}^{N} y_{ij} = pj, \quad \forall j \neq 0$ … pickup demand is satisfied.

$\sum_{i=0}^{N} z_{ji} - \sum_{i=0}^{N} z_{ij} = dj, \quad \forall j \neq 0$ … drop-off demand is satisfied.

$y_{ij} + z_{ij} \leq Q x_{ij}, \quad i, j = 0, \dots, N$ … pickup and delivery demand are transported using arcs included in the solution; imposition of an upper limit on the total volume transported by a vehicle in any given section of the route.

$x_{ij} \in \{0,1\}, \quad i, j = 0, \dots, N$

$y_{ij} \geq 0, \quad i, j = 0, \dots, N$ …each vehicle leaves the depot with the volume equivalent to the sum of the delivery demands of the customers in the route serviced by that vehicle.

$z_{ij} \geq 0, \quad i, j = 0, \dots, N$ …each vehicle returns to the depot with the volume equivalent to the sum of the pick-up demand on the customers in the same route.

3.7 Genetic algorithm (GA)

The *Vehicle Routing Problem* with simultaneous pickup and delivery (VRPSPD) is an NP-Hard problem. Heuristic methods have proved to be more appropriate for dealing with NP-Hard problems in terms of solution quality vs the computational cost (A. Subramanian, 2010). In our simulation, we used the Genetic algorithm (GA) heuristic to solve the VRPSPD problem, with the goal of minimizing the sum of distances traveled by all vehicles. The GA have been implemented in various combinatorial optimization problems, including certain types of vehicle routing problems (Baker, 2003).

The principles of GA are as follows: A population of solutions is maintained, and a reproductive process allows parent solutions from the population to be selected. Offspring solutions with some of each parent's characteristics are produced. Each solution's fitness can be related to the objective function value, in this case the total distance travelled, as well as the level of any constraint violation. Similarly, to biological processes, offspring with relatively high fitness levels are more likely to survive and reproduce, with the expectation that fitness levels will improve as the population evolves (Baker, 2003).

A layout of GA to solve VRPSPD is as follows: Given a list of orders $O_L = \{0,1,2,3 \dots, n\}$ with each order $o \in O_L$ containing a pickup vertex $(o \to i_o)$ and a drop-off vertex $(o \to j_o)$. Let K_h be a set of homogenous trucks.

Initializing:

1. Create a population of solutions $P_{vrt} = \{p_0, p_1, \dots, p_n\}$ by randomly sorting O_L. A 5 order O_L can have following population solutions:

$P_{vrt} = \{\, p_0 \leftarrow (0,1,2,3,4), p_1 \leftarrow (2,4,1,0,3), p_2 \leftarrow (1,2,0,3,4), \ldots p_n \leftarrow (1,2,3,0,4)$

2. Randomly split each population p_i and distribute orders among trucks $k \in K_h$.

For example, populations p_0, p_1 can be assigned among 3 trucks as follow:

$$T_{vrt(0)} = \{k_0 \leftarrow (0,1), k_1 \leftarrow (2,3), k_3 \leftarrow (4)\}$$

$$T_{vrt(1)} = \{k_0 \leftarrow (2,4), k_1 \leftarrow (1,0,3), k_3 \leftarrow \emptyset\}$$

Loop:

$dist_{min} = \infty;\ P_{best}\ \{\}$;

for (int $p = 0; p < P_{vrt}; p++$) **loop**

Step 1: $dist_{sum} = 0;$

for (int $t = 0; t < K_h; t++$) {

waypoints { } ;

waypoints append hub vertex $G \leftarrow h$ … hub location is the starting point for a truck

for (int $o = 0; o < k_t; o++$) {

waypoints append ($i_o \in k_o$) …append pick up vertex corresponding to order o

waypoints append ($j_o \in k_o$) …append drop-off vertex corresponding to order o

}

waypoints append hub vertex $G \leftarrow h$ … hub location is the end point for a truck

for (int $s = 0; s <$ waypoint.length $- 1; s++$) {

dist_{sum} += Floyd-Warshall (waypoint[s], waypoint[$s + 1$])

… calculate sum of distances by adding distance between vertices (s) &

$(s + 1) \in$ waypoints array … }

}

$$if\ (dist_{sum} < dist_{min})\ \{\ dist_{min} = dist_{sum}\ , P_{best} = P_{vrt}\ \}$$

Step 2: $P_{\text{fitness(p)}} = 1/\text{pow}(\text{dist}_{\text{min (p)}}, 8)$

Step 3: $P_{\text{normal(p)}} = P_{\text{fitness(p)}} / \sum_{p=0}^{P_{vrt}} P_{\text{fitness(p)}}$

Step 4: $P_{\text{vrt(p)}_{\text{new}}}$: Perform cross over between two populations, followed by mutation to create a new population.

(Shiffman, 2017)

3.8 Production function (Profit maximization, cost minimization)

The Cobb-Douglas production function has been incorporated into our simulation to indicate the maximum product Q that a firm can produce from a given set of inputs, including land B, labor L, and capital K. The corresponding costs associated with each input is defined by $x(\frac{\$}{acre})$, $w(\frac{\$}{hr})$, and $y(\frac{\$}{unit})$ respectively. Raw and intermediate feeds are used by resource and manufacturing firms, which adds to the cost of each manufacturing run. The additional cost is calculated as $V(Q) = \sum_{i=1}^{n} r_i\, c_i$, where c_i is the cost of intermediate r_i. Firms can change labor inputs in the short term, while land and capital can only be changed over time. Depending on market conditions a firm can pick a profit maximization or cost minimization approach with an exogenous minimum output objective Q_{min}.

The profit maximization function can be written as:

$$\max \pi = M_p(Q) - C - V(Q)\ (3.6),\ Q = AL^p B^q K^r\ (3.7), C = Lw + Bx + Ky\ (3.8)$$

where π is firm's profit, M_p is market price of product, A is technology factor, and p, q, r are exponents of input factors: $p \geq 0, q \geq 0, r \geq 0;\ p + q + r \leq 1$ (concave function – diminishing rate of returns to input factors).

Taking a partial derivative of L, B and K with respect to π results:

$$\frac{d\pi}{dL} = M_p(ApL^{p-1}B^qK^r - w - VApL^{p-1}B^qK^r) = 0 \qquad (3.9)$$

$$\frac{d\pi}{dB} = M_p(AL^pqB^{q-1}K^r - x - VAL^pqB^{q-1}K^r) = 0 \qquad (3.10)$$

$$\frac{d\pi}{dB} = M_p(AL^pB^qrK^{r-1} - y - VAL^pB^qrK^{r-1}) = 0 \qquad (3.11)$$

Solving for L, B, K

$$L = \left(\frac{M_pApB^qK^r - VApB^qK^r}{w}\right)^{\frac{1}{1-p}};\ B = \left(\frac{M_pAqL^pK^r - VAqL^pK^r}{x}\right)^{\frac{1}{1-q}};\ K = \left(\frac{M_pArB^qL^p - VArB^qL^p}{y}\right)^{\frac{1}{1-r}}$$

The optimal production level Q^* to achieve maximum profitability π^* can be calculated by solving the following Equations simultaneously.

$$L = \left[Ap\left(\frac{L^pB^qK^r}{L^p}\right)\left(\frac{M}{w} - \frac{V}{w}\right)\right]^{\frac{-1}{p-1}};\ B = \left[Aq\left(\frac{L^pB^qK^r}{B^q}\right)\left(\frac{M}{x} - \frac{V}{x}\right)\right]^{\frac{-1}{q-1}};\ K = \left[Ar\left(\frac{L^pB^qK^r}{K^r}\right)\left(\frac{M}{y} - \frac{V}{y}\right)\right]^{\frac{-1}{r-1}}$$

$s.t \quad V < M_p$

The *cost minimization* function can be written as:

$$\min C = Lw + Bx + Ky \qquad (3.12)$$

s.t $AL^pB^qK^r = Q_{min}$

The optimal values of L, B, K can be calculated by solving following Lagrangian:

$$\mathcal{L} = Lw + Bx + Ky + \lambda(Q_{min} - AL^pB^qK^r) \tag{3.13}$$

Differentiating with respect to L, B, K and λ yields:

$$\mathcal{L}_L = w - ApL^{p-1}B^qK^r\lambda = 0;\ \mathcal{L}_B = x - AL^pqB^{q-1}K^r\lambda = 0;$$

$$\mathcal{L}_K = y - AL^pB^qrK^{r-1}\lambda = 0;\ \ \mathcal{L}_\lambda = Q_{min} - Lw + Bx + Ky = 0$$

Solving for L and K:

$$\frac{w}{x} = \frac{ApL^{p-1}B^qK^r\lambda}{AL^pqB^{q-1}K^r\lambda} \Longrightarrow L = \frac{Bpx}{qw}\ ; \quad \frac{x}{y} = \frac{AL^pqB^{q-1}K^r\lambda}{AL^pB^qrK^{r-1}\lambda} \Longrightarrow K = \frac{Brx}{qy}$$

Solving for B:

Substituting value of L, K in the production function

$$Q_{min} = A\left(\frac{Bpx}{qw}\right)^p B^q \left(\frac{Brx}{qy}\right)^r \tag{3.14}$$

$$Q_{min} = A\left(\frac{px}{qw}\right)^p \left(\frac{rx}{qy}\right)^r B^{q+p+r} \tag{3.15}$$

$$\frac{Q_{min}}{A}\left(\frac{px}{qw}\right)^{-p}\left(\frac{rx}{qy}\right)^{-r} = B^{q+p+r} \tag{3.16}$$

$$B^* = \left(\frac{Q_{min}}{A}\right)^{\frac{1}{p+q+r}}\left(\frac{px}{qw}\right)^{\frac{-p}{p+q+r}}\left(\frac{rx}{qy}\right)^{-\frac{-r}{p+q+r}} \tag{3.17}$$

Solving for L, K:

$$L = \frac{B^*px}{qw}, \qquad K = \sqrt[r]{\frac{Q_{min}}{AL^pB^{*q}}}$$

3.9 Demand function

In simulation, each boid has a basket of goods $X = (x_o, x_1, \dots, x_n)$ each of which provides a utility u_i from consumption. Consumption of products occurs solely when a person is at home and is calculated using the following function: $x_o = x_o - \log(x_o)$. Important contemporary consumer demand functions i.e., the Hicksian and Marshallian demand functions have been implemented to simulate demand of various commodities in our simulation. The formulation of both functions is as follow:

Consider a profit maximization decision maker (PMDM) with access to n goods in the economy. Let x_i represent the quantity of the i_{th} good consumed $\Longrightarrow i = 1{:}\, n$, let p_i be the price of the ith good and m being the income of the agent. The agent's utility function can be described as $u = u(x_1, x_2, \dots, x_n)$ with a budget constraint of $\sum_{i=1}^{n} p_i x_i = m$. One of the two sub-problems for the PMDM is:

$$\min x_0, x_2, \dots, x_n \sum_{i=1}^{m} p_i x_i \qquad (3.18)$$

$$s.t{:}\, u(x_1, x_2, \dots, x_n) - \bar{u} = 0$$

Solving the 1st order condition of above Equation yields: the Lagrange multiplier $(viz., \lambda = \lambda(p_1, p_2, \dots, p_n, u)$ and the PMDM's jth of n Hicksian demand function viz.,

$$x_j^H = x_j^H(p_1, p_2, \dots, p_n;\, u) = \underset{(x_1, x_2, \dots, x_n)}{\arg\min} \{\sum_{i=1}^{n} p_i x_i | \bar{u} \le u(x_1, x_2, \dots, x_n)\} \qquad (3.19)$$

where superscript H denotes "Hicksian" and the PMDM expenditure function, viz.,

$$m = e(p_1, p_2, \dots, p_n;\, u) = \underset{(x_1, x_2, \dots, x_n)}{\min} \{\sum_{i=1}^{n} p_i x_i | \bar{u} \le u(x_1, x_2, \dots, x_n)\} \qquad (3.20)$$

The second sub-problem of the PMDM is the dual of the constrained utility-maximization problem, viz.,

$$\underset{(x_1, x_2, \dots, x_n)}{max} \quad u(x_1, x_2, \dots, x_n) \qquad (3.21)$$

$$s.t. \sum_{i=1}^{m} p_i x_i - m = 0 \quad (3.22)$$

The related Lagrange function is:

$$\mathcal{L} = u(x_1, x_2, \dots, x_n) - \lambda(\sum_{i=1}^{n} p_i x_i - m) \quad (3.23)$$

Solving the 1st order conditions associated with the above Equation yields: a Lagrange multiplier (viz., $\lambda = \lambda(p_1, p_2, \dots., p_n;\ m)$) and the PMDM's jth of n Marshallian demand functions, viz.,

$$x_j^M = x_j^M(p_1, p_2, \dots, p_n;\ m) = \underset{(x_1, x_2, \dots, x_n)}{\arg\max} \{u(x_1, x_2, \dots, x_n) | \sum_{i=1}^{n} p_i x_i \leq m\} \quad (3.24)$$

where M denotes the "Marshallian" and the PMDM's indirect utility function, viz.,

$$u = v(p_1, p_2, \dots, p_n;\ m) = \max_{(x_1, x_2, \dots, x_n)} \{u(x_1, x_2, \dots, x_n) | \sum_{i=1}^{n} p_i x_i \leq m\} \quad (3.25)$$

A boid spends the least of the Hicksian and Marshallian demands in our scenario (Sproule, 2013).

3.10 Warehouse location problem

In simulation, warehouses are essential components of supply chain. The warehouses nodes act as a material buffer to accommodate variability in supply chain caused by intermittent production and assist in consolidation of products from multiple suppliers for efficient transfer to customers (Jinxiang Gu, 2007). The location of a warehouse is a key factor that affects its profitability; the location of a warehouse should be such that the fixed cost of operation (land, rental, building) and transportation costs associated with material flows from suppliers (industries) – from warehouse to markets are as low as possible. We have implemented the Hub location problem to spatially distribute multiple warehouses such that the above stated objective can be reasonably achieved.

The Hub location problem (HLP) deals with the problem of minimizing the total cost of locating hubs and transporting cargo flows through the hub network. In the p-hub median problem (pHMP) the objective is to locate p hubs in the network such that the total cost of transportation flows through the network is minimized (Mehrdad Mohammadi, 2011). In a multiple allocation p-HLP model, each applicable non-hub node can be allocated to one or multiple hubs. The criterion is $Mini - Sum$, with solution domain being the $network$, the hub nodes are linked together, and every non-hub node can be linked multiple hubs. The number of hubs p is defined exogenously with model outputs being binary. The mathematical formulation of the multiple allocation p-Hub median location problem is defined as follows:

$$\min \sum_i \sum_j \sum_k \sum_m C_{i,j}^{km} h_{i,j} Z_{i,j}^{km} \quad (3.26)$$

Subject to:

$\sum_k X_k = P$ … exactly p hubs are selected.

$\sum_k \sum_m Z_{ij}^{km} = 1, \forall\, i,j$ … each origin-destination pair (i,j) is allocated to hub (i,k)

$Z_{ij}^{km} \leq X_m, \quad \forall\, i,j,k,m$ … demand for origin node i to destination node j cannot be

$Z_{ij}^{km} \leq X_k, \ \forall\, i,j,k,m$ allocated to a hub pair (k,m) unless nodes (k,m) are selected

$Z_{ij}^{km} \geq 0, \quad \forall\, i,j,k,m$ … decision variable type

$X_k \in \{0,1\}, \quad \forall\, k$

The $C_{i,j}^{km}$ is defined as the unit transportation cost between start node i, end node j, and hub nodes k and m. $C_{i,j}^{km} = C_{i,k} + \alpha C_{k,m} + C_{m,j}$ (3.27)

The outputs of the problem are as follows: X_j is 1 when a hub facility is located at node j (and o, otherwise), and Z_{ij}^{km} which is the flow from the origin node i to the

destination j via hub facilities located at nodes k and m (Farahani, 2013).

3.11 M/M/c queuing

The M/M/c queuing model is used to estimate the number of service stations necessary at each market node. The arrival of customers at a given market is assumed to follow a Poisson distribution with an arrival rate λ with each service station having an independent and identical distributed exponential service time, with a mean of $1/u$. The number of service stations c is determined by a cost minimization problem in which only enough service stations are added to each market to ensure that traffic intensity $\rho = \frac{\lambda}{c\mu} < 1$. The probability that all service stations will be idle p_o is:

$$p_o = \left(\frac{r^c}{c!(1-\rho)} + \sum_{n=0}^{c-1} \frac{r^n}{n!}\right)^{-1} \quad , \; r = \lambda/u \tag{3.28}$$

The length of the queue (customer waiting in line) L_q and waiting time W_q is:

$$L_q = \left(\frac{r^c \rho}{c!(1-\rho)^2}\right) p_o \quad , \; W_q = L_q/\lambda \tag{3.29}$$

The system length (total number of customers waiting in line and being served) L and total system waiting time W are given by:

$$L = r + \left(\frac{r^c \rho}{c!(1-\rho)^2}\right) p_o \tag{3.30}$$

$$, \quad W = \frac{1}{\mu} + \left(\frac{r^c \rho}{c!(c\mu)(1-\rho)^2}\right) p_o \tag{3.31}$$

Markets respond dynamically to traffic intensity; as p decreases, the number of service stations decreases accordingly, and as p increases, more service stations are added to the market. The addition of each service station raises the market's operating costs (Donald Gross J. F., 2008).

3.12 Navier-Stokes Equation

Most production and transportation activities produce gaseous emissions, which, depending on the length of exposure and concentration, can cause a variety of health problems and ecological harm. Gaseous pollutants are dispersed and removed from the atmosphere by multiple mechanisms including advection, diffusion, decay, and absorption. The Navier-Stokes Equation can be used to model emission motion in fluid fields under a variety of situations.

The Navier-Stokes Equation is the simplest way to model viscous incompressible fluid motion that is consistent with mass and momentum conservation principles, as well as Stokes hypothesis that internal viscosity forces must be invariant with respect to any superimposed rigid motion of the reference frame (Heywood, 2006). The Navier-Stokes Equation for the motion of an incompressible, constant density, viscous fluid is:

$$\frac{\partial \mathrm{q}}{\partial \mathrm{t}} + (q\nabla)q = -\frac{1}{\rho}\nabla P + \upsilon\nabla^2 q, \quad div\, q = 0 \tag{3.32}$$

where $q(x,t)$ donates the velocity vector, $P(x,t)$ the pressure, and the constants ρ and υ are the density and kinematic viscosity respectively. The system is considered in 2/3 spatial dimensions with a specified initial velocity field $q(x,0) = q_o(x)$ and physically appropriate boundary conditions (Friedlander, 2006). The atmospheric diffusion of pollutant can be assumed to follow Fick's law, which states that the diffusive flux is proportional to the concentration gradient or $(q.\nabla)q = -\mathbf{K}\nabla C$ (3.33). The negative sign ensures that the contaminant flows from regions of high concentration to regions of low concentration and the diffusion coefficient $\mathbf{K}(\vec{x}) =$

daig(K_x, K_y, K_z) (3.34) is a diagonal matrix with entries being the turbulent eddy diffusivities (M.Stockie, 2011).

3.13 Puff dispersion model

The Gaussian plume dispersion is a common model to estimate downwind ambient concentration of air pollutants from sources such as industrial plants, vehicular traffic, or accidental chemical release.

The formulation of Gaussian plume dispersion traces its origin to Navier-Stokes Equations; a set of mathematical Equations defining fluid flows in nature. The turbulent diffusion of a non-reacting pollutant in the atmosphere can be described as:

$$\frac{\partial C}{\partial t} = \vec{\nabla} \cdot \vec{\mathrm{K}} \cdot \vec{\nabla} C - \vec{\nabla} \cdot \vec{\mathrm{u}} C + S \quad (3.35)$$

where C is the concentration gradient, $\vec{K}$ is the diffusivity tensor, $\vec{u}$ is the average wind velocity and S is a source function. The boundary conditions for Eq (3.35), in which the origin of the right-handed coordinate system is at h above the ground with z positive downward, are:

$$C(x, y, z, 0) = I(x, y, z), \lim C(x, y, z, t) = 0, x, y \rightarrow \infty, \quad (3.36)$$

$$\frac{\partial C}{\partial t}(x, y, 0, t) = 0, \frac{\partial C}{\partial z}(x, y, h, t) = \beta C \quad (3.37)$$

… initial concentration I, conservation of pollutant, non-permeability of an inversion layer at height h, and absorption at the ground respectively. Per the formulation discussed by Lamb and Neiburger using the green's function following assumption are made:

1. Initial concentration $I\ (x, y, z) = 0$
2. Steady state emissions from point source (Q)
3. No absorption of generation by ground $(\beta = 0)$
4. Constant wind in one direction $(u = const, v = w = 0)$
5. No inversion layer $(h \rightarrow \infty)$
6. Crosswind and vertical diffusivities wary with downwind distance only and are constant in the diffusion domain.
7. No downwind diffusion $(K_x = 0)$

Given above assumptions, the Equation (3.35) transforms into following:

$$C(x, y, z, t) = \int_0^h \int_{-\infty}^{+\infty} \int_{-\infty}^{+\infty} \int_0^t \frac{E(\mathcal{E}-x', y-y' t-t')}{4\pi \vec{K} x^{1/2}\, \vec{K} y^{1/2}} \times M(z - z', t - t')\, S(x', y', z', t') dt' dx' dy' dz' \quad (3.38)$$

where $E = \exp\left[\frac{-(\mathcal{E}-x')^2}{4\bar{K}_x} - \frac{(\eta-y')^2}{4\bar{K}_y}\right]$ (3.39), $M = \sum_{P^2} \frac{2(P2^2+\beta^2)\cos(P_2 z')\cos(P_2{}^z)}{h(P2^2+\beta^2)+\beta} \exp[-\bar{K}_z P2^2]$ (3.40)

which is summed over the roots, $P_2 h = n\pi, n = 0,1,2, \ldots, of P_2\ \tan(P_2 h) = \beta$.

The quantities $K_{x,y,z} = \int_{t'}^{t} K_{x,y,z}\,(t - t')dt$,

$$\mathcal{E} = x - \int_{t'}^{t} u(x, y,)dt\,, \eta = y - \int_{t'}^{t} v(x, y,)dt$$

For long term avg pollution concentration, it is assumed that u = constant and $\beta = 0$. Then $\bar{K}_i = K_i(t - t')$ (3.41) where $i = x, y, z, \mathcal{E} = x - u(t - t'), \eta = y$. For a steady state point source with mass emission rate

$$Q\colon\ S(x, y, z, t) = Q\delta(x - x')\delta(y - y')\delta(z - z') \quad (3.42)$$

where δ is Dirac delta function.

To neglect downwind diffusion K_x must approach 0. Using the relation

$\lim_{\sigma\to 0} \frac{1}{\sqrt{2\pi\sigma}} exp\left[-\frac{(m-m')^2}{2\sigma^2}\right] = \delta(m-m')$ (3.43) and the definition $\sigma i^2 \equiv$

$2K_i(t - t') \equiv 2K_i \frac{(x_i - x_{io})}{u}$ (3.44), and letting $K_x \to 0$, Eq.(3.38) transforms to;

$$C(x,y,z,t) = \frac{Q}{\sqrt{\pi}hK_y^{1/2}} \sum_{n=0}^{\infty} \cos\left(\frac{\eta\pi}{h}z\right) \cos\left(\frac{\eta\pi}{h}z'\right) \times \int_0^{\infty} \frac{\exp - \left[\frac{(y-y')^2}{4K_y(t-t')} - (\frac{\eta\pi}{h})^2 K_z(t-t')\right]}{(t-t')^{1/2}} \times \delta[x - x' - u(t-t')]dt' \quad (3.45)$$

Now $\delta[x - x' - u(t-t')] = \left(\frac{1}{u}\right)\delta\left[\frac{x-x'}{u} - (t-t')\right]$ (3.46), thus eq (3.45)

integrates to:

$$C(x,y,z,t) = \frac{Q}{\sqrt{\pi}hK_y^{1/2}u} (\frac{u}{x-x'})^{1/2} \sum_{n=0}^{\infty} \cos\left(\frac{\eta\pi}{h}z\right) \cos\left(\frac{\eta\pi}{h}z'\right) \times exp\left[\frac{-(y-y')^2}{4K_y(t-t')} - (\frac{\eta\pi}{h})^2 K_z\left(\frac{x-x'}{u}\right)\right] \quad (3.47)$$

which describes puff of pollutant released at $t = t'$, progress of the front of which at $x = x' + ut$ (3.48) defines a plume. For no inversion layer $h \to \infty$, and using Eq. (3.44), Eq. (3.47) transforms to.

$$C(x,y,z,t) = \frac{2Q}{\sqrt{2\pi}u\sigma_y} \frac{1}{h} \sum_{n=0}^{\infty} \cos\left(\frac{\eta\pi}{h}z\right) \cos\left(\frac{\eta\pi}{h}z'\right) \times exp\left[\frac{-(y-y')^2}{2\sigma_y^2} - (\frac{\eta\pi}{h})^2 K_z t\right] \quad (3.49)$$

$\frac{1}{h}\sum_{n=0}^{\infty} c\,os\left(\frac{\eta\pi z}{h}\right) \cos\left(\frac{\eta\pi z'}{h}\right) = \sum_{n=0}^{\infty} \frac{1}{h} f(\frac{n}{h})$ (3.50), considering the left-hand side Equation as a periodic function with period h extending from $-\infty\, to + \infty$ and writing the period as an interval ΔS one gets $\sum_{n=-\infty}^{\infty} \Delta S f(n, \Delta S)$. Recognizing that as $h \to \infty, \Delta S \to 0$, that

$\lim_{\Delta S\to 0} \sum_{n=-\infty}^{\infty} f(n,\Delta S)\Delta S = \int_{-\infty}^{\infty} f(S)dS$, substituting $\frac{\eta\pi}{h} = k, z' = H$, using the relation $\cos(a\theta)\cos(a\phi) = \frac{1}{2}\{cos[a(\theta+\phi)] + \cos[a(\theta-\phi)]\}$, and Eq (3.44), Eq (3.47) can be written as:

$$C(x,y,z) = \frac{Q}{2\pi u \sigma_y \sigma_z} exp\left[\frac{-(y-y')^2}{2\sigma_y^2}\right]\left\{exp\left[\frac{-(z-H)^2}{2\sigma_z^2}\right] + exp\left[\frac{-(z+H)^2}{2\sigma_z^2}\right]\right\} \quad (3.51)$$

(Wm. J. Veigele, 1978)

The wind velocity u is corrected using the wind power law: $u = u_{ref}(\frac{h_s}{z_{ref}})^p$ (3.52) where u: wind speed at stack outlet height h_s, u_{ref}: wind speed at wind speed measurement height $z_{ref}(\frac{m}{s})$, p is wind profile exponent corresponding to the atmospheric stability. σ_y, σ_z corresponds to the *Pasquil – Gifford* curves. The final plume rise due to thermal buoyancy can be calculated using *CONCAWE* Equation: $H = h_s + \Delta h$ (3.53), $\Delta h = 0.175\sqrt{Q_H}\, u^{\frac{-3}{4}}$ (3.54), $Q_H = \rho C_p Q(T_s - T_A)$ (3.55) where h_s: stack height (m), Q_H: emitted heat quantity (cal/s), ρ: gas density at 0^0C (1.293 x 10^3 g/m^3), C_p: Isobaric specific heat (0.24 cal/K/g), Q: Exhaust gas volume per unit time (m^3_N/s), T_s: Exhaust-gas temperature (C), T_A: Ambient temperature (C) (Ministry of Economy, Trade and Industry (METI), Japan, 2005).

In our simulation, we faced challenges such as variable wind directions, large scale transport distances, varying emission rates, and mobile emissions, which necessitated the use of the puff model. A puff model, unlike a plume model, emits emissions independent of the source, allowing the puff to respond to the meteorology immediately surrounding it. Puffs can also be tracked across multiple sampling periods until they have either been completely diluted or tracked across the entire modeling domain and out of the computational area (Lakes Environmental). The puff model is improved on the Gaussian plume dispersion model to be applied to non-stationary and non-homogenous flow by representing a plume by a series of

independent elements that evolve in time a s function of temporally and spatially varying meteorological condition. The accuracy of the puff model depends on the accurate data of advection velocity field (Young-Rae Jung, 2003). The advection field in our simulation is generated using Perlin noise function.

The contribution of a single puff to a receptor can be formulated as:

$$C(x,y,z) = \frac{M}{(2\pi)^{\frac{3}{2}}\sigma_y^2\sigma_z} \exp\left[-\frac{1}{2}\left(\frac{x}{\sigma_y}\right)^2\right] \exp\left[-\frac{1}{2}\left(\frac{y}{\sigma_y}\right)^2\right] \exp\left[-\frac{1}{2}\left(\frac{z-H}{\sigma_z}\right)^2\right] \qquad (3.56)$$

where M is the mass of a designated puff, i.e., $M = Q\Delta t$. Δt is the time interval of puff emission. The σ_y, σ_z are lateral and vertical dispersion values calculated using the Pasquil-Gifford curves [10].

The total concentration at position $\vec{r}(x,y,z) = \int_0^\infty \dot{C}$, where $\dot{C}$ is all puffs in the domain. The center of a puff is advected according to local time varying wind vector. The growth of σ_y, σ_z at time t and $t+1$ is initialized from computing the virtual horizontal distance d_y and vertical distance d_z.

$$d_y = \left[\frac{\sigma_y(t)}{a_y}\right]^{\frac{1}{b_y}} (3.57), \qquad d_z = \frac{\sigma_z(t)^{1/b_z}}{a_z} \quad (3.58)$$

The computation of Δd, the downwind distance of the puff travelled in the time interval Δt, is given by: $\Delta d = \vec{v}\left(t + \frac{\Delta t}{2}, x, y, z\right)\Delta t$ (3.59) where $\vec{v}(t,x,y,z)$ refers the wind vector. The new standard deviation at $t + \Delta t$ is given as:

[10] See page 10-12 for more detail: (Ministry of Economy, Trade and Industry (METI), Japan, 2005)

$$\sigma_y(t+\Delta t) = a_y\left(d_y + \Delta d\right)^{by}, a_z(t+\Delta t) = a_z(d_z+\Delta d)^{bz} \quad (3.60)$$

The effective emission heigh H is the sum of emitter height h_e and buoyancy induced plume $\Delta h. \rightarrow h_e = h_s + \Delta h$ (3.61)

The Δh is calculated using the CONCAWE Equation:

$$\Delta h = 0.175 Q_H^{1/2} u^{-3/4}, Q_H = \rho C_p Q(T_s - T_A)$$

where ρ: Gas density at $0^o C$ $\left(1.293 \times 10^3 \frac{g}{m^3}\right)$, C_p: Isobaric specific heat $(0.24\ cal/K/g)$, Q: Exhaust gas volume per unit time $(\frac{m_N^3}{s})$, T_s: Exhaust gas temperature (C^o), T_A: Ambient temperature (C^o).

(Ministry of Economy, Trade and Industry (METI), Japan, 2005)

A decay term is integrated in the puff dispersion model to simulate pollutant removal due to physical and chemical processes: $D = \exp(R\frac{x}{u_s})$ (3.62) where R is the decay coefficient (s^{-1}), x is downwind distance, and u_s is wind velocity.

The $R = \frac{0.693}{T_{\frac{1}{2}}}$ (3.63), where $T_{1/2}$ is pollutant half-life.

(U.S. Environmental Protection Agency, 1995)

3.14 Population growth

The population growth in our simulation is modeled using an exponential growth model which assumes that rate of population growth is proportional to the current population: $\frac{dP}{dt} = kP$ (3.64), where k is the rate of population growth per year and P is the population. The differential Equation yields: $P(t) = Ce^{kt}$ (3.65). The

exponential growth model was used because of its simplicity and ability to accurately predict population rise in recent years (Hathout, 2013).

The simulation employs an exponential growth model with an exogenous rate of growth k to calculate the time interval Δt between each successive addition of boid to population array. Given the exponential growth Equation, the Δt can be derived as following:

$$(P+1) = Pe^{kt} \Longrightarrow \frac{P+1}{P} = e^{kt} \Longrightarrow \ln\frac{P+1}{P} = \ln e^{kt} \Longrightarrow \ln\frac{P+1}{P} = kt$$

$$\therefore \Delta t = \frac{\ln\left(\frac{P+1}{P}\right)}{k} \tag{3.66}$$

3.15 Commodities pricing

In our simulation, the price of commodities is dynamic and changes depending on differences in demand and supply volumes. For a commodity x the demand and supply curves can be donated respectively $\rightarrow x_D = D(p, M)$, $x_S = S(p)$ where M is the money income, and p is price of commodity. The equilibrium price p_e is given by:

$$D(p^e, M) - S(p^e) = 0 \tag{3.67}$$

The rate of change of price in response to excess demand can be given by:

$$\frac{dp}{dt} = g\big(D(p, M) - S(p)\big) = g(E(p)) \tag{3.68}$$

where $g' > 0$. The price of the commodity would be adjusted upward or downward in accordance with sign of excess demand. The adjustment mechanism of related to price stability with relation to time t is given by following differential Equation:

$$\frac{dp}{dt} = (g'E')(p - p^e) \Longrightarrow \frac{dp}{dt} = p^e + (p^o - p^e)\exp(g'E')t \quad (3.69)$$

where p^o in the initial price. The equilibrium price chance per change in income M is given by:

$$\frac{\partial \mathrm{p^e}}{\partial \mathrm{M}} = -\frac{D_M}{D_p - S_p} \quad (3.70)$$

The indicates that a rise in income M, increases the demand of commodity x which leads to a new equilibrium price p^e.

(Silberberg, 1990)

3.16 Liquidity preference-money supply (LM) model

In our simulation, the interest rate r is an endogenous variable defined by the LM model.

$$r(t+1) = \left(\frac{h}{f}\right)Y(t) - \left(\frac{1}{f}\right)\left(\frac{M(t)}{P(t)}\right) \quad (3.71)$$

where Y is output, M is money supply, P is price level, h is income responsiveness of the demand for money, and f is the interest rate responsiveness of the money demand. The term of $-\left(\frac{1}{f}\right)\Delta\left(\frac{M(t)}{P(t)}\right)$ represents how much r needs to adjust, given the initial level of Y to maintain money-market equilibrium. The larger the $\Delta\left(\frac{M(t)}{P(t)}\right)$ or smaller the f, the higher the Δr. The f parameter has no impact on the change in Δr .

The change in interest rate r effects the money supply in the following way:

$$M(t+1) = M(t) - M(t)r(t) \quad (3.72)$$

The simulation is initialized with a money supply M_o and an interest rate of $r = 0$. If the money supply stays constant, a rise in output level Y causes the price level P to drop. The LM model reacts by lowering the interest rate $r < 0$, which increases the money supply and causes price level P to return to the desired level. In a different scenario, when output falls and money supply rises, the price level P rises, causing the LM model to raise interest rates until the price level returns to normal (Findlay, 1999). In our model, the price level is calculated using the Fischer inflation index.

3.17 Labor-Leisure model

The simulation is initialized with a minimum wage rate w_{min} and a transport cost per unit distance c. Each boid calculates a reservation wage w by solving a Labor-Leisure utility maximization model $U(Y, L)$, given an alternative income source Y^o, consumption Y, a 2-way distance to work site d, speed of travel s, and a maximum labor Y/w of 8 hours per day. Each boid is loaded with a different value of labor exponent a and leisure b respectively. A basic labor leisure model can be written as

$$U = U(Y^a, L^b) \tag{3.73}$$

$$s.t\ Y = w(24 - L) + Y^o$$

To account for the money and time spent on transit, we included factors of distance, speed, and cost of travels to the above constraint which yield:

$$Y = w\left(24 - L - \frac{d}{s}\right) + Y^o - dc \tag{3.74}$$

Given that we have set a fixed 8-hour workday, any time spent in transit is time taken away from leisure. In addition, the expense of getting from work to home reduced the

overall amount of money available for consuming. The Lagrangian for this model is given by:

$$\mathcal{L} = U(Y^a L^b) + \lambda\left(Y^o - Y - dc + w\left(24 - L - \frac{d}{s}\right)\right) \qquad (3.75)$$

Taking partial derivatives with respect to Y, L, λ

$$\frac{d\lambda}{dL} = bY^a L^{b-1} - \lambda w = 0 \qquad (3.76)$$

$$\frac{d\lambda}{dY} = aL^b Y^{a-1} - \lambda = 0 \qquad (3.77)$$

$$\frac{d}{d\lambda} = -Y + \left(-\frac{d}{s} - L + 24\right)w + Y^o - cd = 0 \qquad (3.78)$$

Solving for wage L, w

$$L = -\frac{cds + dw + s(-Y_o - 24w + Y)}{sw}, w = -\frac{s(cd + Y - Y^o)}{d + (L - 24)s} : L = 16 - \frac{d}{s}$$

Laborers with the lowest reservation salaries are retained by firms.

(Silberberg, 1990)

3.18 Intertemporal choices

The boids` in our simulation use an extension of a two-period utility maximization model to calculate the volume of consumption and savings at each period. Given a boid with savings $S_{(t)}$, market inflation $\Upsilon_{(t)}$, market interest rate $r_{(t)}$, impatience ρ and two period income history $I_{(t)}, I_{(t+1)}$, with utility of consumption modeled as logarithmic function $\rightarrow \log(Y)$, how much to consume $Y_{(t)}$ at current time. The model can be written as:

$$\max: \log(Y_t) + \frac{\log(Y_{t+1})}{1+\rho}\ s.t \tag{3.79}$$

$$Y_{(t+1)} = \left[\left(I_{(t)} + S - Y_t\right)r + I_{(t+1)}\right], r = \frac{1 + r_{(t)}}{1 + \Upsilon_{(t)}} - 1$$

The Lagrangian for above model is given by:

$$\mathcal{L} = \log(Y_t) + \frac{\log(Y_{t+1})}{1+\rho} + \lambda\left(I_{(t)} + \frac{I_{(t+1)}}{1+r} - Y_t - \frac{\log(Y_{t+1})}{1+r}\right) \tag{3.80}$$

$$\frac{d\lambda}{dY_t} = \frac{1}{Y_t} - \lambda = 0; \frac{d\lambda}{dY_{(t+1)}} = \frac{1}{(\rho+1)Y_{(t+1)}} - \frac{\lambda}{r+1} = 0;$$

$$\frac{d}{d\lambda} = -\frac{Y_{(t+1)}}{r+1} - Y_{(t)} + \frac{I_{(t+1)}}{2} + I_{(t)} = 0$$

Solving for $Y_{(t)}, Y_{(t+1)}$

$$Y_{(t)} = \frac{(\rho+1)Y_{(t+1)}}{r+1} \quad , \quad Y_{(t+1)} = \frac{(r+1)Y_{(t)}}{\rho+1}$$

Substituting $Y_{(t)}, Y_{(t+1)}$ in budget constraints yields following solution for $Y_{(t)}, Y_{(t+1)}$

$$Y_{(t)} = \frac{(\rho+1)(I_{(t)}r + I_{(t)} + I_{(t+1)} + S_{(t)} + S_{(t)}r)}{(\rho+2)(r+1)} \tag{3.81}$$

$$Y_{(t+1)} = \frac{(I_{(t)}r + I_{(t)} + I_{(t+1)} + S_{(t)} + S_{(t)}r)}{(\rho+2)} \tag{3.82}$$

Because future earnings are uncertain, we modify current and future earnings as

$I_{(t)} \Longrightarrow I_{(t-2)},\ I_{(t+1)} \Longrightarrow I_{(t-1)}$

(Silberberg, 1990)

3.19 Land price gradient

Our cities are designed in the style of central business districts (CBDs), with market nodes in the heart. Land prices are highest in the CBD model's center and decrease exponentially as one moves away from the center. The following Equation is used to model land prices within city limits:

$$P_{(x)} = P_o e^{-cx} \tag{3.83}$$

where $P_{(x)}$ is price of plot at distance x from city center, P_o is the price of plot at the city center, and c is an exogenous land gradient (Bertaud, 2015). The P_o is based on $\frac{dP_o}{dt} = g\big(D(p,M) - S(p)\big)$ (3.84), where D and S are demand and supply of plots respectively within city limits. Given an n-city distribution on a 2D plane $(M, N) \in \mathbb{R}^2$, the distribution of land prices outside the city limits is approximated using a finite differencing scheme on a nodal network (Waljiyanto, 2004). The price of land on each location m, n is the average of surrounding land prices. Mathematically:

$$P_{m,n,} = \frac{1}{4}\left[P_{m-1,n} + P_{m+1,n} + P_{m,n-1} + P_{m,n+1}\right] \tag{3.85}$$

s.t boundary conditions $t_0 \rightarrow P_{0,(0:N)} = \mathcal{B}, P_{(0:M),0} = \mathcal{B}, P_{(0:M),N} = \mathcal{B}, P_{M,(0:N)} = \mathcal{B}$, where $\mathcal{B}$ is exogenous price declared at the start of simulation such that $\mathcal{B} > 0$. The CBD land price model was implemented because it contains characteristics that are frequently observed in many cities around the world. Examples of cities that follow a CBD model include Midtown Manhattan. Raffles Place in Singapore, La Defense in Paris, Downtown Port of Spain, and New Delhi's Connaught Place (Jagannath, 2020).

3.20 Fisher index

The consumer price index (CPI) tracks price changes in market baskets of consumer goods. A Fisher index is an ideal price level index that is used to approximate price changes and is consistent with price index theory, including time reversibility. The term "temporal reversibility" refers to the fact that multiplying the price index by the volume index yields the current price change. The reversibility factor implies that multiplying a price index and a volume index of the same type should be a proportionate change in current values Equation (Fisher Index, n.d.).

Given N commodities in an economy during the period $[s, t]$, where t and s denotes the current period and base period respectively. Let $P^t = [p_1^t, p_2^t, \dots, p_N^t]^T$ be the vector of N considered prices and $Q^t = [q_1^t, q_2^t, \dots, q_N^t]^T$ be a vector of N considered quantities at any moment t. The Fischer price index P_F can then be calculated by taking a geometric mean of Laspeyres P_{La} and Paasche price index P_{Pa} (Elżbieta Roszko Wójtowicz, 2018).

$$P_F = \sqrt{P_{La} P_{Pa}}\ , \qquad P_{La} = \frac{\sum_{i=1}^{N} q_i^s p_i^t}{\sum_{i=1}^{N} q_i^s p_i^s}\ , P_{Pa} = \frac{\sum_{i=1}^{N} q_i^t p_i^t}{\sum_{i=1}^{N} q_i^t p_i^s}$$

3.21 Emission` exposure

The time averaged pollutant concentration C at a grid point (x, y) is given by:

$$\overline{C_{(x,y)}} = \frac{1}{ds}\int_{s_o}^{s_o+ds} \frac{M_{(s)}}{(2\pi)^{\frac{3}{2}}\sigma_{y_{(s)}}^2 \sigma_{z_{(s)}}} \exp\left[-\frac{1}{2}\left(\frac{x}{\sigma_{y_{(s)}}}\right)^2\right] \exp\left[-\frac{1}{2}\left(\frac{y}{\sigma_{y_{(s)}}}\right)^2\right] \exp\left[-\frac{1}{2}\left(\frac{z-H}{\sigma_{z_{(s)}}}\right)^2\right] ds \tag{3.86}$$

where s_o is the value of s at the beginning of the sampling step[11]. The exponential variation of M due to removal and chemical transformation process is expressed as a linear function:

$$M(s) = M(s_0) + p[M(s_o + d_s) - M(s_0)] \quad (3.87)$$

The exposure level E to a pollutant corresponds to: E= $f[P(x,t), c(x,t)]$, where $P(x,t)$ is population located at point x inhaling pollutant concentration $c(x,t)$ (G.Russell, 1988). All boids are initialized with a health index $H = 1$. The health depreciation of a boid in the system is given by: $H(t+1) = H(t) - H(t)a - H(t)E$, where a represents health depreciation due to normal aging and E represents health depreciation due to exposure to emissions. A boid is removed from the system when $H \leq 0$.

[11] See Puff Dispersion Model section for notation detail.

109

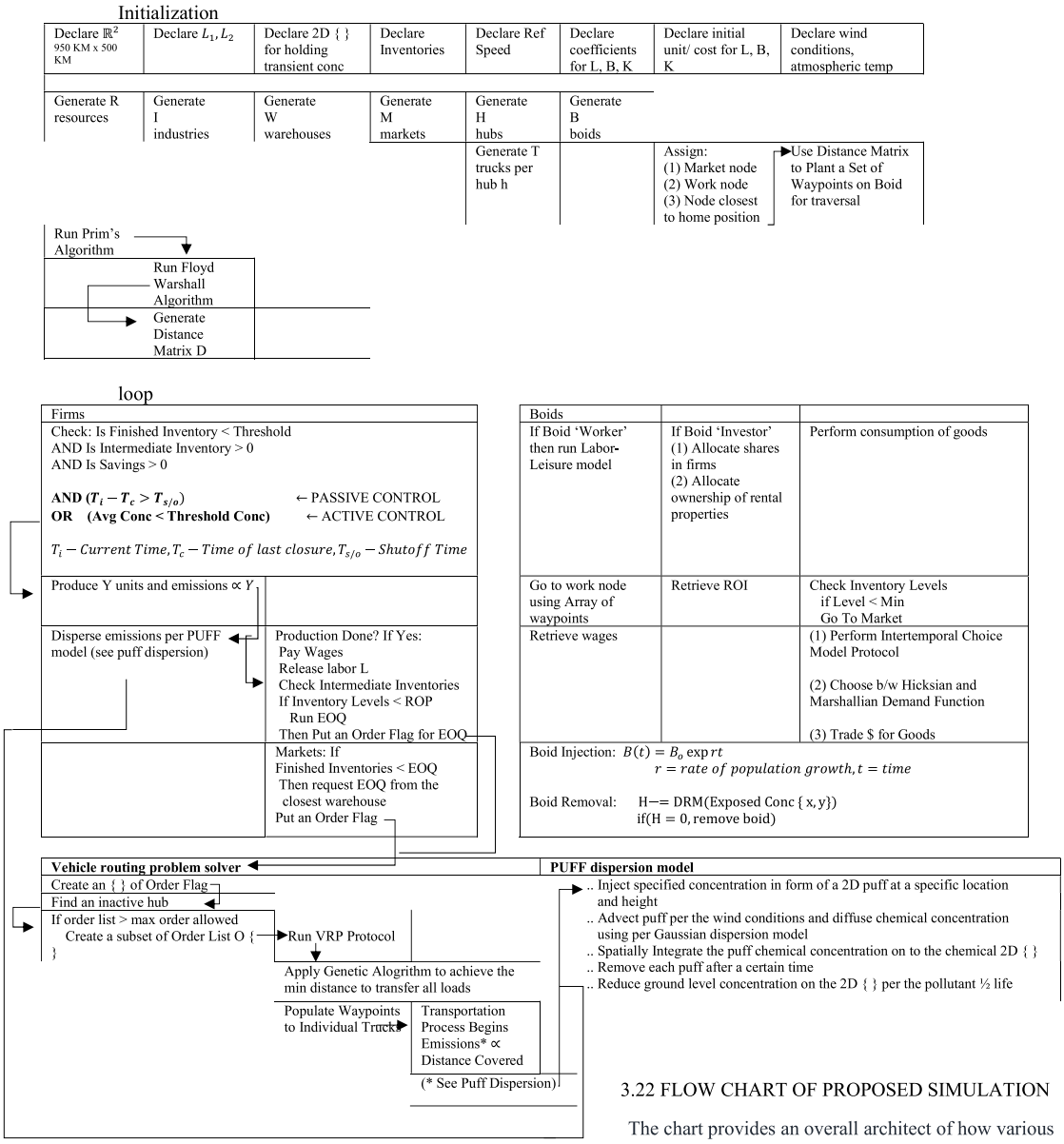

3.22 FLOW CHART OF PROPOSED SIMULATION

The chart provides an overall architect of how various sub-models from operations research, graph theory, economics, and emissions dispersions, etc. have been integrated in the simulation.

FLOW CHART OF THE SIMULATION

4. ASSUMPTIONS OF STUDY

1. The simulation search space spans a 2D area of 950x500 KM.
2. The mines and markets are randomly distributed over the 2D plane.
3. Industries and resources are interdependent on each other’s output for production.
4. Quantity of land, labor and capital acquired by a firm is subject to investment constraint.
5. Boids are regularly introduced in the simulation to represent an increase in population; the rate of population growth is declared by the programmer.
6. All trucks begin and end their journeys at their designated transportation hub.
7. Commodity prices are determined by the difference between commodity demand and supply.
8. Producers require a minimum amount of raw and intermediate material feeds for processing a batch.
9. If the commodity's selling price is zero, all production is halted.
10. Trucks and boids use the road network to travel throughout the region.
11. The minimum price of a product is the greater of the product's manufacturing cost or its market price.
12. A company selects suppliers based on the lowest total cost of product and freight.
13. All production plants have multiple replicas. Purchase orders can only be placed with those replicas where the finished inventory level is larger than the inventory booked level.
14. The order quantity conveyed by each truck is the minimum value of the truck's carrying capacity or the order's EOQ.

15. Firms select between profit maximization and cost minimization strategies based on market pricing, finished inventory quantity, and operational profitability.
16. There is a minimum amount of consumption by all Boids regardless of income.
17. When a Boid's health index falls to zero, it is eliminated from simulation.
18. Reservation wage of worker Boid is calculated using the Labor-Leisure utility maximization model.
19. Population growth rate is exogenous variable.
20. Number of trucks per transport hub is an exogenous variable.
21. Boids replenish goods from the nearest market regardless of market system’s wait time.

5. LIMITATIONS

1. To reduce simulation complexity and processing time, the total population of Boids is limited to 25K.
2. Modeling of atmospheric emissions restricted to mining, industrial, and trucking releases. Emissions from air, sea, and rail transportation sources are not included.
3. No foreign emissions are permitted in the simulation space.
4. To preserve computation memory, Individual puff terminates after a predetermined time or when it is close to the simulation boundary.
5. Population growth rate is an exogenous parameter.
6. The numbers of mining fields, industries, markets, warehouses, and transportation hubs remain constant throughout the simulation run.

6. DELIMITATION

1. Natural sources of atmospheric emissions (volcanic, forest fires, agricultural, etc.) are excluded.
2. A closed-loop economy in which no exports and imports of commodities are permitted.
3. Worker boids are only allowed to work for a maximum of 8 hours per day.
4. To reduce complexity and processing costs, the wind field in the simulation will be approximated using a noise-based approach — Perlin noise (Oyundolgor Khorloo, 2011).
5. GHG emissions' thermal effects are not considered.

7. NUMERICAL SIMULATION

The objective of the research is the theoretical quantification of change in real-gross domestic product (r-GDP) as a direct consequence of restrictions on point and mobile emissions in a closed loop economy. In a closed loop economy, no cross-border trade is permitted, and the economy must fend for itself to generate a diverse range of products for consumption. The closed loop condition ensures that the economic impact of emissions restrictions can be thoroughly examined without any external incentives to replace `production of good with a high net emissions factor` with imports – it is inconsistent to import steel from developing regions with lax emissions controls in the designation of environmental protection when gaseous emissions can disperse unimpeded in the atmosphere.

The study only seeks to establish a relative association between economic key point indicators and emission controls. The effect of any emissions control is evaluated on a hypothetical economy with random distribution of firms and markets. The essential simulation principles will each be independently verified to validate the simulation outcome.

7.1 Experiments

a) Passive controls: Determine the relevant economic output and degree of exposure to pollutants if the subsequent shutdown times are 8, 16, 24, 32, 40, and 48 hours.
b) Active controls: Calculate the corresponding economic productivity if the firms are only allowed to activate production if the average ground level concentrations are below following set of threshold concentrations $\frac{C_\mu}{1}, \frac{C_\mu}{2}, \frac{C_\mu}{4}, \frac{C_\mu}{8}, \frac{C_\mu}{16}$, where C_μ is the average ground level emissions concentration without any emissions constraints.

7.2 Software

The simulation program is written in Processing® platform – a JAVA based applet that supports object-oriented programming with additional benefit of an integrated development environment (IDE) for visual arts (Shiffman, 2012).

7.3 Global Parameters

The simulation platform simulates a geographical area of 950KM x 500KM $\mathbb{R}^2$ with following key parameters that are assumed fixed for all case scenarios:

Table 7.1: Simulation global parameters

#	Parameter	Value	Description
1	Population growth rate	2.0%	
2	Finished commodity types	20	$E = \{e \in \mathbb{N} \mid 0 > e \leq 12\}$
3	N of industry replicates per finished commodity	6x20	$I = \{i \in \mathbb{C} \mid 0 > i \leq 48\}$
4	Raw commodity types	10	$S = \{s \in \mathbb{N} \mid 0 > s \leq 08\}$
5	N of mining replicates per raw commodity	6x18	$R = \{r \in \mathbb{C} \mid 0 > r \leq 16\}$
6	N of market centers	12	$M = \{m \in \mathbb{C} \mid 0 > m \leq 08\}$
7	N of cities	12	
8	N of transport hubs	18	$H = \{h \in \mathbb{C} \mid 0 > h \leq 08\}$
9	N of trucks per transport hub	4x8	$T = \{t \in \mathrm{H} \mid 0 > t \leq 24\}$
10	Radii of a city (CBD) KM	30	
11	Truck delivery speed KM/HR	80	
12	N of boids at instant of initialization	20,000	
13	Health index at instant of initialization	1	
14	Max wind speed m/s	8	

15	Max population for VRPSPD Genetic Algorithm	500
16	Min rest time for boid HR/DAY	8
17	h - income sensitivity to the demand for money L_1	0.8
18	f - interest rate sensitivity to money demand L_2	0.06
19	Markets operating period HR/DAY	16
20	Max life of each puff HR	10
21	Δt between each puff HR	0.5
22	Δx^2 emissions dispersion grid KM^2	0.2x0.2
23	Max carrying capacity of each truck (Tons)	40
24	Max % of population as workforce	70
25	Exhaust rates of point emissions	0.04Y
26	Exhaust rate of mobile emissions (g/KM)	10.54
27	Exhaust temperatures of point emissions (C^o)	109.85
28	Pollutant type	Mix
29	Minimization criteria for genetic algorithm (VRT)	min L (Minimize lead time)
30	Minimum production level (units) Y^o	5 Tons
31	Boundary condition (Puff dispersion model)	None
32	Boundary condition (Land rate) $/Unit Area	1.0
33	Max age of each Boid (s) Max_{Age}	2,400
34	Normal rate of health depreciation	1/ Max_{Age}
35	Compounded rate of health deprecation due to emission`s exposure	$d = \frac{1}{1+\exp^{k(c-c_{50})}}$ *dose response modeling (DRM)*

7.4 Termination conditions

Each simulation scenario is terminated after 130-day equivalent worth of data has been collected. The simulation runs at a frame rate of ~3/60 Hz with 1 second equivalent to 1 hour in real life.

7.5 Validation of key concepts

7.5a Prim's Minimum Spanning Tree (MST)

The Graph Online project, which focuses on graph construction and visualization as well as shortest path search, is used to validate the Prim's MST implementation. The validation is performed on a set of (32) randomly distributed vertices on a (500 KM x 500KM) plane with a n set of edges connecting the vertices. The simulation platform's distance matrix is replicated in the Graph Online project. Fig. 7-1 depicts the final output from the simulation platform and graph online. In both cases, the MST is the same, implying that the Prisms MST implementation is accurate.

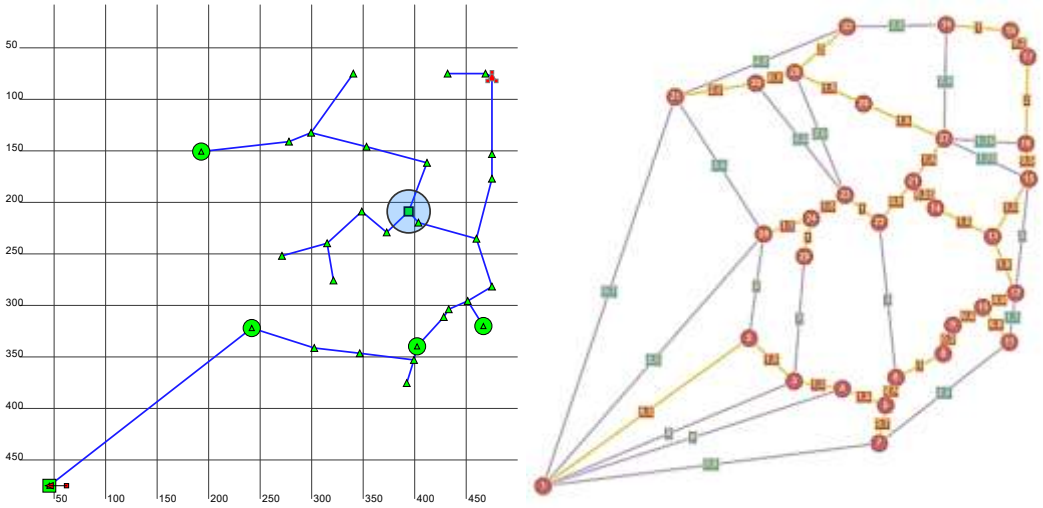

Figure 7-1: Prim's Minimum Spanning Tree output on 32 vertices in simulation (Left) vs Graph Online output (Right)

7.5b Floyd Warshall algorithm

The Graph-Online project is also used to validate the Floyd Warshall Algorithm's implementation. To generate an all-pair shortest path, the Floyd-Warshall Algorithm is applied to the edge set acquired from the Prim's MST in the preceding example. After the shortest path matrix has been successfully calculated, a path reconstruction is executed between vertex (1) and (32). Fig.7-2 represents the shortest path in simulation platform and Graph Online project. The path reconstruction in both instances is identical, proving that Floyd Warshall implementation in the simulation is accurate.

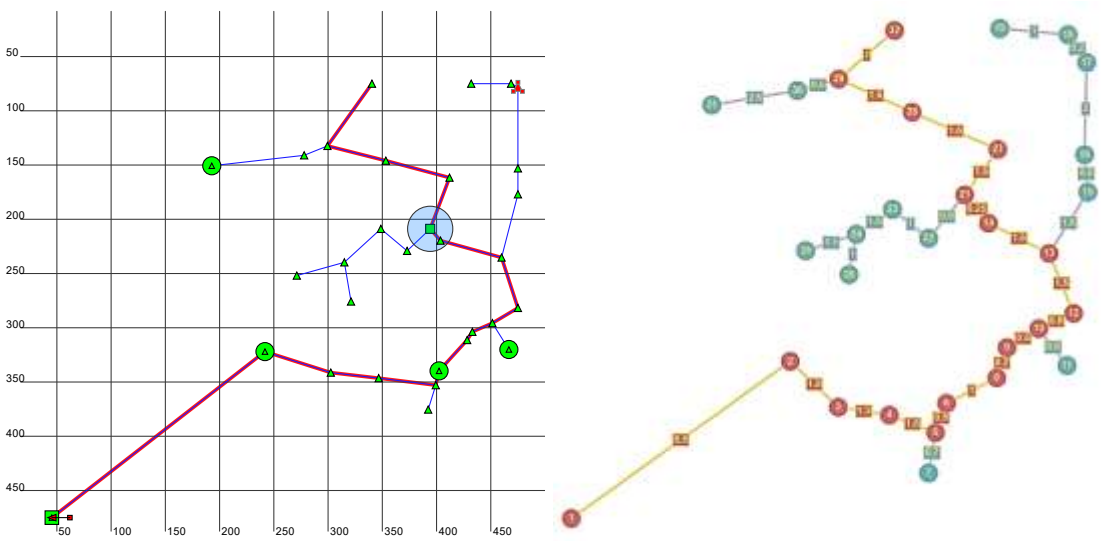

Figure 7-2: Shortest path reconstruction between vertices (1 → 32) using Floyd Warshall Algorithm. Simulation's shortest path output (Left) *edges with red highlight* is identical to the Graph-Online shortest path output (Right) *red vertices with yellow highlighted edges*.

7.5c Production function

The Solver ® program is used to evaluate the validity of the simulation's production function! The Solver ® program has been developed by Frontline systems which is widely used by companies and education sector to solve various forms of optimization problems including Linear, Quadratic, Mixed Integer, etc.

Given a firm with technology factor $A = 1.28$, land input exponent $p = 0.175$, labor input exponent $q = 0.238$, capital input exponent $r = 0.550$, land cost per unit $w = 0.65$, labor cost per unit $x = 3.1$, capital cost per unit $y = 2.2$, market price $M_p = 6.3$, minimum production level $Q_{min} = 1250$ and table of following intermediate feeds: Find the quantities of land B, labor L, and capital K that can generate an output Q such that profit π can be maximized (Profit maximization). Find the quantities of B, L, K such that total cost of operations C is minimum $s.t. Q = Q_0$ (Cost minimization).

raw feeds (S)	unit cost	prop $\propto Q$	intermediate feeds (E)	unit cost	prop $\propto Q$
s_0	0.1287	0.323	e_0	0.5644	0.5638
s_1	0.1477	0.357	e_1	0.7910	0.3545
s_2	0.1902	0.320	e_2	0.5790	0.0817

Profit Maximization

* Simulation Output *

(Land) B	(Labor) L	(Capital) K	(Output) Q	Profit π
3308.9036	943.5713	3072.556	2234.99	454.548

Solver® Output

Engine: GRG Nonlinear

Solution Time: 0.109 Seconds.

Iterations: 3 Subproblems: 0

Solver Options

Max Time Unlimited, Iterations Unlimited, Precision 0.000001, Use Automatic Scaling Convergence 0.0001, Population Size 100, Random Seed 0, Derivatives Forward, Require Bounds Max Subproblems Unlimited, Max Integer Sols Unlimited, Integer Tolerance 1%, Assume Nonnegative

	Objective (Max)	**Initial Value**	**Final Value**
	Profit	1.97	454.55

Variable Cells

Name	**Final Value**	**Reduced Gradient**
B	3307.501233	0
L	943.1704449	0
K	3071.249483	0

Conclusion: In terms of land, labor, and capital inputs and profit output, the (absolute) difference between simulation and Solver ® is 0.0424 %, 0.0425 %, 0.0425 %, and 0.0004 %, respectively.

Cost Minimization

* Simulation Output *

(Land) B	(Labor) L	(Capital) K	(Output) Q	Cost C
516.07495	1809.765	1680.4949	1250.0	6473.2686

Solver® Output

Engine: GRG

Nonlinear

Solution Time: 0.516 Seconds.

Iterations: 11 Subproblems: 0

Solver Options

Convergence 0.0001, Population Size 100, Random Seed 0, Derivatives Forward, Require Bounds

Max Subproblems Unlimited, Max Integer Sols Unlimited, Integer Tolerance 1%, Assume Nonnegative

Objective (Min)	**Initial Value**	**Final Value**
Cost	5.95	6473.27

Variable Cells

Name	**Original Value**	**Final Value**	**Integer**
B	1.00	516.08	Contin

L	1.00	1809.76	Contin
K	1.00	1680.50	Contin

Constraints

Name	Cell Value	Formula	Status	Slack
Q	1250.00	$Q = Q_{min}$	Binding	0

Conclusion: In terms of land, labor, and capital inputs and cost minimization output, the (absolute) difference between simulation and Solver ® is 0.00098%, 0.00028%, 0.00030%, and 0.00002% respectively.

7.5d Demand function

The Solver ® program is used to evaluate the validity of the simulation's demand function!

Given a boid with a budget $m = 227$, minimum utility $u^0 = 8.62$, and a following basket of goods X with corresponding utilities of consumption U and prices P. Find the quantities of X that maximize $'u'$ s.t. budget constraint m (Marshallian). Find the quantities of X that satisfy u^0 (Hicksian demand).

basket of goods (X)	utilities $U \in X$	prices $P \in X$
x_0	u_0 = 0.5224	p_0 = 5.97
x_1	u_1 = 0.1718	p_1 = 3.94
x_2	u_2 = 0.1074	p_2 = 5.08
x_3	u_3 = 0.0946	p_3 = 6.24
x_4	u_4 = 0.1037	p_4 = 5.99

Hicksian Demand

* Simulation Output *

x_0	x_1	x_2	x_3	x_4	C
14.89474	7.4221754	3.5986934	2.5805416	2.9496794	170.21753

Solver® Output

Engine: GRG Nonlinear

Solution Time: 0.375 Seconds.

Iterations: 8 Subproblems: 0

Solver Options

Max Time Unlimited, Iterations Unlimited, Precision 0.000001, Use Automatic Scaling Convergence 0.0001, Population Size 100, Random Seed 0, Derivatives Forward, Require Bounds Max Subproblems Unlimited, Max Integer Sols Unlimited, Integer Tolerance 1%, Assume Nonnegative

Objective (Min)	Initial Value	Final Value
C	27.22	180.6221031

Variable Cells

Name	Original Value	Final Value	Integer
x0 X	1	15.80759126	Contin
x1 X	1	7.875408165	Contin
x2 X	1	3.820741262	Contin
x3 X	1	2.739086317	Contin

x4 X	1	3.125277263	Contin

Constraints

Name	Cell Value	Formula	Status	Slack
u	8.619999754	$u - \bar{u} = 0$	Binding	0

Conclusion: In terms of the quantities of goods $(x_0, x_1, \dots, x_n)$ required to satisfy the minimum utility of consumption u_0 at the lowest possible cost C, the absolute differences between simulation and Solver ® results are 6.1162 % and 6.10042 % respectively.

Marshallian Demand

* Simulation Output *

x_0	x_1	x_2	x_3	x_4	U
19.863453	9.898122	4.799173	3.441378	3.9298666	10.832007

Solver® Output

Engine: GRG Nonlinear

Solution Time: 0.234 Seconds.

Iterations: 9 Subproblems: 0

Solver Options

Max Time Unlimited, Iterations Unlimited, Precision 0.000001, Use Automatic Scaling

Convergence 0.0001, Population Size 100, Random Seed 0, Derivatives Forward, Require Bounds

Max Subproblems Unlimited, Max Integer Sols Unlimited, Integer Tolerance 1%, Assume Nonnegative

Objective (Max)	Initial Value	Final Value
u	1	10.83308888

Variable Cells

Name	Original Value	Final Value	Integer
x0 X	1	19.86548943	Contin
x1 X	1	9.899089325	Contin
x2 X	1	4.799640116	Contin
x3 X	1	3.44168737	Contin
x4 X	1	3.93026963	Contin

Constraints

Name	Cell Value	Formula	Status	Slack
C	226.9999999	$\sum_{i=1}^{n} p_i x_i \leq m$	Binding	0

Conclusion: In terms of the quantities of goods $(x_0, x_1, \ldots, x_n)$ required to maximize utility of consumption u with budget constraint m, the absolute differences between simulation and Solver ® results are 0.009988% and 0.0098%, respectively.

7.5e Puff Dispersion model

The Puff dispersion model is validated using the Gaussian plume dispersion model for Pasquil atmospheric stability classes (A, B, C, D, E, F). The wind field is generated using the Perlin noise function and ground level concentration of pollutant is calculated at several downwind locations. The effective height of the pollutant is calculated using the CONCAWE Equation. The list of parameters used to validate the Puff Dispersion model are as follows:

Class	Emission rate (g/s)	Stack height (m)	Stack diameter (m)	Exit velocity (m/s)	Stack gas exit temp (K)	Ambient temp (K)	Terrain	Wind speed (m/s)	Max[12] Conc ug/m^3	Range to Max Conc (m)
A	28.85	30.48	3.0	18.31	372.04	281.01	Rural	1.0	63.36	1,060
B	-	-	-	-	-	-	-	4.0	39.21	1,082
C	-	-	-	-	-	-	-	5.0	38.22	1,563
D	-	-	-	-	-	-	-	6.0	24.70	3,140
E	-	-	-	-	-	-	-	2.5	29.38	6,388
F	-	-	-	-	-	-	-	2.5	21.88	11,395

Technical Details

Simulation frequency	30-60 Hz	Ground level concentration	$\int_{t=0}^{\infty} \dot{C}\,\Delta t$
Resolution	0.10 KM		
Puff size	1 x 1 KM		
Puff separation	100 milli seconds	Decay rate	0.9999519
Puff removal	Boundary crossing	Wind direction	π
Advection	Wind velocity vector	Wind flow	Perlin Noise

[12] Calculated using EPA SCREEN3

The implementation of the Puff dispersion model in the simulation is validated using the US Environmental Protection Agency's SCREEN3 model. The above parameters are fed into the SCREEN 3 model, and the plume center line concentrations are plotted against the output of the Puff dispersion model. For every atmospheric stability, the Puff dispersion model is run until the centerline concentrations approach steady-state emission levels. The accuracy of the Puff dispersion model is quantified using mean absolute deviation (MAD), mean square error (MSE), root mean square error (RMSE), and mean absolute percentage error (MAPE) (Regression Algorithms: which Machine Learning Metrics?, n.d.).

$\text{MAD} = \frac{1}{n}\sum_{i=1}^{n}\left\|Y_i - \widehat{Y_i}\right\|$	MAD is a measure of how far the reference value and the value predicted by the model diverge from each other on an absolute basis
$\text{MSE} = \frac{1}{n}\sum_{i=1}^{n}\left(Y_i - \widehat{Y_i}\right)^2$	The average of the squared difference between the reference and predicted values. Penalizes outliers
$\text{RMSE} = \sqrt{\frac{1}{n}\sum_{i=1}^{n}\left(Y_i - \widehat{Y_i}\right)^2}$	The average root-squared difference between the reference and predicted values
$\text{MAPE} = \frac{1}{n}\sum_{i=1}^{n}\left\|\frac{Y_i - \widehat{Y_i}}{Y_i}\right\|$	The average absolute difference between the reference value and the value predicted by the model divided by the reference value

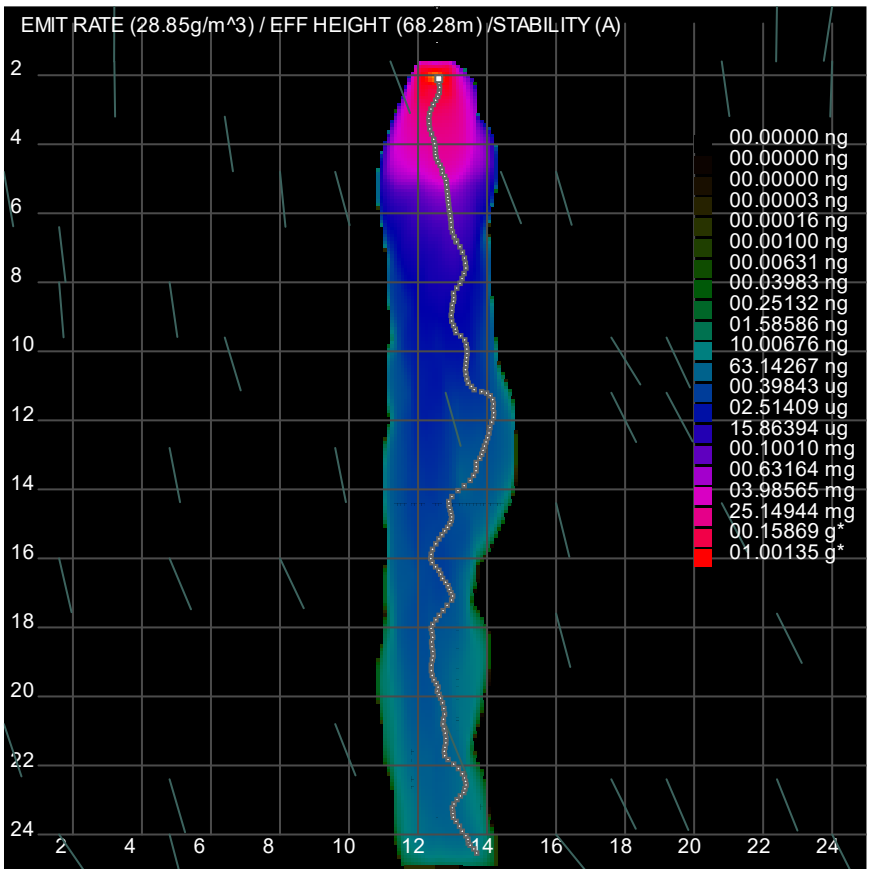

Figure 7-3: Ground level emission's concentration estimated using Puff dispersion model under the atmospheric stability class (A). The central point of gaseous plumes is indicated by white points.

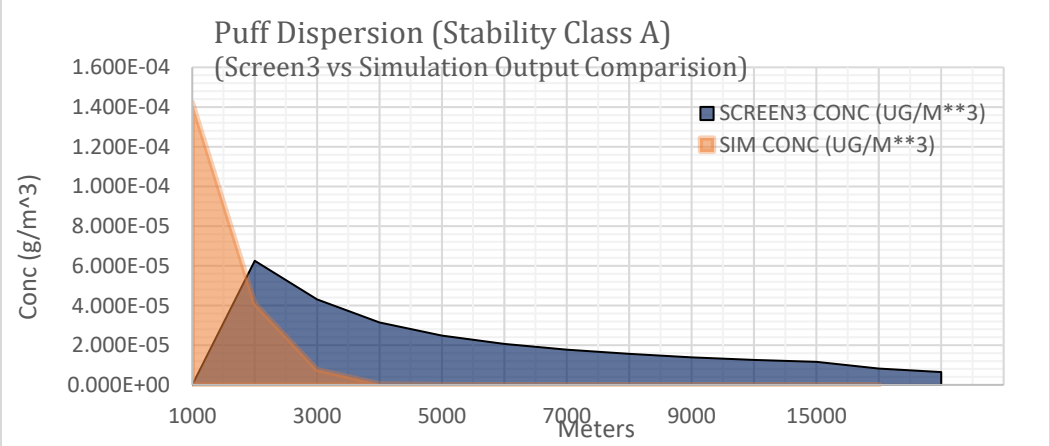

Figure 7-4: Comparison of the steady state concentrations produced by the Puff dispersion model and the EPA Screen 3 model under the stability class (A).

Error measures			
MAD	MSE	RMSE	MAPE
1.97E-05	7.59E-10	2.75E-05	9198%

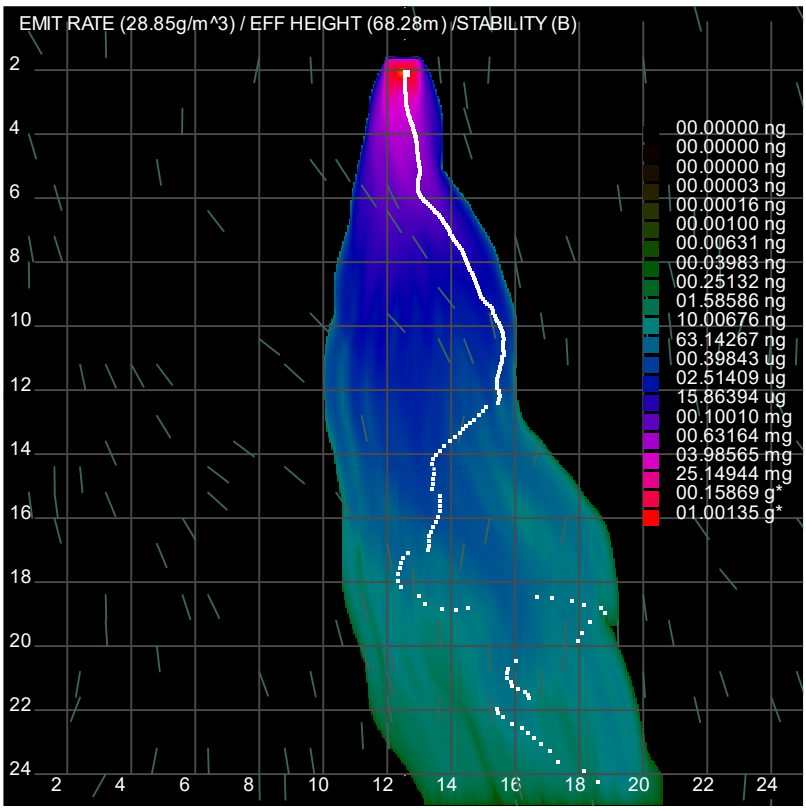

Figure 7-5: Ground level emission's concentration estimated using Puff dispersion model under the atmospheric stability class (B). The central point of gaseous plumes is indicated by white points.

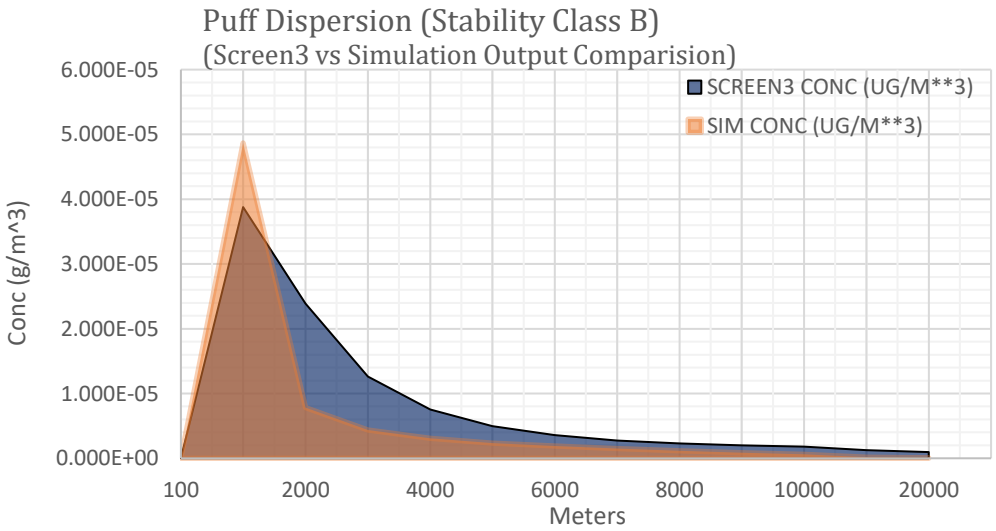

Figure 7-6: Comparison of the steady state concentrations produced by the Puff dispersion model and the EPA Screen 3 model under the stability class (B).

Error measures			
MAD	MSE	RMSE	MAPE
4.13E-06	3.84E-11	6.20E-06	5923%

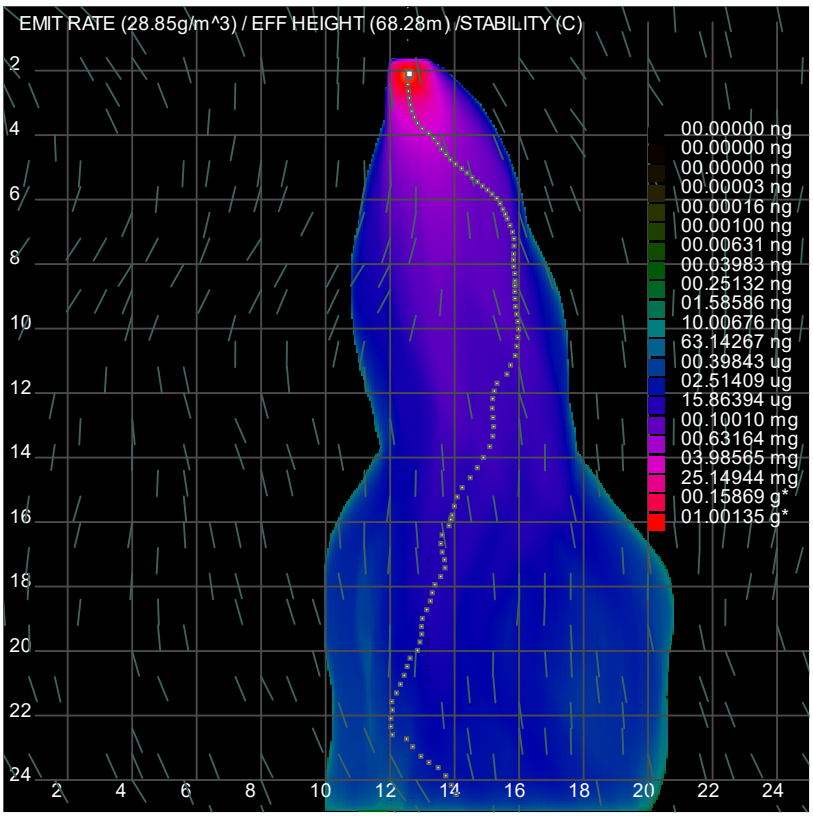

Figure 7-7: Ground level emission's concentration estimated using Puff dispersion model under the atmospheric stability class (C). The central point of gaseous plumes is indicated by white points.

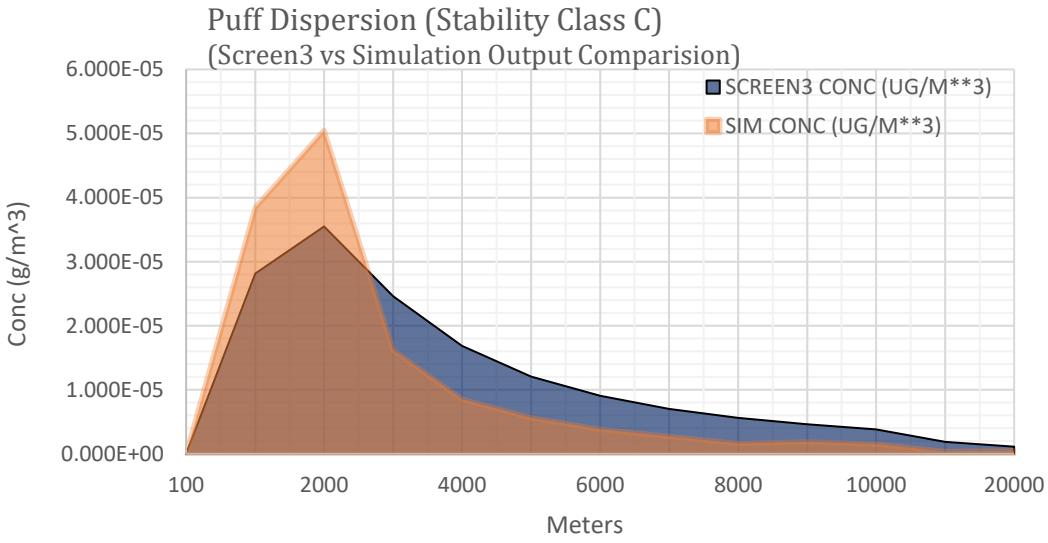

Figure 7-8: Comparison of the steady state concentrations produced by the Puff dispersion model and the EPA Screen 3 model under the stability class (C).

Error measures			
MAD	MSE	RMSE	MAPE
5.78E-06	4.92E-11	7.01E-06	5575%

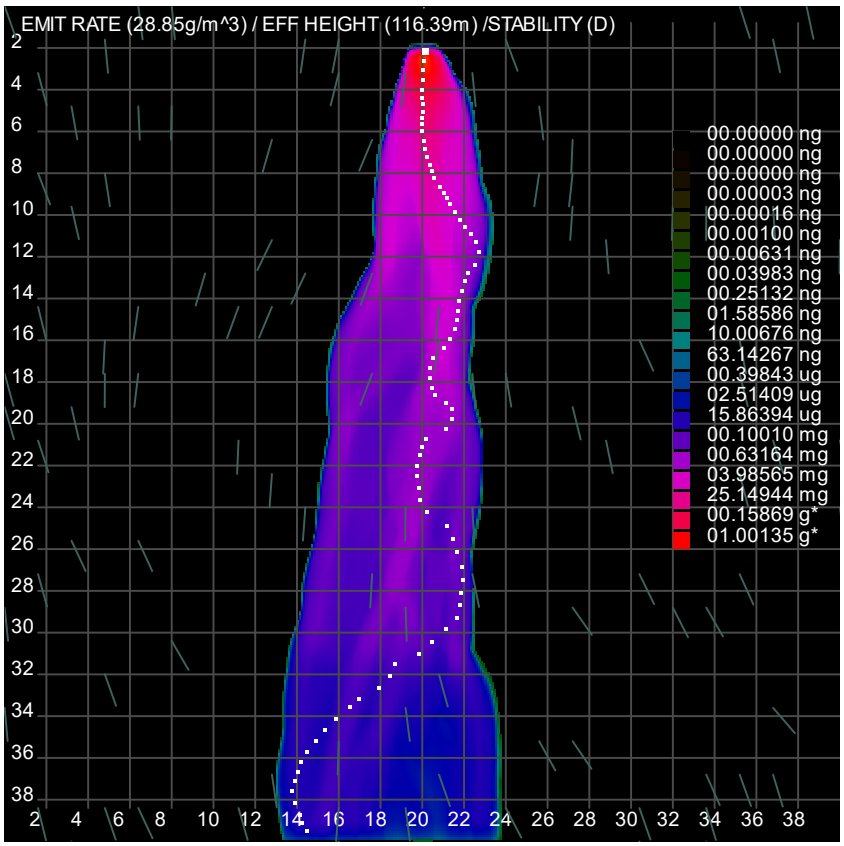

Figure 7-9: Ground level emission's concentration estimated using Puff dispersion model under the atmospheric stability class (D). The central point of gaseous plumes is indicated by white points.

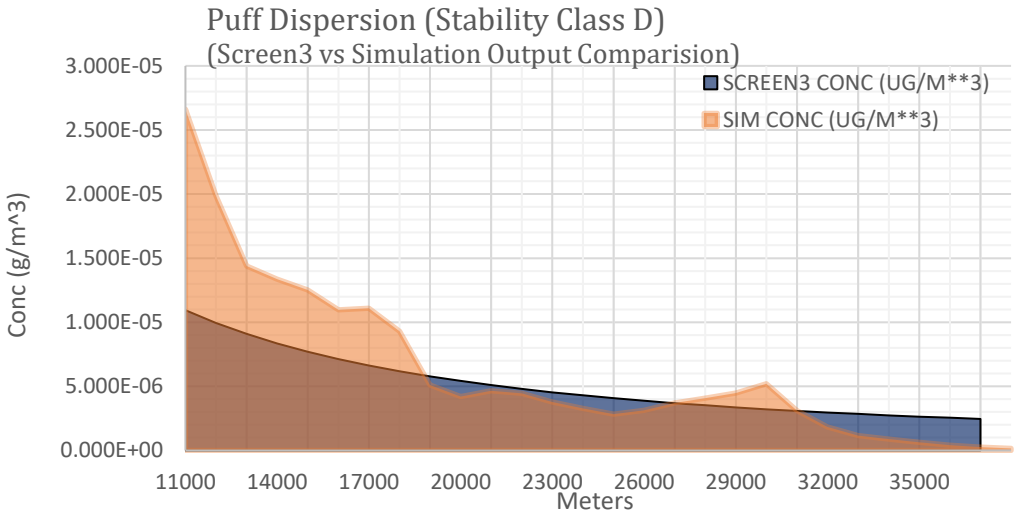

Figure 7-10: Comparison of the steady state concentrations produced by the Puff dispersion model and the EPA Screen 3 model under the stability class (D).

Error measures			
MAD	MSE	RMSE	MAPE
2.59E-06	1.51E-11	3.89E-06	4557%

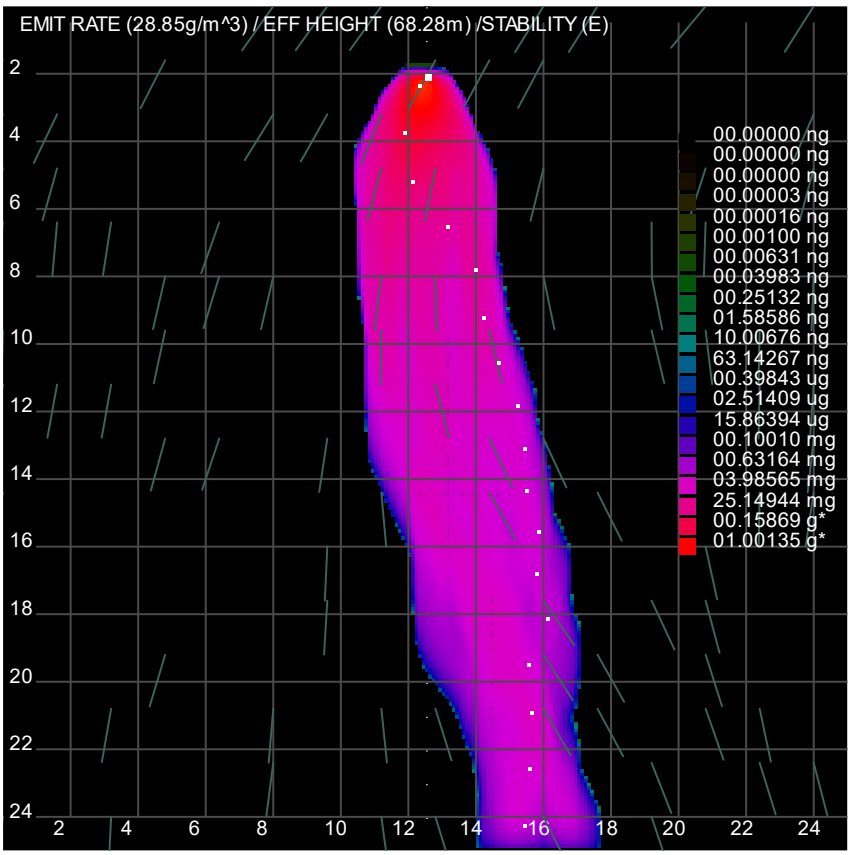

Figure 7-11: Ground level emission's concentration estimated using Puff dispersion model under the atmospheric stability class (E). The central point of gaseous plumes is indicated by white points.

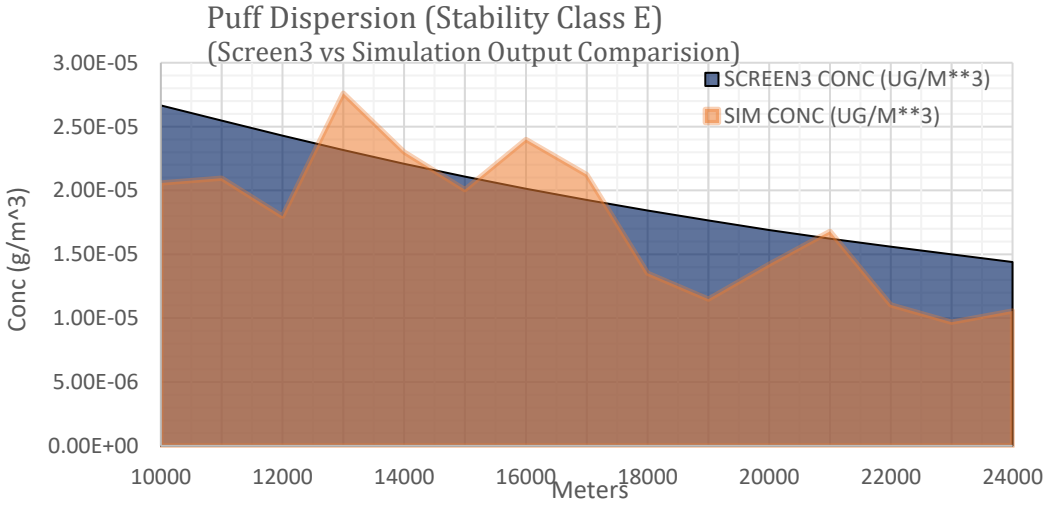

Figure 7-12: Comparison of the steady state concentrations produced by the Puff dispersion model and the EPA Screen 3 model under the stability class (E).

Error measures			
MAD	MSE	RMSE	MAPE
3.81E-06	1.81E-11	4.25E-06	1977%

7.5f VRPSPD

The Solver ® program is used to evaluate the validity of the simulation's VRPSPD!

Vehicle Routing Problem (VRP) is an NP combinatorial optimization problem that aims to find an optimal set of routes for n vehicles ($n \geq 1$) to suffice an objective value i.e., minimize total distance, minimize total lead time, etc. We intend to evaluate the VRPSPD's performance using the Genetic Algorithm (GA) with one hub, one transport unit, and 12 vertices: each vertex requiring delivery from another vertex. The goal of the problem is to reduce the total distance. GA is initialized with a population size of 200, a fitness function given by $\left[\frac{1}{(\sum d_{(i,j)})^{8}+1}\right]$ (7.1) where $\sum d_{(i,j)}$ is the sum of total distances, and a mutation rate of 0.01.

* Simulation Output *

Minimum Distance = 657 (KM)

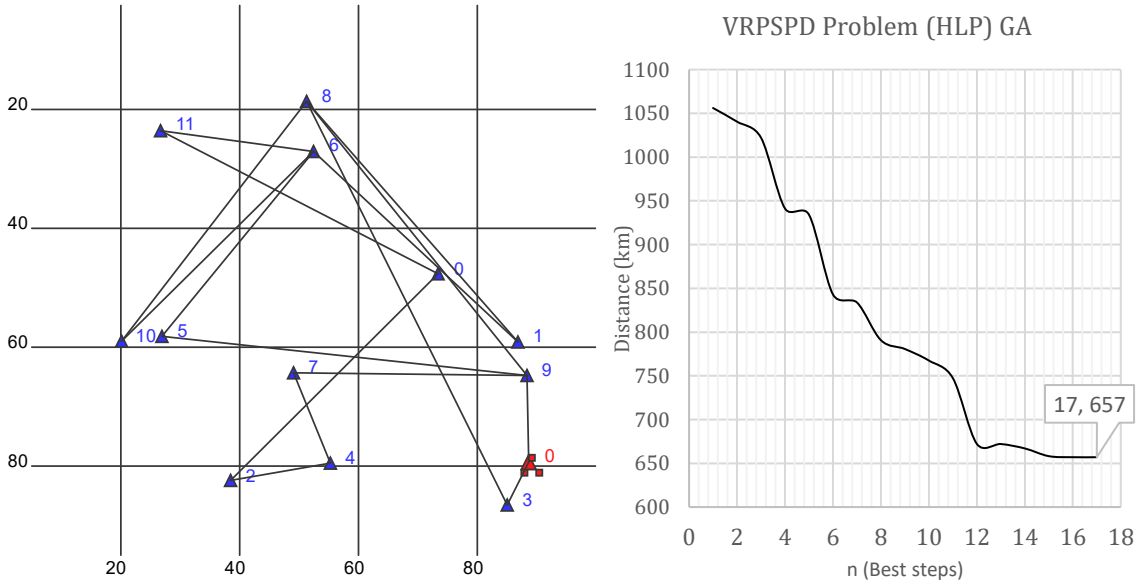

Figure 7-13: The Genetic Algorithm (GA) Heuristic approach is used to solve the VRPSPD problem. To transfer 12 orders between firms, 657 KM must be covered.

Solver® Output

Engine: Evolutionary

Solution Time: 50.063 Seconds.

Iterations: 0 Subproblems: 20118

Solver Options

Max Time Unlimited, Iterations Unlimited, Precision 0.000001, Use Automatic Scaling Convergence 0.0001, Population Size 100, Random Seed 0, Mutation Rate 0.075, Time w/o improve 30 sec Max Subproblems Unlimited, Max Integer Sols Unlimited, Integer Tolerance 1%, Assume Nonnegative

Objective (Min)	**Initial Value**	**Final Value**
$\sum d_{(i,j)}$	1207.5	657.6

FIRMS (Order Matrix)

ORDERS	$j \rightarrow i$		Solution	$j \rightarrow i$	
O 1	13	2	6	11	7
O 2	10	3	12	8	13
O 3	2	4	1	13	2
O 4	10	5	3	2	4
O 5	4	6	5	4	6
O 6	11	7	8	6	9
O 7	3	8	10	9	11
O 8	6	9	9	11	10
O 9	11	10	2	10	3

O	10	9	11	7	3	8
O	11	8	12	11	8	12
O	12	8	13	4	10	5

H	WAYPOINT (Sequence)													
1	11	7	8	13	13	2	2	4	4	6	6	9	9	11
$d_{(i,j)}$	14.6	61.8	40.2	26.0	0.0	52.6	0.0	49.3	0.0	17.0	0.0	16.4	0.0	39.3

11	10	10	3	3	8	8	12	10	5	H
0.0	59.2	0.0	53.9	0.0	47.0	0.0	45.4	51.0	75.8	1	8.1

FIRMS (Distance Matrix)

		1	2	3	4	5	6	7	8	9	10	11	12	13
		H0	F0	F1	F2	F3	F4	F5	F6	F7	F8	F9	F10	F11
1	H0	0.0	35.2	20.3	50.3	8.1	33.4	65.3	63.6	42.3	71.3	14.6	71.5	83.4
2	F0	35.2	0.0	17.7	49.3	40.6	36.7	47.7	29.4	29.5	36.5	22.7	54.5	52.6
3	F1	20.3	17.7	0.0	53.7	27.5	37.6	59.9	47.0	39.1	53.9	5.8	66.7	69.9
4	F2	50.3	49.3	53.7	0.0	46.7	17.0	26.9	57.1	21.0	65.0	52.9	29.8	60.0
5	F3	8.1	40.6	27.5	46.7	0.0	30.6	64.7	67.8	42.3	75.8	22.0	70.5	85.8
6	F4	33.4	36.7	37.6	17.0	30.6	0.0	35.5	52.5	16.4	51.0	36.2	40.7	62.8
7	F5	65.3	47.7	59.9	26.9	64.7	35.5	0.0	40.2	23.0	46.4	61.8	6.8	34.6
8	F6	63.6	29.4	47.0	57.1	67.8	52.5	40.2	0.0	37.4	8.5	52.1	45.4	26.0
9	F7	42.3	29.5	39.1	21.0	42.3	16.4	23.0	37.4	0.0	45.7	39.3	29.4	46.5
10	F8	71.3	36.5	53.9	65.0	75.8	61.0	46.4	8.5	45.7	0.0	59.2	51.0	25.1
11	F9	14.6	22.7	5.8	52.9	22.0	36.2	61.8	52.1	39.3	59.2	0.0	68.5	74.2
12	F10	71.5	54.5	66.7	29.8	70.5	40.7	6.8	45.4	29.4	51.0	68.5	0.0	36.0
13	F11	83.4	52.6	69.9	60.0	85.8	62.8	34.6	26.0	46.5	25.1	74.2	36.0	0.0

Conclusion: The total route distance calculated by the simulation and solver ® is the same, leading to the conclusion that the GA implementation of VRPSPD in the simulation is acceptable.

7.5g Commodities Pricing

Given that the following relationships approximate a commodity's supply $S(p)$ and demand $D(p)$ as a function of price (p). Find the equilibrium price p^e: $p_{(0)} = \$10$.

$$D(p) = 3550 - 266(p)$$

$$S(p) = 1800 + 240(p)$$

The function of price p is given by:

$$\frac{dp}{dt} = k\big(D(p) - S(p)\big) \rightarrow p_{(t+1)} = p_{(t)} - k(S_{(p_t)} - D_{(p_t)})$$

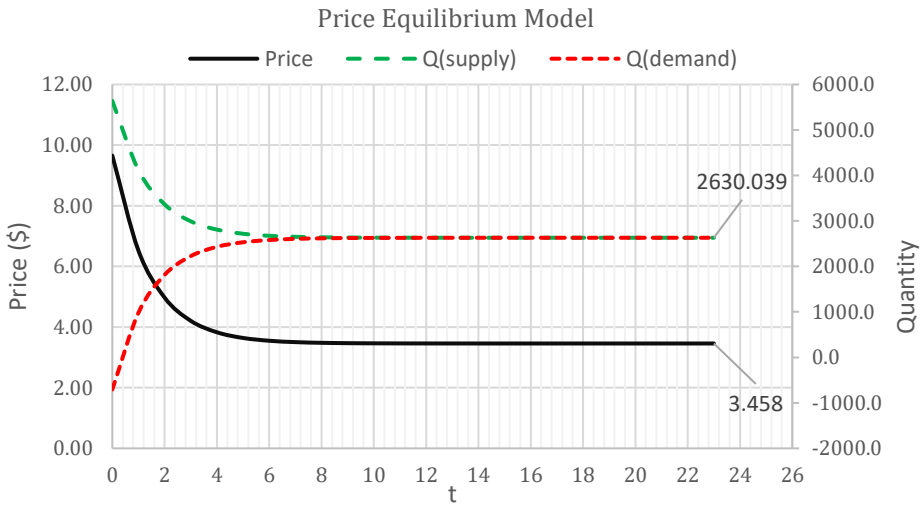

Figure 7-14: Simulation results showing supply, demand, and price changes.

Conclusion: An equilibrium price P_e is achieved when $P_{(i)} = P_{(i+1)}$ and $Q_e = D(p) - S(p) = 0$. In the preceding scenario, the equilibrium price p_e was $

3.458, with a corresponding equilibrium quantity of 2,630 units. The p_e and Q_e values exactly match our reference (Robert Pindyck, 2005)[13].

7.5h Labor-Leisure model

The Solver ® program is used to evaluate the validity of the simulation's Labor-Leisure model!

Given a boid with a labor – leisure utility maximization function:

$$\max U(Y^a L^b)\ \ s.t. Y = w\left(24 - L - \frac{d}{s}\right) + Y^o - dc$$

where a is labor exponent, b is leisure exponent, d is distance to work, c is cost of travel per unit distance, s is speed of transit, Y^0 is non-wage income, and wage w. Calculate L (Hr) and Y ($) that maximizes $U_{Y,L}$.

Y^0 ($)	s ($\frac{\text{km}}{\text{hr}}$)	d (km)	c ($\frac{\$}{km}$)	a	b	w ($\frac{\$}{\text{Hr}}$)
22.32	70	33	0.23	0.38	0.62	16.0

* Simulation Output *

L = 9.290697 Y= 242.53601

Solver® Output

Engine: GRG Nonlinear

Solution Time: 0.063 Seconds.

Iterations: 3 Subproblems: 0

Solver Options

[13] D. R. Robert Pindyck, "Chapter 2: The Basics of Supply and Demand," in *Microeconomics*, New Jersey, Pearson Pentice Hall, 2005, pp. 36-37.

Max Time Unlimited, Iterations Unlimited, Precision 0.000001, Use Automatic Scaling

Convergence 0.0001, Population Size 100, Random Seed 0, Derivatives Forward, Require Bounds

Max Subproblems Unlimited, Max Integer Sols Unlimited, Integer Tolerance 1%, Assume Nonnegative

Objective (Max)	Initial Value	Final Value
$U(Y^a L^b)$	31.35	70.21

Variable Cells

Name	Original Value	Final Value	Integer
L	1	9.76212325	Contin
Y	382.7300000	242.53602788	

Conclusion: The absolute differences between simulation and Solver® results for the quantity of leisure hours L necessary to maximize consumption Y are 4.829136 % and 0.000007 %, respectively.

7.5i Liquidity Preference-Money Supply model

Given an economy with an output $Y_{(t)} = 1{,}280$ units, price level $P_{(t)}$ = 116, money supply $M_{(t)} =$ \$ 4,400, change in demand for money per unit change in income $h = \frac{\Delta M}{\Delta I} = 1.095784$, change in demand for money per unit change in interest rate $f = \frac{\Delta M}{\Delta r} = -0.165937$ (K, n.d.), and interest rate $r_{(0)}$ = 5%. Plot transient interest rate and money supply.

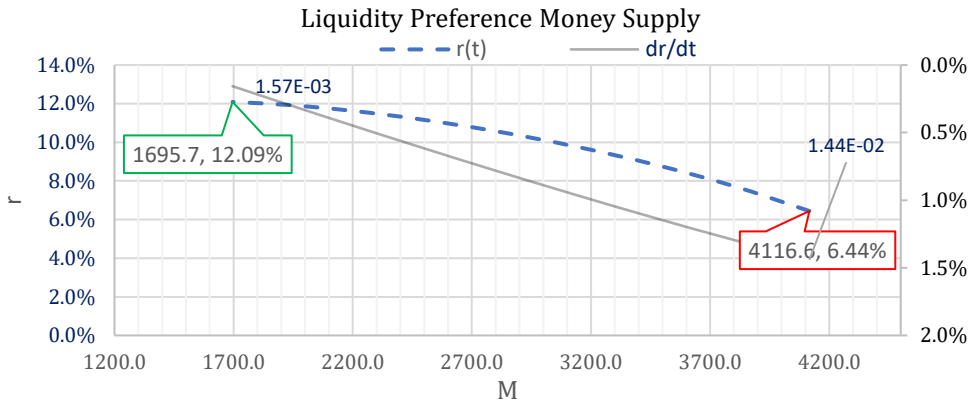

Figure 7-15: Simulation output depicting transient behavior of money supply and interest rate. The approximate money supply equilibrium is established at $ 1,695.70.

7.5j Intertemporal Choice model

The Solver ® program is used to evaluate the validity of the simulation's Labor-Leisure model!

Given an agent with an Additive 2-Period Utility Max function: $V = \mathrm{U}_0 + \frac{\mathrm{U}_1}{1+\rho}$ (7.2): $U_{(i)} = \log(m)$ (7.3), where U_o, U_1 are utilities of consumption in period 0,1 respectively and ρ is impatience parameter. The budget function is defined as:

$$m_1 = [(I_0 + S - m_0)\,\bar{r} + I_1]\,, \bar{r} = \frac{1+r}{1+\gamma} - 1 \qquad (7.4)$$

where m_0, m_1 are consumption in period 0 and 1 respectively, I_0, I_1 are incomes in period 0 and 1 respectively, $r\ is$ nominal interest rate, γ is the inflation rate and $\bar{r}$ is the real interest rate. Given following values of parameters, determine utility maximization consumptions for period m_0 and m_1 subject to total wealth W.

I_0 ($)	I_1($)	S($)	ρ	r	γ
98	110	255	0.12	0.05	0.03

* Simulation Output *

m_0 = 244.60379 m_1= 222.63693

Solver® Output

Engine: GRG Nonlinear

Solution Time: 0.094 Seconds.

Iterations: 3 Subproblems: 0

Solver Options

Max Time Unlimited, Iterations Unlimited, Precision 0.000001, Use Automatic Scaling

Convergence 0.0001, Population Size 100, Random Seed 0, Derivatives Forward, Require Bounds

Max Subproblems Unlimited, Max Integer Sols Unlimited, Integer Tolerance 1%, Assume Nonnegative

Objective (Max)	Initial Value	Final Value
V	0.57	4.48

Variable Cells

Name	Original Value	Final Value	Integer
m_0	1	243.54	Contin
m_1	1	221.58	Contin

Constraints

Name	Cell Value	Formula	Status	Slack
W	460.9048	$\sum \frac{m_i}{(1+r)^{i-1}} = \sum \frac{I_i}{(1+r)^{i-1}}$	Binding	0

Conclusion: The absolute differences between simulation and Solver® results for the quantity of consumption for period (0) and period (1) are 0.43490% and 0.47473% respectively.

7.5k Land Price gradient

Given (8) cities placed randomly on a Euclidean plane $\mathbb{R}^2(100 \times 100)$, each with a unique land value at each city center P_0 and a universal land price gradient c. Simulate the $\mathbb{R}^2$ land price gradient.

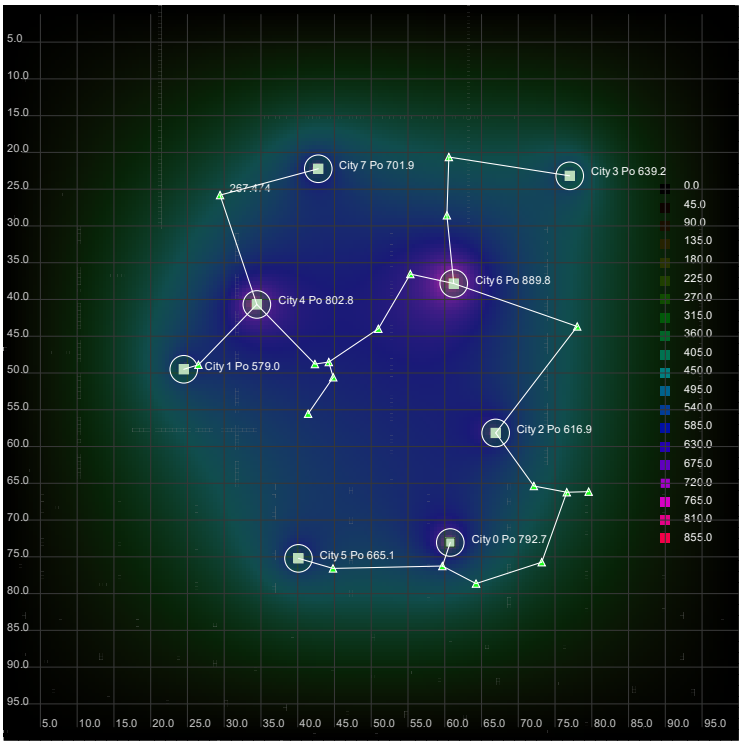

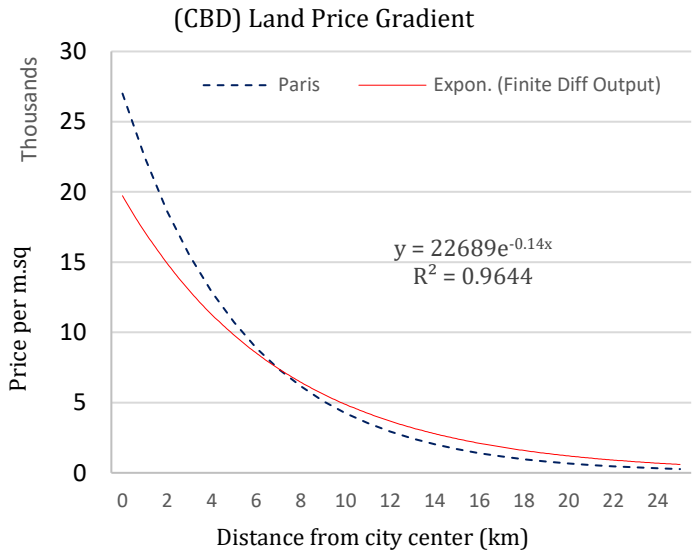

Figure 7-16: (Top) Simulation output of land price gradient achieved using finite differencing scheme. The P_o is the price of land at each city center. (Left) A comparison of land price gradient around a city in the simulation versus the land price gradient for the city of Paris. (The two diagrams shown above are not connected)

Conclusion: The simulated land price gradient achieved the best fit using exponential trend line with an R^2 of 0.9644 and a price gradient of $\exp(-0.14x)$, where x being the distance from the city center in KM. The land prices around the city of Paris are also best represented by an exponential function with an approximate price gradient of $\exp(-0.185)$.

7.5l Hub Location problem

The Solver ® program is used to evaluate the validity of the simulation's HLP implementation!

The Hub Location Problem (HLP) is an NP-hard combinatorial optimization problem that seeks to optimally assign demand points to a single hub while minimizing the total cost of facility operation and transportation. We intend to evaluate the HLP's performance using the Genetic Algorithm (GA) with 4 hubs and 12 demand points. The goal of the problem is to minimize the total transport distance. GA is initialized with a population size of 200, a fitness function of $\frac{1}{\left(\sum d_{(i,j)}\right)^8+1}$ (7.5), and a mutation rate of 0.01.

* Simulation Output *

Minimum Distance = 215.6 (KM)

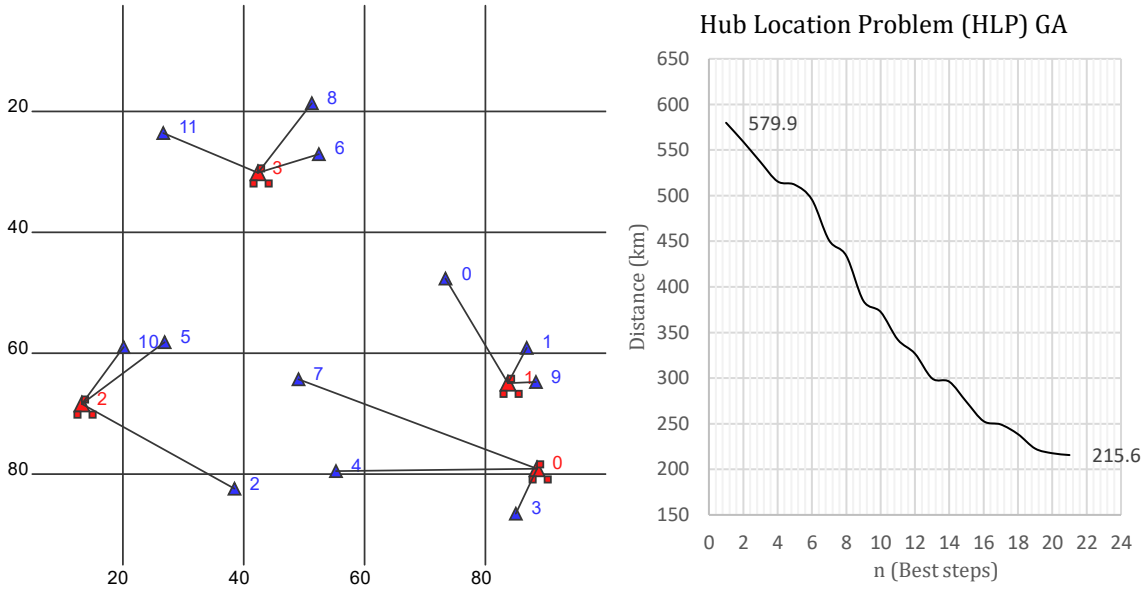

Figure 7-17: The Genetic Algorithm (GA) Heuristic approach is used to solve the HLP problem. To accomplish the shortest possible total transit distance, the 12 demand sites (blue triangles) are each individually connected to 4 hubs.

Solver® Output

Engine: Simplex LP

Solution Time: 0.141 Seconds.

Iterations: 22 Subproblems: 0

Solver Options

Max Time Unlimited, Iterations Unlimited, Precision 0.000001, Use Automatic Scaling

Max Subproblems Unlimited, Max Integer Sols Unlimited, Integer Tolerance 1%, Assume Nonnegative

Objective (Max)	Initial Value	Final Value
V	0.0	206.4

Distance Matrix

HUBS \ FIRMS	F0	F1	F2	F3	F4	F5	F6	F7	F8	F9	F10	F11
H0	35.2	20.3	50.3	8.1	33.4	65.3	63.6	42.3	71.3	14.6	71.5	83.4
H1	20.3	6.9	48.3	21.4	31.8	57.1	49.2	34.6	56.7	4.8	63.8	70.5
H2	63.8	74.4	29.1	74.3	43.7	17.2	57.0	36.3	62.7	75.5	11.7	46.7
H3	35.9	53.3	52.6	71.0	51.2	32.1	10.6	35.0	14.5	57.8	36.5	16.8

Binary Output

HUBS \ FIRMS	F0	F1	F2	F3	F4	F5	F6	F7	F8	F9	F10	F11
H0	0	0	0	1	0	0	0	0	0	0	0	0
H1	1	1	0	0	1	0	0	1	0	1	0	0
H2	0	0	1	0	0	1	0	0	0	0	1	0
H3	0	0	0	0	0	0	1	0	1	0	0	1
	1	1	1	1	1	1	1	1	1	1	1	1

Solution

HUBS \ FIRMS	F0	F1	F2	F3	F4	F5	F6	F7	F8	F9	F10	F11	SUM
H0	0	0	0	8.1	0	0	0	0	0	0	0	0	8.1
H1	20.3	6.9	0	0	31.8	0	0	34.6	0	4.8	0	0	98.4
H2	0	0	29.1	0	0	17.2	0	0	0	0	11.7	0	58
H3	0	0	0	0	0	0	10.6	0	14.5	0	0	16.8	41.9
											Objective		206.4

Conclusion: The total transport distance calculated by the simulation and solver ® has an absolute difference of 4.267161%. Given that HLP is not the primary focus of the research, the current accuracy is sufficient for incorporation into the main model.

8. RESULTS

Upon initialization, the simulation creates a cluster of evenly distributed 2D objects, such as markets, warehouses, industries, resources, transport hubs, trucks, and boids as depicted in Figure 8-1. The fixed nodes are connected to each other by the application of minimum spanning tree to simulate a road network, with additional edges added to create close loops. The resource (mining) nodes serve as the bedrock of the economic supply chain. The mined ore is transferred to industrial sites via use of trucks for refining. The finished product is transferred to warehouses or other industrial and resource sites for consumption. Production nodes continuously monitor the market conditions including cost of intermediaries[14] and respond by varying scales of production per a cost minimization or profit maximization strategy. The consumption points in the economy are simulated as market centers which facilitate trade of finished products between customers and manufacturers. Boids in the simulation are divided into two subgroups of wagers or investors. The wagers earn money through labor at various production sites while the investors earn money through return on their investments. Boids use intertemporal choice function to spend a portion of their savings on consumption. The quantity of various commodities consumed by boids is determined using Hicksian or Marshallian demand functions.

The production process in the simulation is a multistep process starting with resource mining, followed by delivery of ores from mines to industries for refining (tier 1), followed by the transfer of refined products to manufacturing firms (tier 2) for further

[14] Raw materials that are 100% consumed during a production run.

value addition and ultimate transfer of finished products to markets for customer consumption (Timms H. L., 1962). A finished commodity can go through multiple tiers of value addition at numerous production sites before finally making its way to the market. Each tier utilizes a different set of intermediaries during the production process. These intermediaries are basically outputs of other industries in the simulation. The production process is sensitive to the availability of intermediaries since a firm terminates production in case one of the intermediaries falls below a critical level.

Raw, intermediate, and finished products are moved across multiple tiers of production by the logistical units (trucks). Transport hubs are an extension of the main class that are supplied with a set of subservient transport units. Transport hubs are integrated with the minimum spanning tree network with prime responsibility of collecting (pick up – drop off) signals generated by various production and consumption nodes followed by route planning for transport units. Transport hubs operate in binary states of *idle* or *active.* An *idle* state corresponds to all trucks of a corresponding hub being positioned at the hub location. This triggers a search mechanism where the hub checks on the binary value of reorder at various production and consumption nodes. Given that a node's reorder value is (1); the hub checks the binary value of 'order in' variable on all the corresponding input feeds. The hub collects source, sink, container, quantity, and order cost information given a feed's 'order in' state is (0). The source specifies the global id index of node where feed is being procured, sink indicates the global id index of node where feed is getting delivered, container indicates which one of the input feeds is being replenished at sink, quantity indicates the volume of product that is being delivered between source and

sink and is the minimum value between equilibrium order quantity (EOQ) and truck carrying capacity, order price is the combined cost of product purchase and freight.

Upon initialization, the simulation runs an interdependent protocol which links various supplier nodes to production and consumption nodes based on the criteria of minimum distance. Feed quantities are checked at the conclusion of every shift and a reorder signal is generated in the event of a given feed level falling below the reorder point. The simulation runs a modified version of the interdependent protocol in parallel that continuously updates the supplier options based on product availability and combined cost of product and freight. The sale price of a product by a given firm is determined based on the max value of either the cost of production or the market price determined by Walrasian stability equilibrium. The equilibrium order quantity (EOQ) and reorder point (ROP) are updated for a given feed based on the selection of a new supplier.

Transport hubs initiate a vehicle routing problem solver upon receiving a list of pick up - drop off delivery orders. The vehicle routing problem protocol uses combinatorics to sequence a set of deliveries such that the total distance covered by all the corresponding vehicles is minimized. Each vehicle is loaded with a drive plan derived from Floyd Warshall algorithm that defines a set of waypoints on the minimum spanning tree which the vehicle must traverse between hub departure, execution of pickup-drop off deliveries, and arrival back at hub. The freight price per hub is dynamic in nature and calculated based on the utilization factor of transport assets.

During production and transportation, point and mobile units create gaseous emissions that are dispersed in the atmosphere via advection and diffusion mechanisms as depicted in Figure 8-2. The health impact of these emissions on a given boid is estimated using a

logistic dose response curve. If the health level of a given boid falls below a critical level, that boid is removed from the simulation.

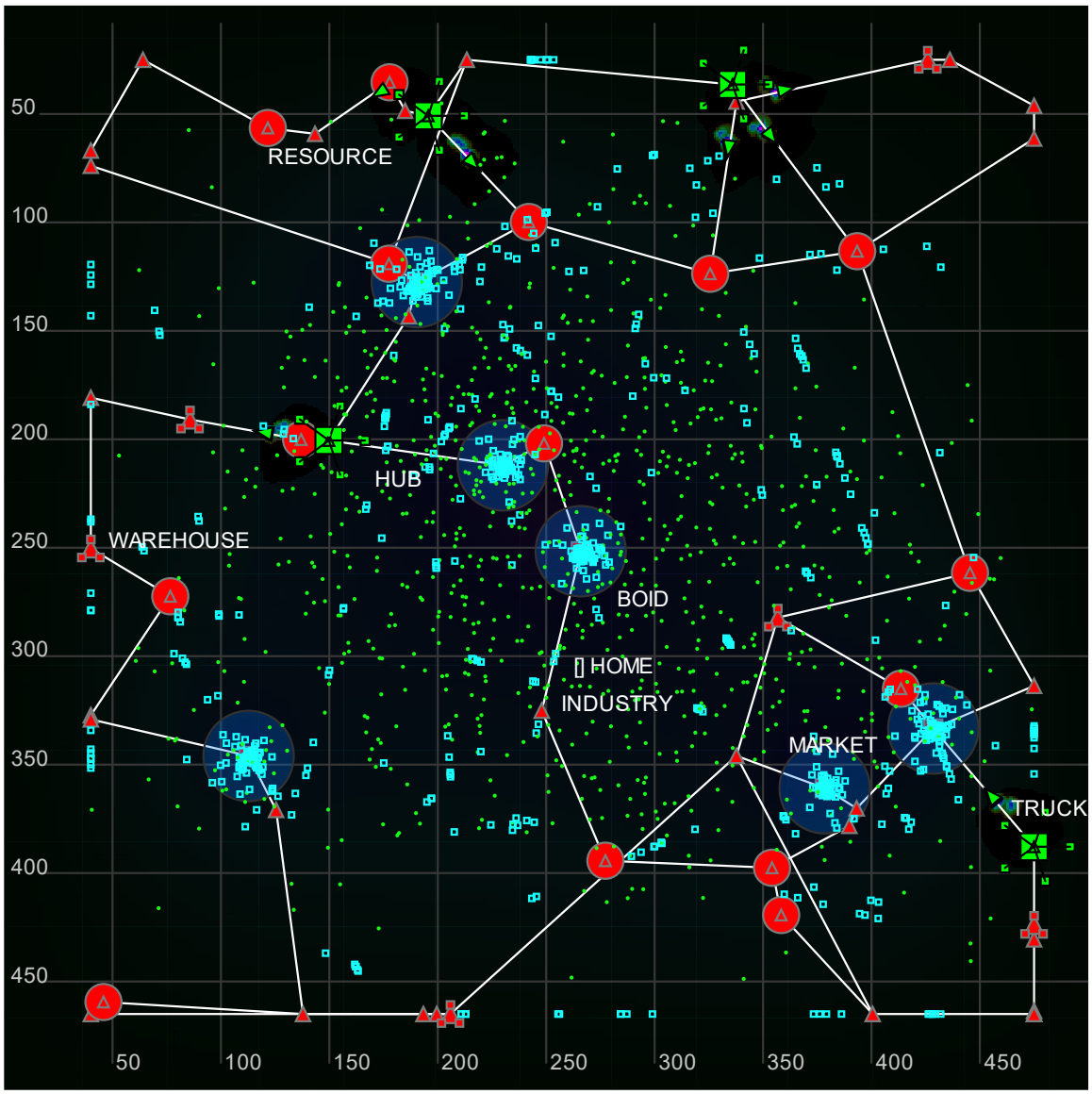

Figure 8-1: A 2D spatial output of the economic assessment platform. The display shows random distribution of various resources, industries, transport hubs and markets over a 500KM x 500 KM area. The road network is conceived by the application of Prim's Minimum Spanning Tree (MST) algorithm, with extra edges added to create close loops. Trucks use the road network to channel goods between pickup and drop-off points.

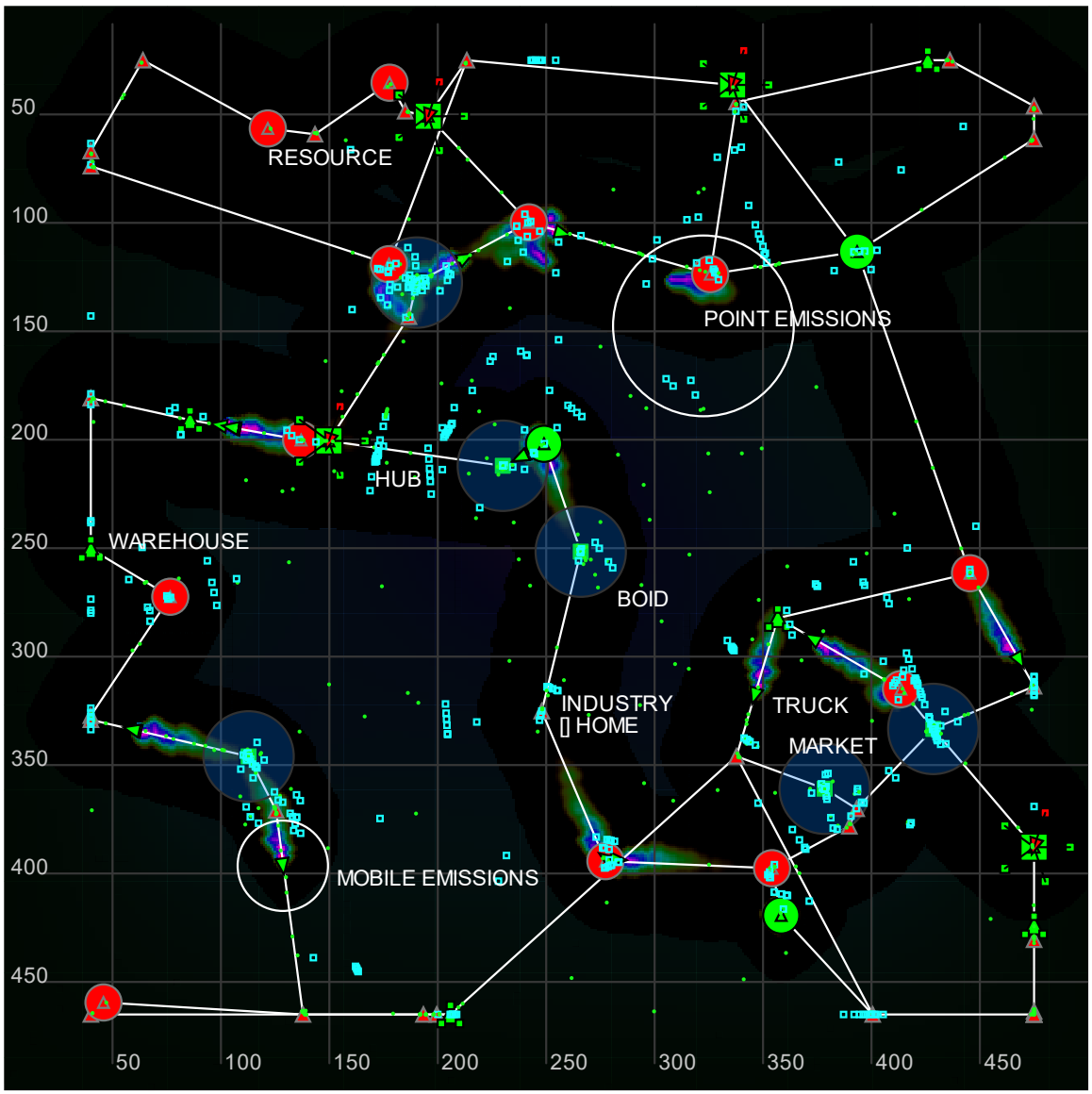

Figure 8-2: Ground level emissions concentrations from mobile and point sources.

Emissions concentrations are estimated using the PUFF dispersion model.

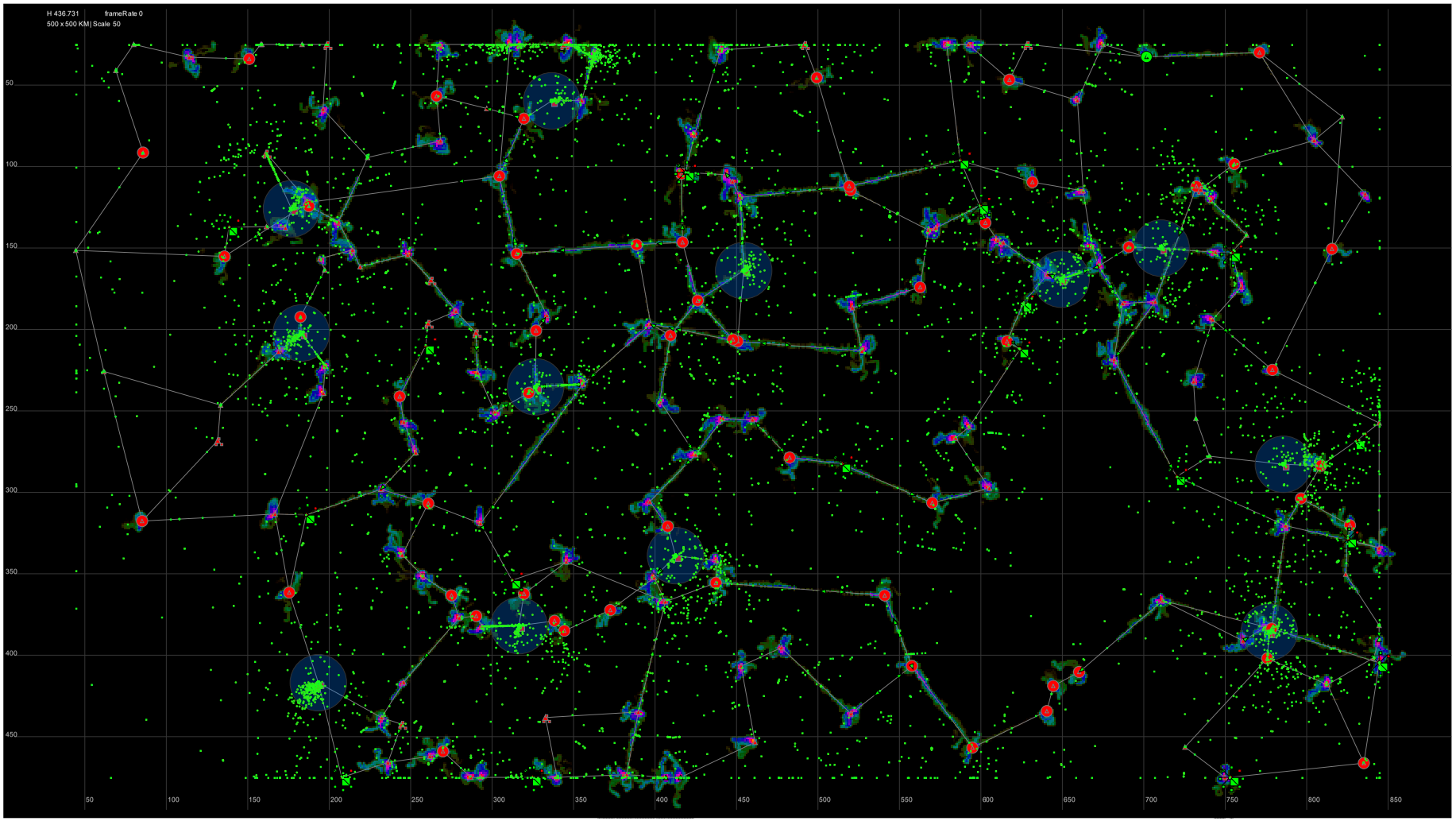

Figure 8-3: Spatial distribution of various entities used in calculating the impact of passive and active emissions control on productivity.

See prior figures for details on entities.

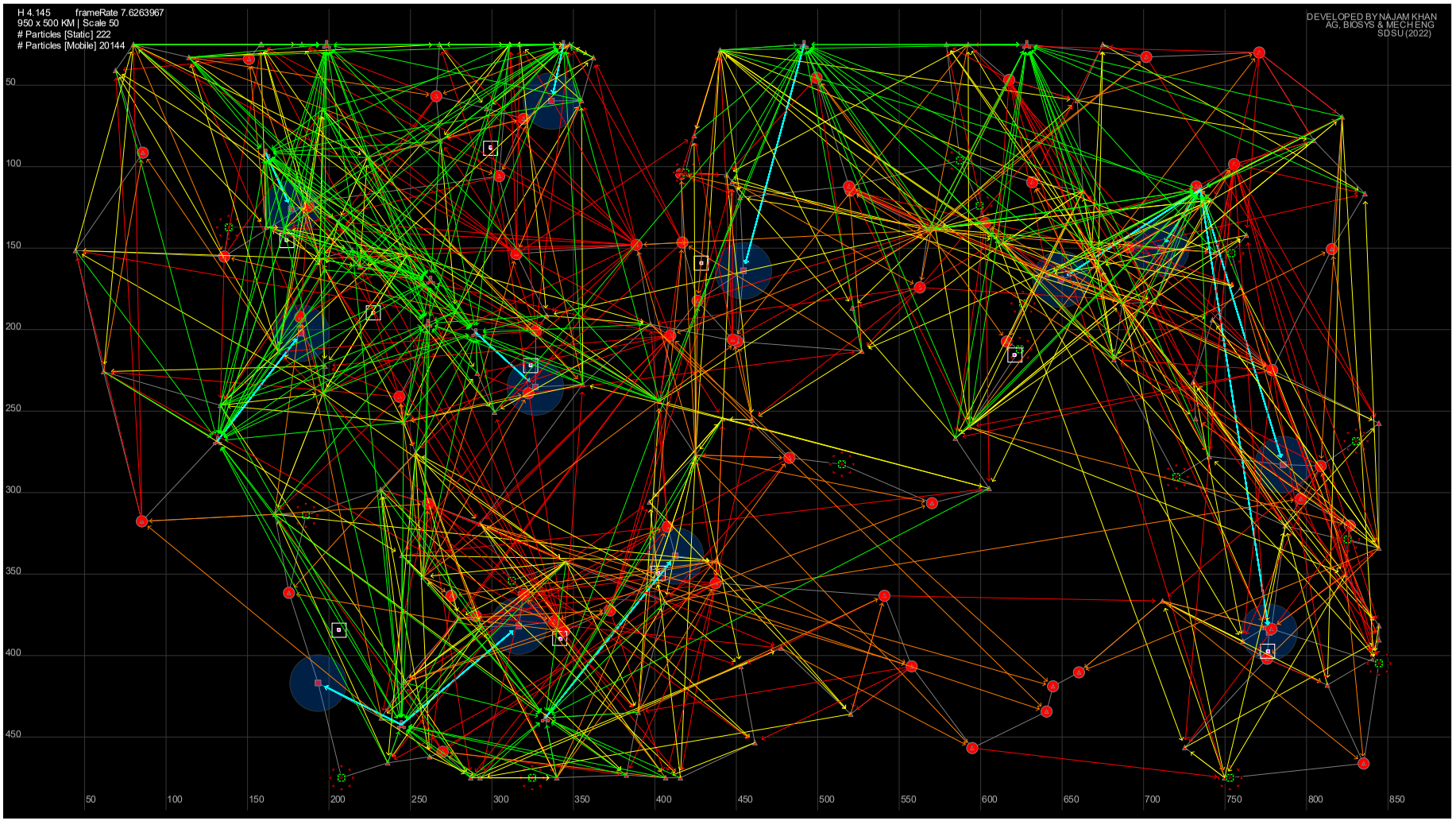

Legend: Warehouse to markets (→) , Industries to Warehouses (→), Industries to industries (→) , Industries to resources (→) , Resources to industries (→)

Figure 8-4: The interdependence of firms on each other's productivity

In the above display, the level of interdependence (M, I, R, W) for industries is (0, 2, 2, 0), for resources (0, 2, 0, 0), for warehouses (0, n, 0, 0), and for markets is (0, 0, 0, n). (M, I, R) indicates number of corresponding markets, industries and resources inputs a given production or consumption node requires to operate.

Legend: Traversal - Unloaded (→) , Traversal - Loaded (→)

Figure 8-5: Vehicle routing problem with multiple pickups-drop offs.
In the above display, the hubs articulated drive plan shows the different waypoints the trucks must traverse to perform successive pickup and drop-off orders. The pathway between any pickup and drop off order is determined using the Floyd

8.1 Passive emissions controls

The emissions exposure levels are evaluated as a function of different shutoff time periods between consecutive operations of industrial and mining facilities. All other firms, including the transport sector, are allowed to operate uninterrupted, and firms are free to vary their scale of production as a function of market price. Firms cannot produce below a minimum threshold and must always maintain a minimum finished inventory levels.

8.1a Earnings ($) / spending ($) / foregone sales ($)

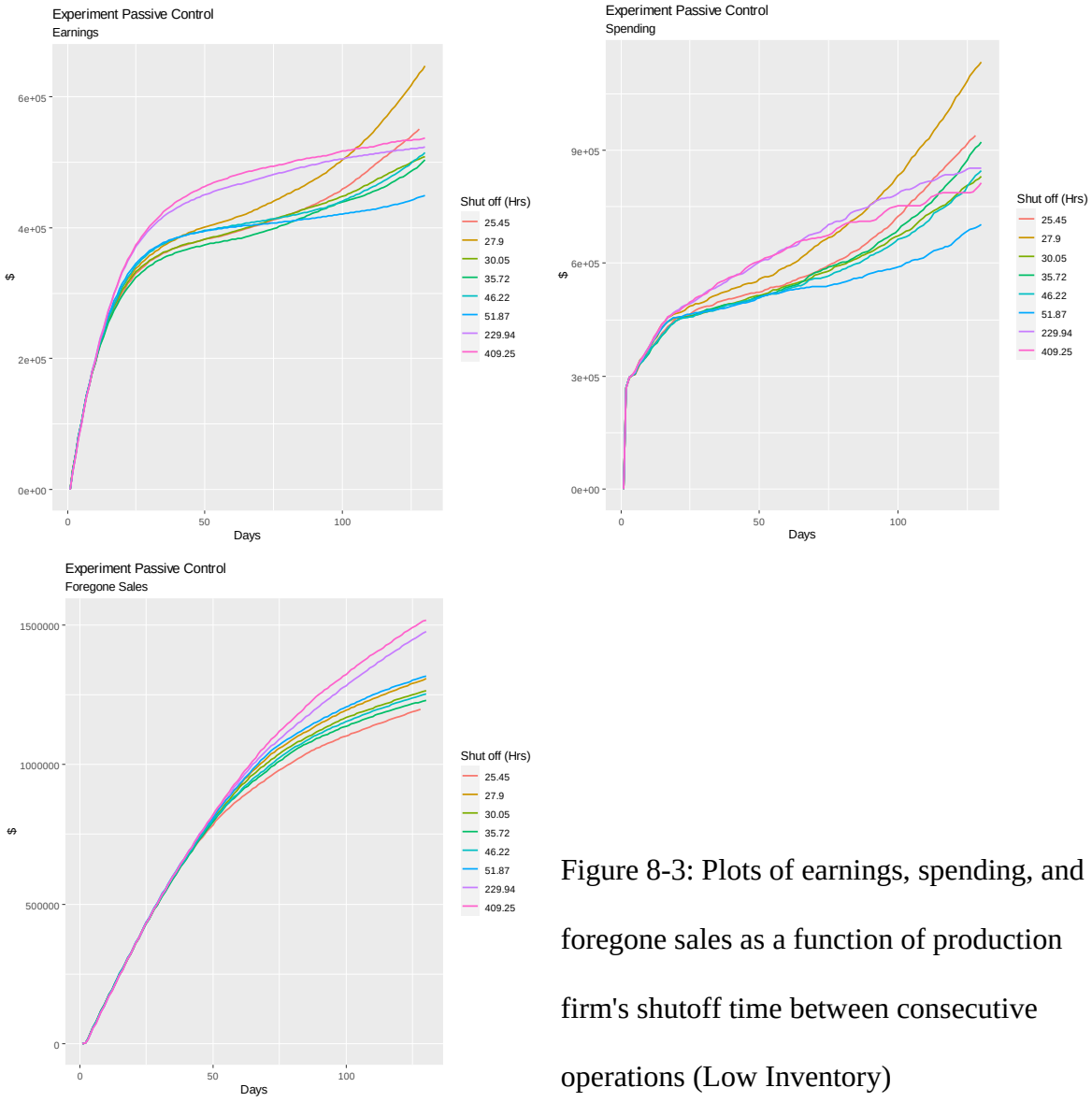

Figure 8-3: Plots of earnings, spending, and foregone sales as a function of production firm's shutoff time between consecutive operations (Low Inventory)

Table 8.1: Summary of earnings, spending, and foregone sales

Shut down time	Earnings (Max)	Spending (Max)	Forgone Sales (Max)
25.45	551308.9	939822.6	1198260
27.90	648133.6	1135869.8	1307759
30.05	509202.6	830658.4	1265033
35.72	503473.9	921556.9	1230993
46.22	515423.9	846423.6	1253976
51.87	449402.4	703220.9	1317709
229.94	523244.9	853797.9	1476442
409.25	537247.4	812590.4	1518916
Correlation	**-0.016284559**	**-0.2928**	**0.950802726 (log)**

Regression Analysis

```
Call:
lm(formula = Earnings ~ ShutdownHrs, data = dataEarn)

Residuals:
   Min     1Q Median     3Q    Max
-80640 -22406 -10141  12439 117933

Coefficients:
             Estimate Std. Error t value Pr(>|t|)
(Intercept) 530383.558  27871.209   19.03 1.36e-06 ***
ShutdownHrs     -6.575    164.810   -0.04    0.969
---
Signif. codes:  0 '***' 0.001 '**' 0.01 '*' 0.05 '.' 0.1 ' ' 1

Residual standard error: 61030 on 6 degrees of freedom
Multiple R-squared:  0.0002652, Adjusted R-squared:  -0.1664
F-statistic: 0.001592 on 1 and 6 DF,  p-value: 0.9695
```

```
Call:
lm(formula = Spending ~ ShutdownHrs, data = dataSpen)

Residuals:
    Min      1Q  Median      3Q     Max
-191797  -55087    8651   26178  234542

Coefficients:
             Estimate Std. Error t value Pr(>|t|)
(Intercept) 908671.8    59346.9   15.31  4.9e-06 ***
ShutdownHrs   -263.2      350.9   -0.75    0.482
---
Signif. codes:  0 '***' 0.001 '**' 0.01 '*' 0.05 '.' 0.1 ' ' 1

Residual standard error: 129900 on 6 degrees of freedom
Multiple R-squared:  0.08573,   Adjusted R-squared:  -0.06664
F-statistic: 0.5626 on 1 and 6 DF,  p-value: 0.4816
```

```
Call:
lm(formula = MissedSales ~ log(ShutdownHrs), data = dataXSales)

Residuals:
   Min     1Q Median     3Q    Max
-39303 -32787   3823  14637  67772

Coefficients:
                Estimate Std. Error t value Pr(>|t|)
(Intercept)       888573      59155  15.021 5.48e-06 ***
log(ShutdownHrs)  105573      14043   7.518 0.000287 ***
---
Signif. codes:  0 '***' 0.001 '**' 0.01 '*' 0.05 '.' 0.1 ' ' 1

Residual standard error: 38840 on 6 degrees of freedom
Multiple R-squared:  0.904,     Adjusted R-squared:  0.888
F-statistic: 56.52 on 1 and 6 DF,  p-value: 0.0002868
```

The regression[15] results show that shutdown hours have no significant impact on earnings or spending volume. However, an increase in shutdown hours increases the opportunity cost due to missed sales. The value of correlation coefficients for earnings, spending, and missed sales are -0.016, -0.293, and 0.951 respectively. The volume of missed sales as a function of shutoff hours can be approximated using the following logarithmic function:

$$\text{sales}_{oc} = 888{,}573 + 105{,}573\log(\text{shutoff hours}) \quad (8.1)$$

The function indicates that a log-hour increase in shutoff period increases opportunity cost due to missed sales by $105,573. The *p*-value for the shutoff period coefficient is 0.000287. The adjusted R-squared for the missed sales in relation to shutoff hours is 0.888, which indicates a relatively strong degree of interrelation and dependence between shutoff hours and foregone sales.

[15] The regression analysis in run in the R® statistical program. The regression analysis is used for modeling a relationship between response variable Y and one or more independent variables, $X_1, \dots, X_p$. Regression analysis have several objectives including prediction of future observations, assessment of effects between explanatory variables on the response, and a general description of data structure. A general form for the model can be:

$$Y = \beta_o + \beta_1 X_1 + \beta_2 X_2 + \beta_3 X_3 + \varepsilon$$

Where Y is output, β_o is intercept term, $\beta_i, i = 0,1,2,3$ are unknown parameters, and ε is the error (Faraway, 2002).

8.1b Units produced versus units consumed

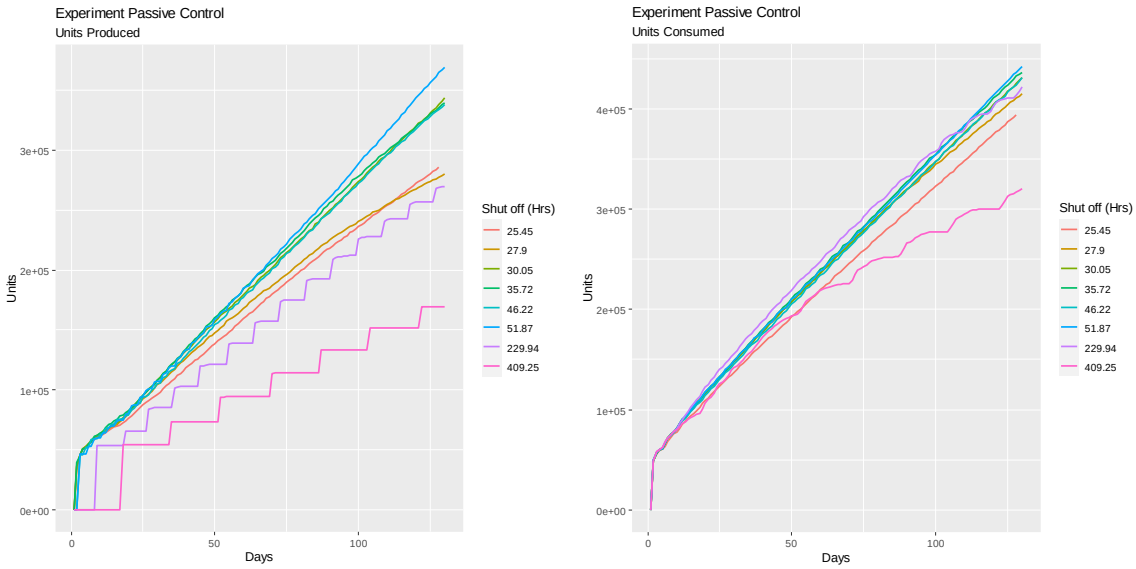

Figure 8-4:Commodities production and consumption as a function of production firm's shutoff time between consecutive operations (Low Inventory)

Table 8.2: Units produced versus units consumed

Shut down time	Units produced	Units consumed
25.45	285759.2	394296.0
27.90	280166.2	414914.9
30.05	344069.8	431177.2
35.72	339643.1	436603.3
46.22	338515.1	430816.7
51.87	369646.9	442457.4
229.94	269655.9	421385.8
409.25	169383.9	320383.2
Correlation	**-0.846994287**	**-0.805846069**

Regression Analysis

```
Call:
lm(formula = UnitsProduced ~ ShutdownHrs, data = dataUProd)

Residuals:
   Min     1Q Median     3Q    Max
-49962 -21588  13650  15949  48762

Coefficients:
             Estimate Std. Error t value Pr(>|t|)
(Intercept) 340888.12   16710.50  20.400 9.02e-07 ***
ShutdownHrs   -385.64      98.81  -3.903  0.00796 **
---
Signif. codes:  0 '***' 0.001 '**' 0.01 '*' 0.05 '.' 0.1 ' ' 1

Residual standard error: 36590 on 6 degrees of freedom
Multiple R-squared:  0.7174,    Adjusted R-squared:  0.6703
F-statistic: 15.23 on 1 and 6 DF,  p-value: 0.007959
```

```
Call:
lm(formula = UnitsConsumed ~ ShutdownHrs, data = dataUConx)

Residuals:
   Min     1Q Median     3Q    Max
-35881 -16518   3722  11164  38003

Coefficients:
             Estimate Std. Error t value Pr(>|t|)
(Intercept) 436001.14   11608.66  37.558 3.38e-08 ***
ShutdownHrs   -228.84      68.65  -3.334   0.0157 *
---
Signif. codes:  0 '***' 0.001 '**' 0.01 '*' 0.05 '.' 0.1 ' ' 1

Residual standard error: 25420 on 6 degrees of freedom
Multiple R-squared:  0.6494,    Adjusted R-squared:  0.591
F-statistic: 11.11 on 1 and 6 DF,  p-value: 0.01574
```

The regression results indicate that there is a relatively strong *negative* correlation between shutoff hours and the total quantity of units produced and consumed in an economy. The correlation factor between shutoff hours and the quantity of units produced and consumed is -0.847 and -0.805 respectively. The units produced in an economy as a function of shutoff hours can be formulated using the following function:

$$\text{units}_{\text{prod}} = 340{,}888.12 - 385.64(\text{shutoff hours}) \qquad (8.2)$$

The linear function indicates that an hour increase in shutoff period reduces productivity by 385.64 units. The shutdown period coefficient has a *p*-value of 0.00796 and the whole model has a *p*-value of 0.007959, indicating that the regression model adequately fits the association between shutoff hours and units produced.

The units consumed in an economy as a function of shutoff hours can be formulated using following function:

$$\text{units}_{\text{consumed}} = 436{,}001.14 - 228.84(\text{shutoff hours}) \qquad (8.3)$$

The function indicates that an hour increase in shutoff period reduces consumption by 228.84 units. The *p*-value for the shutoff period coefficient is 0.0157. The *p*-value for the entire model is 0.01574 which represents that the regression model provides ample fit to the relationship between shutoff hours and units consumed in the economy.

8.1c Maximum product moved ($) vs transportation costs ($)

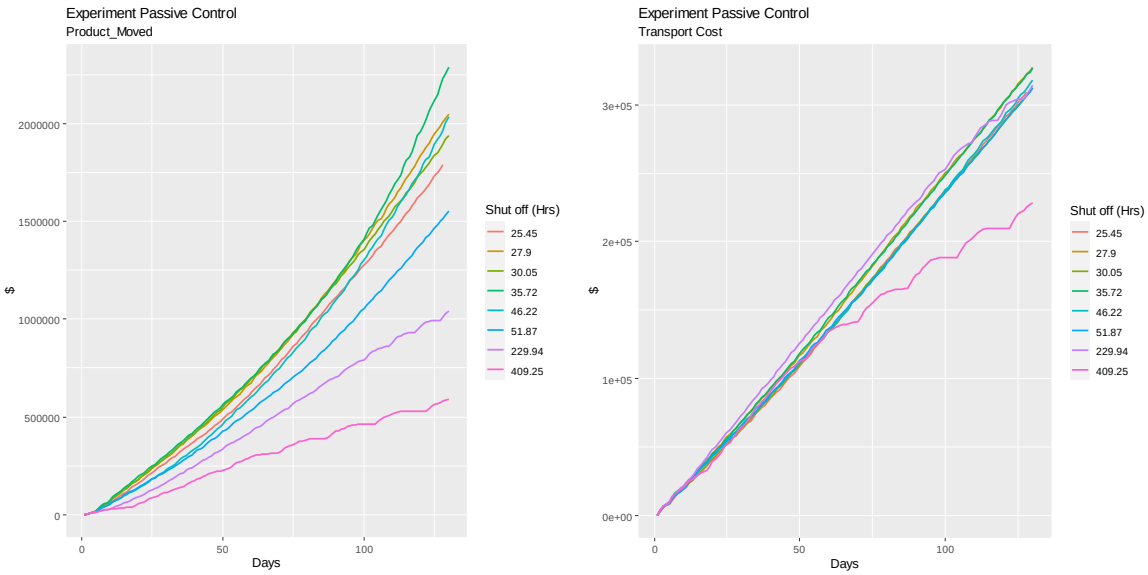

Figure 8-5: Total nominal value of product moved, and the associated transport cost observed at various levels of shutoff time.

Table 8.3: Product moved and corresponding transport cost

Shut down time	Product Moved Max ($)	Transport Max ($)
25.45	1790895.4	309445.0
27.90	2049018.0	327669.1
30.05	1937768.5	312348.4
35.72	2289410.8	326790.7
46.22	2035921.4	318040.5
51.87	1552519.8	312251.6
229.94	1038875.9	314370.7
409.25	590199.5	228693.6
Correlation	**-0.928648822**	**-0.872350283**

Regression Analysis

```
Call:
lm(formula = ProductMoved ~ ShutdownHrs, data = dataProdMvd)

Residuals:
    Min      1Q  Median      3Q     Max
-319064 -159257   33990  100012  356069

Coefficients:
             Estimate Std. Error t value Pr(>|t|)
(Intercept) 2069934.7   105460.7  19.628 1.13e-06 ***
ShutdownHrs   -3824.0      623.6  -6.132  0.00086 ***
---
Signif. codes:  0 '***' 0.001 '**' 0.01 '*' 0.05 '.' 0.1 ' ' 1

Residual standard error: 230900 on 6 degrees of freedom
Multiple R-squared:  0.8624,    Adjusted R-squared:  0.8395
F-statistic:  37.6 on 1 and 6 DF,  p-value: 0.0008602
```

```
Call:
lm(formula = TransportCost ~ ShutdownHrs, data = dataTranCost)

Residuals:
   Min     1Q Median     3Q    Max
-17164 -10184  -2638   5834  32708

Coefficients:
             Estimate Std. Error t value Pr(>|t|)
(Intercept) 327577.11    7725.88  42.400 1.15e-08 ***
ShutdownHrs   -199.68      45.69  -4.371  0.00471 **
---
Signif. codes:  0 '***' 0.001 '**' 0.01 '*' 0.05 '.' 0.1 ' ' 1

Residual standard error: 16920 on 6 degrees of freedom
Multiple R-squared:  0.761,     Adjusted R-squared:  0.7212
F-statistic:  19.1 on 1 and 6 DF,  p-value: 0.004715
```

The regression analysis shows a strong negative relationship between shutdown times and both the max value of the product moved and the associated transportation costs. The respective correlations of the two variables as function of shutdown hours is -0.9286 and -0.87235. The p-value on the value of product moved as a function of shutdown hours is 0.00086 while that of transport cost is 0.00471. An increase in shutoff hours reduces production levels, which in turn reduces the replenishment frequency for intermediate feeds.

8.1d Average and maximum emission's exposure

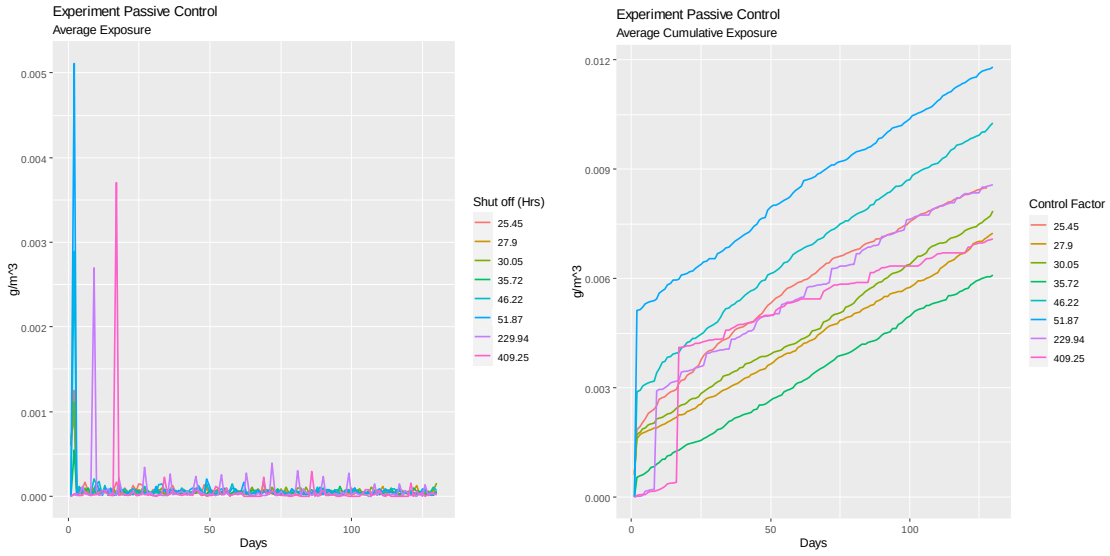

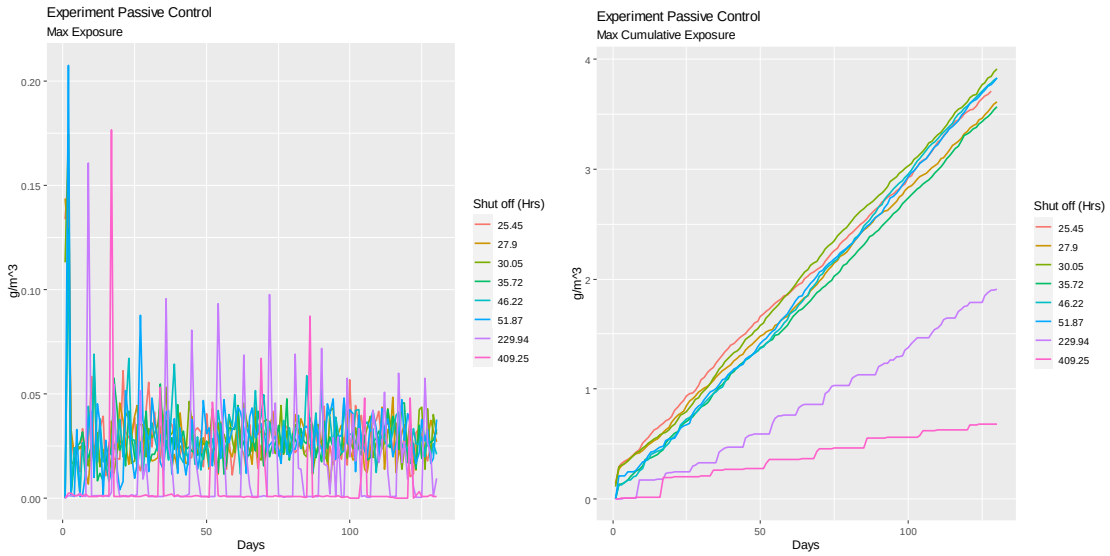

Figure 8-6: Plots of (average) and (maximum) emissions exposure as a function of firm's shutoff time between each production

Table 8.4: Average and Max Emissions Exposure

Shut down time (Hrs.)	Average Emissions Exposure g/m^3	Average Emissions Exposure Cumulative g/m^3	Max Emissions Exposure g/m^3	Max Emissions Exposure Cumulative g/m^3
25.45	6.634984e-05	0.008491695	0.028970091	3.708172
27.90	5.564723e-05	0.007233847	0.027820272	3.616635
30.05	6.047578e-05	0.007861851	0.030119181	3.915494
35.72	4.691038e-05	0.006098350	0.027446379	3.568029
46.22	7.891078e-05	0.010258401	0.029449451	3.828429
51.87	9.088242e-05	0.011814245	0.029442150	3.827479
229.94	6.599750e-05	0.008580000	0.014659952	1.905794
409.25	5.450176e-05	0.007090000	0.005253656	0.683000
Correlation	**-0.21963153**	**-0.213**	**-0.9892**	**-0.9886**

Regression Analysis

```
Call:
lm(formula = uConcentration ~ ShutdownHrs, data = dataAvgExp)

Residuals:
      Min        1Q    Median        3Q       Max
-1.964e-05 -7.415e-06 -2.076e-06  5.981e-06  2.469e-05

Coefficients:
              Estimate Std. Error t value Pr(>|t|)
(Intercept)  6.735e-05  6.834e-06   9.854  6.3e-05 ***
ShutdownHrs -2.229e-08  4.041e-08  -0.551    0.601
---
Signif. codes:  0 '***' 0.001 '**' 0.01 '*' 0.05 '.' 0.1 ' ' 1

Residual standard error: 1.496e-05 on 6 degrees of freedom
Multiple R-squared:  0.04824,   Adjusted R-squared:  -0.1104
F-statistic: 0.3041 on 1 and 6 DF,  p-value: 0.6012
```

```
Call:
lm(formula = uConcentrationSum ~ ShutdownHrs, data = dataAvgExpCS)

Residuals:
      Min        1Q    Median        3Q       Max
-0.0025304 -0.0005413 -0.0003282  0.0007870  0.0032308

Coefficients:
              Estimate Std. Error t value Pr(>|t|)
(Intercept)  8.729e-03  8.889e-04   9.820 6.42e-05 ***
ShutdownHrs -2.806e-06  5.256e-06  -0.534    0.613
---
Signif. codes:  0 '***' 0.001 '**' 0.01 '*' 0.05 '.' 0.1 ' ' 1

Residual standard error: 0.001946 on 6 degrees of freedom
Multiple R-squared:  0.04535,   Adjusted R-squared:  -0.1138
F-statistic: 0.285 on 1 and 6 DF,  p-value: 0.6126
```

```
Call:
lm(formula = MaxConcentration ~ ShutdownHrs, data = dataMaxExp)

Residuals:
      Min        1Q    Median        3Q       Max
-0.0015355 -0.0013460  0.0001019  0.0010870  0.0017275

Coefficients:
              Estimate Std. Error t value Pr(>|t|)
(Intercept)  3.107e-02  6.632e-04   46.85 6.34e-09 ***
ShutdownHrs -6.469e-05  3.922e-06  -16.50 3.16e-06 ***
---
Signif. codes:  0 '***' 0.001 '**' 0.01 '*' 0.05 '.' 0.1 ' ' 1

Residual standard error: 0.001452 on 6 degrees of freedom
Multiple R-squared:  0.9784,    Adjusted R-squared:  0.9748
F-statistic: 272.1 on 1 and 6 DF,  p-value: 3.166e-06
```

```
Call:
lm(formula = MaxConcentrationSum ~ ShutdownHrs, data = dataMaxExpCS)

Residuals:
     Min       1Q   Median       3Q      Max
-0.19662 -0.16521 -0.01237  0.15107  0.23372

Coefficients:
              Estimate Std. Error t value Pr(>|t|)
(Intercept)  4.0381787  0.0881360   45.70 7.35e-09 ***
ShutdownHrs -0.0083751  0.0005212  -16.07 3.69e-06 ***
---
Signif. codes:  0 '***' 0.001 '**' 0.01 '*' 0.05 '.' 0.1 ' ' 1

Residual standard error: 0.193 on 6 degrees of freedom
Multiple R-squared:  0.9773,    Adjusted R-squared:  0.9736
F-statistic: 258.3 on 1 and 6 DF,  p-value: 3.69e-06
```

The regression results show a weak negative correlation between shutoff hours and average exposure to the boids. The correlation factor between shutoff hours and average exposure is -0.219, with a *p*-value of 0.601 for shutoff hour coefficient. The average exposure rate to the boids as a function of shutoff hours can be formulated using the following Equation:

$$\text{exposure}_{\text{u}} = 6.735 \times 10^{-5} - 2.229 \times 10^{-8}(\text{shutoff hours}) \qquad (8.4)$$

The function indicates that an hour increase in shutoff period reduces average exposure by $2.229 \times 10^{-8}\text{g/m}^3$.

There is a strong negative correlation between shutoff hours and the maximum exposure experienced by boids. The correlation factor between shutoff hours and max exposure is -0.9892, with a *p*-value of 3.16×10^{-6} for the shutoff hours coefficient. The adjusted R-squared for the max exposure as function of shutoff hours is 0.9748, which indicates a relatively good degree of interrelation and dependence between shutoff hours and

maximum exposure experienced by the boids. The maximum exposure experienced by the boids as a function of shutoff hours can be formulated using the following Equation:

$$\text{exposure}_{\max} = 3.107 \times 10^{-2} - 6.469 \times 10^{-5}\ (\text{shutoff hours}) \qquad (8.5)$$

The function indicates that an hour increase in shutoff period reduces max exposure by 6.469×10^{-5} g/m^3.

8.1e Active transport hubs, delivery delays

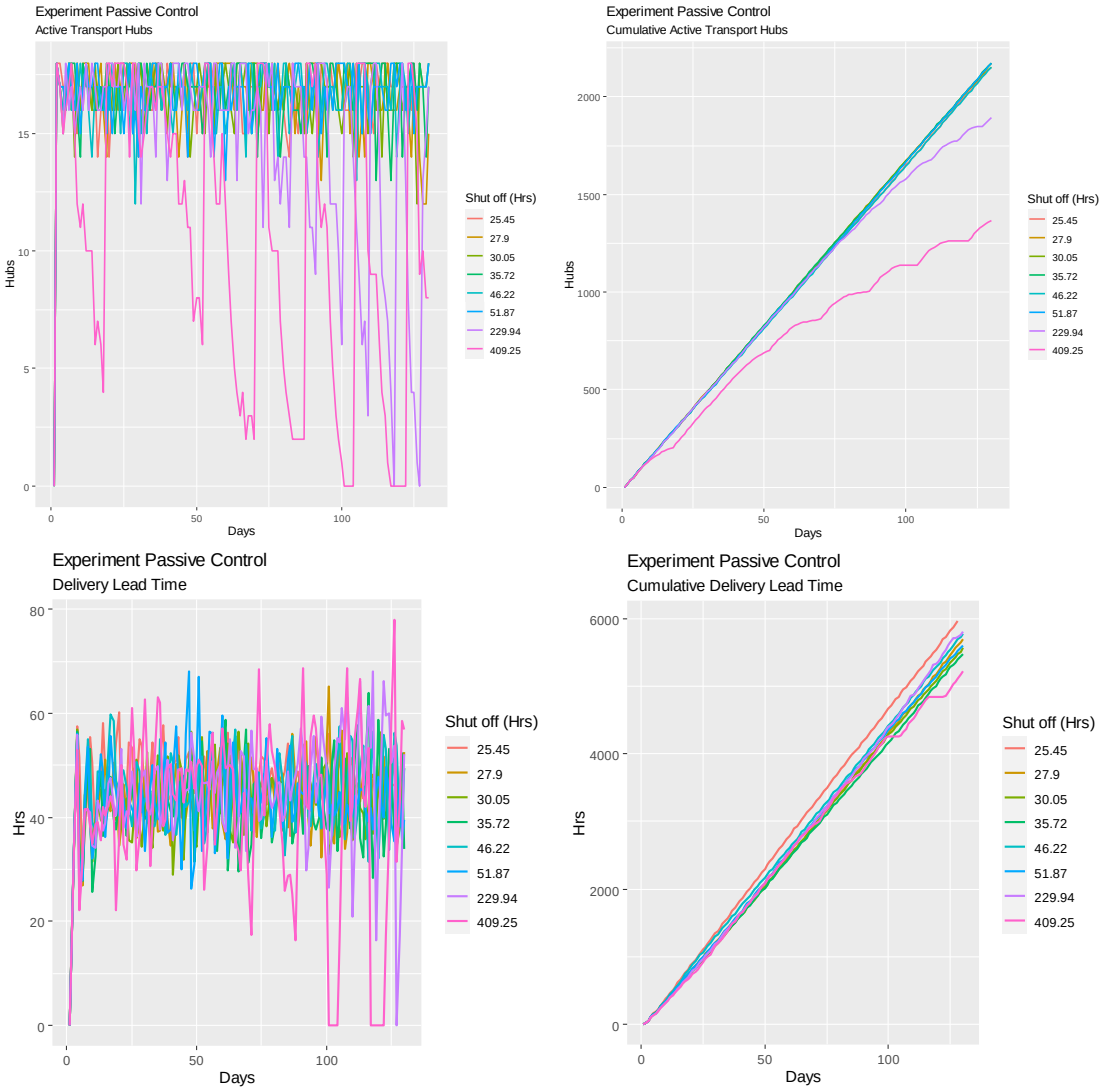

Figure 8-7: Active transport hubs and delivery lead times as a function of shutoff time periods between consecutive production

Table 8.5: Active Transportation Hubs, Delivery Lead Time

Shut down time (Hrs.)	Active Transportation Hubs (Average)	Active Transportation Hubs (Cumulative)	Average Delivery Lead Time (Hrs.)	Delivery Lead Time Cumulative (Hrs.)
25.45	16.60156	2125	46.56212	5959.952
27.90	16.56154	2153	43.85638	5701.329
30.05	16.70769	2172	42.78664	5562.263
35.72	16.71538	2173	42.15607	5480.290
46.22	16.56154	2153	44.44392	5777.710
51.87	16.72308	2174	43.10258	5603.335
229.94	14.57692	1895	44.67832	5808.181
409.25	10.50000	1365	40.20387	5226.502
Correlation	**-0.98252819**	**-0.9793**	**-0.5465**	**-0.5613**

Regression Analysis

```
Call:
lm(formula = nofActiveHubs ~ ShutdownHrs, data = dataActivHub)

Residuals:
     Min       1Q   Median       3Q      Max
-0.46774 -0.27327 -0.04829  0.06905  0.84568

Coefficients:
             Estimate Std. Error t value Pr(>|t|)
(Intercept) 17.26551    0.20126   85.79 1.69e-10 ***
ShutdownHrs -0.01539    0.00119  -12.93 1.32e-05 ***
---
Signif. codes:  0 '***' 0.001 '**' 0.01 '*' 0.05 '.' 0.1 ' ' 1

Residual standard error: 0.4407 on 6 degrees of freedom
Multiple R-squared:  0.9654,    Adjusted R-squared:  0.9596
F-statistic: 167.2 on 1 and 6 DF,  p-value: 1.316e-05
```

```
Call:
lm(formula = nofActiveHubsSum ~ ShutdownHrs, data = dataActivHubCS)

Residuals:
    Min      1Q  Median      3Q     Max
-62.850 -38.184  -0.662  14.301 113.180

Coefficients:
             Estimate Std. Error t value Pr(>|t|)
(Intercept) 3338.303     38.250   79.23 2.73e-10 ***
ShutdownHrs   -1.981      0.167  -11.86 2.18e-05 ***
---
Signif. codes:  0 '***' 0.001 '**' 0.01 '*' 0.05 '.' 0.1 ' ' 1

Residual standard error: 61.86 on 6 degrees of freedom
Multiple R-squared:  0.9591,    Adjusted R-squared:  0.9523
F-statistic: 140.6 on 1 and 6 DF,  p-value: 2.175e-05
```

```
Call:
lm(formula = DelayHrs ~ ShutdownHrs, data = dataDeliveryDelay)

Residuals:
    Min      1Q  Median      3Q     Max
-1.8452 -1.0503 -0.4910  0.9186  2.4849

Coefficients:
             Estimate Std. Error t value Pr(>|t|)
(Intercept) 44.265466   0.782532  56.567 2.05e-09 ***
ShutdownHrs -0.007396   0.004627  -1.598    0.161
---
Signif. codes:  0 '***' 0.001 '**' 0.01 '*' 0.05 '.' 0.1 ' ' 1

Residual standard error: 1.713 on 6 degrees of freedom
Multiple R-squared:  0.2986,    Adjusted R-squared:  0.1817
F-statistic: 2.555 on 1 and 6 DF,  p-value: 0.1611
```

```
Call:
lm(formula = TotalDelayHrs ~ ShutdownHrs, data = dataDeliveryDelayCS)

Residuals:
    Min      1Q  Median      3Q     Max
-224.28 -141.55  -48.47  123.81  279.58

Coefficients:
             Estimate Std. Error t value Pr(>|t|)
(Intercept) 5736.9371    93.3305  61.463 1.16e-05 ***
ShutdownHrs   -0.9040     0.5454  -1.657    0.148
---
Signif. codes:  0 '***' 0.001 '**' 0.01 '*' 0.05 '.' 0.1 ' ' 1

Residual standard error: 201.9 on 6 degrees of freedom
Multiple R-squared:  0.3151,    Adjusted R-squared:  0.2009
F-statistic:  2.76 on 1 and 6 DF,  p-value: 0.1477
```

The regression results indicate that there is a strong *negative* correlation between shutoff hours and the utilization rate of transport hubs. The correlation factor between shutoff hours and average number of active transport hubs is -0.9825. The average number of transportation hubs as a function of shutoff hours can be approximated using following Equation:

$$\text{hubs}_{\text{activated}} = 17.265 - 0.01539(\text{shutoff hours}) \quad (8.6)$$

The function indicates that an hour increase in shutoff period reduces utilization of hubs by -0.01539. (Given that there are 18 hubs this translates to utilization loss of 0.0855% for each hour increase in shutoff period). The *p*-value for the shutoff period coefficient is 1.32×10^{-5}. The adjusted R-squared for the number of active hubs as function of shutoff hours is 0.9596, which indicates a good degree of interrelation and dependence between shutoff hours and transport hubs utilization. The *p*-value for the entire model is 1.316×10^{-5} which represents that the regression model provides ample fit to the relationship between shutoff hours and units produced.

The regression results indicate a relative negative correlation between delivery hours and shutoff hours. The correlation factor between shutoff hours and delivery hours is -0.5465. The average lead time on delivery of an order as a function of shutoff hours can be approximated using following Equation:

$$\text{lead time}_{Hrs} = 44.265 - 0.007396(\text{shutoff hours}) \quad (8.7)$$

The function indicates that an hour increase in shutoff period increases delivery time by 0.007396 hours. The *p*-value for the shutoff period coefficient is 0.161. The *p*-value for the entire model is 0.1611 which represents that the regression model provides a weak fit to the relationship between shutoff hours and delivery lead times.

8.2 Active emissions controls

In the active emissions control mechanism, production firms can engage in production and introduce resultant emissions in the atmosphere only when the regional exposure levels are below a given threshold. The emission controls are tightened with each consecutive simulation run.

8.2a Earnings ($) / spending ($) / foregone sales ($)

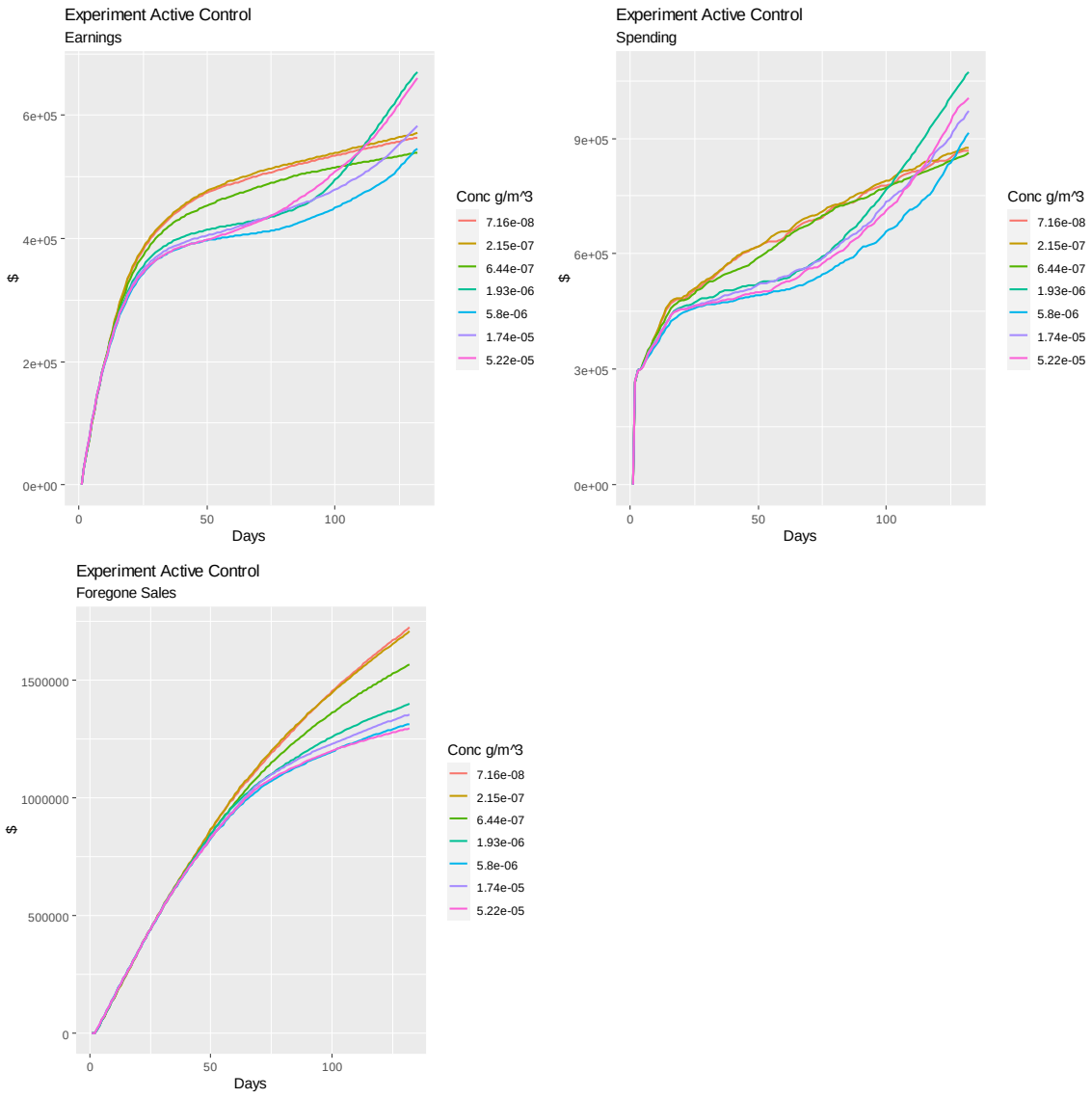

Figure 8-8: Plots of earnings, spending, and foregone sales as a function of production firm's shutoff time between consecutive operations (Active Control)

Table 8.6: Summary of earnings, spending, and foregone sales (Active control)

Concentration (μg)	Earnings (Max)	Spending (Max)	Forgone Sales (Max)
52.20	661034.6	1005946.9	1298470
17.40	582926.7	970052.3	1356126
5.80	546369.4	914601.7	1315400
1.93	670122.2	1071784.2	1400395
0.64	539533.1	862085.9	1568438
0.22	570920.2	876276.4	1707978
0.07	563749.9	868774.6	1725681
Correlation	**0.556267621**	**0.62773359 (log)**	**-0.940896873 (log)**

Regression Analysis

```
Call:
lm(formula = Earnings ~ ThreshConc, data = dataEarn)

Residuals:
    1     2     3     4     5     6     7
 -9693  -2745 -34798  93798 -35955 -17381   6775

Coefficients:
            Estimate Std. Error t value Pr(>|t|)
(Intercept)   573332      21676  26.450 1.44e-06 ***
ThreshConc      1650       1036   1.497    0.195
---
Signif. codes:  0 '***' 0.001 '**' 0.01 '*' 0.05 '.' 0.1 ' ' 1

Residual standard error: 69480 on 5 degrees of freedom
Multiple R-squared:  0.3094,    Adjusted R-squared:  0.1713
F-statistic:  2.24 on 1 and 5 DF,  p-value: 0.1947
```

```
Call:
lm(formula = Spending ~ log(ThreshConc), data = dataSpen)

Residuals:
       1        2        3        4        5        6
   62.33 -15720.35 -53143.77 133312.69 -47171.13 -14985.30  -2355.

Coefficients:
              Estimate Std. Error t value Pr(>|t|)
(Intercept)    1217112     156633   7.770 0.000565 ***
log(ThreshConc)   21177      11743   1.803 0.131187
---
Signif. codes:  0 '***' 0.001 '**' 0.01 '*' 0.05 '.' 0.1 ' ' 1

Residual standard error: 68260 on 5 degrees of freedom
Multiple R-squared:  0.3941,    Adjusted R-squared:  0.2759
F-statistic: 3.253 on 1 and 5 DF,  p-value: 0.1312
```

```
Call:
lm(formula = MissedSales ~ log(ThreshConc), data = dataMSales)

Residuals:
    1     2     3     4     5     6     7
 4095 66398  6683 -81498 -86429 34235 56516

Coefficients:
              Estimate Std. Error t value Pr(>|t|)
(Intercept)     534483     155450   3.374  0.01980 *
log(ThreshConc)  -72763      11654  -6.244  0.00154 **
---
Signif. codes:  0 '***' 0.001 '**' 0.01 '*' 0.05 '.' 0.1 ' ' 1

Residual standard error: 67750 on 5 degrees of freedom
Multiple R-squared:  0.8863,    Adjusted R-squared:  0.8636
F-statistic: 38.98 on 1 and 5 DF,  p-value: 0.001544
```

The regression findings show that threshold concentration has no discernible effect on earnings or spending volume in our simulated economy. However, tightening of threshold concentration increases the opportunity cost due to missed sales. The value of

correlation coefficients for earnings, spending, and missed sales are 0.5563, 0.627, and -0.941 respectively. The opportunity cost of missed sales due to tightening of permissible levels of emissions exposure can be approximated using the following logarithmic function:

$$\text{sales}_{oc} = 524{,}483 - 72{,}763\log(\text{Conc}_{\text{Thresh}}) \qquad (8.8)$$

The function indicates that as the permissibility of threshold concentration is constrained, the level of missed sales increases[16] by a factor of $72{,}763\log(\text{Conc}_{\text{Thresh}})$.The *p*-value for the logarithmic threshold coefficient is 0.00154. The adjusted R-squared for the missed sales in relation to permissible concentration is 0.8636, which indicates a relatively strong degree of interrelation and dependence between threshold concentration and foregone sales.

8.2b Units produced versus units consumed

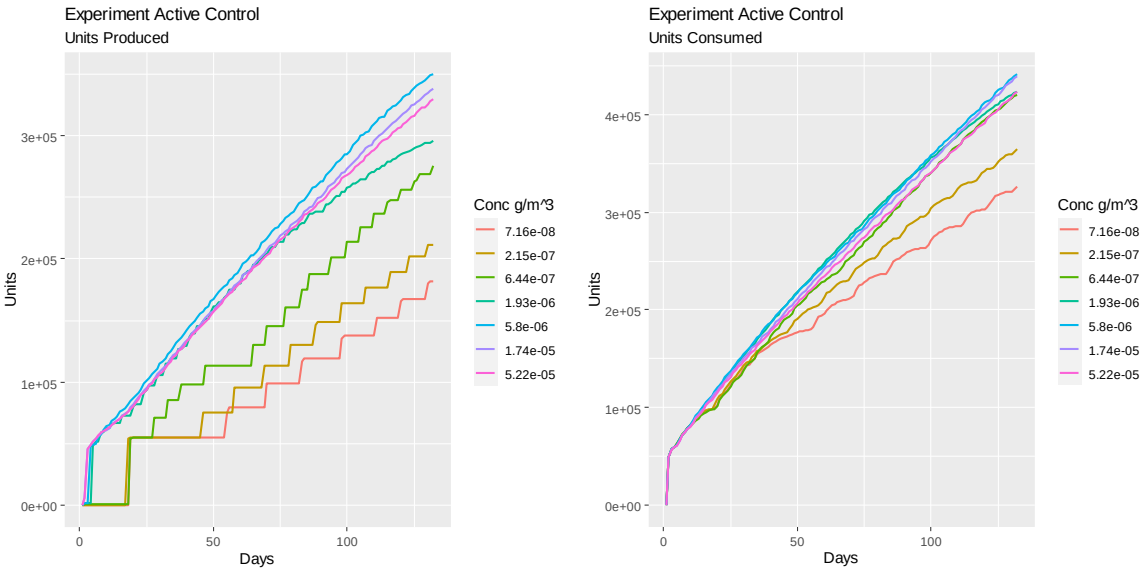

Figure 8-9: Commodities production and consumption as a function of production firm's shutoff time between consecutive operations (Active Control)

[16] The concentration range in our scenario is << 1 g/m^3, the logarithmic relationship returns a negative value. For example, Log (10^{-3}, 10^{-4}, 10^{-5} , 10^{-6} , 10^{-7} , 10^{-8}) ⇒ (-6.908, -9.210, -11.513, -13.816, -16.118, -18.420)

Table 8.7: Units produced versus units consumed (Active control)

Concentration (μg)	Units produced	Units consumed
52.20	329578.4	423276.3
17.40	337400.5	439204.3
5.80	349516.9	441029.8
1.93	296002.9	423366.3
0.64	275240.8	419453.4
0.22	211484.0	364385.2
0.07	181939.9	326464.2
Correlation	**0.916979955 (log)**	**0.826030865 (log)**

Regression Analysis

```
Call:
lm(formula = UnitsProduced ~ log(ThreshConc), data = dataUProd)

Residuals:
      1       2       3       4       5       6       7
-18694.6 -16630.1  19693.3  13016.9  35023.5   -557.3 -35843.7

Coefficients:
              Estimate Std. Error t value Pr(>|t|)
(Intercept)     611924      64831   9.439 0.000225 ***
log(ThreshConc)  24999       4860   5.143 0.003635 **
---
Signif. codes:  0 '***' 0.001 '**' 0.01 '*' 0.05 '.' 0.1 ' ' 1

Residual standard error: 28250 on 5 degrees of freedom
Multiple R-squared:  0.841,     Adjusted R-squared:  0.8093
F-statistic: 26.45 on 1 and 5 DF,  p-value: 0.003635
```

```
Call:
lm(formula = UnitsConsumed ~ log(ThreshConc), data = dataUConx)

Residuals:
      1       2       3       4       5       6       7
-29391.2  -7970.4  30636.0  18077.3  19228.8    917.3 -31496.8

Coefficients:
              Estimate Std. Error t value Pr(>|t|)
(Intercept)     602742      61187   9.851 0.000184 ***
log(ThreshConc)  15006       4587   3.271 0.022165 *
---
Signif. codes:  0 '***' 0.001 '**' 0.01 '*' 0.05 '.' 0.1 ' ' 1

Residual standard error: 26670 on 5 degrees of freedom
Multiple R-squared:  0.6816,    Adjusted R-squared:  0.6179
F-statistic:  10.7 on 1 and 5 DF,  p-value: 0.02216
```

The regression results indicate that there is a strong positive *logarithmic* correlation between threshold concentration and productivity. The correlation factor between threshold concentration and number of units produced is 0.923. The total productivity as a function of threshold concentration can be approximated using the following function:

$$\text{units}_{\text{prod}} = 611{,}924 + 24{,}999\log(\text{threshold conc}) \qquad (8.9)$$

The function indicates that as the permissibility of threshold concentration is reduced, the productivity reduces by a factor of $24{,}999\log(\text{Conc}_{\text{Thresh}})$ units.

The *p*-value for the threshold concentration is 0.003635. The adjusted R-squared for the units produced as function of threshold concentration is 0.8093, which indicates a good degree of interrelation and dependence between threshold concentration and productivity. The *p*-value for the entire model is 0.003635 which represents that the regression model provides ample fit to the relationship between threshold concentration and units produced.

The regression results indicate a positive correlation between units consumed and threshold concentration. The correlation factor between consumption and threshold concentration is 0.826. The total number of units consumed in the economy as a function of threshold concentration can be approximated using following function:

$$\text{units}_{\text{consp}} = 602{,}742 + 15{,}006\log(\text{threshold conc}) \qquad (8.10)$$

The function indicates that as the permissibility of threshold concentration is reduced, the consumption reduces by a factor of $15{,}006\log(\text{Conc}_{\text{Thresh}})$ units. The *p*-value for the threshold concentration coefficient is 0.022165. The adjusted R-squared for the units consumed as function of threshold concentration is 0.6175, which indicates a weak degree of interrelation and dependence between threshold concentration and consumption. The *p*-value for the entire model is 0.02216 which represents that the regression model provides ample fit to the relationship between threshold concentration and units consumed.

8.2c Maximum product moved ($) vs transportation costs ($)

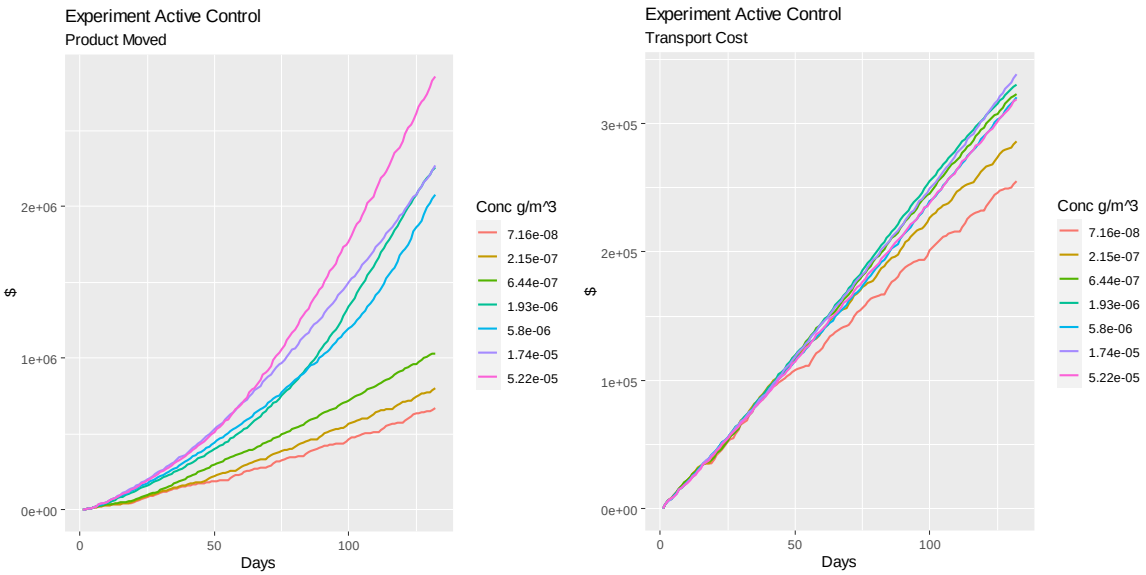

Figure 8-10: Total nominal value of product moved, and the associated transport cost observed at various levels of shutoff time (Active Control)

Table 8.8: Product moved and corresponding transport cost (Active control)

Concentration (μg)	Product Moved Max ($)	Transport Max ($)
52.20	2856306.2	318526.4
17.40	2268104.8	338324.4
5.80	2081109.5	320114.2
1.93	2257903.0	330581.2
0.64	1032150.5	322592.4
0.22	799117.9	286196.2
0.07	672078.8	255420.9
Correlation	**0.945945772 (log)**	**0.770606643 (log)**

Regression Analysis

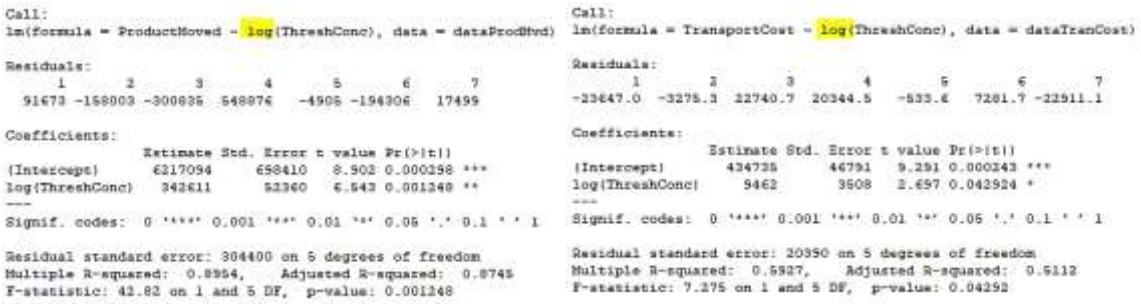

```
Call:
lm(formula = ProductMoved ~ log(ThreshConc), data = dataProdMvd)

Residuals:
      1       2       3       4       5       6       7
  91673 -158003 -300835  548876   -4905 -194306   17499

Coefficients:
              Estimate Std. Error t value Pr(>|t|)
(Intercept)    6217094     658410   8.902 0.000258 ***
log(ThreshConc)  342611      52360   6.543 0.001248 **
---
Signif. codes:  0 '***' 0.001 '**' 0.01 '*' 0.05 '.' 0.1 ' ' 1

Residual standard error: 304400 on 5 degrees of freedom
Multiple R-squared:  0.8954,    Adjusted R-squared:  0.8745
F-statistic: 42.82 on 1 and 5 DF,  p-value: 0.001248
```

```
Call:
lm(formula = TransportCost ~ log(ThreshConc), data = dataTranCost)

Residuals:
      1       2       3       4       5       6       7
-23647.0  -3275.3  22740.7  20344.5   -533.6   7281.7 -22911.1

Coefficients:
              Estimate Std. Error t value Pr(>|t|)
(Intercept)     434735      46791   9.291 0.000243 ***
log(ThreshConc)    9462       3608   2.697 0.042924 *
---
Signif. codes:  0 '***' 0.001 '**' 0.01 '*' 0.05 '.' 0.1 ' ' 1

Residual standard error: 20950 on 5 degrees of freedom
Multiple R-squared:  0.5927,    Adjusted R-squared:  0.5112
F-statistic: 7.275 on 1 and 5 DF,  p-value: 0.04292
```

The regression results indicate that there is a strong positive *logarithmic* correlation between threshold concentration and the value of product transported within the economy. The correlation factor between threshold concentration and product moved is 0.9459. The maximum value of the product transported as a function of threshold concentration can be approximated using the following Equation:

$$\text{Value of product transported (\$)} = 6{,}217{,}094 + 342{,}611\log(\text{threshold conc}) \quad (8.11)$$

The Equation indicates that as the permissibility of threshold concentration is reduced, the maximum value of the product moved reduces by a factor of $342{,}611\log\left(\text{Conc}_{\text{Thresh}}\right)$. The *p*-value for the threshold concentration is 0.001248. The adjusted R-squared for the product moved as function of threshold concentration is 0.8745, which indicates a good degree of interrelation and dependence between threshold concentration and maximum value of product movement in the economy. The *p*-value for the entire model is 0.001248 which represents that the regression model provides ample fit to the relationship between threshold concentration and maximum value of the product moved.

The regression results indicate a positive correlation between value of transportation charges and threshold concentration. The correlation factor between transportation charges and threshold concentration is 0.7706 The maximum transportation charge in our economy as a function of threshold concentration can be approximated using the following Equation:

$$\text{transport (\$)} = 434{,}735 + 9{,}462\log(\text{threshold conc}) \qquad (8.12)$$

The function indicates that as the permissibility of threshold concentration is reduced, the maximum transportation related charges reduce by a factor of $9{,}462\log(\text{Conc}_{\text{Thresh}})$ units. The *p*-value for the threshold concentration coefficient is 0.0429. The adjusted R-squared for the transportation charges as function of threshold concentration is 0.5112, which indicates a weak degree of interrelation and dependence between threshold concentration and transportation costs. The *p*-value for the entire model is 0.04292 which represents that the regression model provides ample fit to the relationship between threshold concentration and transportation costs.

8.2d Average and maximum emission's exposure

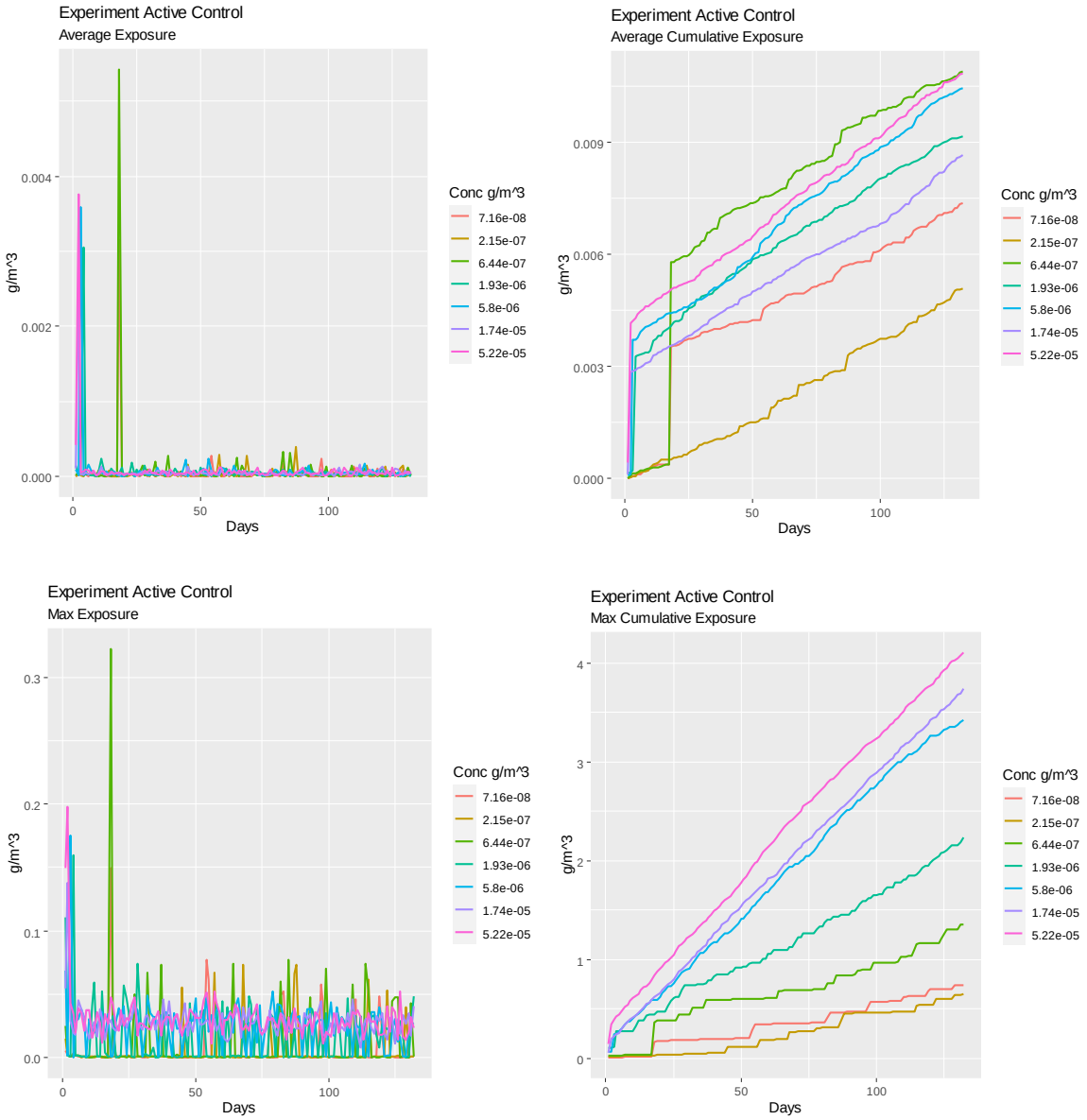

Figure 8-11:Plots of (average) and (maximum) emissions exposure as a function of firm's shutoff time between each production (Active Control)

Table 8.9: Average and Max Emissions Exposure (Active control)

Concentration (μg)	Average Emissions Exposure g/ m^3	Average Emissions Exposure Cumulative g/m^3	Max Emissions Exposure g/m^3	Max Emissions Exposure Cumulative g/ m^3
52.20	8.216330e-05	0.010846330	0.031092893	4.1042618
17.40	6.563338e-05	0.008663156	0.028298208	3.7353635
5.80	7.914277e-05	0.010447839	0.025966619	3.4275941
1.93	6.934819e-05	0.009153247	0.016904196	2.2313571
0.64	8.250012e-05	0.010891661	0.010245413	1.3523894
0.22	3.851194e-05	0.005081873	0.004904974	0.6474606
0.07	5.584888e-05	0.007372843	0.005630485	0.7432233
Correlation	**0.618620 (log)**	**0.6184216 (log)**	**0.973759 (log)**	**0.973759 (log)**

Regression Analysis

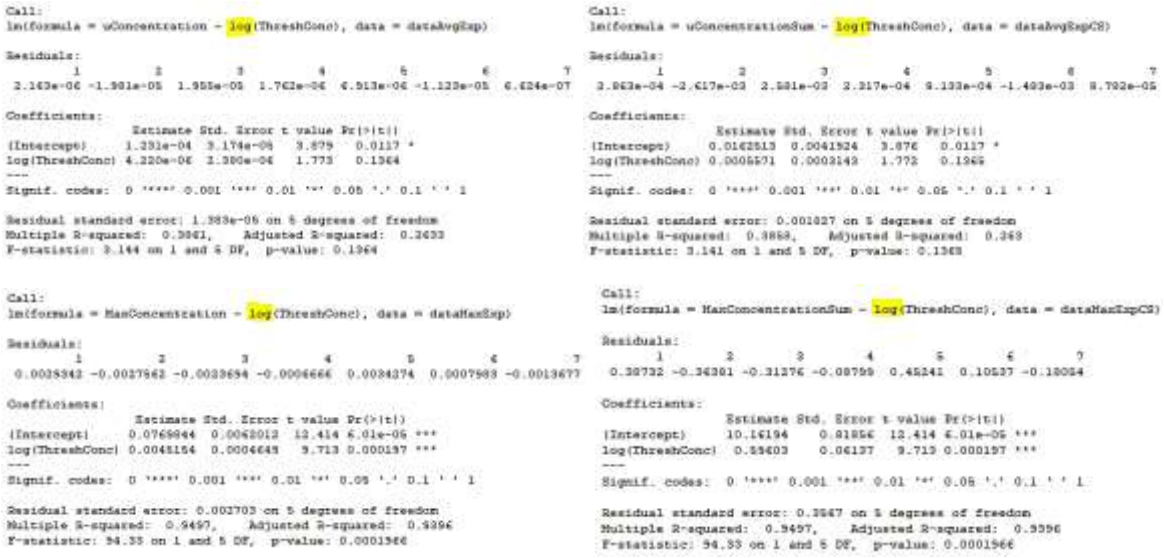

```
Call:
lm(formula = wConcentration ~ log(ThreshConc), data = dataAvgExp)

Residuals:
        1         2         3         4         5         6         7
 2.163e-06 -1.981e-05  1.955e-05  1.762e-06  6.513e-06 -1.122e-05  6.624e-07

Coefficients:
              Estimate Std. Error t value Pr(>|t|)
(Intercept)  1.231e-04  3.174e-06   3.879   0.0117 *
log(ThreshConc) 4.220e-06  2.580e-06   1.773   0.1364
---
Signif. codes:  0 '***' 0.001 '**' 0.01 '*' 0.05 '.' 0.1 ' ' 1

Residual standard error: 1.383e-05 on 5 degrees of freedom
Multiple R-squared:  0.3861,    Adjusted R-squared:  0.2633
F-statistic: 3.144 on 1 and 5 DF,  p-value: 0.1364
```

```
Call:
lm(formula = wConcentrationSum ~ log(ThreshConc), data = dataAvgExpCS)

Residuals:
        1         2         3         4         5         6         7
 3.863e-04 -2.617e-03  2.581e-03  2.317e-04  9.133e-04 -1.483e-03  8.792e-05

Coefficients:
              Estimate Std. Error t value Pr(>|t|)
(Intercept)  0.0162513  0.0041924   3.876   0.0117 *
log(ThreshConc) 0.0005571  0.0003143   1.772   0.1364
---
Signif. codes:  0 '***' 0.001 '**' 0.01 '*' 0.05 '.' 0.1 ' ' 1

Residual standard error: 0.001827 on 5 degrees of freedom
Multiple R-squared:  0.3868,    Adjusted R-squared:  0.263
F-statistic: 3.141 on 1 and 5 DF,  p-value: 0.1365
```

```
Call:
lm(formula = MaxConcentration ~ log(ThreshConc), data = dataMaxExp)

Residuals:
        1         2         3         4         5         6         7
 0.0028542 -0.0027562 -0.0023694 -0.0006666  0.0034274  0.0007983 -0.0013677

Coefficients:
              Estimate Std. Error t value Pr(>|t|)
(Intercept)  0.0769944  0.0062012  12.414 6.01e-05 ***
log(ThreshConc) 0.0045154  0.0004649   9.713 0.000197 ***
---
Signif. codes:  0 '***' 0.001 '**' 0.01 '*' 0.05 '.' 0.1 ' ' 1

Residual standard error: 0.002703 on 5 degrees of freedom
Multiple R-squared:  0.9497,    Adjusted R-squared:  0.9396
F-statistic: 94.33 on 1 and 5 DF,  p-value: 0.0001966
```

```
Call:
lm(formula = MaxConcentrationSum ~ log(ThreshConc), data = dataMaxExpCS)

Residuals:
       1        2        3        4        5        6        7
 0.38732 -0.36301 -0.31276 -0.08799  0.46241  0.10537 -0.18934

Coefficients:
              Estimate Std. Error t value Pr(>|t|)
(Intercept)   10.16194    0.81856  12.414 6.01e-05 ***
log(ThreshConc)  0.59603    0.06137   9.713 0.000197 ***
---
Signif. codes:  0 '***' 0.001 '**' 0.01 '*' 0.05 '.' 0.1 ' ' 1

Residual standard error: 0.3567 on 5 degrees of freedom
Multiple R-squared:  0.9497,    Adjusted R-squared:  0.9396
F-statistic: 94.33 on 1 and 5 DF,  p-value: 0.0001966
```

The regression results show a positive correlation between threshold concentration and average exposure to the boids. The correlation factor between threshold concentration and average exposure is 0.6186, with a *p*-value of 0.1364 for threshold concentration

coefficient. The average exposure rate to the boids as a function of threshold concentration can be formulated using the following Equation:

$$\text{exposure}_{\text{u}} = 1.231 \times 10^{-4} + 4.220 \times 10^{-6}\log(\text{Conc}_{\text{Thresh}}) \qquad (8.13)$$

The function indicates that as the permissibility of threshold concentration is constrained, the level of emission exposure reduces[17] by a factor of $4.22\text{x}10^{-6}\log(\text{Conc}_{\text{Thresh}})$.

There is a strong positive correlation between threshold concentration and the maximum exposure experienced by boids. The correlation factor between threshold concentration and max exposure is 0.9737, with a *p*-value of 0.000197 for the threshold concentration coefficient. The adjusted R-squared for the max exposure as function of threshold concentration is 0.9748, which indicates a relatively good degree of interrelation and dependence between threshold concentration and the maximum exposure experienced by the boids. The maximum exposure experienced by the boids as a function of threshold concentration can be formulated using the following Equation:

$$\text{exposure}_{\text{max}} = 0.0769844 + 0.0045154\log(\text{Conc}_{\text{Thresh}}) \qquad (8.14)$$

The function indicates that as the permissibility of threshold concentration is reduced, the level of maximum exposure reduces by a factor of $4.52\text{x}10^{-3}\log(\text{Conc}_{\text{Thresh}})$.

[17] The concentration range in our scenario is << 1 g/m^3, the logarithmic relationship returns a negative value. For example, Log (10^{-3}, 10^{-4}, 10^{-5}, 10^{-6}, 10^{-7}, 10^{-8}) ⇒ (-6.908, -9.210, -11.513, -13.816, -16.118, -18.420)

8.2e Active transport hubs, delivery delays

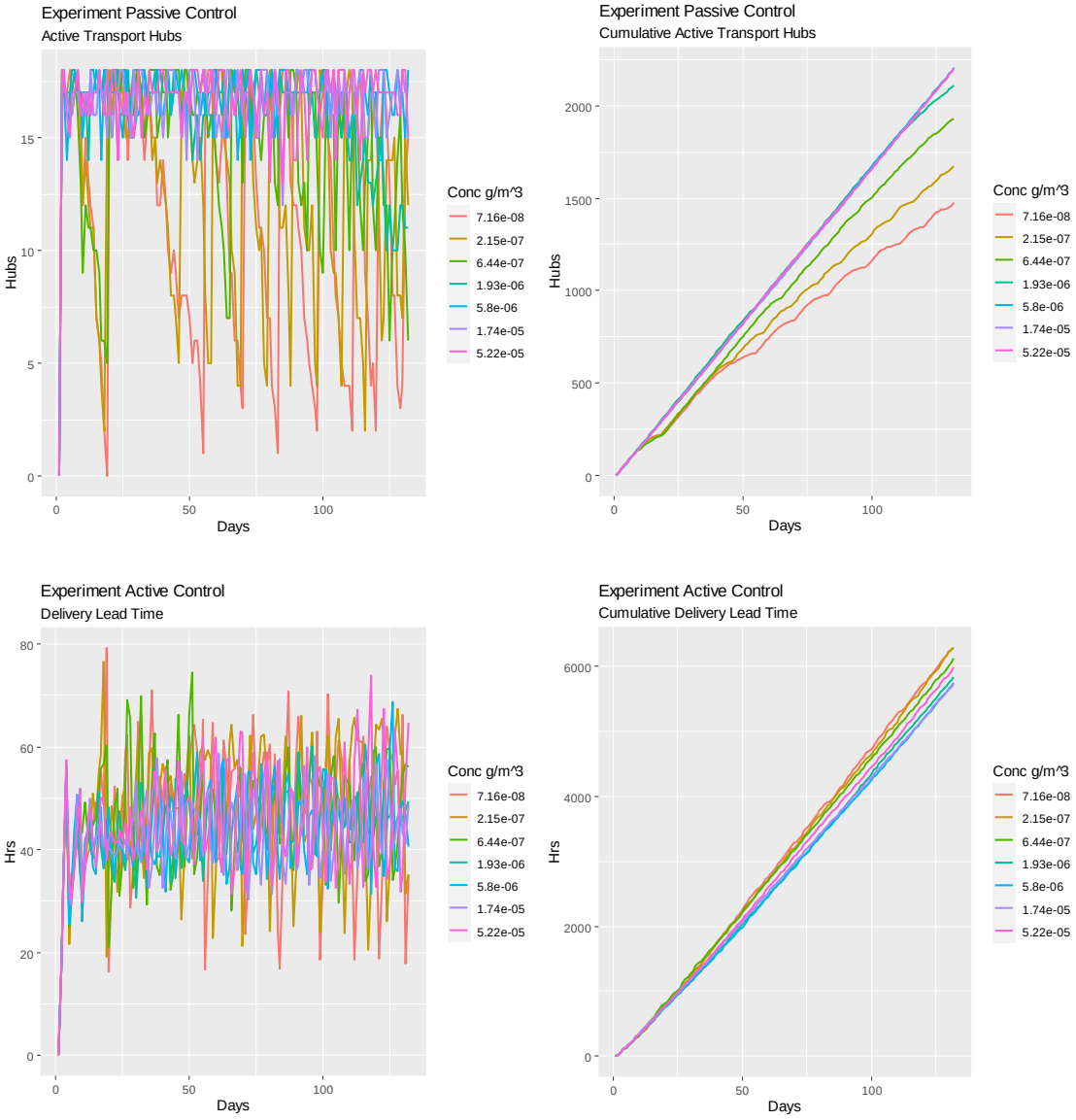

Figure 8-12: Active transport hubs and delivery lead times as a function of shutoff time periods between consecutive production (Active Control)

Table 8.10: Active Transportation Hubs, Delivery Lead Time (Active control)

Concentration (μg)	Active Transportation Hubs (Average)	Active Transportation Hubs (Cumulative)	Average Delivery Lead Time (Hrs.)	Delivery Lead Time Cumulative (Hrs.)
52.20	16.66667	2200	45.36382	5988.025
17.40	16.66667	2200	43.47087	5738.154
5.80	16.70455	2205	43.51810	5744.389
1.93	15.96970	2108	44.25242	5841.319
0.64	14.61364	1929	46.40148	6124.996
0.22	12.67424	1673	47.67213	6292.722
0.07	11.18182	1476	47.67744	6293.422
Correlation	**0.9232853 (log)**	**0.9232854 (log)**	**-0.77173 (log)**	**-0.7717 (log)**

Regression Analysis

```
Call:
lm(formula = nofActiveHubs ~ log(ThreshConc), data = dataActiveHub)

Residuals:
     1      2      3      4      5      6      7
-0.9013 -0.3571  0.6362  1.0457  0.8316 -0.1538 -1.1012

Coefficients:
             Estimate Std. Error t value Pr(>|t|)
(Intercept)    26.2716     2.1441  12.253 6.41e-05 ***
log(ThreshConc)  0.8624     0.1607   5.365  0.00303 **
---
Signif. codes:  0 '***' 0.001 '**' 0.01 '*' 0.05 '.' 0.1 ' ' 1

Residual standard error: 0.9344 on 5 degrees of freedom
Multiple R-squared:  0.852,     Adjusted R-squared:  0.8224
F-statistic: 28.78 on 1 and 5 DF,  p-value: 0.003027
```

```
Call:
lm(formula = nofActiveHubsSum ~ log(ThreshConc), data = dataActiveHubCS)

Residuals:
     1      2      3      4      5      6      7
-118.57  -47.14   83.97  138.03  109.77  -20.30 -145.86

Coefficients:
             Estimate Std. Error t value Pr(>|t|)
(Intercept)    3467.86     283.02  12.253 6.41e-05 ***
log(ThreshConc)  113.84      21.22   5.365  0.00303 **
---
Signif. codes:  0 '***' 0.001 '**' 0.01 '*' 0.05 '.' 0.1 ' ' 1

Residual standard error: 123.3 on 5 degrees of freedom
Multiple R-squared:  0.852,     Adjusted R-squared:  0.8224
F-statistic: 28.78 on 1 and 5 DF,  p-value: 0.003027
```

```
Call:
lm(formula = DelayHrs ~ log(ThreshConc), data = dataDeliveryDelay)

Residuals:
     1      2      3      4      5      6      7
 0.2454  0.8915  0.2705 -1.2279 -1.3103 -0.7067  1.8372

Coefficients:
             Estimate Std. Error t value Pr(>|t|)
(Intercept)    37.6047     2.9075  12.961 4.87e-05 ***
log(ThreshConc) -0.5525     0.2180  -2.718   0.0419 *
---
Signif. codes:  0 '***' 0.001 '**' 0.01 '*' 0.05 '.' 0.1 ' ' 1

Residual standard error: 1.267 on 5 degrees of freedom
Multiple R-squared:  0.5964,    Adjusted R-squared:  0.5157
F-statistic: 7.388 on 1 and 5 DF,  p-value: 0.04187
```

```
Call:
lm(formula = TotalDelayHrs ~ log(ThreshConc), data = dataDeliveryDelayCS)

Residuals:
     1      2      3      4      5      6      7
  32.39  117.68   86.76 -162.09 -172.97  -93.38  243.60

Coefficients:
             Estimate Std. Error t value Pr(>|t|)
(Intercept)    4974.39     383.79  12.961 4.87e-05 ***
log(ThreshConc)  -70.21      25.77  -2.718   0.0419 *
---
Signif. codes:  0 '***' 0.001 '**' 0.01 '*' 0.05 '.' 0.1 ' ' 1

Residual standard error: 167.3 on 5 degrees of freedom
Multiple R-squared:  0.5964,    Adjusted R-squared:  0.5157
F-statistic: 7.388 on 1 and 5 DF,  p-value: 0.04187
```

The regression results indicate that there is a strong positive *logarithmic* correlation between threshold concentration and the utilization rate of the transport hubs. The correlation factor between threshold concentration and average number of active transport hubs is 0.923. The total number of active hubs as a function of threshold concentration can be approximated using the following function:

$$\text{hubs}_{\text{active}} = 26.2 + 0.8624\log(\text{threshold conc}) \qquad (8.15)$$

The function indicates that as the permissibility of threshold concentration is reduced, the utilization factor of active hubs reduces by a factor of $0.8624\log(\text{Conc}_{\text{Thresh}})$.

The *p*-value for the threshold concentration is 0.00303. The adjusted R-squared for the total number of active hubs as function of threshold concentration is 0.8224, which indicates a good degree of interrelation and dependence between threshold concentration and total transport hubs utilization. The *p*-value for the entire model is 0.8224 which represents that the regression model provides ample fit to the relationship between threshold concentration and units produced.

The regression results indicate a relative negative correlation between delivery hours and threshold concentration. The correlation factor between delivery hours and threshold concentration is -0.771. The average lead time on delivery of an order as a function of threshold concentration can be approximated using following function:

$$\text{lead time}_{Hrs} = 37.6847 - 0.5925\log(\text{threshold conc}) \qquad (8.16)$$

The function indicates that as the permissibility of threshold concentration is reduced, the lead time increases by a factor of $0.5925\log(\text{Conc}_{\text{Thresh}})$ hours. The *p*-value for the threshold concentration coefficient is 0.0419.

9. DISCUSSION

The population in many parts of the world has grown rapidly over the past millennia. The population growth compounded by increasing purchasing power has led to a high demand for commodities. To accommodate this rising demand for goods, the industrial and transportation sectors have consistently grown. Although this economic progress has greatly benefited local communities in terms of employment growth, better transportation infrastructure, social services, etc., it has also resulted in a rapid decline in the environment due to air pollution. During normal operations, the industrial and transportation sectors release a variety of pollutants, including Sulphur dioxide, nitrogen oxides, particulate matter, ozone, and volatile organic compounds, among others. Governing bodies in various regions around the world have implemented various emissions control regulations to mitigate health impacts of exposure to air pollutants. This study quantitatively examined the economic impacts of emissions control on economic productivity as well as the rationale of emissions control policies. The key question being:

If the economy needs to produce Y units of output to meet total demand $D|D = \sum_{i=1}^{B} \Delta y$ and maximize labor opportunity $l \subseteq B$. Calculate the economic productivity Y of a closed loop economy and the corresponding health indices $H \in B$ as a function of constrain on point source emissions?

To address the given problem, a simulation-based approach was utilized to merge core concepts from areas of operations research, economics, and mechanics. The simulation primary objectives were:

1. To create a customizable program using object-oriented programming that can allow testing of various economic scenarios involving value added production and transportation of goods.
2. Generate autonomous objects with embedded production, consumption, and intertemporal choice models.
3. Create a transportation model to facilitate efficient channeling of goods between supply and demand points.
4. Integrate a Puff dispersion model to simulate transient modeling of emissions from point and mobile sources.
5. Quantify the emissions exposure levels on the pseudo-inhabitants.

The above-stated primary objectives have been accomplished and all core concepts have been validated on an individual basis.

To thoroughly examine the impact of emissions control on productivity, two approaches were used. The *passive* approach examined the impact of different shutoff time periods on changes in productivity and exposure levels. The *active* approach determined how tightening of permitted levels of emission's exposure impact productivity. The simulation used an autonomous monetary policy with the main goal of achieving a balance between the money supply and total availability of goods. The impact of emissions control was analyzed using following set of indicators:

1.	Earnings ($)	To gauge total earnings from production and investments
2.	Spending ($)	To gauge total spending from consumption
3.	Foregone sales ($)	To gauge volume of revenue lost due to non-availability of goods
4.	Units produced	To gauge total number of units produced by all industries (↑)

5.	Units consumed	To gauge total number of units consumed by all customers (↓)
8.	Product moved	$ value of all products moved in the economy
9.	Transportation	Transportation cost associated with the product moved
10.	Avg emissions exposure	Average value of the chemical exposure endured by all boids in the 2D space of the simulation
11.	Max emissions exposure	Maximum value of the chemical exposure endured by a boid in the 2D space of the simulation
12.	# of active hubs	To gauge utilization of transport hubs in the economy
13.	Delivery lead time	To gauge average delivery time between orders placed and orders received

Here are the answers to the research questions posed in paper:

Research Question 1

Calculate the change in industrial production in a geographically confined, closed-loop economy as a function of emission restrictions, assuming no breakthroughs in emissions control technologies.

According to the simulation results, both passive and active emissions controls reduce industrial productivity. A small increase in shutdown time (about 4.6 hours) had no effect on productivity in the passive control analysis, but as the shutdown time limits were raised further, production levels did begin to decline. In the active control analysis, changing the threshold concentration from 52.20 μg to 5.80 μg has no appreciable effect on productivity, but as the threshold concentration is further restricted the production levels begin to fall.

Regression results on passive controls indicate that there is a negative linear relationship between shutdown time and productivity (correlation -0.84699). The slope of the linear relationship is approximately: -385.64 x Shutoff Hours with a corresponding *p*-value of

0.0079. In terms of active control, there exists a logarithmic relationship between threshold concentration and productivity (correlation 0.91697). The slope of the logarithmic relation is given by 24,999 x log (threshold conc) with a corresponding *p*-value of 0.003635. The logarithmic relation indicates a decreased loss in productivity with a consecutive increased restriction on threshold concentration.

Despite some very strict emissions control restrictions, it is also seen that productivity levels in our fictitious economic scenarios are quite resilient. This can be attributed to saturated presence of firms of various types leading to production over-capacity and liberal expansion of production levels per profit maximization function. The LM function also encourages production by making capital readily available to businesses so they can pay employees' salaries and buy intermediate raw materials.

Conclusion: Under a set of restricted scenarios, passive and active emissions control policies have been found to negatively impact the rate of industrial productivity in a closed loop economy.

Research Question 2

Calculate the change in consumption in a geographically confined, closed-loop economy as a function of emission restrictions, assuming no breakthroughs in emissions control technologies.

Simulation results indicate that both passive and active emissions controls depress consumption in an economy. The correlation factor between shutdown hours and units consumed is -0.8058. The consumption of goods stays resilient when the shutdown times stays below 37.72 hours, however beyond that the consumption volume starts to trend downwards. Application of linear regression indicates that the slope of reduction in

consumption is ~ -228.84 x shutoff hours with a corresponding *p*-value of 0.01574. Compared to production, consumption is more insensitive to passive control.

The correlation factor between threshold concentration and units consumed is 0.826. It is determined that the logarithmic conversion of threshold concentration provides the best fit in the regression modelling. The slope of reduction in consumption as a function of threshold concentration is 15,006 x log (Threshold Concentration) with a corresponding *p*-value of 0.022165. Compared to production the consumption is more insensitive to active control. The logarithmic fit indicates decreased change in consumption per an increased constraint on emissions.

The reduction in consumption can be simply attributed to a combined unavailability of products at the market level as well as a reduction in purchasing power due to less frequency of wage releases. Inflation can also styme consumption by reducing the volume of per unit good that can be purchased at a fixed level of income.

Conclusion: Under a set of restricted scenarios, passive and active emissions control policies have been found to negatively impact the rate of consumption in a closed loop economy.

Research Question 3

Calculate the change in emissions exposure levels experienced by boids as a function of change in emissions restrictions.

In our simulation, the boids exposure to emissions is quantified at both the average and maximum exposure levels. The simulation results indicate a weak correlation between both the passive and active emissions control and average exposure to pollutants. The correlation factor between shutdown time and average exposure to emissions is -0.21. In

terms of regression analysis, the shutdown hours coefficient produced an estimated value of $-2.229E^{-08}$x Shutoff Hours with a corresponding *p*-value of 0.601. The correlation factor between log-threshold concentration and average exposure to emissions is 0.61862. In terms of log-regression analysis, the threshold concentration coefficient produced an estimated value of $4.220E^{-06}$x log (Threshold Concentration) with a corresponding *p*-value of 0.1366.

The simulation results indicate a strong negative correlation between both the passive and active emissions control and the maximum exposure to pollutants. The correlation factor between threshold concentration and maximum exposure of a pollutant to a boid is -0.9892. The linear regression on the eight passive control scenarios produced an estimated shutdown hours coefficient of $-6.469E^{-05}$x Shutoff Hours with a corresponding *p*-value of $-3.16E^{-06}$. The correlation factor between log-threshold concentration and maximum exposure to emissions is 0.973759. In terms of log-regression analysis, the threshold concentration coefficient produced an estimated value of $4.5154E^{-03}$x log (Threshold Concentration) with a corresponding *p*-value of 0.000197.

The limited association between passive and active emissions control on the average amount of emissions exposure suggests that point source emissions have little impact on the typical level of pollution exposure that boids experience. This finding may be explained by several variables, including the geographic distribution of boids on the 2D plane, the wind speed and direction, the atmospheric conditions that prevailed during the dispersion of pollutants, the pollutants half-life, and the fact that mobile emissions contributed more than point source emissions.

The high correlation between passive and active emissions control on the maximum amount of emission exposure experienced by a boid suggests that the point source emitters play a significant role in saturated levels of pollutant concentrations in the atmosphere. In essence, according to the results of our simulations, passive and active emissions control can significantly reduce the extreme levels of exposure to emissions, but these controls have little impact on the average exposure levels experienced by the members of a community.

Conclusion: Passive and active emissions control policies do not appear to have any statistically significant impact on average rates of emissions exposure under a set of restricted scenarios, but they do impact the maximum amount of emission exposure experienced by members of a population.

Research Question 4

Quantify the impact on transportation sector as a function of emissions restrictions on point sources.

The impact of point source emissions control on transport sectors is quantified in three ways:

a) Utilization factor of transport assets

b) Lead time of deliveries

c) Value of product transported.

The simulation results indicate that point source emission's control negatively impacts the utilization rate of transport hubs. The passive control strategy indicates a very strong negative correlation between shutdown hours and the total number of transport hubs activated with correlation value of -0.9825. The linear regression analysis estimates the

shutdown coefficient as -0.01539 x Shutoff Hours with a corresponding *p*-value of $1.32\mathrm{E}^{-05}$. The active control strategy also indicates a strong correlation between log-threshold concentration and the total number of transport hubs activated with a corresponding correlation factor of 0.9232. The log regression estimates the threshold concentration of 0.8624 x log (Threshold Concentration) with a corresponding *p*-value of 0.00303.

Emissions restrictions have reduced transportation hub activation for a variety of reasons. The reduction in productivity caused by emissions constraints reduces the frequency with which raw and intermediate feeds are replenished, including the channeling of finished goods to warehouses and markets. The tightening of emissions controls also indirectly reduces the addition of pollutants in the atmosphere.

According to the simulation results, emissions constraints have no statistically significant impact on delivery lead times for both passive and active emissions control strategies. The value of correlation coefficient between shutoff hours and delivery times is -0.5465. The linear regression analysis estimates the shutoff hours coefficient of -0.007396 x Shutoff Hours with a corresponding *p*-value of 0.161. The correlation coefficient between log-threshold concentration and delivery lead times is -0.771. The logarithmic regression analysis estimates the threshold concentration coefficient of -0.5925 x log (threshold concentration) with corresponding *p*-value of 0.0419.

The negative value of the shutdown hours coefficient indicates that the delivery time decreases as the level of passive emissions control increases. In contrast, as the level of active emissions control increases, so does the delivery time. The decrease in productivity and consumption of goods provides additional delivery capacity, ensuring that a truck is

available to execute the transfer of goods as soon as a delivery order is received. Extreme levels of emissions control reduce the total amount of finished goods available in active control scenarios, where the unavailability of goods exceeds transportation capacity factor.

The simulation results indicate a negative correlation between emissions control and the total value of product moved within the economy. The correlation coefficient between shutdown time and the maximum value of product moved is -0.9286. The regression analysis estimates the coefficient value for shutdown hours to be -3824 x Shutdown hours, with the corresponding *p*-value of 0.00086. The correlation coefficient between threshold concentration and the maximum value of product moved is 0.9459. The log-regression estimates the coefficient value of threshold concentration to be 342,611 x log (Threshold Concentration) with a corresponding *p*-value of 0.001248. In a nutshell, tighter emission control reduces the volume of goods transported within the closed loop economy in both passive and active emission control regimes.

Conclusion: Under a set of restricted scenarios, passive and active emissions control policies have been found to negatively impact the utilization rate of transport hubs and the volume of product moved across the economy. No adverse effects on delivery times have been detected.

10. CONCLUSION

The current program has effectively combined numerous concepts from the literature relevant to macro/microeconomics, operations research, and the advection-diffusion process with a particle systems model to give a platform for researchers to analyze the cost vs benefit of emission controls. The proposed methodology allows researchers to create customized economic scenarios for a specific region, including the spatial distribution of industries, markets, transportation hubs, and population to study various trade interactions and the dispersion of harmful emissions over a 2D surface. The simulation platform is highly versatile, adaptable, and scalable to adapt endless combinations of scenarios with processing power being the limiting factor.

The impact of emissions control on industrial productivity and air quality was examined through a series of passive and active emission control scenarios. The key findings on 7 different scenarios of passive and active emissions controls indicated that in the absence of alternatives, the rate of productivity and consumption is negatively impacted with increased levels of emissions controls on point sources. In addition to lowering the productivity of industrial units, these emissions restrictions were also found to indirectly impact the transportation industry in an improper way. The increased level of restrictions is helpful in reducing the maximum quantity of pollutant dose received by a member of a community, however the average rates of exposures stayed very much static. This leads to the possibility of mobile emissions being the main culprit of pollutant exposure to the public. The random distribution of industries and resource sites in our simulation avoided them being clustered around cities which may be the primary reason that the average

level of emissions exposure did not significantly change with increased restrictions on point source emissions.

If the thermal impacts of GHG emissions from point sources are neglected, the mere spatial dispersal of industrial sites should be sufficient to keep hazardous emissions from interacting with the public.

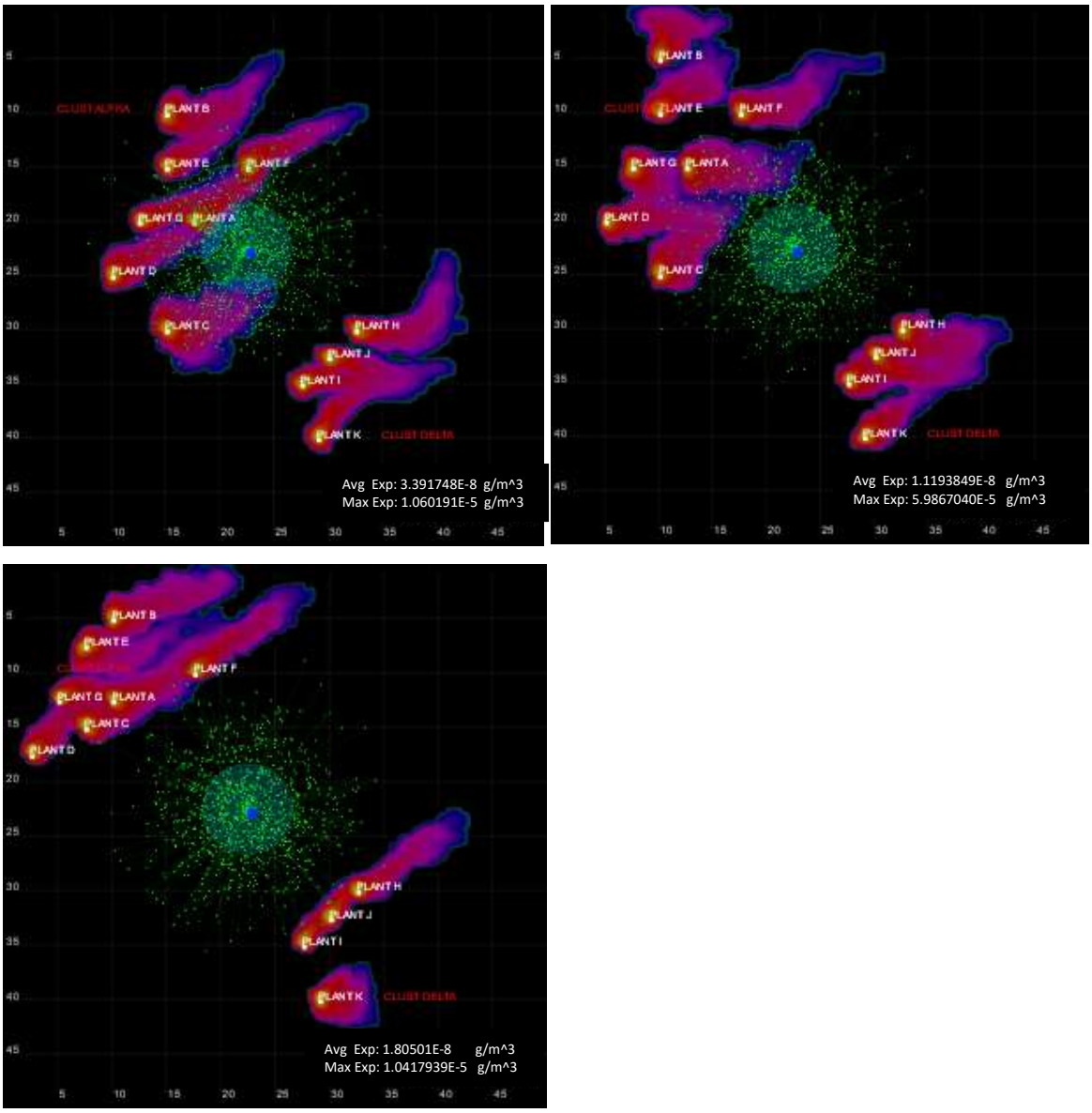

Figure 10-1: Average and maximum ground level concentrations experienced by a set of 1000 boids from industrial clusters (alpha) and (delta) as a function of varying distances.

11. RECOMMENDATIONS

The current methodology has a great deal of space for improvement.

1. The current emissions control policies only apply to point source emissions. The emission control policies can be extended to mobile sources and the corresponding exposure levels can be studied.
2. The current model has only integrated fossil fuel-based transport units. However, electric and hydrogen powered vehicles can be integrated in the simulation, which should significantly reduce the total amount of emissions exposure.
3. Current models assume a linear relationship between productivity and emissions, however other forms of relationships (quadratic, non-linear) can be investigated.
4. The markets and industrial units were distributed at random across the 2D plane in all scenarios of the simulation run, with the population mainly centered around market hubs. Given that much of the pollutant concentration is greatly reduced within a 25 KM radius of the point source, it will be important to look into how exposure levels to emissions change with distance from different industrial clusters.
5. The ability of boids to exhibit emergent behavior through interactions with other boids and the economy was left out of the current research. The boids can be configured in the simulation so that they can pick up on other boids actions and improve their corresponding utilities.

12. REFRENCES

A. Mustafin, A. K. (2018). Opening the Leontief's black box. *Heliyon, 4*(5). doi:https://doi.org/10.1016/j.heliyon.2018.e00626.

A. Subramanian, L. D. (2010). A parallel heuristic for the Vehicle Routing Problem with Simultaneous Pickup and Delivery. *Computers & Operations Research, 37*(11), 1899-1911. doi:https://doi.org/10.1016/j.cor.2009.10.011

A.D. Bhanarkar, S. G. (2005). Assessment of contribution of SO2 and NO2 from different sources in Jamshedpur region, India. *Atmospheric Environment, 39*(40), 7745-7760. doi:https://doi.org/10.1016/j.atmosenv.2005.07.070.

Agency, E. E. (2021, 12 3). *Air quality standards*. (Europen Environment Agency) Retrieved 05 23, 2022, from https://www.eea.europa.eu/themes/air/air-quality-concentrations/air-quality-standards

Ahfazh Fauzy Nurunnajib, E. R. (2018). Application of Cobb-Douglas Production Function to Manufacturing Industries in West Sumatra Indonesia. *World Scientific News, 101*, 145-156. Retrieved from http://www.worldscientificnews.com/wp-content/uploads/2018/04/WSN-101-2018-145-156.pdf

Air quality monitoring. (2017, 03 27). (Queensland Government) Retrieved 05 11, 2022, from https://www.qld.gov.au/environment/pollution/monitoring/air/air-monitoring

Alessandro Franco, A. R. (2009). The future challenges for “clean coal technologies”: Joining efficiency increase and pollutant emission control. *Energy, 34*(3), 348-354. doi:https://doi.org/10.1016/j.energy.2008.09.012.

Alexander H. DeGolia, E. H. (2019). Economic losses or environmental gains? Framing effects on public support for environmental management. *PLOS ONE, 14*(7), 1-17.

Alexandra Fedorets, C. S. (2021). Great expectations: Reservation wages and minimum wage reform. *Journal of Economic Behavior & Organization, 183*, 397-419. doi:https://doi.org/10.1016/j.jebo.2021.01.006

AMEC Environment & Infrastructure UK Limited. (2014). *Study on: "Contribution of industry to pollutant emissions to air and water"*. London: European Union. doi:10.2779/25422

An empirical investigation of air pollution from fossil fuel combustion and its impact on health in India during 1973–1974 to 1996–1997. (2005). *Ecological Economics, 55*, 235-250. doi:10.1016/j.ecolecon.2004.09.022

Andrew J Ghio, Y.-C. T. (2004). Exposure to concentrated ambient particles (CAPs): a review. *Inhalation Toxicology, 16*, 53-59. doi:10.1080/08958370490258390

Arif, I. (2021). Productive knowledge, economic sophistication, and labor share. *World Development, 139*. Retrieved from https://doi.org/10.1016/j.worlddev.2020.105303

Arne Henningsen, G. H. (2012). On estimation of the CES production function—Revisited. *Economics Letters, 115*(1), 67-69. doi:https://doi.org/10.1016/j.econlet.2011.12.007.

Arora, J. S. (2004). 15 - Discrete Variable Optimum Design Concepts and Methods. In J. S. Arora (Ed.), *Introduction to Optimum Design (Second Edition)* (pp. 513-530). Academic Press. doi:https://doi.org/10.1016/B978-012064155-0/50015-X

ATSDR. (2016, 12). Public health statement Hydrogen Sulfide. Atlanta, GA: Agency for Toxic Substances and Disease Registry.

Barrie M. Baker, M. A. (2003). A genetic algorithm for the vehicle routing problem. *Computers & Operations Research, 30*(5), 787-800. doi:https://doi.org/10.1016/S0305-0548(02)00051-5

Bellman Ford's Algorithm. (n.d.). (Programiz) Retrieved 06 05, 2022, from https://www.programiz.com/dsa/bellman-ford-algorithm

Benassy, J.-P. (2007). IS-LM and the multiplier: A dynamic general equilibrium model. *Economic Letters (Science Direct)*, 189-195.

Bereg, S. (n.d.). *Applications of minimum spanning trees*. (University of Texas at Dallas) Retrieved 06 04, 2022, from https://personal.utdallas.edu/~besp/teaching/mst-applications.pdf

Bertaud, A. (2015). The Spatial Distribution of Land Prices and Densities. New York: NYU, Marron Institute of Urban Management.

Blender. (2023, 05 11). *Boids*. Retrieved from Blender 3.5 Manual: https://docs.blender.org/manual/en/latest/physics/particles/emitter/physics/boids.html

Bon-Gang, H. (2018). Chapter 3 - Methodology. In *Performance and Improvement of Green Construction Projects* (pp. 15-22). Butterworth-Heinemann. doi:https://doi.org/10.1016/B978-0-12-815483-0.00003-X

Bruno Sauce, L. D. (2017). Inductive Reasoning. In *Encyclopedia of Animal Cognition and Behavior*. Springer International Publishing. doi:10.1007/978-3-319-47829-6_1045-1

C.Chen, G. Y. (2010). Environmental impact of cement production: detail of the different processes and cement plant variability evaluation. *Journal of Cleaner Production, 18*(5), 478-485. doi:https://doi.org/10.1016/j.jclepro.2009.12.014

Çağrı Koç, G. L. (2020). A review of vehicle routing with simultaneous pickup and delivery. *Computers & Operations Research, 122*. doi:https://doi.org/10.1016/j.cor.2020.104987

Carlos J. Garcia, J. M. (2018). Macroeconomic stabilization of primary commodities price cycles in developing economies. *Journal of Policy Modeling, 40*(5), 1050-1066. doi:https://doi.org/10.1016/j.jpolmod.2018.07.004

Cayuela, R. (2013, 10 11). *Market outlook: Speedy growth for chemicals by 2050*. (Independent Commodity Intelligence Services) Retrieved 05 18, 2022, from https://www.icis.com/explore/resources/news/2013/10/13/9714353/market-outlook-speedy-growth-for-chemicals-by-2050/

Cedergren, M. (2012). *The Aggregate Production Function*. New York: NYU Stern. Retrieved from https://pages.stern.nyu.edu/~dbackus/2303/notes_production.pdf

CEH. (2020). *Chemical Economics Handbook (CEH)*. (S&P Global) Retrieved 05 18, 2022, from https://ihsmarkit.com/products/chemical-economics-handbooks.html

Charles Gottlieb, J. O.-E. (2021). On the measurement of the elasticity of labour. *European Economic Review, 139*. Retrieved from https://doi.org/10.1016/j.euroecorev.2021.103879

CIA. (2023). *GDP – composition, by sector of origin*. (CIA) Retrieved 05 07, 2022, from The World Factbook: https://www.cia.gov/the-world-factbook/field/gdp-composition-by-sector-of-origin/?msclkid=6fa8ec6bce6d11ecb25dbfaf2b34cb4c

Cleland, J. (2013). World population growth; past, present and future. *Environmental and Resource Economics, 55*(4), 543–554. doi:10.1007/s10640-013-9675-6

Coal and Air Pollution. (2017, 12 19). (Union of Concerned Scientists) Retrieved 05 19, 2022, from https://www.ucsusa.org/resources/coal-and-air-pollution

Danan Gu, K. A. (2021). Major Trends in Population Growth Around the World. *China CDC weekly, 3(28)*, 604-613. doi:10.46234/ccdcw2021.160

Donald G. Rogich, G. R. (2008). *The global flows of metals and minerals.* Reston: U.S. Geological Survey. Retrieved from https://pubs.usgs.gov/of/2008/1355/pdf/ofr2008-1355.pdf

Donald Gross, J. F. (2008). *Fundamentals of Queueing Theory, Fourth Edition.* John Wiley & Sons, Inc.

Edi Munawar, M. U. (2003). Estimation CO2, Non-CO2 GHGs and Other Gas pollutant Emissions of Indonesia's Urea Fertilizer Factories. *World*(45), 100.

Ellyatt, H. (2021, 10 18). *Supply chain chaos is already hitting global growth. And it's about to get worse*. (CNBC) Retrieved 05 29, 2022, from https://www.cnbc.com/2021/10/18/supply-chain-chaos-is-hitting-global-growth-and-could-get-worse.html

Elżbieta Roszko Wójtowicz, J. B. (2018). How to approximate the ideal fisher price index? *The 12th International Days of Statistics and Economics.* Prague. Retrieved from https://msed.vse.cz/msed_2018/article/168-Roszko-Wojtowicz-Elzbieta-paper.pdf

Emilio Carrizosa, B. M.-B. (2014). A nested heuristic for parameter tuning in Support Vector Machines. *Computers & Operations Research, 43*, 328-334. doi:https://doi.org/10.1016/j.cor.2013.10.002

Enkeleida Lushi, J. M. (2010). An inverse Gaussian plume approach for estimating atmospheric pollutant emissions from multiple point sources. *Atmospheric Environment, 44*, 1097-1107.

EPA. (1984). *Locating and estimating emissions from sources of chromium* . Durham : Unites States Environmental Protection Agency .

EPA. (n.d.). *2014 National Emissions Inventory Report*. (Environmental Protection Agency) Retrieved 05 08, 2022, from https://gispub.epa.gov/neireport/2014/

EPA. (2021, 10 18). *AP 42, Fifth Edition, Volume I Chapter 12: Metallurgical Industry*. (Environmental Protection Agency (EPA)) Retrieved 05 18, 2022, from https://www.epa.gov/air-emissions-factors-and-quantification/ap-42-fifth-edition-volume-i-chapter-12-metallurgical-0

EPA. (2021, 10 06). *Greenhouse Gas Reporting Program (GHGRP) Metals*. (EPA) Retrieved 05 18, 2022, from https://www.epa.gov/ghgreporting/ghgrp-metals

EPA. (2021, 10 06). *National Air Quality: Status and Trends of Key Air Pollutants*. (EPA) Retrieved 05 23, 2022, from https://www.epa.gov/air-trends

EPA. (2022, 06 02). *Community Multiscale Air Quality Modeling System (CMAQ) (Max 8 Hr Ozone Concentration)*. (United States Environmental Protection Agency) Retrieved 06 09, 2022, from https://www.epa.gov/cmaq/cmaq-models-0

EPA. (2022, 01 05). *Initial List of Hazardous Air Pollutants with Modifications*. (Environmental Protection Agency) Retrieved 05 18, 2022, from https://www.epa.gov/haps/initial-list-hazardous-air-pollutants-modifications

EPA. (2022, 03 11). *Summary of Proposed NO_x Emission Limits for Industrial Sources*. (US EPA) Retrieved 05 22, 2022, from https://www.epa.gov/csapr/summary-proposed-no-emission-limits-industrial-sources

EPA. (2022, 05 06). *Support Center for Regulatory Atmospheric Modeling (SCRAM)*. (EPA) Retrieved 05 23, 2022, from https://www.epa.gov/scram

Eric Koomen, J. B. (2002). Economic Theory and Land Prices in Land Use Modeling. *5th AGILE Conference on Geographic Information Science.* Palma.

Eric Walling, C. (2020). Greenhouse gas emissions from inorganic and organic fertilizer production and use: A review of emission factors and their variability. *Journal of Environmental Management, 276*(15), 1-16. doi:https://doi.org/10.1016/j.jenvman.2020.111211

European Environment Agency. (2018, 10 29). *Air pollution: Half a million early deaths in Europe despite progress*. (BBC) Retrieved 05 23, 2022, from https://www.bbc.com/news/world-europe-46017339

Ewan KB, P. R. (1996). Increased inorganic mercury in spinal motor neurons following chelating agents. *Neurotoxicology, 17*(2), 343-349.

Fabio Caiazzo, A. A. (2013). Air pollution and early deaths in the United States. Part I: Quantifying the impact of major sectors in 2005. *Atmospheric Environment, 79*, 198-208. doi:https://doi.org/10.1016/j.atmosenv.2013.05.081

Faraway, J. J. (2002, July). *Practical Regression and Anova using R.* Retrieved from The Comprehensive R Archive Network: https://cran.r-project.org/doc/contrib/Faraway-PRA.pdf

Fermin Alfredo Tang Montane, R. D. (2002). Vehicle Routing Problems with Simultaneous Pick-up and Delivery Service. *Operational Research Society of India, 39*(1), 20-33. Retrieved

from https://link-springer-com.excelsior.sdstate.edu/content/pdf/10.1007/BF03398667.pdf

Filip, N. &. (2014). The role of transportation in economic development. *"Mircea cel Batran" Naval Academy Scientific Bulletin, XVII*, 10-12.

Findlay, D. W. (1999). The IS-LM Model: Is There a Connection between Slopes and the Effectiveness of Fiscal and Monetary Policy? *The Journal of Economic Education, 30*(4), 373-382. Retrieved from https://www.jstor.org/stable/1182951

Fisher Index. (n.d.). (Breaking Down Finance) Retrieved 06 19, 2022, from https://breakingdownfinance.com/

Friedlander, S. (2006). Stability of Flows. In G. L. Jean-Pierre Françoise (Ed.), *Encyclopedia of Mathematical Physics* (pp. 1-7). Academic Press. doi:https://doi.org/10.1016/B0-12-512666-2/00252-2

G.Russell, A. (1988). Mathemetical Modeling of the Effect of Emission Sources on Atmospheric Pollutant Concentrations. In *Air Pollution, the Automobile, and Public Health.* Washington (DC): National Academies Press (US). Retrieved from https://www.ncbi.nlm.nih.gov/books/NBK218138/

Gali, J. (1992). How Well Does the IS-LM Model Fit Postwar U.S. Data? *The Quarterly Journal of Economics, 107*(2), 709-738. Retrieved from https://www.jstor.org/stable/2118487

Gang Wang, J. D. (2020). Air pollutant emissions from coal-fired power plants in China over the past two decades. *Science of The Total Environment, 741*. doi:https://doi.org/10.1016/j.scitotenv.2020.140326.

Gasparino, C. (2022, 03 10). *Inflation is Biden's fault, and only Biden's fault*. (New York Post) Retrieved 12 2022, 05, from https://nypost.com/2022/03/10/inflation-is-bidens-fault-and-only-bidens-fault/

Graham Glen, V. Z. (2012, 05 21). *Stochastic Human Exposure and Dose Simulation (SHEDS) to estimate human exposure to chemicals*. (United States Environmental Protection Agency) Retrieved 06 09, 2022, from https://www.epa.gov/chemical-research/stochastic-human-exposure-and-dose-simulation-sheds-estimate-human-exposure

Greenberg, H. J. (1998). *Greedy alogrithm for minimum spanning tree*. University of Colorado at Denver. Retrieved from https://glossary.informs.org/notes/spanningtree.pdf

Gu Y, W. T. (2018). Impacts of sectoral emissions in China and the implications: air quality, public health, crop production, and economic costs. *Environmental Research Letters*, 1-13. Retrieved from https://iopscience.iop.org/article/10.1088/1748-9326/aad138/pdf

Haluk Ozkaynak, L. K. (2013). Air pollution exposure prediction approaches used in air pollution. *Journal of Exposure Science and Environmental Epidemiology, 23*, 566-572.

Hannah Ritchie, M. R. (2013). *Fertilizers*. (Our World In Data) Retrieved 05 17, 2022, from https://ourworldindata.org/fertilizers

Hannah Ritchie, M. R. (2018). *Plastic Pollution*. (Our World in Data) Retrieved 05 17, 2022, from https://ourworldindata.org/plastic-pollution#citation

Hathout, D. (2013). Modeling Population Growth: Exponential and Hyperbolic Modeling. *Applied Mathemetics, 4*, 299-304. doi:http://dx.doi.org/10.4236/am.2013.42045

Helga Weisz, F. D. (2006). Physical and monetary input–output analysis: What makes the difference? *Ecological Economics, 57*(3), 534-541. doi:https://doi.org/10.1016/j.ecolecon.2005.05.011

Henderson. (n.d.). *Attraction/Repulsion*. (Open Processing) Retrieved 06 17, 2022, from https://openprocessing.org/sketch/18798

Hewings, G. J. (1985). *Regional Input-Output Analysis.* (G. I. Thrall, Ed.) WVU Research Repository: Sage Publications. Retrieved from https://researchrepository.wvu.edu/cgi/viewcontent.cgi?article=1009&context=rri-web-book

Heywood, J. (2006). Viscous Incompressible Fluids: Mathematical Theory. In G. L. Jean-Pierre Françoise (Ed.), *Encyclopedia of Mathematical Physics* (pp. 369-379). Academic Press. doi:https://doi.org/10.1016/B0-12-512666-2/00158-9

Hiroyuki Iseki, R. P. (2018). Analysis of firm location and relocation in relation to Maryland and Washington, DC metro rail stations. *Research in Transportation Economics, 67*, 29-43. doi:https://doi.org/10.1016/j.retrec.2016.11.003.

Horowitz, J. a. (1994). Advances in Random Utility Models. *Marketing Letters, 5:4*, 311-322. Retrieved from https://mpra.ub.uni-muenchen.de/53026/

Hougardy, S. (2010). The Floyd-Warshall alogrithm on graphs with negative cycles. *ELSEVIER. Information Processing Letter*, 279-281.

House, T. W. (2021, 11 02). *Fact Sheet: President Biden Tackles Methane Emissions, Spurs Innovations, and Supports Sustainable Agriculture to Build a Clean Energy Economy and Create Jobs*. (The White House) Retrieved 05 12, 2022, from https://www.whitehouse.gov/briefing-room/statements-releases/2021/11/02/fact-sheet-president-biden-tackles-methane-emissions-spurs-innovations-and-supports-sustainable-agriculture-to-build-a-clean-energy-economy-and-create-jobs/

Hubacek, K. (2002). *The Role of Land in Economic Theory.* Laxenburg: International Institute for Applied Systems Analysis.

Hui Xu, Y. Z.-J. (2019). Source contribution analysis of mercury deposition using an enhanced CALPUFF-Hg in the central Pearl River Delta, China. *Environmental Pollution, 250*, 1032-1043. doi:https://doi.org/10.1016/j.envpol.2019.04.008.

Imem Haj Hamad, A. C. (2021). A Takagi-Sugeno Fuzzy Model for Greenhouse Climate . *Engineering, Technology & Applied Science Research, 11*(4), 7423-7429.

Institue for energy reseach (IER). (2021, 10 26). *EIA Expects Energy Demand to Increase Almost 50 Percent Worldwide by 2050*. (IER) Retrieved 05 18, 2022, from https://www.instituteforenergyresearch.org/international-issues/eia-expects-energy-demand-to-increase-almost-50-percent-worldwide-by-2050/

Jagannath, T. (2020, 08 13). *Central Business District (CBD) | Characteristics, Examples, Pros and Cons*. (Planning Tank) Retrieved 06 19, 2022, from https://planningtank.com/city-insight/central-business-district-cbd

Ji Luo, C. W. (2022). Heavy-duty truck routing strategy for reducing community-wide exposure to associated tailpipe emissions. *Transportation Research Part D*. doi:https://doi.org/10.1016/j.trd.2022.103289

Jinxiang Gu, M. G. (2007). Research on warehouse operation: A comprehensive review. *European Journal of Operational Research, 177*(1), 1-21. doi:https://doi.org/10.1016/j.ejor.2006.02.025

John R. Balmes, J. M. (1987). Symptomatic Bronchoconstriction after Short-Term Inhalation of Sulfur Dioxide. *American Review of Respiratory Disease, 136*(5), 1117. doi:https://doi.org/10.1164/ajrccm/136.5.1117

Jonathan Lee, N.-L. H. (2013). On Fuzziness. In *Studies in Fuzziness and Soft Computing* (pp. 365–370). Berlin, Heidelberg: Springer. doi:https://doi.org/10.1007/978-3-642-35641-4_53

José I. Huertas, M. E. (2012). Air quality impact assessment of multiple open pit coal mines in northern Colombia. *Journal of Environmental Management, 93*(1), 121-129. doi:https://doi.org/10.1016/j.jenvman.2011.08.007.

Jun Wang, L. J.-Y. (2013). Investigation of speciated VOC in gasoline vehicular exhaust under ECE and EUDC test cycles. *Science of The Total Environment*(0048-9697), 445–446. Retrieved from https://doi.org/10.1016/j.scitotenv.2012.12.044.

Junming Lao, H. S. (2022). Research on atmospheric pollutant and greenhouse gas emission reductions of trucks by substituting fuel oil with green hydrogen: A case study. *International Journal of Hydrogen Energy*. doi:https://doi.org/10.1016/j.ijhydene.2022.02.230

K, N. (n.d.). *Demand Function for Money | Economics*. (Economics Discussion) Retrieved 07 05, 2022, from https://www.economicsdiscussion.net/money/demand-for-money/demand-function-for-money-economics/24694#:~:text=Similarly%2C%20the%20responsiveness%20of%20demand%20for%20money%20with,known%20as%20interest%20elasticity%20of%20demand%20for%20money.

Kanbay, P. P. (2018). A Fuzzy Approch to the Emission Estimation. *International Scientific Journal "Mathemetical Modeling"*(4), 136-138. Retrieved from https://stumejournals.com/journals/mm/2018/4/136.full.pdf

Khandakar Md Habib Al Razi, M. H. (2012). Modeling of atmospheric dispersion of mercury from coal–fired power plants in Japan. *Atmospheric Pollution Research, 3*(2), 226-237. doi:https://doi.org/10.5094/APR.2012.025.

Kopsch, M. (2012, 04 02). *Delaunay triangulation*. (Wikipedia) Retrieved 06 04, 2022, from https://en.wikipedia.org/wiki/Delaunay_triangulation

Kris Braekers, K. R. (2016). The vehicle routing problem: State of the art classification and review. *Computers & Industrial Engineering, 99*, 300-313. doi:https://doi.org/10.1016/j.cie.2015.12.007

Kröcher, O. (2018). Selective Catalytic Reduction of NOx. *Catalysts, 8*(459), 1-4. doi:http://dx.doi.org/10.3390/catal8100459

L. Fu, D. S. (2006). Heuristic shortest path algorithms for transportation applications: State of the art. *Computers & Operations Research, 33*(11), 3324-3343. doi:https://doi.org/10.1016/j.cor.2005.03.027

Lakes Environmental. (n.d.). *CALPUFF View Leading Interface for Puff Dispersion.* Lakes Environmental. Retrieved 06 16, 2022, from https://www.addlink.es/images/pdf/agdweb1201.pdf#:~:text=Different%20than%20a%20plume%20model%2C%20a%20puff%20model,to%20respond%20to%20the%20meteorology%20immediately%20surrounding%20it.

Lasley SM, G. M. (2000). Glutamatergic components underlying lead-induced impairments in hippocampal synaptic plasticity. *Neurotoxicology, 21*(6), 1057-1068.

Laurent Lebreton, A. A. (2019). Future scenarios of global plastic waste generation and disposal. *Springer Nature*, 1-11. doi:https://doi.org/10.1057/s41599-018-0212-7

Lazenby, H. (2022, 05 12). *Mining Indaba: Russia-Ukraine war triggers policy shifts, supply chain disruptions*. (Mining.com) Retrieved 05 30, 2022, from https://www.mining.com/mining-indaba-world-order-at-a-critical-inflection-point/

Lee J.Krajewski, M. K. (2022). Using operations to create value. In *Operations Management, Processes and Supply Chains* (Vol. 13, pp. 22-23). Pearson.

Leggett, R. (2004). *Real-Time Crowd Simulation: A Review*.

Li Li, Y. L. (2018). Evaluation of future energy consumption on PM2.5 emissions and public health economic loss in Beijing. *Journal of Cleaner Production, 187*, 1115-1128. doi:https://doi.org/10.1016/j.jclepro.2018.03.229

Liang Fu, R. S. (2016). Tobin's q Ratio and Firm Performance. *International Research Journal of Applied Finance, 7*(4). Retrieved from https://www.researchgate.net/publication/307847236_Tobin%27s_q_Ratio_and_Firm_Performance

Lili Wang, A. S. (2012). Capital inputs in the Chinese economy: Estimates for the total economy, industry and manufacturing. *China Economic Review, 23*(1), 81-104. doi:https://doi.org/10.1016/j.chieco.2011.08.002

Lloyd-Smith, P. (2018). A new approch to calculating welfare measures in Kuhn-Tucker demand models. *Journal of Choice Modelling, 26*, 19-27. doi:https://doi.org/10.1016/j.jocm.2017.12.002

Lucino Fanti, P. M. (2007). Chaotic business cycles and fiscal policy: An IS-LM model with distributed tax collection lags. *Chaos, Solitions & Fractals, 32*(2), 736-744.

M.Shekar Reddy, C. V. (2002). Inventory of aerosol and sulphur dioxide emissions from India: I—Fossil fuel combustion. *Atmospheric Environment, 36*(4), 677-697. doi:https://doi.org/10.1016/S1352-2310(01)00463-0

M.Stockie, J. (2011). The Mathematics of Atmospheric Dispersion Modeling. *Society for Industrial and Applied Mathematics, 53*(2), 349-372. doi: 10.1137/10080991X

Mahlia, T. (2002). Emissions from electricity generation in Malaysia. *Renewable Energy, 27*, 293-300.

Manoela Kohler, M. M. (2019). PSO+: A new particle swarm optimization algorithm for constrained problems. *Applied Soft Computing, 85*. doi:https://doi.org/10.1016/j.asoc.2019.105865

Marilena Kampa, E. C. (2008). Human health effects of air pollution. *Environmental Pollution, 151*(2), 362-367. doi:https://doi.org/10.1016/j.envpol.2007.06.012

Martel, C. (2002). The expected complexity of Prim's minimum spanning tree alogrithm. *ELSEVIER. Information Processing Letters*, 197-201.

Mary E Deily, W. B. (1991). Enforcement of pollution regulations in a declining industry. *Journal of Environmental Economics and Management, 21*(3), 260-274.

McCall, J. (2005). Genetic algorithms for modelling and optimisation. *Journal of Computational and Applied Mathematics, 184*(1), 205-222. doi:https://doi.org/10.1016/j.cam.2004.07.034

Mehrdad Mohammadi, F. J. (2011). An M/M/c queue model for hub covering location problem. *Mathematical and Computer Modelling, 54*(11-12), 2623-2638. doi:https://doi.org/10.1016/j.mcm.2011.06.038

Midwest Research Institute. (1993). *Locating and estimating air toxic emissions from sources of cyanide compounds.* Cary: US Environmental Protection Agency.

Ministry of Economy, Trade and Industry (METI), Japan. (2005). *Low Rise Industrial Source Dispersion Model (METI-LIS Model Ver.2.0).* Tokyo: Ministry of Economy, Trade and Industry.

Nadja Popovich, L. A.-R.-L. (2021, 01 20). *The Trump Administration Rolled Back More Than 100 Environmental Rules.* (The New York Times) Retrieved 05 12, 2022, from https://www.nytimes.com/interactive/2020/climate/trump-environment-rollbacks-list.html

Newburger, E. (2021, 11 16). *What the COP26 climate conference really accomplished*. (CNBC) Retrieved 05 11, 2022, from https://www.cnbc.com/2021/11/16/un-cop26-climate-summit-what-was-accomplished.html?msclkid=4db2a63bd12f11eca919351eb79cee72

Nicholas A. Mailloux, D. W. (2022). Nationwide and Regional PM2.5-Related Air Quality Health Benefits from the Removal of Energy-Related Emissions in the United States. *GeoHealth, 6*, 1-19. doi:https://doi.org/10.1029/2022GH000603

NIOSH. (2007). *NIOSH pocket guide to chemical hazards.* Cincinnati: NIOSH Publications.

Nsikan Paul Akpan, I. I. (2017). A Minimum Spanning Tree Approach of Solving a Transportation Problem. *International Journal of Mathematics and Statistics Invention (IJMSI), 5*(3), 8-17.

NTP. (2018, 07 26). *14th Report on Carcinogens.* Retrieved from National Toxicological Program: https://ntp.niehs.nih.gov/ntp/roc/content/profiles/cokeovenemissions.pdf

OECD. (2023). *Industrial production*. (OECD) doi:10.1787/39121c55

OECD. (2023). *Material consumption*. (OECD) doi:10.1787/84971620

Olivier Vidal, F. R. (2017). Global Trends in Metal Consumption and Supply: The Raw Material–Energy Nexus. *Elements, 13*, 319-324. doi:10.2138/gselements.13.5.319

Oren, T. (2018). On the Advantages of Simulation based Approach in Engineering. *COJ Electronics and Communications, 1*(1). doi:http://dx.doi.org/10.31031/COJEC.2018.01.000501

Oyundolgor Khorloo, Z. G. (2011). Wind Field Synthesis for Animating Wind-induced Vibration. *International Journal of Virtual Reality, 10*(1), 53-60. doi:https://doi.org/10.20870/IJVR.2011.10.1.2802

Parivesh Bhawan, E. A. (1998). *Emission Regulation.* Delhi: Central Pollution Control Board. Retrieved from https://cpcb.nic.in/openpdffile.php?id=UmVwb3J0RmlsZXMvTmV3SXRlbV8xNjRfRU1JU1NJT05fUkVHVUxBVElPTlNfUEFSVF8yLnBkZg==

Patrick Heffer, M. P. (2014). *Global nitrogen fertiliser demand and supply: trend, current level and outlook.* Paris: International Fertilizer Industry Association (IFA). Retrieved from https://www.fertilizer.org/images/Library_Downloads/2016%20Global%20nitrogen%20fertiliser%20demand%20and%20supply.pdf

Pavelescu, F. M. (2014). *Some aspects of the translog production.* Bucharest: Institute of National Economy Bucharest Romania. Retrieved from https://www.researchgate.net/profile/Florin-Marius-Pavelescu

Pratima Meshram, B. P. (2014). Extraction of lithium from primary and secondary sources by pre-treatment, leaching and sepration: A comprehensive review. *Hydrometallurgy, 150*, 192-208. Retrieved from http://dx.doi.org/10.1016/j.hydromet.2014.10.012

Qing Lu, J. Z. (2013). Emissions trends and source characteristics of SO2, NOx, PM10 and VOCs in the Pearl River Delta region from 2000 to 2009. *Atmospheric Environment, 76*, 11-20. doi:http://dx.doi.org/10.1016/j.atmosenv.2012.10.062

Quality, O. o. (2008). *Average In-Use Emissions from Heavy Duty Trucks.* EPA. Retrieved from https://nepis.epa.gov/Exe/ZyPDF.cgi/P100EVY6.PDF?Dockey=P100EVY6.PDF

Rahila Rahman Khan, M. S. (2014). Review on effects of Particulates; Sulfur Dioxide and Nitrogen Dioxide on Human Health. *International Research Journal of Environment Sciences, 3*(4), 70-73.

Raquel A. Silva, Z. A. (2016). The Impact of Individual Anthropogenic Emissions Sectors on the Global Burden of Human Mortality due to Ambient Air Pollution. *Environmental Health Perspectives, 124*(11), 1776-1784. doi:https://doi.org/10.1289/EHP177

Ratnaike, R. N. (2003). Acute and chronic arsenic toxicity. *Postgraduate Medical Journal, 79*(933), 391.

Reeves, C. (2010). Genetic Alogrithms. In *Handbook of Metaheuristics* (pp. 56-82). Springer.

Reeves, W. T. (1983). Particle Systems- A Technique for Modeling a Class of Fuzzy Objects. *Computer Graphics, 17*(3). Retrieved from https://course.ccs.neu.edu/cs5310sp13/resources/readings/fuzzyParticles.pdf

Regression Algorithms: which Machine Learning Metrics? (n.d.). (MyDataModels) Retrieved 07 13, 2022, from https://www.mydatamodels.com/learn/guide/a-path-to-discover-ai/regression-algorithms-which-machine-learning-metrics/

Reynès, F. (2019). The Cobb–Douglas function as a flexible function: A new perspective on homogeneous functions through the lens of output elasticities. *Mathematical Social Sciences, 97*, 11-17. doi:https://doi.org/10.1016/j.mathsocsci.2018.10.002.

Reza Zanjirani Farahani, M. H. (2013). Hub location problems: A review of models, classification, solution techniques, and applications. *Computers & Industrial Engineering, 64*(4), 1096-1109. doi:https://doi.org/10.1016/j.cie.2013.01.012

Robert Pindyck, D. R. (2005). Chapter 2: The Basics of Supply and Demand. In *Microeconomics* (pp. 36-37). New Jersey: Pearson Pentice Hall.

Robert Sedgewick, R. S. (2017). Object-Oriented Programming. In *Computer Science, An interdisciplinary approch* (pp. 329-478). Crawfordsville: Pearson Education, Inc.

RTI International. (2015). *Emissions Estimation Protocol for Petroleum Refineries.* Research Triangle Park: Office of Air Quality Planning and Standards (EPA). Retrieved from https://www.epa.gov/sites/default/files/2020-11/documents/protocol_report_2015.pdf

S. Brusca, F. R. (2016). Theoretical and experimental study of Guassian Plume model in small scale system. *Energy Procedia, 101*, 58-65. doi:10.1016/j.egypro.2016.11.008

Salam, H. A. (2013). Prediction of pollutants emissions dispersion of phosphate fertilizers production facility. *International Journal of Research in Engineering and Technology, 2*(11), 306-311.

Samanez-Larkin, G. R. (2015). Chapter 3 - Decision Neuroscience and Aging. In J. S. Thomas M. Hess (Ed.), *Aging and Decision Making* (pp. 41-60). Academic Press. doi:https://doi.org/10.1016/B978-0-12-417148-0.00003-0

Sanaa ElFadily, A. K. (2019). Modeling and Mathematical Analysis of Labor Force Evolution. *Modelling and Simulation in Engineering*, 1-5. doi:https://doi.org/10.1155/2019/2562468

SCMR Staff. (2022, 5 25). *Supply chain disruptions could cost European economies up to €920 billion in GDP by 2023*. (Supply Chain Management Review) Retrieved 5 30, 2022, from https://www.scmr.com/article/supply_chain_disruptions_could_cost_european_economies_up_to_920_billion_in

Senthilnathan, S. (2019). Economic Order Quantity (EOQ). *SSRN Electronic Journal*. doi:10.2139/ssrn.3475239

Shiffman, D. (2012). *The Nature of Code, Simulating Natural Systems with Processing.* (S. Fry, Ed.) California: Daniel Shiffman.

Shiffman, D. (2017). *Coding Challenge 35: Traveling Salesperson with Genetic Algorithm*. (The Coding Train) Retrieved 06 15, 2022, from https://www.youtube.com/watch?v=hnxn6DtLYcY

Shiwen Huang, H. L. (2021). Long-term exposure to nitrogen dioxide and mortality: A systematic review and meta-analysis. *Science of The Total Environment, 776*, 1-12. doi:https://doi.org/10.1016/j.scitotenv.2021.145968.

Silberberg, E. (1990). *The Structure of Economics A Mathemetical Analysis* (Second ed.). (S. D.Stratford, Ed.) McGraw-Hill,Inc.

Silberberg, E. (1990). *The structure of economics: A mathemetical analysis.* (S. D.Stratford, Ed.) McGraw Hill, Inc.

Skiena, S. S. (2008). *The Alogrithm Design Manual.* New York: Springer.

Skinderowicz, R. (2022). Improving Ant Colony Optimization efficiency for solving large TSP instances. *Applied Soft Computing, 120*. doi:https://doi.org/10.1016/j.asoc.2022.108653

Smith, J. M. (1998). *Steiner Minimal Trees in E3: Theory, Alogrithms, and Applications.* Kluwer Academic Publishers.

Sommer, B. (2022, 05 14). *How Do Higher Interest Rates Bring Down Inflation?* (The New York Times) Retrieved 06 02, 2022, from https://www.nytimes.com/2022/05/14/business/inflation-interest-rates.html#:~:text=One%20way%20of%20looking%20at,more%20expensive%20to%20borrow%20money.

Soularidis, A. (n.d.). *An Introduction to Kruskal's Algorithm: Theory and Python Implementation*. (Python in Plain English) Retrieved 06 04, 2022, from https://python.plainenglish.io/an-introduction-to-kruskals-algorithm-theory-and-python-implementation-6117c164fbc6

Sproule, R. (2013). A systematic analysis of the links amongst the Marshallian, Hicksian, and Frischian demand functions: A note. *Economics Letters, 121*(3), 555-557. doi:https://doi.org/10.1016/j.econlet.2013.10.004

Stevens, J. R. (2010). Intertemporal Choice. In *Encyclopedia of Animal Behavior* (pp. 203-208). Elsevier Ltd. doi:10.1016/B978-0-08-045337-8.00093-0

T. Rajkumar, H. W. (1996). Fuzzy Exposure Model. Auckland. doi:10.1109/ICSMC.1996.571226

Takashi Nagatani, D. H. (2004). Stability analysis and stabilization strategies for linear supply chains. *Physica A: Statistical Mechanics and its Applications, 335*(3-4), 644-660. doi:https://doi.org/10.1016/j.physa.2003.12.020

Tang, L. (2022). The dynamic demand for capital and labor: Evidence from Chinese industrial firms. *Economic Modelling, 107*. Retrieved from https://doi.org/10.1016/j.econmod.2021.105731.

The World Bank. (n.d.). *Indicators*. (World Bank Corp) Retrieved 05 16, 2022, from https://data.worldbank.org/indicator?tab=all

Thomas D Durbin, X. Z. (2003). The effects of diesel particulate filters and a low-aromatic, low-sulfur diesel fuel on emissions for medium-duty diesel trucks. *Atmospheric Environment, 37*(15), 2105-2116. doi:https://doi.org/10.1016/S1352-2310(03)00088-8.

Tiffany Vass, P. L. (2021, 11). *Chemials*. (IEA) Retrieved 05 18, 2022, from https://www.iea.org/reports/chemicals

Timms, H. L. (1962). Plant Planning, Fundamentals and Analysis for Management . In *The production function in business* (pp. 293-324). Homewood: Richard D. Irwin, Inc.

Timms, H. L. (1962). *The production functions in business, Fundamentals and analysis for management* . Illinois: Richard D. Irwin, Inc.

Tsitsas, A. M. (2021). Particle Swarm Optimization Algorithms with Applications to Wave Scattering Problems. In *Optimization Algorithms [Working Title]*. London, United Kingdom: IntechOpen. doi:10.5772/intechopen.97217

U.S. Environmental Protection Agency. (1995). *User's guide for the Industrial Source Complex (ISC3) dispersion models.* Research Triangle Park, North Carolina: Office of Air Quality Planning and Standards Emissions, Monitoring, and Analysis Division.

U.S. Environmental Protection Agency. (2019, 08). *Community Multiscale Air Quality (CMAQ) Modeling System.* Retrieved 06 09, 2022, from https://www.epa.gov/system/files/documents/2021-11/cmaq_factsheet_august2019.pdf

Uzair Ali, J. W. (2021). The impact of climate change on the economic perspectives of crop farming in Pakistan: Using the ricardian model. *Journal of Cleaner Production, 308*. doi:https://doi.org/10.1016/j.jclepro.2021.127219.

Valdovinos, C. G. (2003). Inflation and economic growth in long run. *Economic Letters, 80*(2), 167-173.

Varadhan, S. (2022, 05 10). *India lets coal mines hike output without feedback*. (Reuters) Retrieved 05 11, 2022, from https://www.reuters.com/business/energy/india-lets-coal-mines-hike-output-without-feedback-2022-05-11/?msclkid=09e2bdd0d12f11ecacf399b285461393

Venkatachalam, K. (2017, 03 03). *Report: China and India have World's deadlist air pollution*. (The Diplomat) Retrieved 05 23, 2022, from https://thediplomat.com/2017/03/report-china-and-india-have-worlds-deadliest-air-pollution/

Vimal Chandra Pandeya, J. S. (2011). Arsenic hazards in coal fly ash and its fate in Indian scenario. *Elsevier*, 819-835.

Waljiyanto, N. W. (2004). Application of Finite Difference Method to Develop Land Value Map. *3rd FIG Regional Conference.* Jakarta. Retrieved from

https://www.fig.net/resources/proceedings/fig_proceedings/jakarta/papers/ts_07/ts_07_5_waljiyanto_etal.pdf

Wang, X. Z. (2011). The Comparison of Three Algorithms in Shortest Path Issues. *First International Conference on Advanced Algorithms and Control Engineering*. doi:10.1088/1742-6596/1087/2/022011

Wm. J. Veigele, J. H. (1978). Derivation of the Guassian Plume Model. *Journal of the Air Pollution Control Association, 28*(11), 1139-1140. doi:https://doi.org/10.1080/00022470.1978.10470720

Yaroslav Bezyk, D. O. (2021). Evaluation of the CALPUFF model performance for the estimation of the urban ecosystem CO2 flux. *Atmospheric Pollution Research, 12*(3), 260-277. doi:https://doi.org/10.1016/j.apr.2020.12.013.

Yoon Soo Park, L. K. (2020). The Positivism Paradigm of Research. *Academic Medicine, 95*(5), 690-694. doi:doi: 10.1097/ACM.0000000000003093

Young-Rae Jung, W.-G. P.-H. (2003). Pollution dispersion analysis using the puff model with numerical flow field data. *Mechanics Research Communications, 30*, 277-286. doi:10.1016/S0093-6413(03)00024-7

Zaratiegui, J. M. (2002). Marshallian demand function and the adjustment of competitive markets. *International Journal of Applied Economics and Econometrics, 10*(3), 369-380. Retrieved from https://dadun.unav.edu/bitstream/10171/6313/1/Demand%20function%20%28IJAEE%29.pdf

Zhang, Y. S. (2021). Global health effects of future atmospheric mercury emissions. *Nature Communications, 12*(3035), 1-10. doi:https://iopscience.iop.org/article/10.1088/1748-9326/aad138/pdf

Zhdannikov, N. B. (2022, 05 09). *Exclusive-Biden sidelined global energy partners with record emergency oil release*. (Reuters) Retrieved 05 12, 2022, from https://news.yahoo.com/exclusive-biden-sidelined-global-energy-051733939.html

Zhenyu Luo, Y. W. (2022). Impacts of vehicle emission on air quality and human health in China. *Science of The Total Environment, 813*. doi:https://doi.org/10.1016/j.scitotenv.2021.152655